1,3,2-diazaphospholene-catalysed reduction of unsaturated bonds

Chong, Che Chang

2016

1,3,2-DIAZAPHOSPHOLENE-CATALYSED REDUCTION OF UNSATURATED BONDS

CHONG CHE CHANG

SCHOOL OF PHYSICAL AND MATHEMATICAL SCIENCES

2016

1,3,2-DIAZAPHOSPHOLENE-CATALYSED REDUCTION OF UNSATURATED BONDS

CHONG CHE CHANG

CHONG CHE CHANG

School of Physical and Mathematical Sciences

A thesis submitted to Nanyang Technological University in partial fulfilment
of the requirements for the degree of Doctor of Philosophy

2016

Acknowledgements

Table of Contents

List of Abbreviations

9-BBN	9-borabicyclo[3.3.1]nonane
δ	chemical shift
μL	microliter
atm	atmospheres
Ar	aryl (substituted aromatic ring)
br	broad
^{n}Bu	*n*-butyl
^{t}Bu	*tert*-butyl
CAAC	cyclic alkyl amino carbene
calcd	calculated
d	doublet
DABCO	1,4-diazabicyclo[2.2.2]octane
Dipp	2,6-diisopropylphenyl
DFT	Density Functional Theory
eq	(chemical) equation
equiv	equivalent
FLPs	frustrated Lewis Pairs
g	gram
h	hour
H	hydrogen
HBpin	pinacolborane (4,4,5,5-tetramethyl-1,3,2-dioxaborolane)
HBcat	catecholborane
HRMS	High Resolution Mass Spectrometry
Hz	Hertz
IR	infra-red
J	coupling constant
m	multiplet

M	concentration in mol/L
M^+	parent ion peak in mass spectrum
Me	methyl
Mes	2,4,6-trimethylphenyl
MHz	megahertz
mL	milliliter
mmol	millimole
mol%	mole percent
M.p.	melting point
m/z	mass to charge ratio (mass spectrum)
NHC	N-heterocyclic carbene
NMR	Nuclear Magnetic Resonance
$HNTf_2$	triflimide (trifluoromethanesulfonimide)
OTf	triflate (trifluoromethanesulfonate)
Ph	phenyl
ppm	parts per million
^{i}Pr	*iso*-propyl
q	quartet
quint	quintet
rt	room temperature
s	singlet
sept	septet
sext	sextet
t	triplet
THF	tetrahydrofuran

List of Schemes

Abstract

The development of main group catalysts has been gaining increasing attention in recent years. Several of these catalysts are shown to be efficient in various organic reactions and thus, provide a potential replacement for toxic, expensive transition metal catalysts. Nonetheless, high catalytic loading and catalyst decomposition are often the cause of concern for main group catalysts. Hence, exploring new reactivity and understanding its mechanism in these systems are of utmost importance to increase catalytic efficiency.

This thesis mainly focuses on the novel usage of 1,3,2-diazaphospholene as an efficient catalyst in various reduction reactions including transfer hydrogenation of azo compounds (N=N), hydroboration of carbonyl compounds (C=O) as well as N-formylation of amines using CO_2. More importantly, the mechanisms of these reactions were investigated using experimental and DFT studies. Understanding these catalytic systems plays a crucial role in the development of a more robust and effective catalyst in the near future.

Chapter 1   **Introduction**

1.1   **Main group compounds – alternative to transition metal complexes**

Understanding the fundamentals of the natural world and applying them to improve our daily lives are key aspects in science. A crucial observation from the natural world is the way living organisms transform relatively inert molecules into chemically important compounds for sustaining life. These transformations generally involve the breaking of chemically inert bonds to form new chemical bonds, usually with the help of enzymes. For instance, plants contain enzyme such as 1,5-bis(phosphate)-carboxylase-oxidase (RuBisCO), which uses CO_2 available in the atmosphere for C-carboxylation reactions to yield glucose during photosynthesis. [1] Another significant example involves the oxidation of methane by means of a methane monooxygenase (MNO) to give methanol. [2] Likewise, organic transformations are of paramount importance for chemical industries in affording various useful commodities which include pharmaceutical drugs, organic dyes or storage materials.

An important feature in these transformations is that it requires overcoming the typically high kinetic barrier associated with these bonds. It has been well established that transition metal complexes could activate a variety of bonds such as C-H, C-C, H_2, N_2 and N-H through binding and coordination of these bonds to its partially filled d-orbitals. [3] In addition, the versatility of transition metal complex to possess variable oxidation states makes them an ideal catalyst and capable of participating in various mechanisms. Oxidative addition, reductive elimination, olefin metathesis are some of the key mechanisms found in notable transition metal catalysts like the Wilkinson's catalyst (**I**), Grubbs' catalyst (**II**) and Shvo's catalyst (**III**) (Figure 1.1). Despite the prevalent use of transition metal catalysts in bond activation reactions, issues of toxicity, cost fluctuation, and uncertainty in future supplies constitute major disadvantages. [4] Further exploitation and mining of these metals may also pose serious problems for the environment, especially so with the exponential increase in demand for transition metals for other uses. [5] Therefore, it is reasonable to source for suitable alternatives to replace transition metals in the long run.
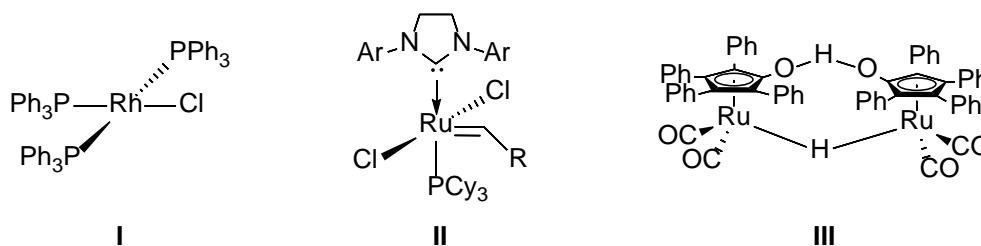
Figure 1.1   Examples of some notable transition metal catalysts: Wilkinson' catalyst **I**, Second Generation Grubbs' catalyst **II**, Shvo's catalyst **III**.

In recent decades, there has been a growing trend in the development of main group compound as a viable alternative to transition metal complex.[6] Unlike transition metals, main group elements usually have fixed oxidation states and therefore, do not undergo oxidative addition/reductive elimination-type reaction. Furthermore, a limited number of coordination sites or accessible vacant orbitals restrict reactivity at the main group element centre. Nonetheless, designing novel main group compounds featuring appropriate ligands or substituents could circumvent these difficulties.

A key breakthrough was discovered by Power et al. in 2005 in which they demonstrated that a Ge alkyne analogue ArGe-GeAr readily reacted with H_2 (1 atm) at room temperature to yield a mixture of digermane and primary germane (eq 1).[7] The Ge-Ge bonding in ArGe-GeAr can be described formally as a double bond with significant non-bonding electron density on the two Ge centres. A second-order Jahn-Teller σ^*-π-orbital mixing leads to a decrease in Ge-Ge bond order from an idealized triple bond. Such Jahn-Teller distortion also explains its deviation from ideal linear geometry to a more stable trans-bent structure.[8] Further work by the same group also demonstrated that the Sn analogue gave similar reactivity with H_2 under ambient conditions.[9] Importantly, theoretical studies gave insights into the bonding interactions between the heavier element alkyne analogues and H_2 (Figure 1.2a). The reaction between ArE-EAr (where E = Ge, Sn) and H_2 can be described using synergistic bonding description based on frontier molecular orbital interactions as follows: donation of electrons from the σ(H-H) bonding orbital into the LUMO(n^+, non-bonding orbital) of ArE-EAr and a back donation from the HOMO(π) of ArE-EAr to the σ^*(H-H) orbital, thus, weakening the H-H bond. Such synergistic bonding description is

akin to the extension of the Dewar-Chatt-Duncanson model for transition metal-dihydrogen complexes (Figure 1.2b) which was first described by Kubas et al. in 1984.[10]

$$Ar\diagdown Ge\equiv\equiv Ge\diagup Ar \xrightarrow[\text{hexane, r.t.}]{H_2} Ar\diagdown Ge=Ge\diagup Ar \diagup H \quad + \quad H\diagdown Ge-Ge\diagup Ar \diagup H \quad + \quad H\diagdown Ge-H \diagup Ar \quad (1)$$

Ar =

Dipp   Dipp
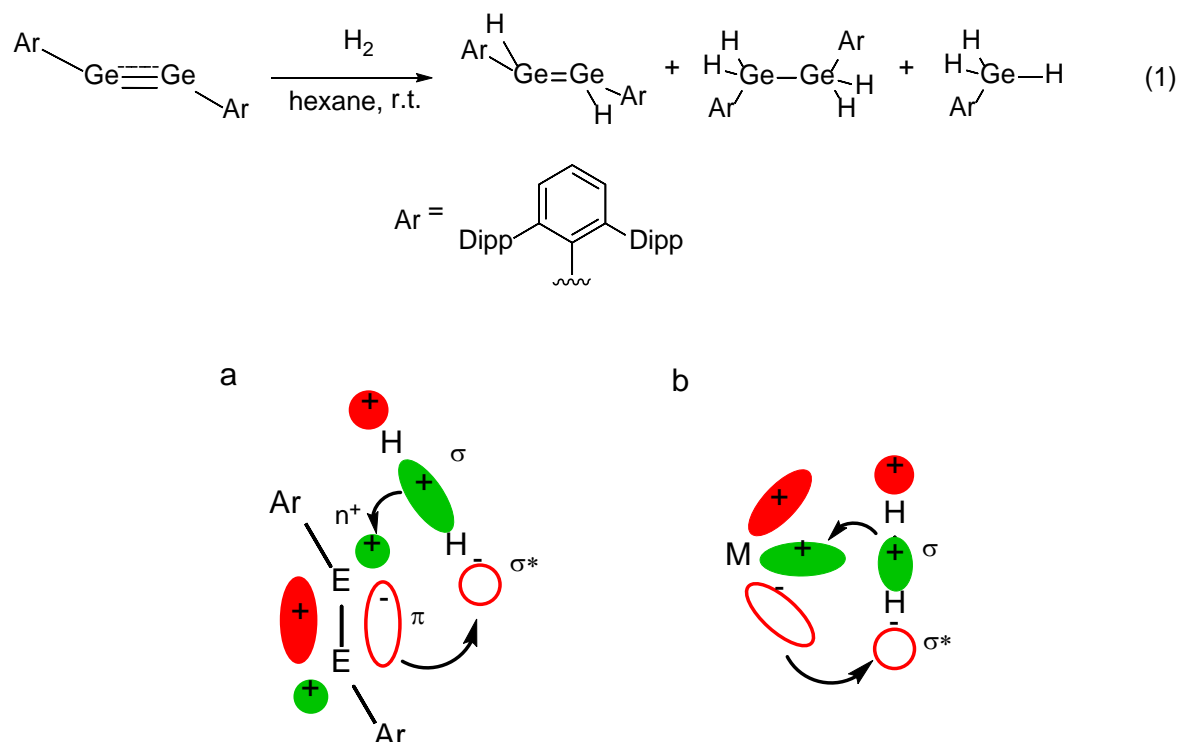
Figure 1.2   Interactions of the frontier molecular orbitals in H_2 activation by a) heavier group 14 alkyne analogues and b) transition metal complexes.

In the case of non-metal main group compounds employed in bond activation reactions, the bulky Lewis acid-base compound, termed as frustrated Lewis pair (FLP) is a notable example. In 2006, Stephan et al. demonstrated the first example of a metal-free reversible activation of H_2 using $[Mes_2P(C_6F_4)B(C_6F_5)_2]$ FLP system (eq 2).[11] The mechanism for this reaction was initially proposed as a two-step pathway: H_2 addition onto either the B-C bond or the P-C bond and subsequent intramolecular hydride transfer to the B atom or proton transfer to the P atom, respectively. However, DFT studies conducted by Li et al. suggested a familiar synergistic bonding description as that in Figure 1.2, where the electrons on the P atom interact with the σ* orbital of H_2 while the σ-bond of H_2 interacts with the empty p-orbital on the B atom of another molecule of $[Mes_2P(C_6F_4)B(C_6F_5)_2]$ in an intermolecular fashion.[12]

3

$$(Mes)_2P\text{-----}B(C_6F_5)_2 \quad \underset{-H_2,\ 150\ ^\circ C}{\overset{H_2,\ 25\ ^\circ C}{\rightleftharpoons}} \quad (Mes)_2\overset{\oplus}{\underset{H}{P}}H\cdots\overset{\ominus}{B}(C_6F_5)_2 \quad (2)$$
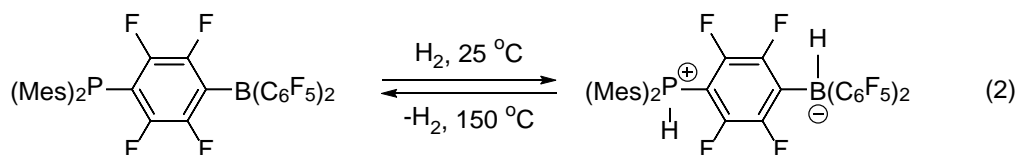
Besides activation of H_2, many other substrates are susceptible to activation by FLPs.[13] For instance, $Mes_2PCH_2CH_2B(C_6F_5)_2$ can activate the C-H bond of terminal alkynes and also undergo addition reactions with phenyl isocyanate, and CO_2 (eq 3).[14]

$$(3)$$

$$(4)$$

IV
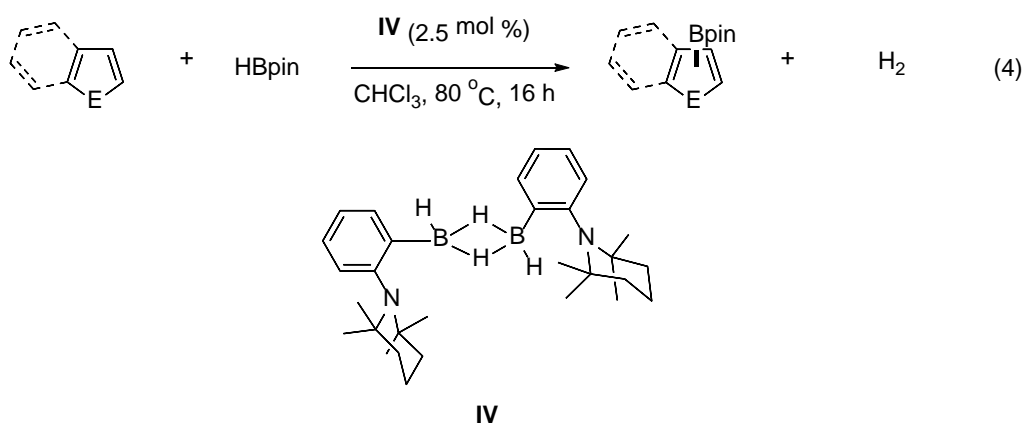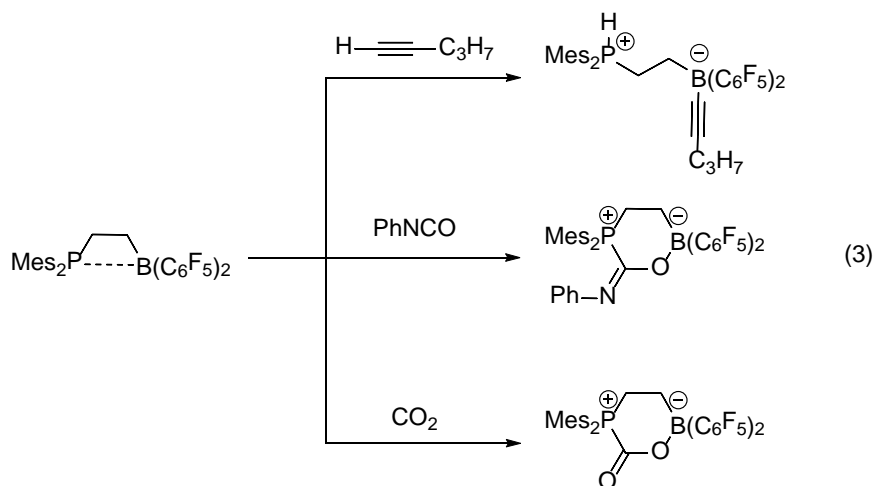
Recently, Fontaine et al. achieved the $C(sp^2)$-H borylation of heteroarenes under relatively mild conditions using a catalytic amount (2.5 mol%) of intramolecular FLP (**IV**) (eq 4).[15] The borylation occurs through an initial C-H activation at the *ortho* position of the heteroarene, releasing H_2 in the process (Scheme 1.1a). Then, regeneration of the catalyst

4

proceeds via a proposed four-membered σ-bond metathesis in the presence of HBpin to yield the borylated product (Scheme 1.1b). A variety of heteroarenes such as electron-rich thiophenes and furan derivatives (E = O, S) were shown to be susceptible to borylation using this intramolecular FLP catalyst. This instance further illustrates the ability of main group catalyst to mimic that of transition metal catalyst in C-H bond activation.
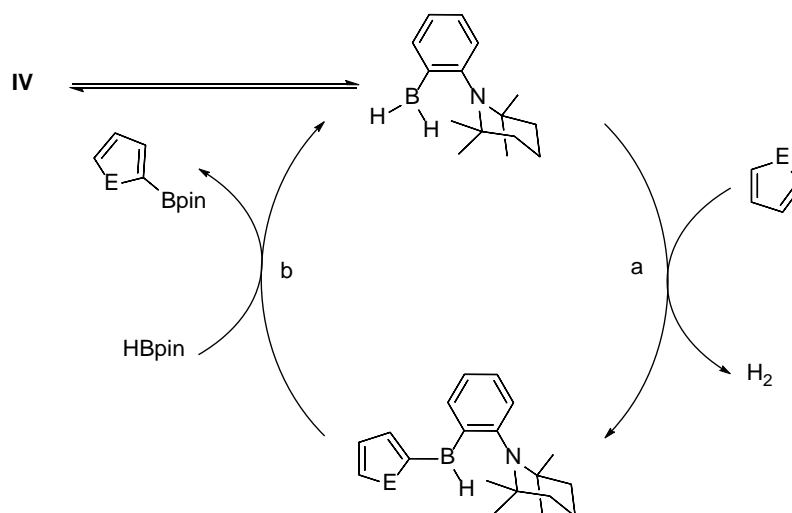
Scheme 1.1   Mechanism for the first example of FLP-catalysed borylation of heteroarenes.

Stable carbenes are another class of non-metal main group compound with great importance in bond activation. Since the isolation of N-heterocyclic carbenes (NHC)s by Arduengo et al. in 1991, NHC has been proven to be an excellent ligand for transition metals and could also act as an efficient organocatalyst.[16] In 2005, Bertrand et al. synthesized a novel stable carbene, cyclic (alkyl)(amino)carbene (CAAC) which features a quaternary sp^3 carbon next to the carbene carbon centre.[17] CAAC, which has both strong σ-donating and π-accepting properties, are useful in the stabilisation of many reactive species.[18] Significantly, CAACs could activate small molecules including CO, P_4 and E-H [E = H, $(RO)_2B$, $Ph(H)_2Si$, $Ph(H)P$, H_2N] (eq 5).[19] The reaction of CAAC with E-H bonds can be seen fundamentally as an oxidative addition on the carbon centre, resembling those observed in transition metal complexes. Notably, the activation of the N-H bond of ammonia was rarely observed in transition metal complexes due to the formation of Werner-type complexes. However, N-H bond was undoubtedly cleaved in an oxidative manner by CAAC.

5

$$(5)$$
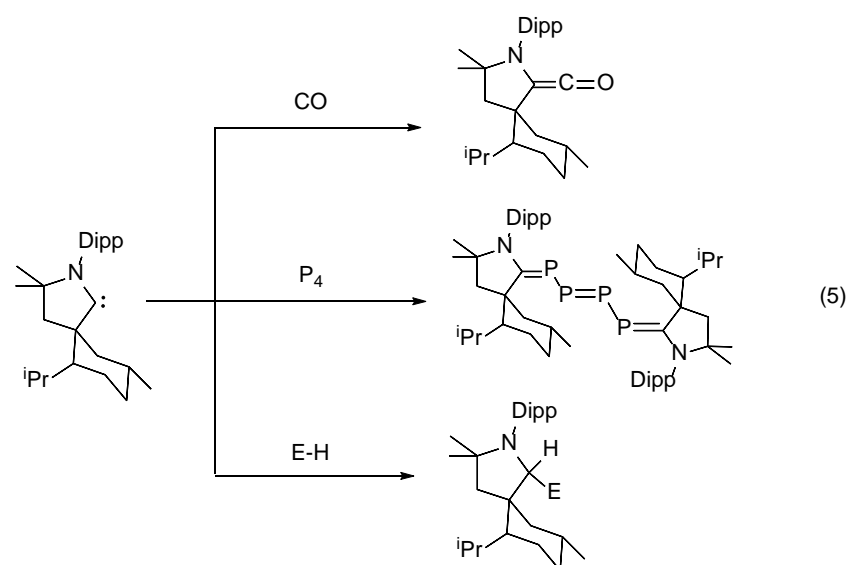
These examples clearly demonstrate that main group compounds could undergo a variety of bond activations. Given that most of these reactions are stoichiometric reactions, extending these reactions to catalytic scale would be a remarkable achievement in this field.

1.2   Development of main group catalysts for reduction reactions

As aforementioned, main group compounds could potentially replace transition metal catalysts in organic transformations. One such area of interest is the catalytic reduction reaction of organic substrates, which is an effective methodology to obtain useful and valuable compounds. Indeed, catalytic hydrogenation, hydrosilylation, and hydroboration are common synthetic methodologies commonly employed in laboratories and chemical industries.[20] In homogeneous catalysis, transition metal-catalysed hydrogenation, hydroboration, and hydrosilylation of unsaturated bonds have been extensively studied in the past decades.[21] In contrast, the use of main group compounds as effective catalysts are relatively uncommon.[22] In the case of hydrogenation, boranes, bismuth compounds, and some organocatalysts were shown to have some catalytic activity; however, high pressures of H_2, high catalytic loading, and harsh reaction conditions are usually required.[23]

An extension of the work on FLPs, Stephan et al. demonstrated the use of FLP as an efficient catalyst (5 mol%) for the hydrogenation of imines, nitriles, and aziridine using approximately 1 – 5 atm of H_2 under relatively mild conditions.[24] To investigate the reaction mechanism, stoichiometric reactions were conducted. The mechanism can be summarised as follows: the activation of H_2 by FLP occurs initially, follow by the proton transfer from P-H moiety to the imine substrate to afford an iminium cation and borohydride anion. Subsequent hydride insertion into C=N occurs to give a borane-amine adduct. Under heating conditions, the borane-amine adduct could dissociate to give the corresponding amine (Scheme 1.2).

Surprisingly, Stephan et al. and Klankermayer et al. showed that the use of bulky and highly Lewis acidic borane, $B(C_6F_5)_3$ alone could also perform similar hydrogenation reaction under catalytic conditions (5 mol%).[25] In this case, the imine substrates act as the Lewis base partner of $B(C_6F_5)_3$ in the FLP system, hence, activating H_2 to afford iminium cation and borohydride anion, $[HB(C_6F_5)_3]^-$ (eq 6). Subsequent hydride transfer from $[HB(C_6F_5)_4]^-$ to iminium cation afford an amine-borane adduct. Under heating condition, the amine-borane adduct would dissociate to afford the catalyst, $B(C_6F_5)_3$ concomitant with the release of the amine. $B(C_6F_5)_3$ has also been utilized in numerous catalytic applications such as catalytic transfer

hydrogenation of alkenes, hydrosilylation of carboxylic acids to acetals, deoxygenation of carbonyls, carboxyls, alcohols, and also in hydrodefluorination reactions.[26]
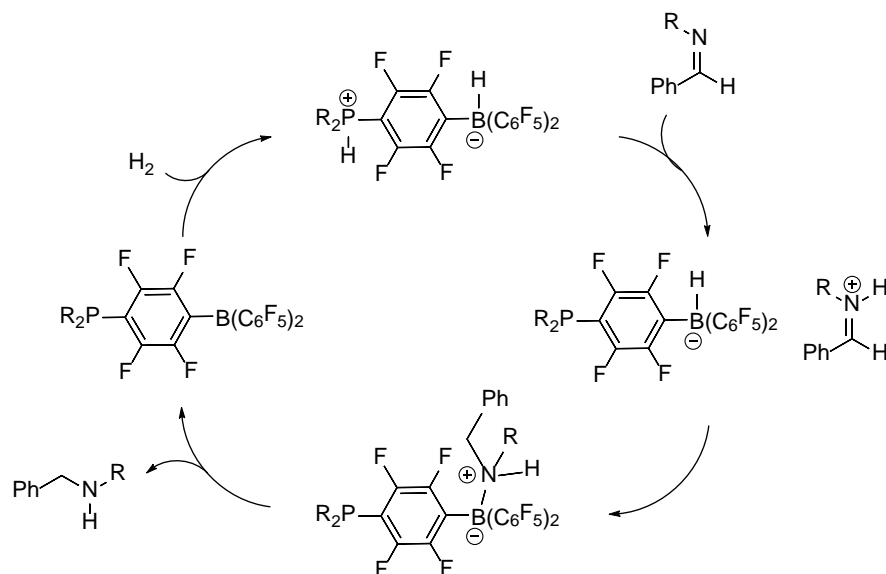
Scheme 1.2   Proposed mechanism for FLP-catalysed hydrogenation of imines.

$$\tag{6}$$
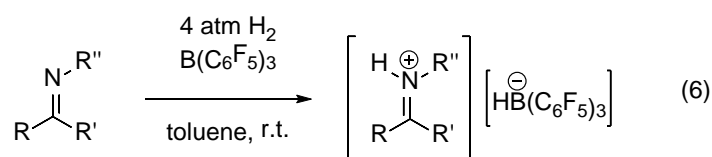
Prior to the use of $B(C_6F_5)_3$ in the hydrogenation of imines, seminal work by Piers et al. revealed that $B(C_6F_5)_3$ could catalyse the hydrosilylation of carbonyl compounds.[27] The proposed mechanism consists of an initial activation of the Si-H bond of the silane by $B(C_6F_5)_3$ (Scheme 1.3a) rather than the coordination of $B(C_6F_5)_3$ to the Lewis basic oxygen atom on the C=O moiety. [28] This is followed by the coordination of Lewis basic oxygen atom to the activated Lewis acidic Si moiety. Further studies by Oestreich et al. suggested an energetically favourable S_N2-type mechanism for the activation of carbonyl moiety via a penta-coordinated Si as the transition state (Scheme 1.3b).[29] Regeneration of $B(C_6F_5)_3$ occurred via hydride transfer, releasing the hydrosilylated product in the process (Scheme 1.3c). This mechanism, namely the Piers-Oestreich mechanism, was supported by theoretical studies.[30]
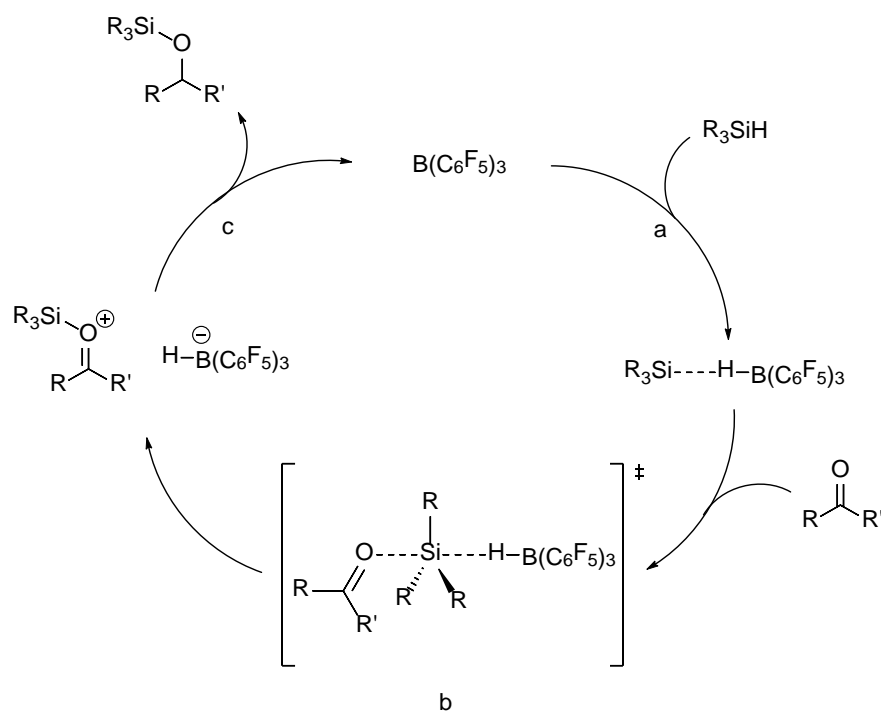
Scheme 1.3 Piers-Oestreich mechanism for $B(C_6F_5)_3$-catalysed hydrosilylation of carbonyl compounds.

Lately, the structure for the borane-silane adduct as proposed in Scheme 1.3 was confirmed by Piers and Tuononen et al. using a bulkier and a more Lewis acidic borane, 1,2,3-tris(pentafluorophenyl)-4,5,6,7-tetrafluoro-1-boraindene. [31] Cooling the borane-silane reaction mixture to -78 $^{\circ}$C drives the equilibrium towards the formation of the borane-silane adduct (eq 7). This provides another concrete evidence on the role of $B(C_6F_5)_3$ in the catalytic hydrosilylation of carbonyl compounds.

$$(7)$$
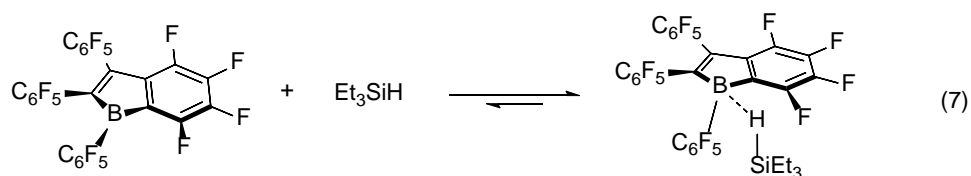
In recent times, highly electrophilic main group cations like borenium cations or phosphenium cations have been demonstrated to act as effective catalysts in several reactions. [32] Fundamentally, these positively charged Lewis acids contain low-lying LUMO which serves as an active site for catalytic reactions. For instance, borenium cation, a three-coordinated cationic

boron species, could catalyse reactions such as hydroboration and hydrogenation.[33] Curran and Vedejs et al. employed NHC–stabilised borane for hydroboration of alkenes at room temperature to obtain various isomeric alcohols after oxidation (eq 8).[34] The presence of catalytic amount HNTf$_2$ (5 – 30 mol%) is crucial for the formation of catalytically active borenium species in the reaction (eq 9).

$$
\text{(NHC)}-BH_3 \xrightarrow[\substack{3)\ NaOH/H_2O_2, \\ MeOH,\ 16h}]{\substack{1)\ Tf_2NH\ (5\ mol\ \%) \\ 2)\ (E)\text{-}3\text{-hexene}}} C_6H_{13}OH \qquad (8)
$$

$$
\text{(NHC)}-BH_3\ +\ Tf_2NH \xrightarrow{-H_2} \left[\text{(NHC)}-BH_2\right]^{\oplus}\ {}^{\ominus}NTf_2 \quad \text{or} \quad \left[\text{(NHC)}-BH_2\cdots H\cdots BH_2-\text{(NHC)}\right]^{\oplus}\ {}^{\ominus}NTf_2 \qquad (9)
$$
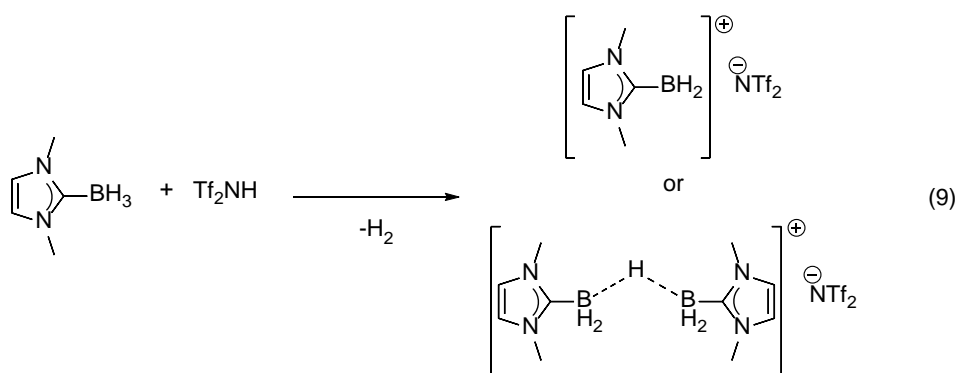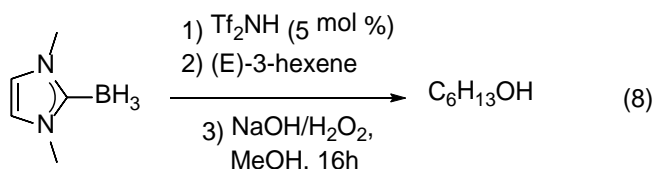
In 2012, Stephan et al. demonstrated the use of NHC-stabilised borenium cation, formed from the reaction of NHC and 9-BBN, for H$_2$ activation as well as the catalytic hydrogenation of imines (eq 10a).[35] Although a high pressure of H$_2$ (102 atm) is required, the reaction proceeds readily at room temperature using a relatively low catalytic loading (1 – 5 mol%). The proposed mechanistic cycle is similar to the mechanism proposed for the B(C$_6$F$_5$)$_3$-catalysed hydrogenation of imines. Crudden et al. reported an analogous borenium cation catalyst containing mesoionic carbene with triazole moiety (eq 10b).[36] The slightly milder hydrogenation conditions required (1 atm of H$_2$) can be attributed to the formation of a more hydridic B-H bond after H$_2$ activation, hence, hydride insertion into the iminium cation is deemed to be energetically more feasible.

$$(10a)$$

$$(10b)$$
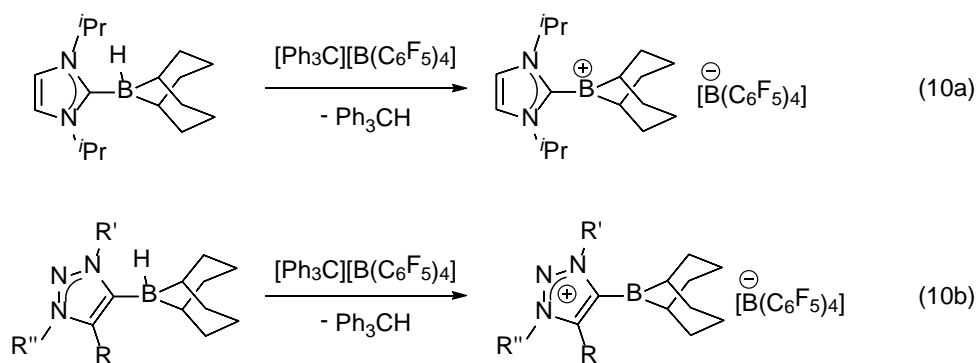
Another borenium type cation was synthesized by the same group, Crudden et al., from the reaction of a bulky base DABCO-B($C_6F_5)_3$ adduct and HBpin (eq 11).[37] Importantly, they were able to employ these borenium cations in catalytic hydroboration of imines. Unexpectedly, the borenium cation containing no hydridic counterion (eq 11b) has a higher catalytic activity than the borenium cation containing hydridic counterion (eq 11a). Thus, a mechanism involving B-H insertion from its counterion [HB($C_6F_5)_3$]$^-$ to the C=N bond of the imines can be excluded. A plausible mechanism involves the coordination of cationic boron moiety to the lone pair electrons on the N atom of the imine (Scheme 1.4a). Subsequent hydroboration of the activated C=N bond by HBpin/DABCO affords the hydroborated products and regenerates the catalyst (Scheme 1.4b).

$$(11a)$$

$$(11b)$$
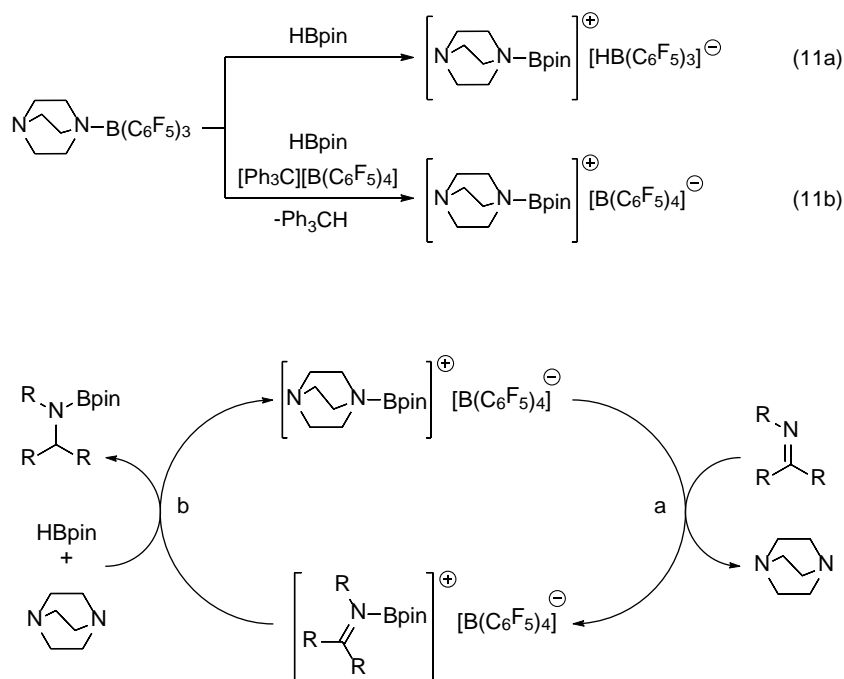
Scheme 1.4   Crudden's DABCO-Bpin cation-catalysed hydroboration of imines.

Phosphorus compounds are known to be Lewis bases, however, strong electron-withdrawing substituents can alter the electronic environment around the phosphorus centre to a great extent.[32, 38] Stephan et al. synthesized a highly Lewis acidic P(V) phosphenium cation, $[(C_6F_5)_3PF][B(C_6F_5)_4]$, containing four electron-withdrawing substituents ($-C_6F_5$) around the phosphorus centre (eq 12).[39]

$$P(C_6F_5)_3 \xrightarrow{XeF_2} \quad \begin{array}{c} F \\ | \\ C_6F_5-P\cdots C_6F_5 \\ | \quad \diagdown C_6F_5 \\ F \end{array} \qquad (12a)$$

$$\begin{array}{c} F \\ | \\ C_6F_5-P\cdots C_6F_5 \\ | \quad \diagdown C_6F_5 \\ F \end{array} \xrightarrow[- Et_3SiF]{[Et_3Si][B(C_6F_5)_4]} \quad \begin{array}{c} F \\ | \\ C_6F_5-\overset{\oplus}{P}\cdots C_6F_5 \\ \diagdown C_6F_5 \end{array} \quad \overset{\ominus}{B}(C_6F_5)_4 \qquad (12b)$$
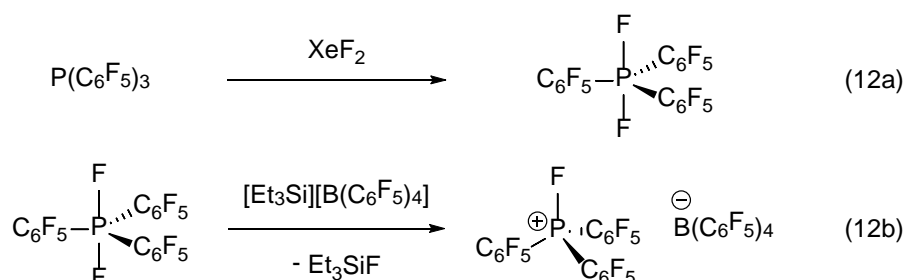
This phosphenium cation was shown to catalyse several reduction reactions such as hydrodefluorination of fluoroalkanes, hydrosilylation of alkenes, alkynes, ketones, imines and nitriles.[40] In addition, $[(C_6F_5)_3PF][B(C_6F_5)_4]$ is also active in the catalytic dehydrocoupling of amines, alcohols, thiols and carboxylic acids with silanes (Scheme 1.5).[41] Further work by the same group demonstrated that the phosphenium cation with no strong electron withdrawing substituents (eq 13) can act as an effective catalyst in those catalytic reactions as aforementioned.[42]
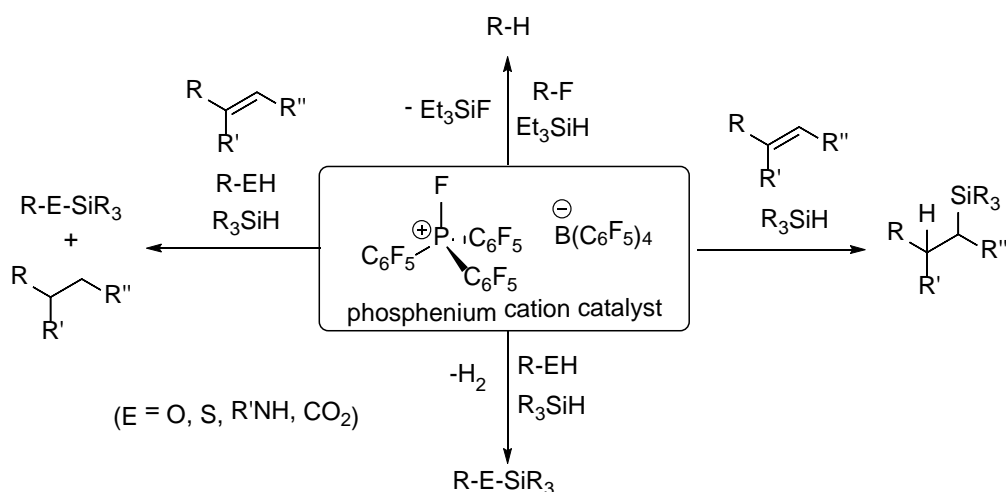
Scheme 1.5   Various reactions catalysed by $[P(C_6F_5)_3F][B(C_6F_5)_4]$.

$$[\text{structure}] \quad \xrightarrow{\text{XeF}_2} \quad [\text{structure}] \qquad (13a)$$

$$[\text{structure}] \quad \xrightarrow{[\text{Et}_3\text{Si}][\text{B(C}_6\text{F}_5)_4]} \quad [\text{structure}] \qquad (13b)$$
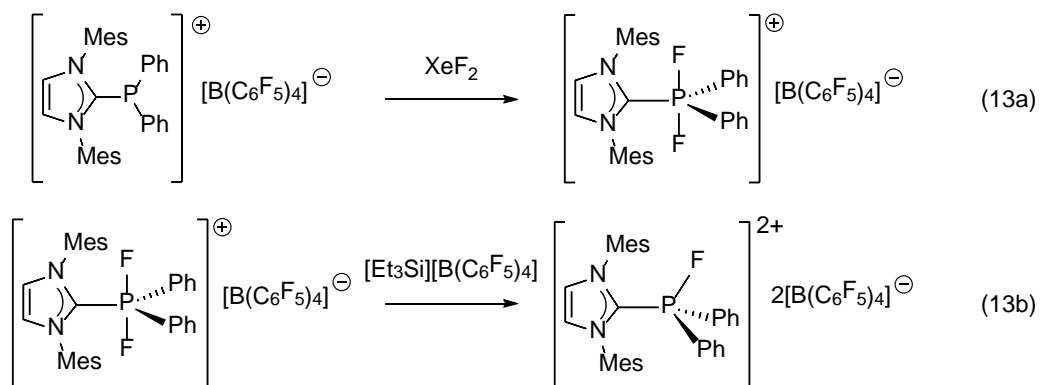
These studies demonstrated the versatility of non-metal main group compounds as catalysts for a variety of reactions. In some of these reactions, the catalytic activity is comparable to that of the transition metal complexes. Currently, main group catalysis are still in its early stage development, and further work is anticipated from viewpoints of i) better catalytic efficiency, ii) milder reaction conditions iii) new and unique mechanistic pathways.

1.3   Main Group Hydrides as Potential Catalyst in Reduction Reactions

Based on those background studies mentioned in section 1.2, an effective main group catalytic system for reduction reactions should consist of firstly, an electrophilic main group centre bearing accessible empty orbitals. Secondly, the presence of hydride source is also essential for such catalytic process.

With this in mind, we began to explore the possibility of using main group hydrides as a catalyst. Contrary to the well-established transition metal hydrides[43], main group hydrides are used primarily as reducing agents or in metathesis reactions but rarely as catalysts.[44] Therefore, to tune the stability and reactivity of main group hydrides, designing suitable ligands is crucial.

A key aspect in many catalysts lies in its ability to activate small molecules. In 2001, Roesky et al. reported the synthesis of the first three-coordinated Ge(II) hydride compound stabilized by β-diketiminato ligand (Ar = Dipp or Mes) (eq 14).[45] Analogous Sn(II) hydrides were also synthesized using modified procedures.[46] Interestingly, the monohydride Ge(II) compound was shown to activate various small molecules including CO_2 (eq 15a) and carbonyl compounds (eq 16) to form germylene formate and germylene alkoxide respectively.[47] Importantly, the addition of LiH_2NBH_3 to germylene formate compound resulted in the regeneration of the Ge(II) hydride concomitant with the formation of lithium formate (eq 15b), hence, suggesting that the Ge(II) hydride could potentially catalyse the reduction of CO_2.[48]

14

$$(16)$$
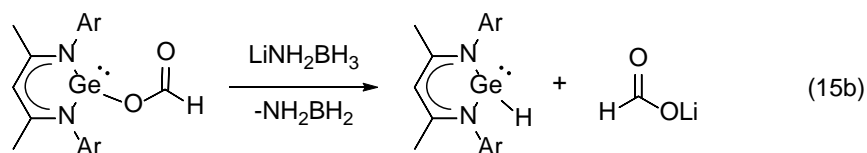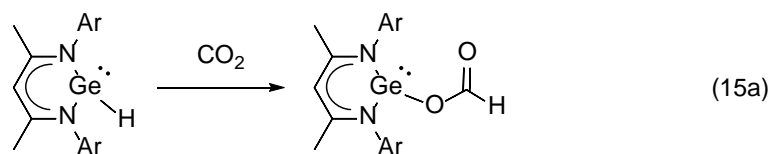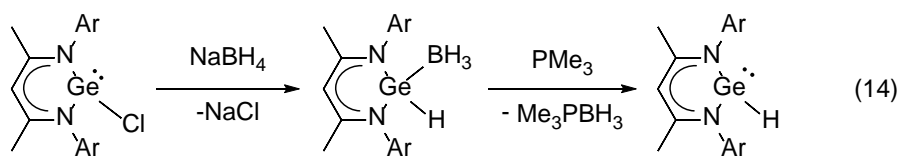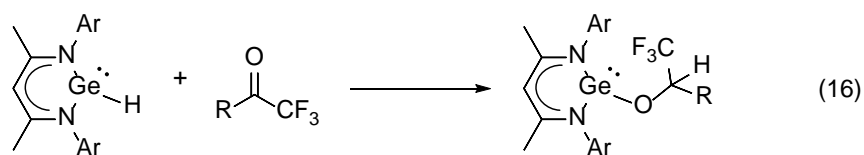
A comprehensive computational study on the application of the Ge(II) hydride as a catalyst in hydrosilylation and hydrogenation reactions was reported by Sakaki et al. in 2013.[49] The calculation results suggest that the charge transfer interaction from σ-bonding of the Ge-H bond to the π* antibonding of the C=O moiety plays a vital role in the initial hydride insertion step. Two pathways, namely hydrogenation and hydrosilylation of a Ge-alkoxide complex, via a metathesis-type transition state were investigated (Scheme 1.6). For the hydrogenation of the Ge-alkoxide complex, the calculated activation energy ($E_a^{\ddagger}$) and the Gibbs free energy of activation ($\Delta G^{\ddagger}$) were found to be relatively high (+46.6 and +51.3 kcal/mol respectively) as compared to those for the hydrosilylation process using $HSiF_3$ (+13.3 and +23.1 kcal/mol). The stabilization of the transition state for the hydrosilylation process can be attributed, firstly, to the charge transfer from lone pair of electrons on the O atom of the Ge-alkoxide complex to the vacant p-orbital of the Si centre and secondly, the charge transfer from the Si-H σ-bonding to the LUMO of the Ge complex, which is mainly localized on the unoccupied 5p orbital of the Ge centre.

In addition, the Gibbs free energy (ΔG^{o}) for hydrogenation of the Ge-alkoxide complex is endergonic (+16.2 kcal/mol) while the hydrosilylation process is exergonic (–3.7 kcal/mol). This can be explained by comparing the bond energies involve in these two processes. For hydrogenation of the Ge-alkoxide complex, the cleavage of the strong Ge-O bond (106.2 kcal/mol) and formation of a weaker Ge-H bond (69.2 kcal/mol) is disfavoured. On the other hand, the hydrosilylation process is driven by the formation of a much stronger F_3Si-O bond (135.2 kcal/mol), hence, offsetting the effect of forming a weaker Ge-H bond.
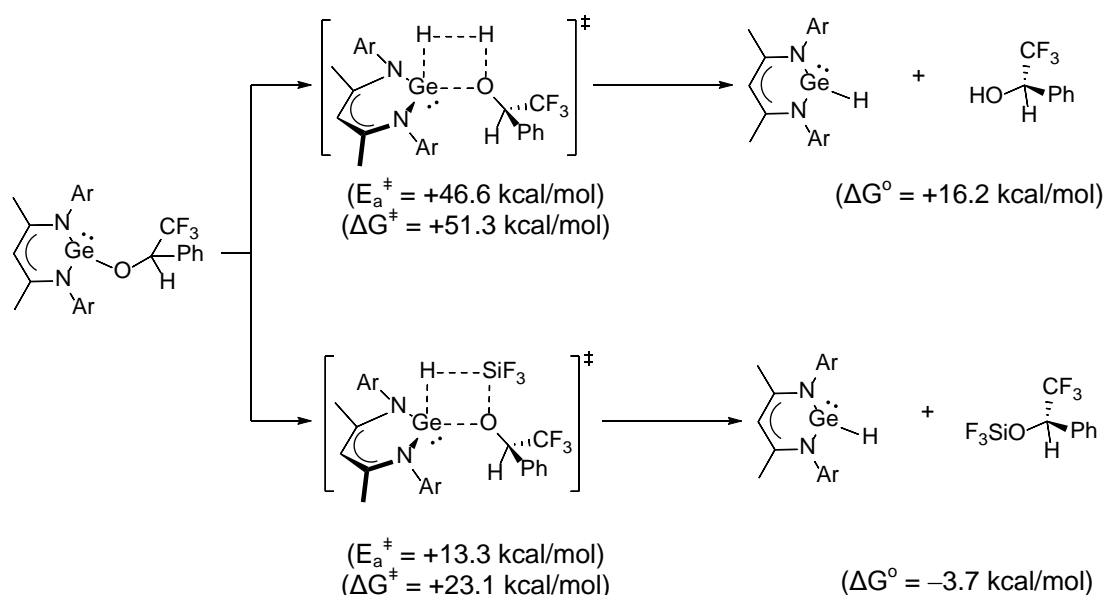
Scheme 1.6   Mechanistic pathway for Ge(II)-alkoxide hydrogenation and hydrosilylation with the calculated thermodynamic data by Sakaki et al. shown in parenthesis.

Based on these information, we seek to explore the catalytic efficiency of a metal-free main-group hydride in reduction reactions. N-heterocyclic phosphanes (NHPs) have gained prominence, mostly driven by the isolation of stable N-heterocyclic carbenes.[50] In particular, 1,3,2-diazaphospholenes are known for its elongated and polarised P-X bond as well as its electrophilic property of the phosphorus centre (Figure 1.3a).[51] The bond polarization and lengthening in the P-X bond can be attributed mostly to the hyperconjugative interaction between non-bonding electrons on N to the σ^*(P-X) orbital (Figure 1.3b-c). Both structural and computational studies demonstrated the planarity of the 5-membered ring, indicating a delocalised 6π-electron aromatic system.[50, 51] These hyperconjugative effects make its corresponding phosphenium (III) cation stable, which can be obtained by halide abstraction reaction of neutral NHPCl with TMSOTf (eq 17).
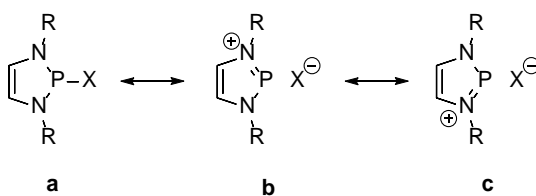
Figure 1.3 Resonance structures depicting the polarized P-X bond in 1,3,2-diazaphospholenes.
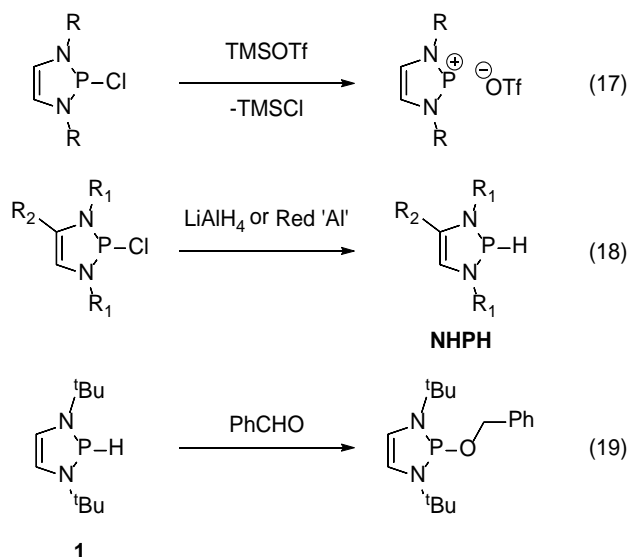
In 2000, Gudat et al. reported the first three-coordinated phosphorus species containing umpolung P-H polarity from the reduction of P-chloro-1,3,2-diazaphospholene to yield P-hydrido-1,3,2-diazaphospholene (NHPH) (eq 18).[52 a] Importantly, the isolated structures of **NHPH** (R_1 = Mes, R_2 = Cl and R_1 = Dipp, R_2 = H) show particularly long P-H bond distances (1.51 Å and 1.48 Å, respectively) which are in agreement with the canonical structures as depicted in Figure 1.3. The hydridic character in the polarized P-H bond of NHPH stands in contrast to the acidic character of the hydrogen in a typical secondary phosphines R_2PH. Indeed, the reaction of **1** and benzaldehyde resulted in a hydridic insertion of the P-H bond onto the C=O moiety of PhCHO to yield a NHP-alkoxide compound (eq 19).[52]

To understand the electronic structure of NHPH, we conducted a simple theoretical calculation for **1** at B3LYP/6-311G(d,p) level of theory. Similar to the Ge(II) hydride species, the HOMO of **1** consists of mainly the π-system over the NHP backbone with significant contribution

from the σ(P-H) bonding orbital (Figure 1.4a). The LUMO of **1** lies mainly on the empty p-orbital

of the P atom which indicates the electrophilic nature on the P centre (Figure 1.4b).

a)   b)
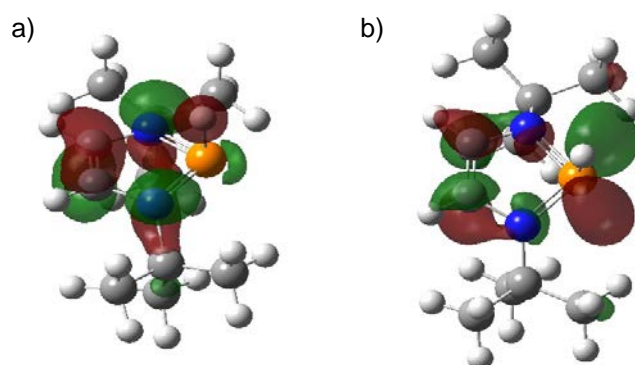
Figure 1.4   Molecular orbitals depicting a) HOMO and b) LUMO of **1**. (Isovalue = 0.05).

1.3.1   Objectives and aims of this project

Given the similarities in the frontier orbital description of **1** and the Ge(II) hydride species

as well as their reactivity with unsaturated bonds such as C=O, we hypothesized that similar

catalytic reactions such as hydrosilylation, hydroboration could be carried out using **1** as a metal-

free catalyst. Therefore, the main objective of this project is to examine the catalytic efficiency of

1,3,2-diazaphospholene **1** in various reductions reactions of unsaturated bonds such as N=N and

C=O. In addition, we would also investigate the catalytic cycle to understand its mechanistic

pathway which could play a crucial role in designing more robust and effective metal-free catalyst

in the future.

1.4   References

1.   Akazawa, T.; Incharoensakdi, A.; Takabe, T. in *Carbon Dioxide as a Source of Carbon: Chemical and Biochemical Uses*; Aresta, M., Forti, G., Eds.; NATO-ASI Series: Reidel, Dordrecht, 1987; pp 83–91.

2.   a) Tinberg, C. E.; Lippard, S. J. *Acc. Chem. Res*. **2011**, *44*, 280–288.; b) Merkx, M.; Kopp, D. A.; Sazinsky, M. H.; Blazyk, J. L.; Müller, J.; Lippard, S. J. *Angew. Chem. Int. Ed*. **2001**, *40*, 2782–2807; c) Wallar, B. J.; Lipscomb, J. D. *Chem. Rev.* **1996**, *96*, 2625–2658.

3.   *Activation of Small Molecules*; Tolman, W. B., Ed.; WILEY-VCH Verlag GmBH & Co. KGaA: Weinheim, Germany, 2006.

4 .   a) Hurd, A. J.; Kelley, R. L.; Eggert, R. G.; Lee, M. *MRS Bulletin* **2012**, *37*, 405–410; b) *Energy Critical Elements: Securing Materials for Emerging Technologies*; American Physical Society, Materials Research Society; American Physical Society: New York, 2011; c) *Critical Materials Strategy*; U.S Department of Energy, U.S. Government Printing Office: Washington, DC, 2010.

5.   Öhrlund, F.; *Future Metal Demand from Photovoltaic Cells and Wind Turbines – Investigating the Potential Risk of Disabling a Shift to Renewable Energy Systems*; Science and Technology Options Assessment (STOA); European Parliament: Brussels, 2011.

6.   a) Hounjet, L. J.; Stephan, D. W. *Org. Process Res. Dev.* **2014**, *18*, 385–391; b) Leitao, E. M.; Jurca, T.; Manners, I. *Nat. Chem.* **2013**, *5*, 817–829; c) Power, P. P. *Nature* **2010**, *463*, 171–177.

7.   Spikes, G. H.; Fettinger, J. C.; Power, P. P. *J. Am. Chem. Soc.* **2005**, *127*, 12232–12233.

8.   a) Power, P. P. *Chem. Commun.* **2003**, 2091–2101; b) Stender, M.; Philips, A. D.; Wright, R. J.; Power, P. P. *Angew. Chem. Int. Ed*. **2002**, *41*, 1785–1787; b) Allen, T. L.; Fink, W. H.; Power, P. P. *J. Chem. Soc., Dalton Trans*. **2000**, 407–412.

9. a) Peng, Y.; Brynda, M.; Ellis, B. D.; Fettinger, J. C.; Rivard, E.; Power, P. P. *Chem. Commun.* **2008**, 6042–6044; b) Pu, L.; Philips, A. D.; Richards, A. F.; Stender, M.; Simons, R. S.; Olmstead, M. M.; Power, P. P. *J. Am. Chem. Soc*. **2003**, *125*, 11626–11636.

10. a) Kubas, G. J. In *Metal Dihydrogen and σ-Bond Complexes: Structures, Theory, and Reactivity*; Fackler, J. P., Jr., Ed.; Kluwer Academic: New York, U.S.A., 2001; pp 99–135; b) Kubas, G. J.; Ryan, R. R.; Swanson, B. I.; Vergamini, P. J.; Wasserman, H. J. *J. Am. Chem. Soc*. **1984**, *106*, 452–454.

11. Welch, G. C.; San Juan, R. R.; Masuda, J. D.; Stephan, D. W. *Science* **2006**, *314*, 1124–1126.

12. Li, S.; Guo, Y. *Inorg. Chem.* **2008**, *47*, 6212–6219.

13. For recent reviews on FLP, see: a) Stephan, D. W. *Acc. Chem. Res*. **2015**, *48*, 306–316; b) Stephan, D. W. *J. Am. Chem. Soc.* **2015**, *137*, 10018–10032; c) Stephan, D. W.; Erker, G. *Angew. Chem. Int. Ed*. **2015**, *54*, 6400–6441; d) Stephan, D. W.; Erker, G. *Angew. Chem. Int. Ed*. **2010**, *49*, 46–76. For activation of H_2 by aromatic triphosphabenzene, see Longobardi, L. E.; Russell, C. A.; Green, M.; Townsend, N. S.; Wang, K.; Holmes, A. J.; Duckett, S. B.; McGrady, J. E.; Stephan, D. W. *J. Am. Chem. Soc*. **2014**, *136*, 13453–13457.

14. a) Mömming, C. M.; Kehr, G.; Wibbeling, B.; Fröhlich, R.; Erker, G. *Dalton Trans*. **2010**, *39*, 7556–7564; b) Mömming, C. M.; Otten, E. Kehr, G.; Fröhlich, R.; Grimme, S.; Stephan, D. W.; Erker, G. *Angew. Chem. Int. Ed.* **2009**, *48*, 6643–6646; c) Mömming, C. M.; Frömel, S.; Kehr, G.; Fröhlich, R.; Grimme, S.; Erker, G. *J. Am. Chem. Soc.* **2009**, *131*, 12280–12289.

15. Légaré, M.; Courtemanche, M.; Rochette, E.; Fontaine, F. *Science* **2015**, *349*, 513–516.

16. For recent reviews, see a) Flanigan, D. M.; Romanov-Michailidis, F.; White, N. A.; Rovis, T. *Chem. Rev*. **2015**, *115*, 9307–9387; b) Visbal, R.; Gimeno, M. C. *Chem. Soc. Rev.* **2014**, *43*, 3551–3574; c) Hopkinson, M. N.; Richter, C.; Schedler, M.; Glorius, F. *Nature* **2014**, *510*, 485–496.

17.   Lavallo, V.; Canac, Y.; Präsang, C.; Donnadieu, B.; Bertrand, G. *Angew. Chem. Int. Ed.* **2005**, *44*, 5705–5709.

18.   For review on CAACs-stabilized reactivity species, see: a) Soleilhavoup, M.; Bertrand, G. *Acc. Chem. Res.* **2015**, *48*, 256–266; b) Martin, D.; Soleilhavoup, M.; Bertrand, G. *Chem. Sci.* **2011**, *2*, 389–399.

19.   a) Frey, G. D.; Masuda, J. D.; Donnadieu, B.; Bertrand, G. *Angew. Chem. Int. Ed.* **2010**, *49*, 9444–9447. b) Frey, G. D.; Lavallo, V.; Donnadieu, B.; Schoeller, W. W.; Bertrand, G. *Science* **2007**, *316*, 439–441; c) Masuda, J. D.; Schoeller, W. W.; Donnadieu, B.; Bertrand, G. *Angew. Chem. Int. Ed.* **2007**, *46*, 7052–7055; d) Frey, G. D.; Masuda, J. D.; Donnadieu, B.; Bertrand, G. *Angew. Chem. Int. Ed.* **2010**, *49*, 9444– 9447; e) Lavallo, V.; Canac, Y.; Donnadieu, B.; Schoeller, W. W.; Bertrand, G. *Angew. Chem. Int. Ed.* **2006**, *45*, 3488–3491.

20.   *Modern Reduction Methods*; Andersson, P. G.; Munslow, I. J., Eds.; WILEY-VCH Verlag GmBH & Co. KGaA: Weinheim, Germany, 2008.

21.   For selected reviews, see: a) Chong, C. C.; Kinjo, R. *ACS Catalysis* **2015**, *5*, 3238–3259; b) Foubel, F.; Yus, M. *Chem. Rec.* **2015**, *15*, 907–924; c) Yoshimaru, M.; Tanaka, S.; Kitamura, M. *Tetrahedron Lett.* **2014**, *55*, 3635–3640; d) Troegel, D.; Stohrer, J. *Coord. Chem. Rev.* **2011**, *255*, 1440–1459; e) Díez-González, S.; Nolan, S. P. *Org. Prep. Proced. Int.* **2007**, *39*, 523–559; f) Crudden, C. M.; Edwards, D. *Eur. J. Org. Chem.* **2003**, 4695–4712; g) Blaser, H.; Malan, C.; Pugin, B.; Spindler, F.; Steiner, H.; Studer, M. *Adv. Synth. Catal.* **2003**, *345*, 103–151; h) Noyori, R.; *Angew. Chem. Int. Ed.* **2002**, *41*, 2008– 2022; i) Noyori, R.; Ohkuma, T.; *Angew. Chem. Int. Ed.* **2001**, *40*, 40–73.

22.   Revunova, K.; Nikonov, G. I. *Dalton Trans.* **2015**, *44*, 840–866.

23.   a) MacMillan, D. W. C. *Nature* **2008**, *455*, 304–308; b) Ouellet, S. G.; Walji, A. M.; MacMillan, D. W. C. *Acc. Chem. Res.* **2007**, *40*, 1327–1339; c) Haenel, M. W.; Narangerel, J.; Richter, U. B.; Rufińska, A. *Angew. Chem. Int. Ed.* **2006**, *45*, 1061–1066; d) Lelais, G. MacMillan, D. W. C. *Aldrichchim. Acta.* **2006**, *39*, 79–87; e) Walling, C.; Bollyky, L. *J. Am. Chem. Soc.* **1964**, *86*, 3750–3752; f) Walling, C.; Bollyky, L. *J. Am.*

Chem. Soc. **1961**, *83*, 2968–2969; g) DeWitt, E. J.; Ramp, F. L.; Trapasso, L. E. *J. Am. Chem. Soc.* **1961**, *83*, 4672–4672.

24.   Chase, P. A.; Welch, G. C.; Jurca, T.; Stephan, D. W. *Angew. Chem. Int. Ed.* **2007**, *46*, 8050–8053.

25.   a) Chase, P. A.; Jurca, T.; Stephan, D. W. *Chem. Commun.* **2008**, 1701–1703; b) Chen, D.; Klankermayer, J. *Chem. Commun.* **2008**, 2130–2131.

26.   For an overview of B(C$_6$F$_5$)$_3$-catalysed reactions, see: a) Oestreich, M.; Hermeket, J.; Mohr, J. *Chem. Soc. Rev.* **2015**, *44*, 2202–2220; b) Erker, G. *Dalton Trans.* **2005**, 1883–1890; c) Piers, W. E. *Adv. Organomet. Chem.* **2004**, *52*, 1–76; d) Ishihara, K.; Yamamoto, H.; *Eur. J. Org. Chem.* **1999**, 527–538; e) Piers, W. E.; Chivers, T. *Chem. Soc. Rev.* **1997**, *26*, 345–354.

27.   Parks, D. J.; Piers, W. E. *J. Am. Chem. Soc.* **1996**, *118*, 9440–9441.

28.   Parks, D. J.; Blackwell, J. M.; Piers, W. E. *J. Org. Chem.* **2000**, *65*, 3090–3098.

29.   Rendler, S.; Oestreich, M. *Angew. Chem. Int. Ed.* **2008**, *47*, 5997–6000.

30.   Sakata, K.; Fujimoto, H. *J. Org. Chem.* **2013**, *78*, 12505–12512.

31.   Houghton, A. Y.; Hurmalainen, J.; Mansikkamäki, Piers, W. E.; Tuononen, H. M. *Nat. Chem.* **2014**, *6*, 983–988.

32.   For overview, see: a) Caputo, C. B.; Stephan, D. W in *Structure and Bonding*; Mingos, M. P., Ed.; Springer International: Switzerland, 2015; doi: 10.1007/430_2015_177; b) Weicker, S. A.; Stephan, D. W. *Bull. Chem. Soc. Jpn.* **2015**, *88*, 1003–1016.

33.   For overview of borenium chemistry, see: De Vries, T. S.; Prokofjevs, A.; Vedejs, E. *Chem. Rev.* **2012**, *112*, 4246–4282. For hydroboration using borenium cations, see: a) Nerkar, S.; Curran, D. P. *Org. Lett.* **2015**, *17*, 3394–3397; b) Watanabe, T.; Curran, D. P.; Taniguchi, T. *Org. Lett.* **2015**, *17*, 3450–3453; c) Taniguchi, T.; Curran, D. P. *Angew. Chem. Int. Ed.* **2014**, *53*, 13150–13154; d) Pan, X.; Boussonnière, A.; Curran, D. P. *J. Am. Chem. Soc.* **2013**, *135*, 14433–14437; e) Boussonnière, A.; Pan, X.; Geib, S. J.; Curran, D. P. *Organometallics* **2013**, *32*, 7445–7450.

34. Prokofjevs, A.; Boussonnière, A.; Li, L.; Bonin, H.; Lacôte, E.; Curran, D. P.; Vedejs, E. *J. Am. Chem. Soc*. **2012**, *134*, 12281–12288.

35. a) Farrelll, J. M.; Posaratnanathan, R. T.; Stephan, D. W. *Chem. Sci*. **2015**, *6*, 2010–2015; b) Farrell, J. M.; Hatnean, J. A.; Stephan, D. W. *J. Am. Chem. Soc*. **2012**, *134*, 15728–15731.

36. Eisenberger, P.; Bestvater, B. P.; Keske, E. C.; Crudden, C. M. *Angew. Chem. Int. Ed.* **2015**, *54*, 2467–2471.

37. Eisenberger, P.; Bailey, A. M.; Crudden, C. M. *J. Am. Chem. Soc*. **2012**, *134*, 17384–17387.

38. Bayne, J. M.; Stephan, D. W. *Chem. Soc. Rev*. **2016**, *45*, 765–774.

39. Caputo, C. B.; Hounjet, L. J.; Dobrovetsky, R.; Stephan, D. W. *Science* **2013**, *341*, 1374–1377.

40. a) Pérez, M.; Mahdi, T.; Hounjet, L. J.; Stephan, D. W. *Chem. Commun*. **2015**, *51*, 11301–11304; b) Mehta, M.; Holthausen, M. H.; Mallov, I.; Pérez, M.; Qu, Z.; Grimme, S.; Stephan, D. W. *Angew. Chem. Int. Ed.* **2015**, *54*, 8250–8254; c) Pérez, M.; Qu, Z.; Caputo, C. B.; Podgorny, V.; Hounjet, L. J.; Hansen, A.; Dobrovetsky, R.; Grimme, S.; Stephan, D. W. *Chem. Eur. J.* **2015**, *21*, 6491–6500; d) Pérez, M.; Hounjet, L. J.; Caputo, C. B.; Dobrovetsky, R.; Stephan, D. W. *J. Am. Chem.* **2013**, *135*, 18308–18310.

41. Pérez, M.; Caputo, C. B.; Dobrovetsky, R.; Stephan, D. W. *Proc. Nat. Acad. Sci.* **2014**, *111*, 10917–10921.

42. Holthausen, M. H.; Mehta, M.; Stephan, D. W. *Angew. Chem. Int. Ed*. **2014**, *53*, 6538–6541.

43. For review on transition metal hydrides, see: a) Andrews, L. *Chem. Soc. Rev*. **2004**, *33*, 123–132; b) Hoskin, A. J.; Stephan, D. W. *Coord. Chem. Rev*. **2002**, *233–234*, 107–129; c) *Recent Advances in Hydride Chemistry*; Peruzzini, M.;Poli, R. Eds.; Elsevier Science B. V.: Amsterdam, Netherlands, 2001; d) Murahashi, S.; Takaya, H. *Acc. Chem. Res*. **2000**, *33*, 225–233; e) Sabo-Etienne, S.; Chaudret, B. *Chem. Rev*. **1998**, *98*, 2077–2092.

44.   a) Heiden, Z. M.; Lathem, A. P. *Organometallics* **2015**, *34*, 1818–1827; b) Harder, S. *Chem. Commun.* **2012**, *48*, 11165–11177; c) Mandal, S. K.; Roesky, H. W. *Acc. Chem. Res*. **2012**, *45*, 298–307; d) Aldridge, S.; Downs, A. J. *Chem. Rev*. **2001**, *101*, 3305–3366.

45.   Ding, Y.; Hao, H.; Roesky, H. W.; Noltemeyer, M.; Schmidt, H. *Organometallics* **2001**, *20*, 4806–4811.

46.   Pineda, L. W.; Jancik, V.; Starke, K.; Oswald, R. B.; Roesky, H. W. *Angew. Chem. Int. Ed.* **2006**, *45*, 2602–2605.

47.   a) Jana, A.; Roesky, H. W.; Schulzke, C. *Dalton. Trans*. **2010**, *39*, 132–138; b) Jana, A.; Ghoshal, D.; Roesky, H. W.; Objartel, I.; Schwab, G.; Stalke, D. *J. Am. Chem. Soc.* **2009**, *131*, 1288–1293; c) Jana, A.; Roesky, H. W.; Schulzke, C.; Döring, A. *Angew. Chem. Int. Ed*. **2009**, *48*, 1106–1109.

48.   Jana, A.; Tavčar, G.; Roesky, H. W.; John, M. *Dalton Trans*. **2010**, *39*, 9487–9489.

49.   Takagi, N.; Sakaki, S. *J. Am. Chem. Soc*. **2013**, *135*, 8955–8965.

50.   a) Gudat, D. in *Comprehensive Inorganic Chemistry II*; Reedijk, J.; Poeppelmeier, K., Eds.; Elsevier: Oxford, U.K., 2013, pp 587–621; b) Gudat, D. in *Comprehensive Inorganic Chemistry II*; Reedijk, J.; Poeppelmeier, K., Eds.; Elsevier: Oxford, U.K., 2013, pp 587–621; c) Gudat, D. in *Topics in Heterocyclic Chemistry*; Bansal, R. K., Ed.; Springer: Berlin, Germany, 2010; pp 63–102.

51.   a) Gudat, D. *Dalton Trans.* **2016**, *45*, 5896–5907; b) Gudat, D. *Acc. Chem. Res*. **2010**, *43*, 1307–1316.

52.   a) Burck, S.; Gudat, D.; Nieger, M.; Du Mont, W. *J. Am. Chem. Soc.* **2006**, *128*, 3946–3955; b) Gudat, D.; Haghverdi, A.; Nieger, M. *Angew. Chem. Int. Ed*. **2000**, *39*, 3084–3086.

Chapter 2   1,3,2-Diazaphospholene-Catalysed Transfer Hydrogenation of N=N Bond with Ammonia Borane

2.1   Introduction

An addition of two hydrogen atoms to an unsaturated bond using a source other than dihydrogen (H_2), namely transfer hydrogenation, has seen considerable attention in recent years as an alternative and convenient methodology for the hydrogenation of unsaturated bonds in organic reactions.[1] One of the important sources of hydrogen atoms other than H_2 gas is ammonia-borane (**AB**: H_3NBH_3). **AB** is an air-stable and non-flammable solid that contains high gravimetric hydrogen density (19.6 wt%) which aligns with the U.S. Department of Energy (DoE) target of 9 wt % for hydrogen storage material practicability.[2] In the past decades, the utilisation of **AB** as a H_2 storage material as well as a potential source of H_2 has been subjected to extensive research. [3, 4, 5, 6]

For successful utilisation of **AB** as a hydrogen source, understanding its elementary hydrogen transfer step is important to establish efficient transfer hydrogenation systems. [7] Recently, Berke et al. performed several hydrogenation reactions on various unsaturated bonds including polarized alkenes, aldehydes, ketones, and imines using **AB**. [8] For the transfer hydrogenation reaction of imines, it was proposed that the reaction proceeded via a concerted six-membered transition state (Scheme 2.1a). An analogous mechanism has been reported for the Meerwein-Pondorf-Verley reaction which involves the reduction of ketones or aldehydes to corresponding alcohols using Al-alkoxide catalyst.[9] Likewise, Manner et al. also showed that the metal-free hydrogen transfer between $R_2N=BH_2$ and R_2NHBH_3 occurred via concerted double H-transfer transition state (Scheme 2.1b) as confirmed by both experimental studies and DFT calculations.[10]

It has to be noted that the double H-transfers reactions as aforementioned were observed for hydrogen acceptor with polarized π bonds such as C=N or B=N. On the contrary, the concerted pathway for hydrogen transfer between non-polarized molecules such as ethane and ethylene were found to involve high activation energy (+58.2 kcal/mol) according to theoretical

calculations.[11] The presence of polarized π bonds in hydrogen acceptors may provide lower activation barrier and therefore, facilitate hydrogen transfer in a concerted manner.

a) *Transfer hydrogenation of imines*
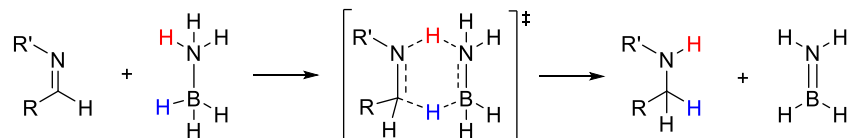
b) *H-transfer between amine-borane and iminoborane*
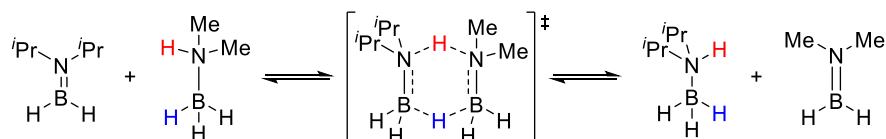
Scheme 2.1 Proposed concerted six-membered double H-transfers in a) transfer hydrogenation of imines; b) H-transfer between amine-borane and iminoborane.

There have been relatively few accounts on the simultaneous activation of N-H and B-H bonds in **AB** using main group compounds.[12] In 2012, Radosevich et al. reported that a catalytic amount of P(III) compound **I** promotes the transfer hydrogenation of azobenzene using excess **AB** (Scheme 2.2a).[13] The planar geometry of **1** resulted in the phosphorus centre to contain both donating and accepting orbitals, hence, accepting both protic and hydridic hydrogen from **AB** to form dihydridophosphorane **II** (Scheme 2.2a).

a)

b)
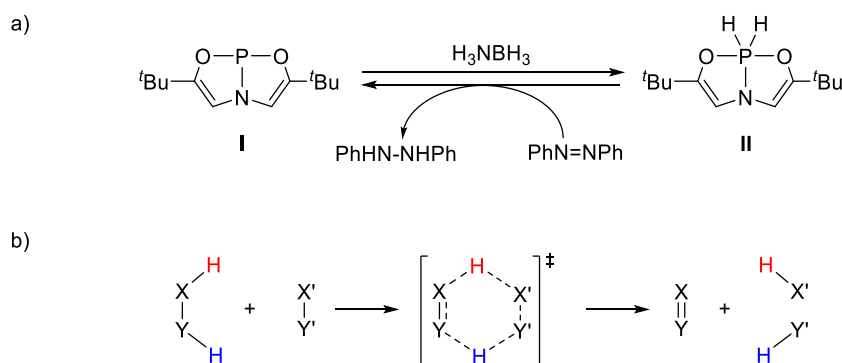
Scheme 2.2 a) **I** (P^{III}) / **II** (P^{IV}) redox catalyst for the transfer hydrogenation of azobenzene with **AB**; b) Transfer hydrogenolysis using donor HX-YH and saturated acceptor X'-Y'.

Subsequently, hydrogen transfer from **II** to azobenzene gave hydrobenzene and regenerate catalyst **I** in a proposed concerted pathway. This suggests that the phosphorus centre undergoes formally oxidative addition and reductive elimination [P(III) $\leftrightarrow$ P(V)], akin to the mechanism found in transition metal catalyst although there is a controversial argument on such mechanism. According to DFT calculations reported by Vanka et al. and Sakaki et al., the P(III) $\leftrightarrow$ P(V) mechanism involves a high activation barrier. Instead, pathways involving P-O cleavage and bond metathesis were found to entail lower activation energies.[14]

These studies prompted us to investigate whether a strongly polarized saturated bond, X'-Y' (where χX' < χY', χ = electronegativity) could activate **AB**. The negatively polarized Y' could accept a proton from the N-H bond of **AB** while the positively polarized X' could receive a hydride from the B-H bond of **AB**, to achieve a unique hydrogenolysis (Scheme 2.2b). In this chapter, we demonstrate a non-metal catalytic transfer hydrogenation of a N=N bond which involves a concerted double hydrogen transfer between **AB** and 1,3,2-diazaphospholene-derived intermediate in the hydrogenolysis process.

2.2 Results and Discussions

2.2.1 *Stoichiometric reaction between 1, azobenzene and ammonia-borane*

As mentioned in the previous chapter, N-heterocyclic phosphane **1** contains a substantial P-H bond polarity and it bears an accessible empty p-orbital on the P centre. Despite the extensive studies on **1**, the reaction of **1** with a N=N bond has not been reported. Treatment of **1** with azobenzene at room temperature resulted in a P-H insertion into the N=N bond to form N-heterocyclic phosphinohydrazine **2** (Scheme 2.3a). Quantitative formation of **2** was confirmed by ^{31}P NMR spectroscopy, which showed a singlet at δ = 90.0 ppm in CD$_3$CN. For comparative studies, we also synthesized **1'**, featuring a saturated C-C backbone in the five-membered ring, and subjected to a similar reaction. Expectedly, a clean formation of **2'** was observed with a singlet at δ = 101.9 ppm in the ^{31}P NMR spectrum. A single crystal structure of **2'** was obtained from a benzene solution and subjected to X-ray diffraction analysis (Figure 2.1). The P centre displays a distorted trigonal pyramidal geometry and the P1-N1, P1-N2 and P1-N3 bond distances are 1.6774(15) Å, 1.7229(15) Å and 1.7721(15) Å respectively.

Subsequently, the addition of 4 equivalents of **AB** to **2 / 2'** at 50 ^{o}C in CD$_3$CN afforded diphenylhydrazine **3** concomitant with formation of **1 / 1'** as confirmed by ^{31}P NMR spectroscopy (Scheme 2.3b). Importantly, the hydrogenolysis step occurred selectively at the exocyclic P-N bond due to the stability of the endocyclic P-N bonds, which can be attributed to both thermodynamic and kinetic effects. The ^{31}P NMR spectrum showed a full conversion of **2** into **1** after heating at 50 ^{o}C for 1.25 h (Appendix A, Figure A2-1a). On the other hand, when heating **2'** for long hours, further cleavage of endocyclic P-N bonds occurred competitively, and generation of PH$_3$ was observed at δ = –243.8 ppm (q, ^{P-H}J = 191.2 Hz) in the ^{31}P NMR spectrum (Appendix A, Figure A2-1b).

Significantly, when H$_3$NBD$_3$ was utilised for the reaction with **2**, only the 2-[D]-1,3,2-diazaphospholene **1**[D] was generated, hence, showing regiospecificity in the H-transfer reaction (Appendix A, Figure A2-2).
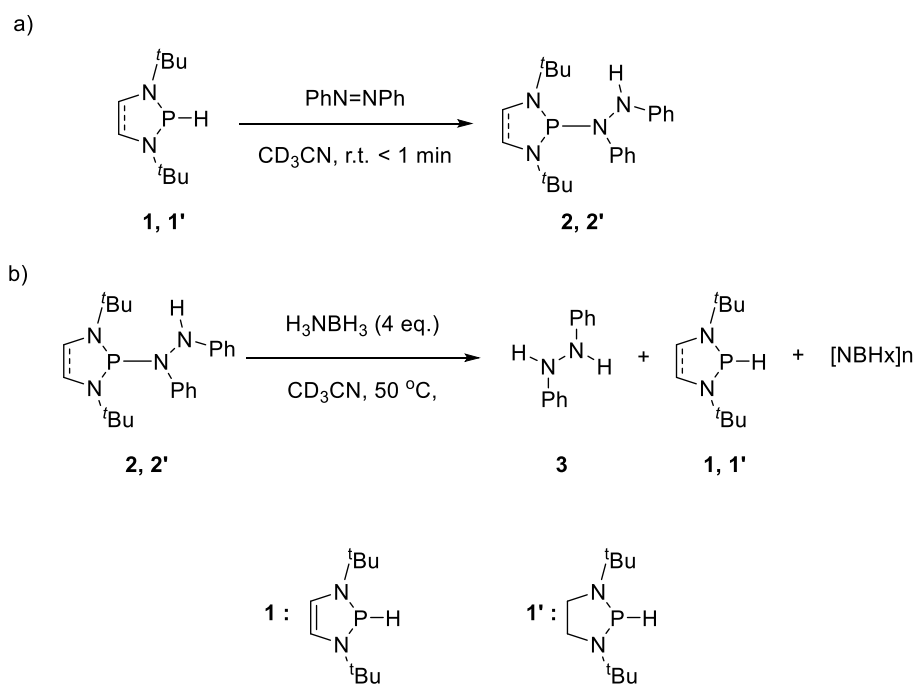
Scheme 2.3   a) Synthesis of N-heterocyclic phosphinohydrazine **2, 2'**; b) Reaction of **2, 2'** with **AB** at 50 °C.
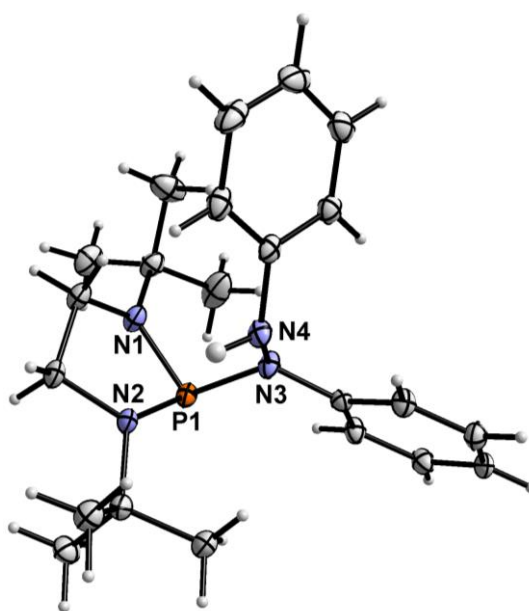
Figure 2.1   ORTEP drawing of **2'** with thermal ellipsoids set at 30% probability level. Selected bond lengths [Å] and angles [°]: P1-N3 1.7721(15), P1-N1 1.6774(15), P1-N2 1.7229(15), N3-N4 1.4246(19), N1-P1-N2 91.12(7), N1-P1-N3, 106.87(7), N2-P1-N3 98.26(7).

2.2.2 *Catalytic Transfer Hydrogenation of Azobenzene using 1*

We applied these stoichiometric reactions as described in the last section in a catalytic process. A control experiment in the absence of the catalyst was performed and an insignificant amount of diphenylhydrazine was produced (Table 2.1, entry 1). We also attempted the use of dibutyl- and diphenylphosphines for the reaction; however, no H-transfer occurred even with stoichiometric amount of phosphines (Table 2.1, entries 2–3). In contrast, 5 mol% of **1** promoted the transfer hydrogenation reaction with an observable NMR yield of 94% (Table 2.1, entry 4). When using **1'** as the catalyst, only a small amount of diphenyhydrazine was detected (Table 2.1, entry 5) due to decomposition as previously mentioned. Solvent screening showed that both dichloromethane and acetonitrile are appropriate for this reaction (Table 2.1, entries 6–10). In addition, we confirmed that the full conversion of azobenzene to **3** took only 4 h in deuterated acetonitrile (Table 2.1, entry 11). Decreasing the catalyst loading to 2 mol%, resulted in a low yield of diphenylhydrazine (36%) after 4 h (Table 2.1, entry 12). In addition, 1 equivalent of **AB** resulted in a slightly lower yield of 77% after 12 h (Table 2.1, entry 13). Notably, the catalytic transfer hydrogenation could also take place at room temperature, however, the reaction is much slower as diphenylhydrazine **3** was obtained in 77% yield only after 72 h (entry 14, Table 2.1). Importantly, during the reaction, only a single peak corresponding to **2** was observed in the ^{31}P NMR spectroscopy, hence implying that **2** is the resting state of the catalyst. Therefore, the oxidation state of the phosphorus centre remains unchanged throughout the catalytic cycle.

Table 2.1   Optimisation for the catalytic transfer hydrogenation of azobenzene.[a]

cat. R_2PH

$Ph{\sim}_N{\nwarrow}^N{\diagdown}_{Ph}$ $\xrightarrow[\text{Solvent}]{H_3NBH_3}$ $Ph{\sim}_N{\diagup}^{N}{\diagdown}_{Ph}$ (with H above and below N)
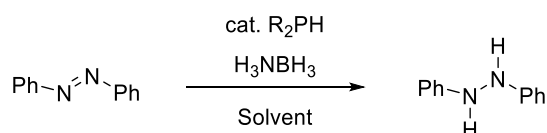
Entry	cat. (mol%)	AB (eq)	Solvent	T [ºC]	Time (h)	Yield (%)[b]
1	None (0 mol%)	4	$CDCl_3$	80	48	<5
2	Ph_2PH (100 mol%)	4	$CDCl_3$	50	24	0
3	$^tBu_2PH$ (100 mol%)	4	$CDCl_3$	50	24	0
4	**1** (5 mol%)	4	$CDCl_3$	50	24	94
5	**1'** (5 mol%)	4	$CDCl_3$	50	24	18
6	**1** (5 mol%)	4	$CDCl_3$	50	12	67
7	**1** (5 mol%)	4	d_8-THF	50	12	6
8	**1** (5 mol%)	4	C_6D_6	50	12	21
9	**1** (5 mol%)	4	CD_2Cl_2	50	12	**>99**
10	**1 (5 mol%)**	**4**	**CD_3CN**	**50**	**12**	**>99**
11	**1** (5 mol%)	4	CD_3CN	50	4	**98**
12	**1** (2 mol%)	4	CD_3CN	50	4	36
13	**1** (5 mol%)	1	CD_3CN	50	12	77
14	**1** (5 mol%)	4	CD_3CN	r.t.	72	79

(a)   Reaction conditions: azobenzene (0.30 mmol), **AB** (1.20 mmol), solvent (1.0 ml). Catalyst loading relative to azobenzene.

(b)   Yields are determined by ^1H NMR using 1,3,5-trimethoxybenzene as an internal standard.

After optimizing the reaction conditions, we examined the catalytic reactions with various azo–compounds (Figure 2.2). Azoarenes containing electron-withdrawing groups including chloro, fluoro, and trifluoromethoxy group afforded corresponding hydrazine (**3a**-**d**) in good to excellent yields. Alkyl-substituted azoareans were also well tolerated (**3e**-**f**); however, strong electron-donating substituents including 4-amino or 4-methoxy phenyl groups, resulted in the formation of corresponding anilines derivatives (**3g-h**). Unsymmetrical hydrazine derivatives were also obtained in excellent yields (**3i-l**).

31
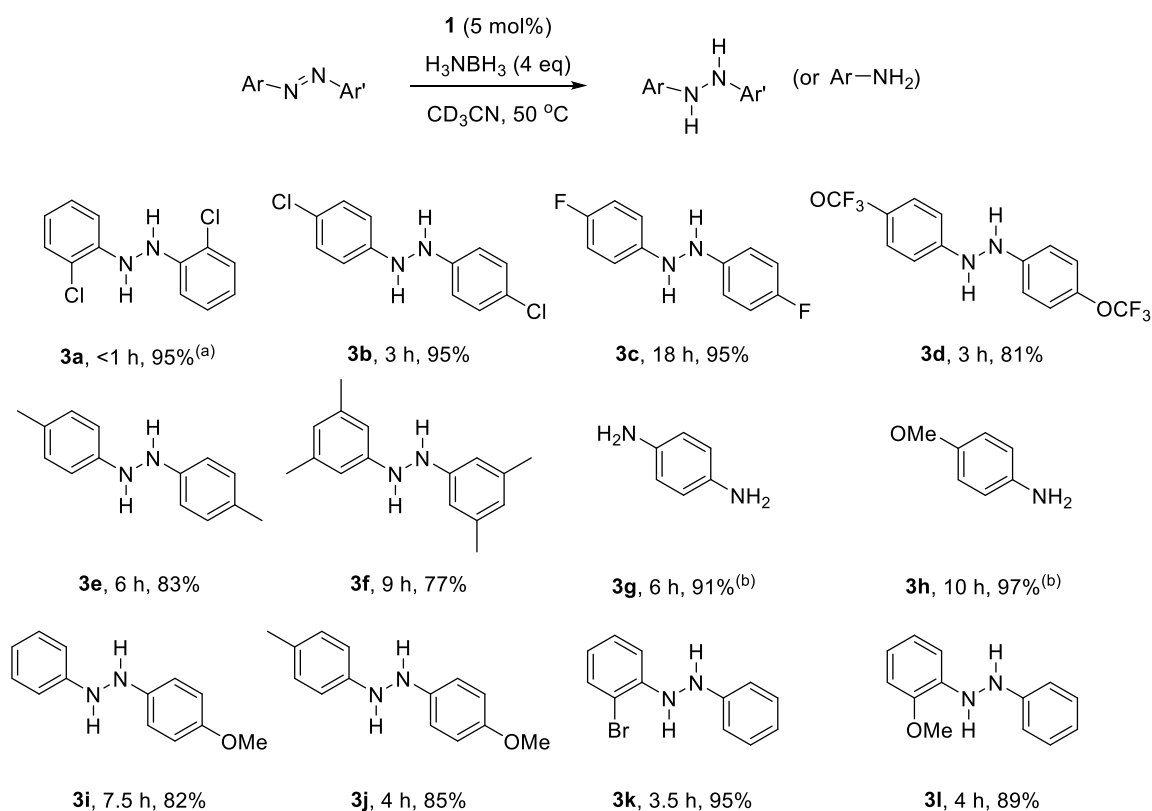
Figure 2.2   NMR Yields and reaction times for the transfer hydrogenation of azoarenes using **AB** and 5 mol% **1**. (a) Reaction conducted at r.t.; (b) Corresponding aniline derivatives observed instead of its hydrazine derivatives.

2.2.3   *Kinetic Studies and Mechanism Elucidation*

To gain further insights into the reaction mechanism, we conducted several kinetic studies theoretical calculations. Firstly, a first-order plot of ln[azobenzene] against time at various temperatures (40 $^\circ$C – 70 $^\circ$C) (Appendix B, Figure B2-1) allowed us to determine an Eyring Plot (Appendix B, Table B2-1, Figure B2-2) from which we were able to obtain free energy ($\Delta G^\ddagger$), enthalpy change ($\Delta H^\ddagger$) and entropy change ($\Delta S^\ddagger$) of activation using the Eyring Equation (Appendix B, eq B1).

DFT calculations for the catalytic cycle were conducted using M05-2X (SCRF)/6-311G(d,p) level of theory[15] (See Appendix C, Figure C2-1 for the energy profile for the initial step). For the second step, a concerted double hydrogen transfer via a six-membered cyclic transition state (TS4) was obtained as a plausible energetically favourable pathway (Figure 2.3). The six-membered transition state involved the hydrogen bonding between the N atom from **2** and

the N-H from **AB** as well as the P atom from **2** and the B-H from **AB**. This is in line with the polarized atomic charge distribution for the exocyclic P-N bond (P: +1.35, N: –0.62) as obtained from the natural population analysis (Figure 2.4).[16] Furthermore, the bonding interactions among the N, P, H, B atoms were confirmed by the bond lengths of the optimized structures and the Wiberg bond index (WBI) values obtained based on the NBO analysis (Table 2.2). The experimentally determined activation parameters ($\Delta H^{\ddagger}$= 21.8 ± 2.2 kcal/mol, $\Delta G^{\ddagger}_{(298)}$ = 25.2 ± 4.2 kcal/mol, $\Delta S^{\ddagger}$ = –11.6 ± 6.8 e.u) agree relatively well with the calculated results ($\Delta H^{\ddagger}$= 20.1 kcal/mol, $\Delta G^{\ddagger}_{(298)}$ = 23.3 kcal/mol, $\Delta S^{\ddagger}$ = –10.9 e.u). We also examined a plausible stepwise hydrogen transfer mechanism (see Appendix C, Figure C2-2), however, neither proton nor hydridic hydrogen transfer provided a stable transition state, hence, implying that such mechanism is unlikely.

We also further investigated the catalytic reaction using deuterated **AB** (D_3NBH_3, H_3NBD_3, and D_3NBD_3) in order to assess the deuterium kinetic isotope effects (DKIEs). 5 mol% of **1**, azobenzene and excess deuterated ammonia-borane were dissolved in CD_3CN and heated at 50 °C in a sealed NMR tube. The reaction was monitored by NMR spectroscopy at 5 minutes interval. The DKIE values were determined based on rate constants obtained from the kinetic conversion chart (Appendix B, Figure B2-3). Notably, we observed normal DKIEs of 1.44 and 3.05 for the reactions of azobenzene with H_3NBD_3 and D_3NBH_3 respectively. The double DKIE reaction with D_3NBD_3 was found to have the largest DKIE of 4.67, hence, suggesting that both B-H and N-H transfers are involved in the rate-determining step. Theoretical DKIE values, computed based on the zero-point energy (ZPE) of various optimized structures and deuterated **AB**s (Appendix C, Table C2-1), agree reasonably with experimental data, hence, supporting the proposed concerted double hydrogen transfer mechanism involving a six-membered transition state. The full catalytic cycle for transfer hydrogenation can therefore be described as shown in Scheme 2.4.

a)

RC2: **2** + **AB**

Pro: **1** + Ph$_2$N$_2$H$_2$ + H$_2$N=BH$_2$
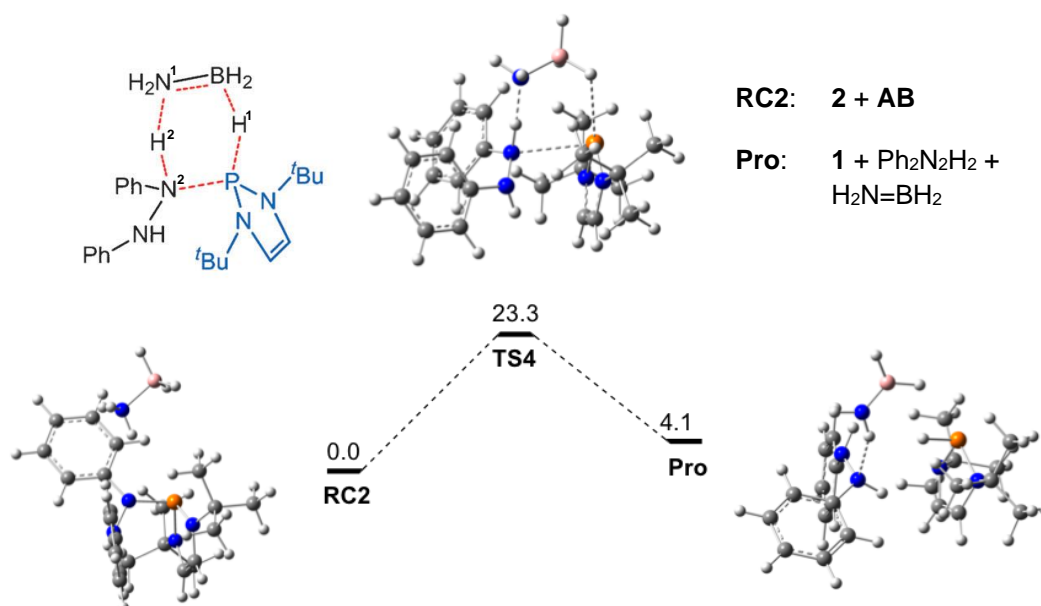
Figure 2.3   DFT-calculated free energy (kcal/mol) for mechanism between **2** and **AB**. The ΔG in CH$_3$CN at 298 K were obtained from M05-2X/6-311G(d,p) gas–phase harmonic frequency and the energy in CH$_3$CN. Atom sphere colours: C = grey; N = blue, P = orange; H = white; B = pink.

Table 2.2   NBO analysis for the second step from **RC2** (**2** + **AB**) to **Pro** (**1** + Ph$_2$N$_2$H$_2$ + H$_2$N=BH$_2$) as determined at the B3LYP/6-311+G(d,p) level of theory.

	RC2	TS4	Pro
N^2-P distance (Å)	1.79037	2.83166	4.09430
WBI	0.6660	0.0889	0.0013
P-H^1 distance (Å)	4.45636	2.80558	1.43757
WBI	0.0005	0.0206	0.9059
B-H^1 distance (Å)	1.21067	1.23503	3.18104
WBI	0.9797	0.9350	0.0005
N^1-B distance (Å)	1.65234	1.58594	1.38769
WBI	0.6422	0.7758	1.2841
N^1-H^2 distance (Å)	1.01467	1.66093	2.90335
WBI	0.8193	0.1731	0.0013
N^2-H^2 distance (Å)	3.01359	1.08476	1.00852
WBI	0.0016	0.5853	0.8171
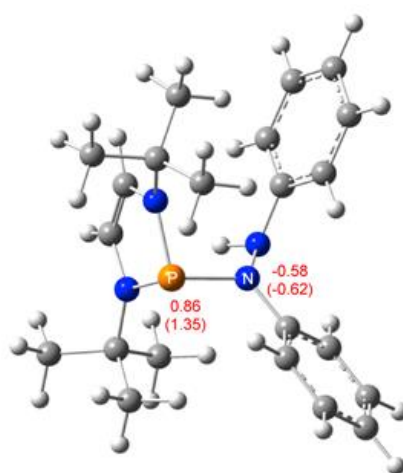
Figure 2.4 Key atomic charges of **2** calculated using Mulliken (out of parentheses) and natural (in parentheses) population analyses at the M05-2X(SCRF)/6-311G(d,p)//M05-2X/6-311G(d,p) level. Atom sphere colours: C = grey; N = blue, P = orange; H = white; B = pink.
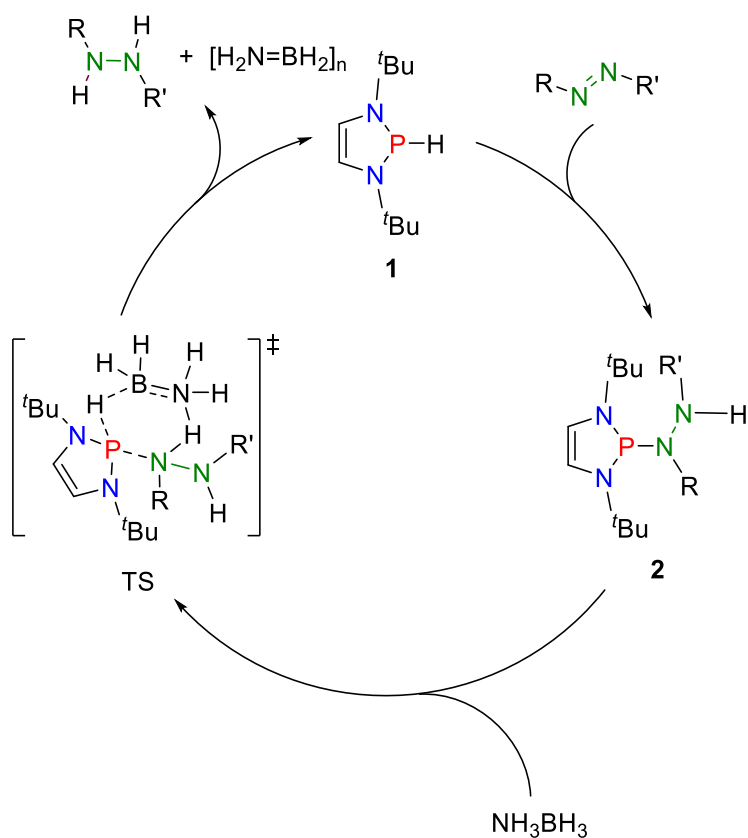
Scheme 2.4 Full catalytic cycle for the transfer hydrogenation of azo-compounds catalysed by **1**.

2.3 Conclusion

In conclusion, we have demonstrated that 1,3,2-diazaphospholene **1** could catalyse the transfer hydrogenation of N=N bond using ammonia-borane. Importantly, we have shown that the catalytic mechanism involves a unique hydrogenolysis step featuring a polarized saturated acceptor in compound **2**. The P-N bond in compound **2** is polarized in such a way that the P(δ+) would accept hydride from B-H while N(δ-) would accept a proton from N-H to achieve a six-membered ring transition state (TS). This was further evident from both kinetic and DFT studies which suggest a favourable concerted mechanism for the second step of the catalytic cycle involving **2** and ammonia-borane. We also investigated the deuterated kinetic isotopic effects (DKIE) for the catalytic reaction using various deuterated ammonia-boranes which show normal KIEs, thus, indicating that the cleavage of N-H and B-H bonds occur in the rate determining step.

2.4   Experimental Section

2.4.1   *Synthesis, physical and spectroscopic data for all new compounds*

General considerations: All reactions were performed under an atmosphere of argon by using standard Schlenk or dry box techniques; solvents were dried over Na metal, K metal or CaH_2. Reagents were of analytical grade, obtained from commercial suppliers and used without further purification. ^1H, ^{13}C, ^{11}B, and ^{19}F NMR spectra were obtained with a Bruker AV 400, AVIII 400 MHz BBFO2 or AV 500, spectrometers at 298 K unless otherwise stated. Coupling constants *J* are given in Hz. Electrospray ionization (ESI) mass spectra were obtained at the Mass Spectrometry Laboratory at the Division of Chemistry and Biological Chemistry, Nanyang Technological University. Melting points were measured with OptiMelt (Stanford Research System). Azo substrates were synthesized according to reported procedures [17] 4-methoxyazobenzene is commercially available at Sigma-Aldrich. The spectroscopic data for the **3i** were identical to those reported in the literature. [18] ND_3BH_3 **[A(D)B]**, NH_3BD_3**[AB(D)]**, and ND_3BD_3**[A(D)B(D)]** were synthesized according to literature procedures. [19]

Synthesis of compound 1: A solution of 1,3-bis(*tert*-butyl)-2-chloro-1,3,2-diazaphospholene (6.12 g, 26.1 mmol) in THF (100 mL) was cooled to -78 ºC and a 70 wt. % solution of sodium bis(2-methoxy)aluminium hydride in toluene (3.7 mL, 13.3 mmol) was slowly added. The mixture was warmed to room temperature and stirred overnight. Solvents were evaporated in a vacuum, and then the residue was dissolved in hexane (100 mL) and filtered. The product **1** was obtained after fractionated distillation of the filtrate in vacuum. The spectroscopical data were similar to those as reported in the literature (Chapter 1 ref. 52).

Synthesis of compound 1': 1,3-bis(tert-butyl)-2-chloro-1,3,2-diazaphospholidine (3.00 g, 12.7 mmol) and $LiAlH_4$ (0.20 g, 13.1 mmol) added to a 100 mL Schlenk flask and cooled to -78 ºC. THF (40 mL) was then added slowly to the reaction mixture. The reaction mixture was allowed to warm to room temperature and stirred overnight. Solvents were evaporated in a vacuum, and the residue was dissolved in pentane (50 mL) and filtered. The product **1'** was obtained after

fractionated distillation of the filtrate in vacuum. The spectroscopical data were similar those as reported in the literature.[20]

Synthesis of compounds 2 and 2': **1** / **1'** (0.120 mmol) and azobenzene (18.2 mg, 0.100 mmol) were dissolved in toluene (5 mL) and stirred for a minute. The solvent and volatiles were then removed under vacuum, and the residue was washed with a minimum amount of pentane to yield **2**. A single crystal of **2'** was obtained by recrystallization from a benzene solution.

2 (67%): brown oil.

^{1}H NMR (500 MHz, C$_6$D$_6$): δ = 7.63 (d, ^3J = 7.5 Hz, 2H, *m*-C*H*), 7.25 (t, ^3J = 7.5 Hz, 2H, *o*-C*H*), 7.03 (t, ^3J = 7.5 Hz, 2H, *o*-C*H*), 6.86 (t, ^3J = 7.5 Hz, 1H, *p*-C*H*), 6.75 – 6.72 (m, 3H, *aromatic*-C*H*), 5.88 (br, 1H, =C*H*), 5.62 (br, 1H, =C*H*), 5.29 (s, 1H, N*H*), 1.05 (br, 18H, C*H*$_3$).

^{13}C NMR (125 MHz, C$_6$D$_6$): 30.3 (br, *C*H$_3$), 52.8 (br, *C*Me$_3$), 53.7 (br, *C*Me$_3$), 112.2 (br, =*C*H), 113.4 (br, =*C*H), 113.6 (C*H*), 115.4 (d, $^{C\text{-}P}J$ = 15.1 Hz, *C*H), 119.3 (*C*H), 120.4 (*C*H), 128.3 (*C*H), 129.3 (*C*H), 148.1 (d, $^{C\text{-}P}J$ = 16.4 Hz, PN*C*), 149.8 (NN*C*).

^{31}P NMR (202 MHz, C$_6$D$_6$): 88.2.

HRMS (ESI): *m/z* calcd for C$_{22}$H$_{32}$N$_4$P: 383.2365 [(*M+H*)]$^+$; found: 383.2357.

2' (53%): White solid, M.p.: 104 ^{o}C.

^{1}H NMR (500 MHz, C$_6$D$_6$): δ = 7.67 (d, ^3J = 7.2 Hz, 2H, *m*-C*H*), 7.27 (t, ^3J = 7.2 Hz, 2H, *o*-C*H*), 7.07 (t, ^3J = 7.2 Hz, 2H, *o*-C*H*), 6.86 (t, ^3J = 7.2 Hz, 1H, *p*-C*H*), 6.78 – 6.72 (m, 3H, *aromatic*-C*H*), 6.64 (s, 1H, N*H*), 2.96 (br, 2H, NC*H*$_2$), 2.66 (br, 2H, NC*H*$_2$), 1.06 (br, 18H, C*H*$_3$).

^{13}C NMR (125 MHz, C$_6$D$_6$): 29.1 (br, *C*H$_3$), 44.9 (br, *C*H$_2$), 46.7 (br, *C*H$_2$), 52.3 (br, *C*Me$_3$), 53.0 (br, *C*Me$_3$), 114.2 (*C*H), 115.1 (d, $^{C\text{-}P}J$ = 15.1 Hz, *C*H), 119.4 (*C*H), 120.0 (*C*H), 129.1 (*C*H), 129.4 (*C*H), 149.1 (NN*C*), 150.5 (d, $^{C\text{-}P}J$ = 18.9 Hz, PN*C*).

^{31}P NMR (202 MHz, C$_6$D$_6$): 99.9.

HRMS (ESI): *m/z* calcd for C$_{22}$H$_{34}$N$_4$P: 385.2521 [(*M+H*)]$^+$; found: 385.2522.

Reaction of compound 2 and AB: Compound **2** / **2'** (0.042 mmol) and 4 eq. **AB** (5.2 mg, 0.168 mmol) or 4 eq. **AB(D)** (5.7mg, 0.168 mmol) were dissolved in CD$_3$CN (1 mL), and loaded in a

Carius NMR tube under argon atmosphere. The tube was sealed, and the reaction was monitored by NMR spectroscopy at 50 °C.

General catalytic procedures for the transfer hydrogenation of various azo-compounds: Compound **1** (3 mg, 0.015 mmol), azo-compound (0.300 mmol), ammonia-borane (37 mg, 1.199 mmol), the internal standard 1,3,5-trimethoxybenzene (17 mg, 0.101 mmol) and CD$_3$CN (1.0 mL) were loaded in a dried Carius NMR tube under argon atmosphere. The tube was sealed, placed in an oil bath, and heated at 50 °C. The reaction was monitored by NMR spectroscopy. Products were then purified by flash column chromatography on silica gel (9:1 = hexane : ethyl acetate) in a glove box. Isolated yield is given in parenthesis.
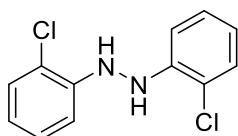
3a

3a (83%): M.p.: 88 °C.

^{1}H NMR (500 MHz, CDCl$_3$): δ = 7.30 (d, ^3J = 8.0 Hz, 2H, C*H*), 7.13 (t, ^3J = 8.0 Hz, 2H, C*H*), 6.96 (d, ^3J = 8.0 Hz, 2H, C*H*), 6.79 (t, ^3J = 8.0 Hz, 2H, C*H*), 6.21 (s, 2H, N-*H*).

^{13}C NMR (125 MHz, CDCl$_3$): δ = 113.1 (*C*H), 118.2 (*C*H), 120.4 (*C*H), 128.2 (*C*H), 129.5 (*C*-Cl), 144.0 (*C*-N).

HRMS (ESI): *m/z* calcd for C$_{12}$H$_{11}$N$_2$Cl$_2$: 253.0299 [(*M+H*)]$^+$; found: 253.0292.
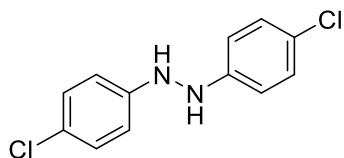
3b

3b (89%): M.p.: 125 °C.

^{1}H NMR (500 MHz, CDCl$_3$): δ = 7.17 (d, ^3J = 9.0 Hz, 4H, C*H*), 6.76 (d, ^3J = 9.0 Hz, 4H, C*H*), 5.63 (s, 2H, N-*H*).

^{13}C NMR (125 MHz, CDCl$_3$): δ = 113.7 (*C*H), 124.9 (*C*-Cl), 129.5 (*C*H), 147.2 (*C*-N).

HRMS (ESI): *m/z* calcd for C$_{12}$H$_{11}$N$_2$Cl$_2$: 253.0299 [(*M+H*)]$^+$; found: 253.0306.

3c
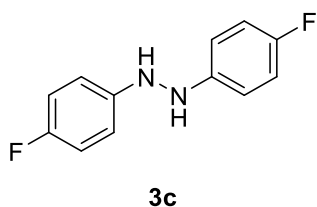
3c (61%): M.p.: 75 °C.

^{1}H NMR (400 MHz, CDCl$_3$): δ = 6.93 (t, ^3J = 9.0 Hz, 4H, C*H*), 6.81 – 6.78 (m, 4H, C*H*), 5.55 (s, 2H, N*H*).

^{13}C NMR (100 MHz, CDCl$_3$): δ = 113.5 (d, $^{\text{C-F}}J$ = 7.5 Hz, *C*H), 116.0 (d, $^{\text{C-F}}J$ = 22.6 Hz, *C*H), 145.0 (*C*-N), 157.3 (d, $^{\text{C-F}}J$ = 236.4 Hz, *C*-F).

^{19}F NMR (376 MHz, CDCl$_3$): δ = −128.4.

HRMS (ESI): *m/z* calcd for C$_{12}$H$_{11}$N$_2$F$_2$: 221.0890 [(*M*+*H*)]$^+$; found: 221.0899.

3d
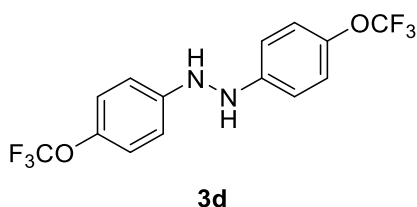
3d (53%) M.p.: 55 °C.

^{1}H NMR (400 MHz, CDCl$_3$): δ = 7.09 (d, ^3J = 9.0 Hz, 4H, C*H*), 6.83 (d, ^3J = 9.0 Hz, 4H, C*H*), 5.70 (s, 2H, N*H*).

^{13}C NMR (100 MHz, CDCl$_3$); δ = 113.0 (*C*H), 120.8 (q, $^{\text{C-F}}J$ = 255.6 Hz, *C*F$_3$), 122.7 (*C*H), 142.7 (*C*-N), 147.3 (*C*-CF$_3$).

^{19}F NMR (376 MHz, CDCl$_3$): δ = −59.1.

HRMS (ESI): *m/z* calcd for C$_{14}$H$_{11}$N$_2$O$_2$F$_6$: 353.0725 [(*M*+*H*)]$^+$; found: 353.0719.

3e
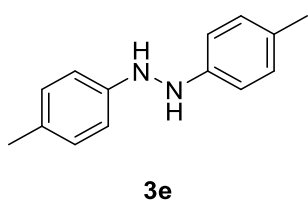
3e (61%): M.p.: 113 °C.

^{1}H NMR (500 MHz, CDCl$_3$): δ = 7.04 (d, ^3J = 8.0 Hz, 4H, C*H*), 6.78 (d, ^3J = 8.0 Hz, 4H, C*H*), 5.50 (s, 2H, N*H*), 2.28 (s, 3H, C*H*$_3$).

^{13}C NMR (125 MHz, CDCl$_3$): δ = 20.6 (CH$_3$), 112.6 (CH), 129.2 (C-CH$_3$), 130.0 (CH), 146.9 (C-N).

HRMS (ESI): *m/z* calcd for C$_{14}$H$_{17}$N$_2$: 213.1392 [(*M+H*)]$^+$; found: 213.1387.
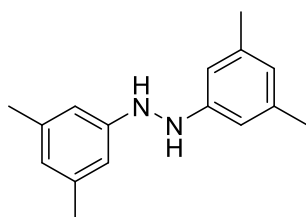
3f

3f (67%): M.p.: 116 $^\circ$C.

^{1}H NMR (400 MHz, CDCl$_3$): δ = 6.51 (s, 6H, *aromatic*-C*H*), 5.46 (s, 2H, N*H*), 2.25 (s, 12H, C*H*$_3$).

^{13}C NMR (100 MHz, CDCl$_3$): δ = 21.6 (CH$_3$), 110.2 (CH), 121.9 (CH), 139.3 (C-Me), 149.4 (C-N).

HRMS (ESI): *m/z* calcd for C$_{16}$H$_{21}$N$_2$: 241.1705 [(*M+H*)]$^+$; found: 241.1700.
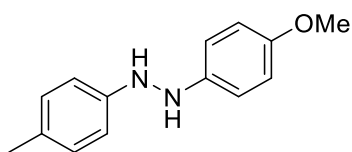
3j

3j (62%) M.p.: 99 $^\circ$C.

^{1}H NMR (400 MHz, CDCl$_3$): δ = 7.02 (d, ^3J = 8.0 Hz, 2H, C*H*), 6.81 – 6.76 (m, 6H, *aromatic*-C*H*), 5.50 (s, 1H, N*H*), 5.42 (s, 1H, N*H*), 3.75 (s, 3H, OC*H*$_3$), 2.26 (s, 3H, C*H*$_3$).

^{13}C NMR (100 MHz, CDCl$_3$): δ = 20.7 (CH$_3$), 55.9 (OCH$_3$), 112.7 (CH), 113.9 (CH), 115.0 (CH), 129.3 (C-Me), 130.0 (CH), 143.1 (C-N), 147.0 (C-N), 153.9 (C-OMe).

HRMS (ESI): *m/z* calcd for C$_{14}$H$_{17}$N$_2$O: 229.1341 [(*M+H*)]$^+$; found: 229.1346.
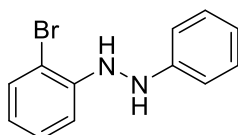
3k

3k (73%): M.p.: 80 $^\circ$C.

^{1}H NMR (400 MHz, CDCl$_3$): δ = 7.45 (d, ^3J = 8.0 Hz, 1H, C*H*), 7.22 (t, ^3J= 8.0 Hz, 2H, C*H*), 7.15 (t, ^3J = 8.0 Hz, 1H, C*H*), 7.02 (d, ^3J = 8.0 Hz, 1H, C*H*), 6.87 – 6.80 (m, 3H, C*H*), 6.70 (t, 8.0 Hz, 1H, C*H*), 6.17 (s, 1H, N*H*), 5.66 (s, 1H, N*H*).

^{13}C NMR (100 MHz, CDCl$_3$): δ = 107.4 (*C*Br), 112.5 (*o*-*C*H), 113.5 (*C*H), 120.4 (*p*-*C*H), 120.6 (*C*H), 128.7 (*C*H), 129.6 (*m*-*C*H), 132.6 (*C*H), 145.4 (*C*-N), 148.4 (ipso-*C*-N).

HRMS (ESI): *m/z* calcd for C$_{12}$H$_{12}$N$_2$Br: 263.0184 [(*M*+*H*)]$^+$; found: 263.0186.

3l
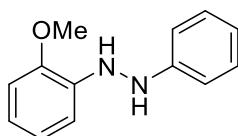
3l (70%): M.p.: 83 $^{\circ}$C.

^{1}H NMR (400 MHz, CDCl$_3$): δ = 7.21 (t, ^3J = 8.0 Hz, 2H, C*H*), 6.93 (d, ^3J = 8.0 Hz, 1H, C*H*), 6.87 – 6.79 (m, 6H, C*H*), 6.15 (s, 1H, N*H*), 5.52 (s, 1H, N*H*), 3.90 (s, 3H, OC*H*$_3$).

^{13}C NMR (100 MHz, CDCl$_3$): δ = 55.7 (O*C*H$_3$), 110.1 (*C*H), 112.0 (*C*H), 112.5 (*o*-*C*H), 119.3 (*p*-*C*H), 119.9 (CH), 121.5 (*C*H), 129.5 (*m*-*C*H), 138.3 (*C*-OMe), 146.5 (*C*-N), 149.2 (ipso-*C*-N).

HRMS (ESI): *m/z* calcd for C$_{13}$H$_{15}$N$_2$O: 215.1184 [(*M*+*H*)]$^+$; found: 215.1176.

2.4.2   Kinetic study results

General procedures for the transfer hydrogenation of azobenzene: Compound **1** (3 mg, 0.015 mmol), azobenzene (55 mg, 0.302 mmol), ammonia-borane (37 mg, 1.199 mmol), the internal standard 1,3,5-trimethoxybenzene (17 mg, 0.101 mmol) and CD$_3$CN (1.0 mL) were loaded in a dried Carius NMR Tube under argon atmosphere. The tube was sealed and heated over a temperature range from 40 $^{\circ}$C to 70 $^{\circ}$C. The reaction progress was monitored by NMR spectroscopy with 5 minutes interval. Based on the integration of azobenzene, the logarithmic plot of the concentration of azobenzene was plotted against time. The Eyring plot was also obtained based on the rate at each temperature and plotted against inverse of time.

General procedures for study of the deuterium kinetic isotope effect: Compound **1** (3 mg, 0.015 mmol), azobenzene (55 mg, 0.302 mmol), deuterated ammonia-borane (1.199 mmol), the internal standard 1,3,5-trimethoxybenzene (17 mg, 0.101 mol), and CD_3CN (1.0 mL) were loaded in a dried Carius NMR Tube under argon atmosphere. The reaction was monitored at 50 ^{o}C with 5 minutes interval. Based on the integration of azobenzene, logarithmic plot against time was obtained.

2.4.3   *Crystal Structure Determination of Compound 2'*

X-ray data collection and structural refinement. Intensity data for compound **2'** were collected using a Bruker APEX II diffractometer. A crystal of **2'** was measured at 103(2) K. The structure was solved by direct phase determination (SHELXS-97) and refined for all data by full-matrix least squares methods on F^2.[21] All non-hydrogen atoms were subjected to anisotropic refinement. The hydrogen atoms were generated geometrically and allowed to ride on their respective parent atoms; they were assigned appropriate isotropic thermal parameters and included in the structure-factor calculations. CCDC–978856 contains the supplementary crystallographic data for this paper. The data can be obtained free of charge from the Cambridge Crystallography Data Centre via www.ccdc.cam.ac.uk/data_request/cif.

Table 2.3   Summary of Data Collection and Structure Refinement for **2'**.

	2'
Formula	$C_{22}H_{33}N_4P$
*F*w	384.49
Cryst syst	monoclinic
Space group	$P\,1\,2_1/c\,1$
Size (mm³)	0.20 x 0.24 x 0.30
T, K	103(2)
a, Å	11.576(2)
b, Å	13.771(3)
c, Å	13.694(2)
α, deg	90
β, deg	90.037(3)
γ, deg	90
V, A³	2181.6(7)
Z	4
*d*calcd g·cm⁻³	1.171
μ, mm⁻¹	0.140
Refl collected	21102
*T*min / *T*max	0.9856
Nmeasd	5383
[*R*int]	[0.0568]
R [I>2sigma(I)]	0.0486
*R*w[I>2sigma(I)]	0.1322
GOF	1.044
Largest diff peak/hole[e·Å⁻³]	0.499/-0.456

2.5   References

1. For recent review on transfer hydrogenation reactions, see: a) Wang, D.; Astruc, D. *Chem. Rev*. **2015**, *115*, 6621–6686; b) Zhu, C.; Saito, K.; Yamanaka, M.; Akiyama, T. *Acc. Chem. Res*. **2015**, *48*, 388–398; c) Li, Y.; Yu, S.; Shen, W.; Gao, J. *Acc. Chem. Res*. **2015**, *48*, 2587–2598.

2. Dresselhaus, M.; Crabtree, G.; Buchanan, M., Eds. *Basic Energy Needs for the Hydrogen Economy*; Basic Energy Sciences, Office of Science, U.S. Department of Energy; Washington, DC, 2003.

3. For selected reviews, see: a) Li, H.; Yang, Q.; Chen, X.; Shore, S. G. *J. Organomet. Chem*. **2014**, *751*, 60–66; b) Leitao, E. M.; Jurca, T.; Manners, I. *Nat. Chem*. **2013**, *5*, 817–829; c) Stubbs, N. E., Robertson, A. P. M.; Leitao, E. M.; Manners, I. *J. Organomet. Chem*. **2013**, *730*, 84–89; d) Staubitz, A.; Robertson, A. P. M.; Manners, I. *Chem. Rev*. **2010**, *110*, 4079–4124; e) Smythe, N. C.; Gordon, J. C. *Eur. J. Inorg. Chem*. **2010**, 509–521; f) Hamilton, C.W.; Baker, R. T.; Staubitz, A.; Manners, I. *Chem. Soc. Rev*. **2009**, *38*, 279–293; g) Yang, J.; Sudik, A.; Wolverton, C.; Siegel, D. J. *Chem. Soc. Rev*. **2010**, *39*, 656–675; h) Alcaraz, G.; Sabo-Etienne, S. *Angew. Chem. Int. Ed*. **2010**, *49*, 7170–7179; i) Stephens, F. H.; Pons, V.; Baker, R. T. *Dalton Trans*. **2007**, 2613–2626; j) Marder, T. B. *Angew. Chem. Int. Ed*. **2007**, *46,* 8116–8118.

4. a) Sutton, A. D.; Burrell, A. K.; Dixon, D. A.; Garner III, E. B.; Gordon, J. C.; Nakagawa, T.; Ott, K. C.; Robinson, J. P.; Vasiliu, M. *Science* **2011**, *331*, 1426–1429; b) Luo, W.; Zakharov, L. N.; Liu, S.-Y. *J. Am. Chem. Soc*. **2011**, *133*, 13006–13009; c) Davis, L. B.; Dixon, D. A.; Garner, E. B.; Gordon, J. C.; Matus, M. H.; Scott, B; Stephens, F. H. *Angew. Chem. Int. Ed*. **2009**, *48*, 6812 – 6816.

5. For recent examples of transition metal-catalysed dehydrogenation of ammonia borane, see: a) Glüer, A.; Förster, M.; Celinski, V. R.; auf der Güne, J. S.; Holthausen, M. C.; Schneider, S. *ACS Catalysis* **2015**, *5*, 7214–7217; b) Hu, X.; Soleilhavoup, M.; Melaimi, M.; Chu, J.; Bertrand, G. *Angew. Chem. Int. Ed.* **2015**, *54*, 6008–6011; c) Buss, J.

A.; Edouard, G. A.; Cheng, C.; Shi, J.; Agapie, T. *J. Am. Chem. Soc*. **2014**, *136*, 11272–11275; d) Helten, H.; Dutta, B.; Vance, J. R.; Sloan, M. E.; Haddow, M. F.; Sproules, S.; Collison, D.; Whittell, G. R.; Lloyd-Jones, G. C.; Manners, I. *Angew. Chem. Int. Ed*. **2012**, *52*, 437–440.

6.　For recent examples on metal-catalysed transfer hydrogenation using ammonia-borane derivatives, see: a) Pagano, J. K.; Stelmach, J. P. W.; Waterman, R. *Dalton Trans*. **2015**, *44*, 12074–12077; b) Hartmann, C. H.; Jurčík, V.; Songis, O.; Cazin, C. S. J. *Chem. Comm.* **2013**, *49*, 1005–1007; c) Sloan, M. E.; Staubitz, A.; Lee, K.; Manners, I. *Eur. J. Org. Chem.* **2011**, 672–675; d) Barrios-Francisco, R.; García, J. J. *Appl. Catal. A* **2010**, *385*, 108–115.

7.　For recent studies on the mechanism for transfer hydrogenation using ammonia-borane, see: a) Stubbs, N. E.; Schäfer, A.; Robertson, A. P. M.; Leitao, E. M.; Jurca, T.; Sparkes, H. A.; Woodall, C. H.; Haddow, M. F.; Manners, I. *Inorg. Chem.* **2015**, *54*, 10878–10889; b) Ganguly, G.; Malakar, T.; Paul, A. *ACS Catal.* **2015**, *5*, 2754–2769; c) Butera, V.; Russo, N.; Sicilla, E. *Chem. Eur. J*. **2014**, *20*, 5967–5976; d) Berke, H.; Jiang, Y.; Yang, X.; Jiang, C.; Chakraborty, S.; Landwehr, A. *Top Curr. Chem.* **2013**, *334*, 27–57; e) Berke, H. *ChemPhysChem* **2010**, *11*, 1837–1849; f) Comas-Vives, A.; Ujaque, G.; Lledós, A.; *J. Mol. Struct. THEOCHEM* **2009**, *903*, 123–132.

8.　a) Yang, X.; Fox, T.; Berke, H. *Org. Biomol. Chem*. **2012**, *10*, 852–860; b) Yang, X.; Fox, T.; Berke, H. *Chem. Commun*. **2011**, *47*, 2053–2055; c) Yang, X.; Fox, T.; Berke, H. *Tetrahedron* **2011**, *67*, 7121–7127; d) Yang, X.; Zhao, L.; Fox, T.; Wang, Z.-X.; Berke, H. *Angew. Chem. Int. Ed*. **2010**, *49*, 2058–2062.

9.　a) Campbell, J. E.; Zhou, H.; Nguyen, S. T. *Org. Lett*. **2001**, *3*, 2391–2393; b) Ponndorf, W. *Angew. Chem*. **1926**, *39*, 138–143; c) Meerwin, H.; Schmidt, R. *Justus Liebigs Ann. Chem*. **1925**, *444*, 221–238; d) Varley, A. *Bull. Soc. Chim. Fr*. **1925**, *37*, 871–874.

10.　Leitao, E. M.; Stubbs, N. E.; Robertson, A. P. M.; Helten, H.; Cox, R. J.; Lloyd-Jones, G. C.; Manners, I. *J. Am. Chem. Soc*. **2012**, *134*, 16805–16816.

11.   a) Fernández, I.; Sierra, M. A.; Cossio, F. P. *J. Org. Chem*. **2007**, *72*, 1488–1491; b) Miller, D. J.; Smith, D. M.; Chan, B.; Radom, M. *Mol. Phys*. **2006**, *104*, 777–794.

12.   For selected examples, see: a) Di, W.; Li, Y.; Ganguly, R.; Kinjo, R. *Chem. Commun.* **2014**, *50*, 12378–12381; b) Appelt, C.; Slootweg, J. C.; Lammertsma, K.; Uhl, W. *Angew. Chem. Int. Ed.* **2013**, *52*, 4256–4259; c) Hansmann, M. M.; Melen, R. L.; Wright, D. S.; *Chem. Sci.* **2011**, *2*, 1554–1559; d) Mènard, G.; Stephan, D. W. *J. Am. Chem. Soc*. **2010**, *132*, 1796–1797; e) Jana, A.; Schulzke, C.; Roesky, H. W. *J. Am. Chem. Soc.* **2009**, *131*, 4600–4601.

13.   Dunn, N. L.; Ha, M.; Radosevich, A. T. *J. Am. Chem. Soc*. **2012**, *134*, 11330–11333.

14.   a) Pal, A.; Vanka, K. *Inorg. Chem*. **2016**, *55*, 558–565; b) Zeng, G.; Maeda, S.; Taketsugu, T.; Sakaki, S. *Angew. Chem. Int. Ed*. **2014**, *53*, 4633–4637.

15.   Zhao, Y.; Schultz, N. E.; Truhlar, D. G. *J. Chem. Theory Comput*. **2006**, *2*, 364–382.

16.   Reed, A. E.; Curtiss, L. A.; Weinhold, F. *Chem. Rev*. **1988**, *88*, 899–926.

17.   a) Yin, Z.; Jiang, X.; Sun, P. *J. Org. Chem*. **2013**, *78*, 10002–10007; b) Ma, X.; Tian, S. *Adv. Synth. Catal*. **2013**, *355*, 337–340; c) Ma, H.; Li, W.; Wang, J.; Xiao, G.; Gong, Y.; Qi, C.; Feng, Y.; Li, X.; Bao, Z.; Cao. W.; Sun, Q.; Veaceslav, C.; Wang, F.; Lei, Z. *Tetrahedron* **2012**, *68*, 8358–8366; d) Zhang, C.; Jiao, N. *Angew. Chem. Int. Ed*. **2010**, *49*, 6174–6177.

18.   Drug, E.; Gozin, M. *J. Am. Chem. Soc*. **2007**, *129*, 13784–13785.

19.   Penner, G. H.; Chang, Y. C. P.; Hutzal, *J. Inorg. Chem*. **1999**, *38*, 2868–2873.

20.   King, R. B.; Sundaram, P. M. *J. Org. Chem*. **1984**, *49*, 1784–1789.

21.   Sheldrick, G. M., SHELXL-97; Universität Göttingen, Göttingen, Germany, 1997.

Chapter 3 Metal-Free σ-Bond Metathesis in 1,3,2-Diazaphospholene-Catalysed Hydroboration of Carbonyl Compounds

3.1 Introduction

One of the most efficient methodologies for the construction of new bonds is the metathesis process, which has been widely utilized in various organic synthesis, material science as well as biochemistry. [1,2] Extensive experimental and theoretical studies on the metathesis process have enabled an in-depth understanding of its mechanism, especially in the case of alkene and alkyne metathesis reaction.[3] It has been established that alkene metathesis takes place via a metallocyclobutane intermediate while alkyne metathesis goes through a cycloaddition-cycloreversion steps via a metallocyclobutadiene intermediate (Scheme 3.1a, b).[4] In the case of alkane metathesis, however, bonding exchange between two molecules may progress through either a σ-bond metathesis four-membered transition state (Scheme 3.2c, path 1) or a two-step process involving oxidative addition and reductive elimination (Scheme 3.2c, path 2), depending on the electronic structure of the transition metal complexes.[5]

Notably, for the metathesis reaction, a four-membered ring transition state is proposed which is conceptually formed by a [2+2] cycloaddition. Despite being forbidden by orbital symmetry[6], [2+2] cycloaddition could proceed owing to the empty d or f–orbitals on the metal centre. Hence, several transition metal complexes have been shown to be catalytically active in metathesis reactions.[7] On the other hand, metal-free σ-bond metathesis reactions are relatively uncommon. In 2013, Wang and Li reported a metal-free hydrogenation of alkenes using $HB(C_6F_5)_2$ in which they proposed a four-membered transition involving H_2 molecule and borane-alkene insertion product (Figure 3.1a).[8] Nikonov and Vyboishchikov also reported similar σ-bond metathesis transition state for the activation of H_2 and Si-H bond by boranes (Figure 3.1b).[9] More recently, our group demonstrated an σ-bond metathesis involving ammonia activation by a non-planar diazadiphosphapentalene (Figure 3.1c).[10] These results imply that non-metal p-block compounds bearing an accessible vacant orbital could also undergo formal [2+2] interactions.

a) *Alkene Metathesis*
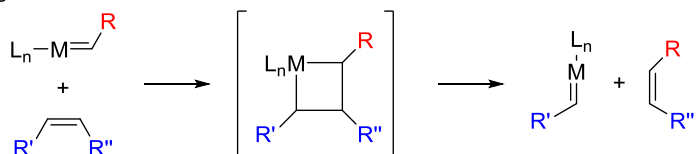
b) *Alkyne Metathesis*
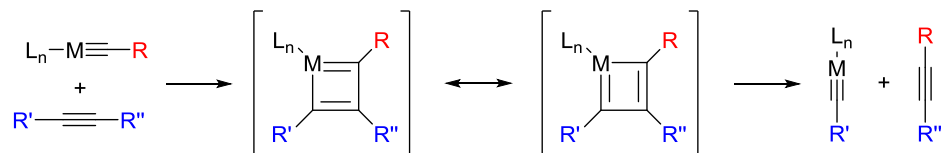
c) *Alkane Metathesis*
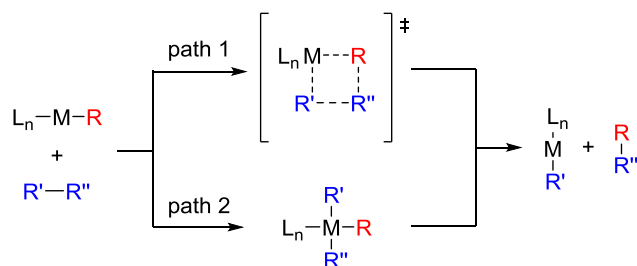
Scheme 3.1   General mechanism for a) alkene metathesis, b) alkyne metathesis, and c) alkane metathesis (path 1 corresponds to σ-bond metathesis pathway while path 2 corresponds to oxidative addition/reductive elimination pathway).

a)   b)   c)
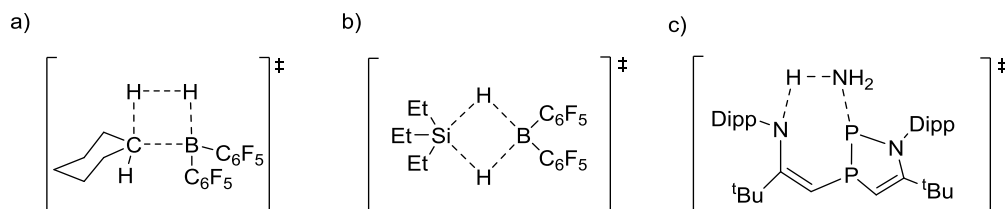
Figure 3.1   Proposed transition state for the σ-bond metathesis between a) Lewis acidic boranes with H_2; b) Et_3SiH and $HB(C_6F_5)_2$; c) NH_3 activation by diazadiphosphapentalene.

   As mentioned in Chapter 2, 1,3,2-diazaphospholene **1** promotes the transfer hydrogenation of a N=N bond using ammonia-borane via a concerted double hydrogen transfer in a six-membered ring transition state. Intrinsically, the electrophilicity of the phosphorus atom in **1** could allow strong interaction with σ-bond of other substrates, hence, we reasoned that similar σ-bond metathesis reaction observed in highly Lewis acidic boranes could be applied to **1**. As it has been reported that main group hydride species like Ge-H, Sn-H, Mg-H and Al-H species (Figure

49

3.2) could catalyse hydroboration of carbonyl compounds[11], we examined hydroboration reactions of carbonyl compounds with a catalytic amount of **1**.[12] The subsequent formation of the strong B-O bond could allow for the formation of the four-membered-ring transition state and hence, proceed in σ-bond metathesis manner. In this chapter, we discuss a σ-bond metathesis mechanism in catalytic hydroboration of carbonyl compounds using **1**.
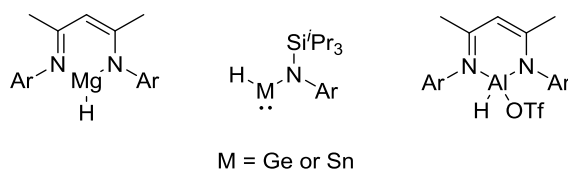
Figure 3.2   Main-Group hydride species in the catalytic hydroboration of carbonyl compounds.

3.2 Results and Discussions

3.2.1 Stoichiometric reaction of 1 with benzaldehyde and pinacolborane

In Chapter 1, it was mentioned that **1** could react with carbonyl compounds to generate alkoxyphosphines. Following this protocol, we treated **1** with benzaldehyde (PhCHO) in CD_3CN (Scheme 3.2a). As expected, the reaction proceeds readily at room temperature as observed by ^{31}P NMR spectroscopy with a singlet at δ = 93.0 ppm, corresponding to the formation of **4**. Subsequently, the addition of one equivalent of HBpin to alkoxyphosphine **4** at room temperature regenerated **1** concomitant with the formation of boric ester, Ph_2CH_2OBpin as monitored by ^{11}B and ^{31}P NMR spectroscopy (Scheme 3.2b). The result demonstrates a metal-free σ-bond metathesis involving the cleavage of a P(III)-O bond.[10] Importantly, the metathesis occurred only at the exocyclic P-O bond in **4** and the cleavage of the endocyclic P-N bond was not observed. This is most likely due to the polarized P-O bond as well as the kinetic stability of the endocyclic P-N bond.
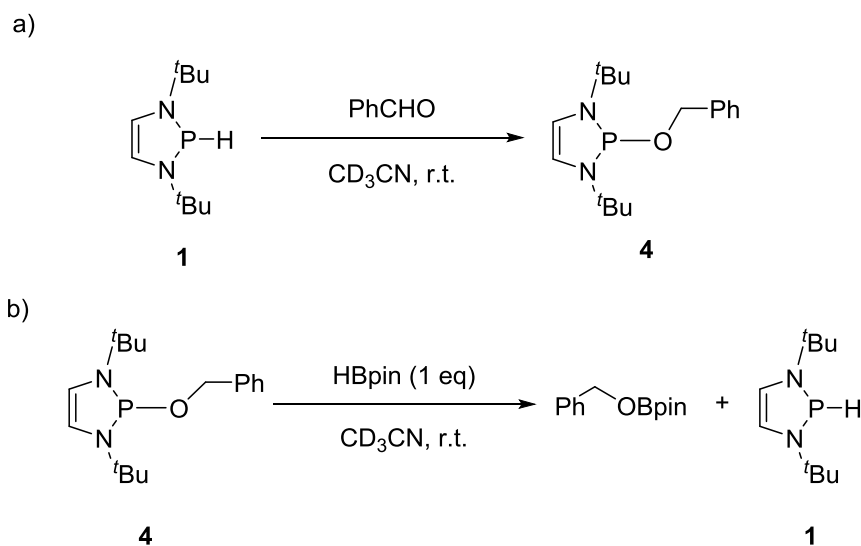
Scheme 3.2 a) Quantitative synthesis of alkoxyphosphine **4** and, b) stoichiometric reaction between **4** and HBpin.

3.2.2 Hydroboration of ketones and aldehyde catalysed by 1

Next, we attempted to apply the stoichiometric reactions in a catalytic process. Without any catalysts, there was negligible formation of $PhCH_2OBpin$, **5** (Table 3.1, entry 1). Similarly, in the presence of a stoichiometric amount of diphenylphosphine or di-tert-butylphosphine (Table 3.1, entries 2 and 3) only small amount of $PhCH_2OBpin$ was produced. In contrast, the addition of 1 mol% of **1** resulted in the quantitative formation of $PhCH_2OBpin$ after 1 h (Table 3.1, entry 4). Both dichloromethane and acetonitrile are shown to be suitable solvents for the reaction (Table 3.1, entries 4–8). A reaction time of 15 minutes was required for near completion of the reaction (Table 3.1, entry 9). When the catalyst loading was decreased to 0.5 mol%, the hydroborated product was quantitatively formed after 45 minutes (Table 3.1, entry 10).

Table 3.1   Optimization of the reaction condition for the hydroboration of benzaldehyde.[a]
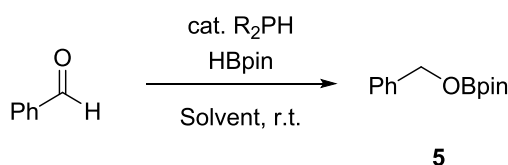
Entry	cat. (mol%)	Solvent	Time (h)	Yield (%)[b]
1	None (0 mol%)	CD_3CN	1	6
2	Ph_2PH (100 mol%)	CD_3CN	1	6
3	$^tBu_2PH$ (100 mol%)	CD_3CN	1	6
4	**1** (1 mol%)	CD_3CN	1	>99
5	**1** (1 mol%)	C_6D_6	1	79
6	**1** (1 mol%)	d_8-THF	1	57
7	**1** (1 mol%)	$CDCl_3$	1	93
8	**1** (1 mol%)	CD_2Cl_2	1	>99
9	**1** (1 mol%)	CD_3CN	<0.25	>99
10	**1** (0.5 mol%)	CD_3CN	0.75	**>99**

(a)   Reaction conditions: benzaldehyde (1.50 mmol), HBpin (1.50 mmol), solvent (0.3 ml). Catalyst loading relative to benzaldehyde.

(b)   Yields are determined by ^1H NMR using 1,3,5-trimethoxybenzene as an internal standard.

Using the optimised conditions, we examined the scope of substrates employing various aldehydes (Figure 3.3). Aliphatic aldehydes afforded the corresponding boric esters (**5a, b**) in

good to high yields. In addition, both electron-withdrawing (**5c–g**) and electron-donating (**5h–k**) aromatic substituents also afford the corresponding boric esters in reasonable yields (70 – >99%). Moreover, heterocyclic substrates were also well tolerated to give excellent yields (**5l**: 99%, **5m**: 99%). In particular, no dearomatization product was observed, unlike those hydroboration reactions that were previously reported, hence, highlighting the chemoselectivity of the catalyst. In the presence of two equivalents of HBpin, terephthalaldehyde was readily converted to bis(hydroborated) derivative (**5n**) in 99% NMR yield. More importantly, when 4-acetylbenzaldehyde was employed, hydroboration only occurred selectively at the aldehyde functional group (**5o**), which was previously not reported.
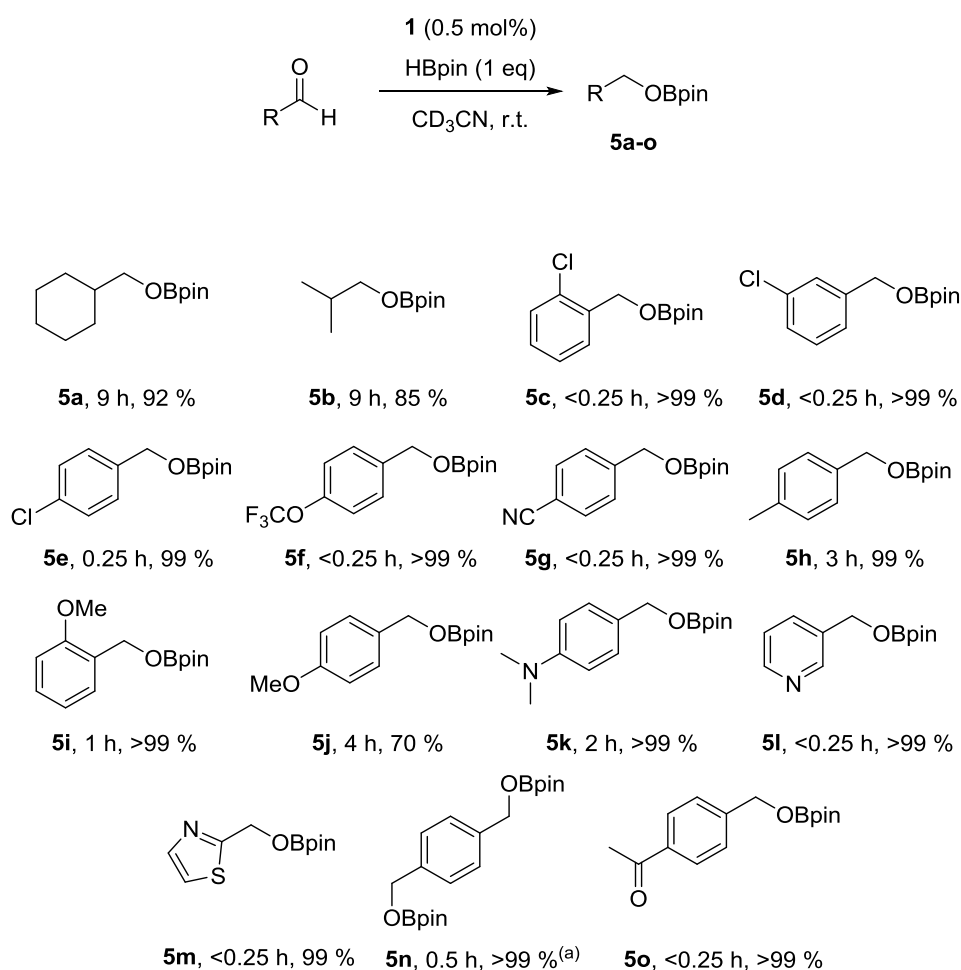
Figure 3.3   NMR yields and reaction times for the hydroboration of aldehydes using HBpin (1 eq) and 0.5 mol% **1** at r.t. (a) 2 eq of HBpin added.

To expand the substrate scope, we also attempted catalytic hydroboration of ketones. Due to steric hindrance and the less electrophilic carbonyl carbon, a harsher reaction condition (10 mol% **1** and heating at 90 °C) is required for the quantitative formation of the corresponding boric ester derivatives (Figure 3.4). Both acyclic and cyclic ketones containing electron-withdrawing or electron-donating groups were well tolerated and afforded a reasonable yield of boric esters (**6a–j**: > 98%).
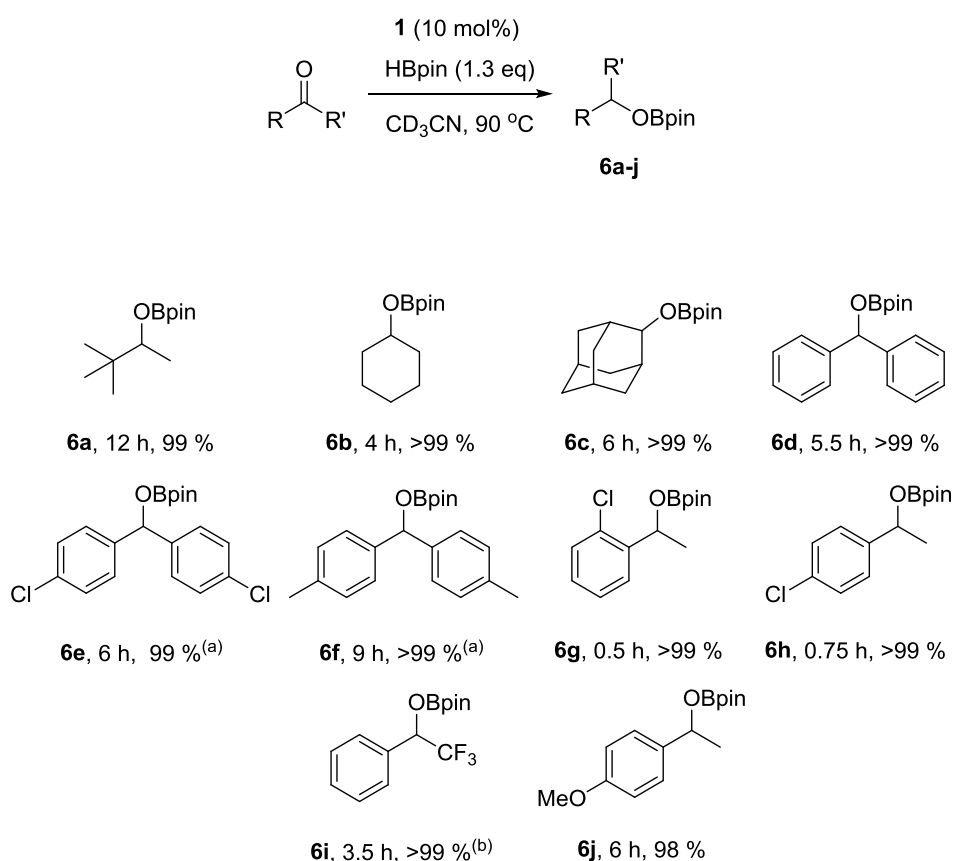
Figure 3.4 NMR yields and reaction times for the hydroboration of ketones using HBpin (1.3 eq) and 10 mol% **1** at 90 °C. (a) Reaction was conducted in C_6D_6. (b) Reaction was conducted at r.t.

3.2.3   *Kinetic and theoretical studies*

To elucidate the reaction mechanism for the hydroboration reaction, we conducted kinetic studies for the hydroboration of benzophenone (Ph_2CO) in the presence of **1** and HBpin. Thermodynamic parameters ($\Delta G^\ddagger$, $\Delta H^\ddagger$, $\Delta S^\ddagger$) for the second step could be obtained using the Eyring plot. Compound **7** was synthesized by the method similar to that as shown in Scheme 3.2a and reacted with excess HBpin to obtain a pseudo first-order plot of ln[**7**] against time at various temperatures (Appendix B, Figure B3-1). Based on the determined rate constant k for each temperature as shown in Figure B3-1, we obtained the Eyring plot for the reaction (Appendix B, Table B3-1, Figure B3-2).

DFT calculations were also carried out for the catalytic hydroboration reaction (See Appendix C, Figure C1-1 for full energy profile).[13] Theoretical calculations for the second step gave an energetically probable pathway involving a stepwise σ-bond metathesis (Figure 3.5) which was akin to the proposed mechanism for the reaction between Et_3SiH and $HB(C_6F_5)_2$.[8] The two transition states (TS3 and TS4) encompass an H-bonding interaction between the B and P atoms, consistent with the polarized natural bond orbital (NBO) atomic-charge distribution (P = +1.39, O = -0.86).[14] The differences between TS3 and TS4 lie in the elongation of the P-O and the B-H bonds in TS4, as well as the stronger P-H and B-O interactions (Table 3.2). In addition, the bonding interactions among the P, B, H and O atoms were confirmed by Wiberg bond index (WBI) values obtained based on NBO analysis (Table 3.2).[13] The experimentally determined thermodynamic parameters ($\Delta H^\ddagger = +13.0 \pm 0.6$ kcal/mol, $\Delta G^\ddagger_{(298)} = +23.4 \pm 1.2$ kcal/mol, $\Delta S^\ddagger = -34.9 \pm 2.0$ e.u) agreed reasonably well with the theoretical calculated values ($\Delta H^\ddagger = +9.5$ kcal/mol, $\Delta G^\ddagger_{(298)} = +25.1$ kcal/mol, $\Delta S^\ddagger = -52.3$ e.u.).
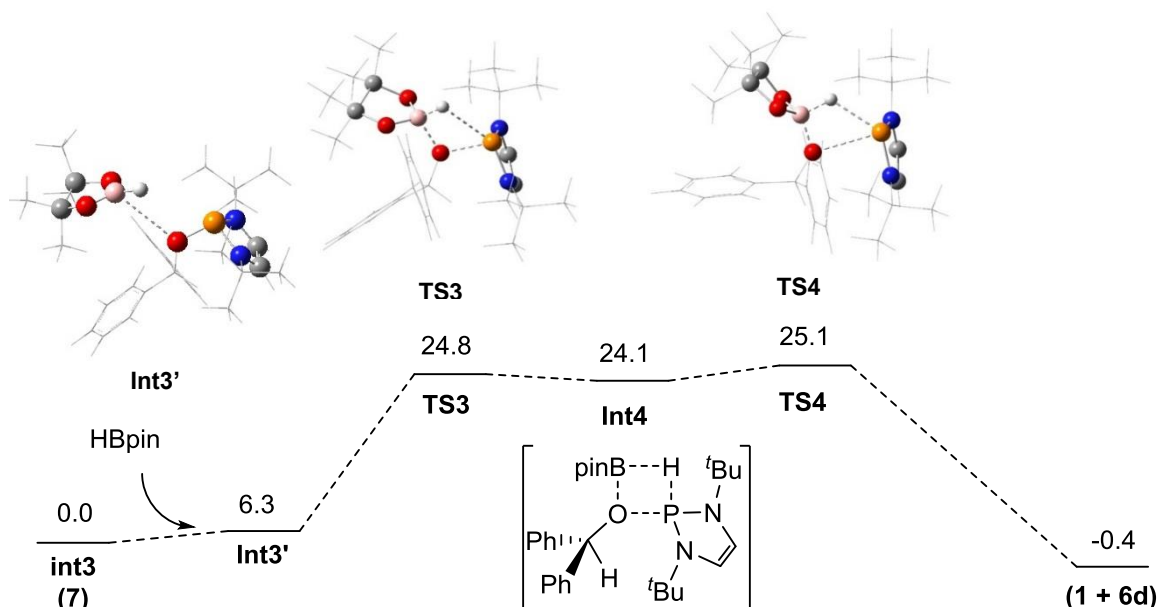
Figure 3.5   DFT-calculated free energy profile (kcal/mol) in CH$_3$CN at 298 K for the reaction between **7** and HBpin as determined at the B3LYP-D3(SCRF)/B2//B3LYP-D3/B1 level. B1: 6-311+G(d,p) for B, N, O, P and 6-31+G(d,p) for C,H. B2: 6-311+G(d,p). Atom sphere colours: C = grey; N = blue; P = orange; H = white; O = red; B = pink.

Table 3.2   NBO analysis for the metathesis process from **Int3** to products (**1 + 6d**) as determined at the B3LYP/6-311+G(d,p) level of theory.

	Int3'	TS3	Int4	TS4
P-O distance (Å)	1.697	1.975	2.012	2.679
WBI	0.6531	0.3907	0.3636	0.0631
P-H distance (Å)	3.311	2.619	2.620	2.238
WBI	0.0015	0.0148	0.0159	0.1089
B-H distance (Å)	1.179	1.208	1.213	1.275
WBI	0.9591	0.9002	0.8952	0.7523
B-O distance (Å)	3.196	1.705	1.658	1.473
WBI	0.0103	0.4179	0.4532	0.6642

Further analysis of the catalytic reactions was performed using deuterated pinacolborane (DBpin) to examine deuterated kinetic isotope effects (DKIEs) for the reaction with benzophenone. A normal DKIE of 2.69 was observed based on the rate constants simulated from the kinetic conversion chart (Appendix B, Figure B3-6). We also carried out the same reaction using ^{18}O-labelled benzophenone and gave a ^{16}O/^{18}O KIE value of 1.05.[15] The double KIE reaction with DBpin and **7**(^{16}O) showed the largest KIE value of 2.96, hence, implying that both P-O bond and B-H bond exchange are involved in the rate-determining transition state. The

overall catalytic cycle for hydroboration of aldehydes and ketones could be described as shown in Scheme 3.3.
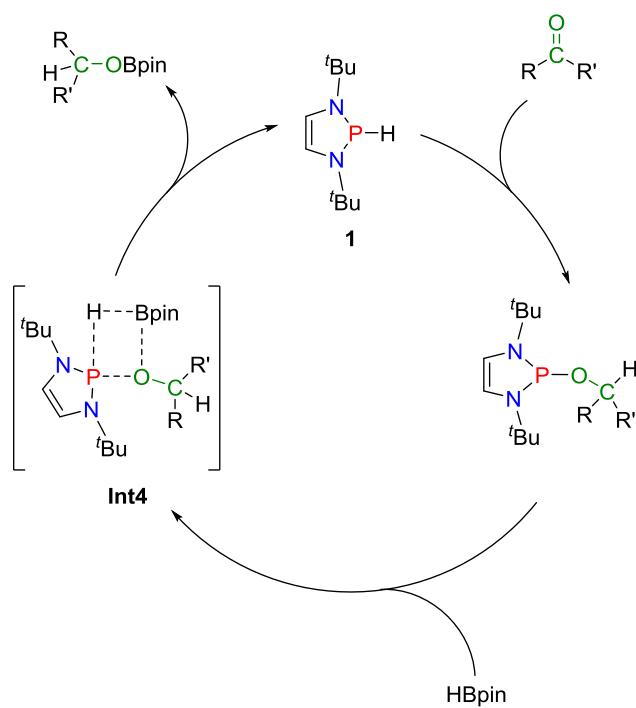
Scheme 3.3 Proposed catalytic cycle for the hydroboration of carbonyl compounds catalysed by **1**.

3.3   Conclusion

In conclusion, we developed a metal-free hydroboration of carbonyl compounds catalysed by **1**. A 0.5 mol% of **1** in CD_3CN could catalyse the hydroboration of benzaldehyde to afford the corresponding boric acid **5** in >99% NMR yield within 0.75 h at room temperature. Screening of various aldehyde substrates was performed and afforded the corresponding hydroborated products under the same catalytic conditions. Due to the steric hindrance and less electrophilic carbonyl carbon, the hydroboration of ketones can only proceed under harsher conditions: 10 mol% of **1** at 90 ^{o}C in CD_3CN.

To elucidate the mechanism, we examined two stoichiometric reactions. The first involves the insertion of the P-H bond of **1** into the C=O bond of PhCHO to form an alkoxyphosphine derivative **4**. Subsequently, σ-bond metathesis occurs at the exocyclic P-O bond in the presence of HBpin to yield desired boric ester and **1**. We also performed DKIE studies and DFT calculations, which indicated that cleavage of both the P-O and B-H bonds are involved in the rate-determining transition steps in a nearly concerted pathway.

3.4   Experimental Section

3.4.1   *Synthesis, physical and spectroscopic data for all new compounds*

*General considerations***:** All reactions were performed under an atmosphere of argon by using standard Schlenk or dry box techniques. Solvents were dried over Na metal, K metal or CaH_2. Reagents were of analytical grade, obtained from commercial suppliers and used without further purification. ^{1}H, ^{13}C, ^{11}B, and ^{19}F NMR spectra were obtained with a Bruker AV 400 or AVIII 400 MHz BBFO2 spectrometers at 298 K unless otherwise stated. Coupling constants *J* are given in Hz. Electrospray ionization (ESI) mass spectra were obtained at the Mass Spectrometry Laboratory at the Division of Chemistry and Biological Chemistry, Nanyang Technological University. Melting points were measured with OptiMelt (Stanford Research Systems). Compounds **1**, **4**, and **7** were prepared according to the literature procedures (refer to Chapter 1 reference 52). All aldehyde and ketone substrates are commercially available either from Sigma-Aldrich or Tokyo Chemical Industry (TCI). The spectroscopic data for products **5a-b, 5i-j, 5l, 5n, 6b-d, 6i-j** were identical to those reported in the literature.[10d,e] All new compounds were isolated by removing volatiles under vacuum for several hours.

General catalytic procedures for the hydroboration of various aldehydes **5***:* Compound **1** (0.3 mL of 0.025 M of **1** in CD_3CN, 0.0075 mmol), aldehyde **5** (1.50 mmol), HBpin (0.22 mL, 1.54 mmol) and the internal standard 1,3,5-trimethoxybenzene (10 mg) were loaded into a dried Carius NMR tube under argon atmosphere. The tube was sealed, shaken and monitored by NMR spectroscopy. The corresponding borate esters **5c**-**f**, **5i**-**j**, **5l** were isolated by removing volatiles under vacuum for several hours. Isolated yields are given in parenthesis.
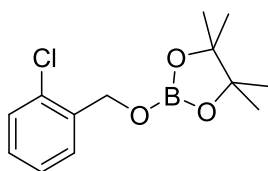
5c

5c (87%): Colourless liquid.

^{1}H NMR (400 MHz, CDCl$_3$): δ = 7.51 (d, ^3J = 7.6 Hz, 1H, Ar*H*), 7.32 – 7.18 (m, 3H, Ar*H*), 5.02 (s, 2H, C*H$_2$*), 1.27 (s, 12H, C*H$_3$*).

^{13}C NMR (100 MHz, CDCl$_3$): δ = 24.6 (*C*H$_3$), 64.1 (*C*H$_2$), 83.1 (*C*(CH$_3$)$_2$), 126.8 (*C*H), 127.7 (*C*H), 128.4 (*C*H), 129.0 (*C*H), 132.0 (Ar*C*-R), 136.8 (*C*-Cl).

^{11}B NMR (128 MHz, CDCl$_3$): δ = 22.5

HRMS (ESI): *m/z* calcd for C$_{13}$H$_{19}$BO$_3$Cl: 269.1116 [(*M*+*H*)]$^+$; found: 269.1112.
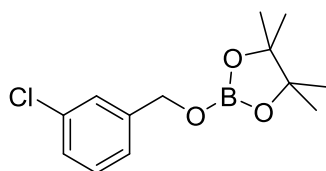
5d

5d (88%): Colourless liquid.

^{1}H NMR (400 MHz, CDCl$_3$): δ = 7.34 (s, 1H, Ar*H*), 7.20 – 7.17 (m, 3H, Ar*H*), 4.86 (s, 2H, C*H$_2$*), 1.23 (s, 12H, C*H$_3$*).

^{13}C NMR (100 MHz, CDCl$_3$): δ = 24.6 (*C*H$_3$), 65.8 (*C*H$_2$), 83.0 (*C*(CH$_3$)$_2$), 124.7 (*C*H), 126.7 (*C*H), 127.4 (*C*H), 129.6 (*C*H), 134.2 (Ar*C*-R), 141.3 (*C*-Cl).

^{11}B NMR (128 MHz, CDCl$_3$): δ = 22.4.

HRMS (ESI): *m/z* calcd for C$_{13}$H$_{19}$BO$_3$Cl: 269.1116 [(*M*+*H*)]$^+$; found: 269.1112.
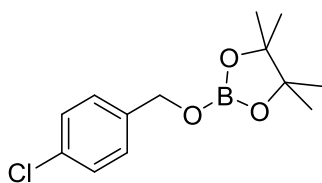
5e

5e (80%): Colourless liquid.

^{1}H NMR (400 MHz, CDCl$_3$): δ = 7.28 (s, 4H, ArH), 4.88 (s, 2H, CH_2), 1.25 (s, 12H, CH_3).

^{13}C NMR (100 MHz, CDCl$_3$): δ = 24.7 (*C*H$_3$), 66.0 (*C*H$_2$), 83.1 (*C*(CH$_3$)$_2$), 128.2 (*C*H), 128.5 (*C*H), 133.1 (Ar*C*-R), 137.8 (*C*-Cl).

^{11}B NMR (128 MHz, CDCl$_3$): δ = 22.4.

HRMS (ESI): *m/z* calcd for C$_{13}$H$_{19}$BO$_3$Cl: 269.1116 [(*M*+*H*)]$^+$; found: 269.1107.
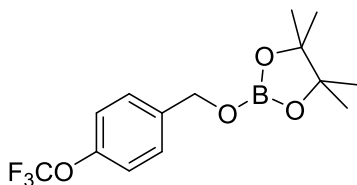
5f

5f (92%): Colourless liquid.

^{1}H NMR (400 MHz, CDCl$_3$): δ = 7.37 (d, ^3J = 8.8 Hz, 2H, ArH), 7.18 (d, ^3J = 8.8 Hz, 2H, ArH), 4.92 (s, 2H, CH_2), 1.26 (s, 12H, CH_3).

^{13}C NMR (100 MHz, CDCl$_3$): δ = 24.7 (*C*H$_3$), 66.0 (*C*H$_2$), 83.2 (*C*(CH$_3$)$_2$), 120.6 (q, $^{C\text{-}F}J$ = 257.6 Hz, O*C*F$_3$), 121.0 (*C*H), 128.2 (*C*H), 138.1 (Ar*C*-R), 148.6 (*C*-OCF$_3$).

^{11}B NMR (128 MHz, CDCl$_3$): δ = 22.4.

^{19}F NMR (376 MHz, CDCl$_3$): δ = -58.0.

HRMS (ESI): *m/z* calcd for C$_{14}$H$_{19}$BO$_4$F$_3$: 319.1328 [(*M*+*H*)]$^+$; found: 319.1336.
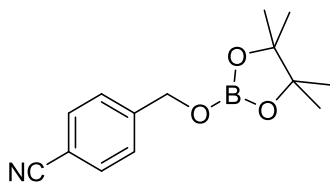
5g

5g (82%): Colourless solid; M.p.: 93.4^{o}C.

¹H NMR (400 MHz, CDCl$_3$): δ = 7.63 (d, ^3J = 8.0 Hz, 2H, ArH), 7.45 (d, ^3J = 8.0 Hz, 2H, ArH), 4.98 (s, 2H, CH_2), 1.27 (s, 12H, CH_3).

¹³C NMR (100 MHz, CDCl$_3$): δ = 24.7 (*C*H$_3$), 65.9 (*C*H$_2$), 83.5 (*C*(CH$_3$)$_2$), 111.3 (*C*CN), 119.0 (*C*N), 127.0 (*C*H), 132.3 (*C*H), 144.7 (Ar*C*-R).

¹¹B NMR (128 MHz, CDCl$_3$): δ = 22.4.

HRMS (ESI): *m/z* calcd for C$_{14}$H$_{19}$BNO$_3$: 260.1458 [(*M*+*H*)]$^+$; found: 260.1462.
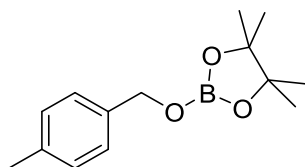
5h

5h (81%): Colourless liquid.

¹H NMR (400 MHz, CDCl$_3$): δ = 7.24 (d, ^3J = 8.0 Hz, 2H, ArH), 7.13 (d, ^3J = 8.0 Hz, 2H, ArH), 4.88 (s, 2H, CH_2), 2.33 (s, 3H, Ar-CH_3), 1.26 (s, 12H, CH_3).

¹³C NMR (100 MHz, CDCl$_3$): δ = 21.3 (*C*H$_3$), 24.8 (*C*H$_3$), 66.7 (*C*H$_2$), 83.0 (*C*(CH$_3$)$_2$), 127.0 (*C*H), 129.1 (CH), 136.4 (*C*-Me), 137.1 (Ar*C*-R).

¹¹B NMR (128 MHz, CDCl$_3$): δ = 22.4.

HRMS (ESI): *m/z* calcd for C$_{14}$H$_{22}$BO$_3$: 249.1662 [(*M*+*H*)]$^+$; found: 249.1657.
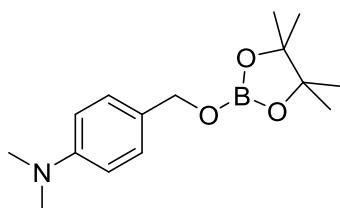
5k

5k (80%): Colourless liquid.

¹H NMR (400 MHz, CDCl$_3$): δ = 7.22 (d, ^3J = 8.8 Hz, 2H, ArH), 6.68 (d, ^3J = 8.8 Hz, 2H, ArH), 4.80 (s, 2H, CH_2), 2.90 (s, 6H, N(CH_3)$_2$), 1.24 (s, 12H, CH_3).

¹³C NMR (100 MHz, CDCl$_3$): δ = 24.6 (*C*H$_3$), 40.6 (*C*H$_3$), 66.7 (*C*H$_2$), 82.7 (*C*(CH$_3$)$_2$), 112.4 (*C*H), 127.2 (Ar*C*-R), 128.5 (*C*H), 150.2 (*C*-N).

¹¹B NMR (128 MHz, CDCl$_3$): δ = 22.4.

HRMS (ESI): *m/z* calcd for C$_{15}$H$_{25}$BNO$_3$: 278.1927 [(*M*+*H*)]$^+$; found: 278.1938.
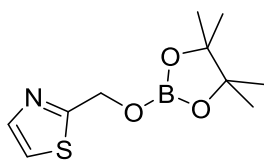
5m

5m (80%): Yellow liquid.

^{1}H NMR (400 MHz, CDCl$_3$): δ = 7.74 (d, ^3J = 3.4 Hz, 1H, =CH), 7.31 (d, ^3J = 3.4 Hz, 1H, =CH), 5.20 (s, 2H, CH_2), 1.28 (s, 12H, CH_3).

^{13}C NMR (100 MHz, CDCl$_3$): δ = 24.7 (CH_3), 64.6 (CH_2), 83.6 (C(CH$_3$)$_2$), 119.1 (CH), 142.7 (CH), 169.8 (C=N).

^{11}B NMR (128 MHz, CDCl$_3$): δ = 22.4.

HRMS (ESI): m/z calcd for C$_{10}$H$_{17}$BNO$_3$S: 242.1022 [(M+H)]$^+$; found: 242.1020.
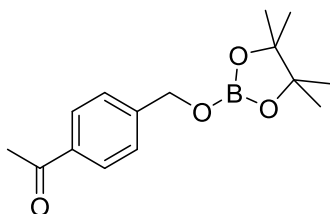
5o

5o (78%): Colourless liquid.

^{1}H NMR (400 MHz, CDCl$_3$): δ = 7.92 (d, ^3J = 8.0 Hz, 2H, Ar-H), 7.42 (d, ^3J = 8.0 Hz, 2H, Ar-H), 4.98 (s, 2H, CH_2), 2.58 (s, 3H, CH_3), 1.26 (s, 12H, CH_3).

^{13}C NMR (100 MHz, CDCl$_3$): δ = 24.8 (CH_3), 26.8 (CH_3), 66.2 (CH_2), 83.3 (C(CH$_3$)$_2$), 126.5 (CH), 128.6 (CH), 136.3 (ArC-R), 144.8 (ArC-R), 197.9 (C=O).

^{11}B NMR (128 MHz, CDCl$_3$): δ = 22.4.

HRMS (ESI): m/z calcd for C$_{15}$H$_{22}$BO$_4$: 277.1611 [(M+H)]$^+$; found: 277.1617.

General catalytic procedures for the hydroboration of various ketones 6: Compound **1** (12 mg, 0.0600 mmol), ketone **6** (0.600 mmol), HBpin (0.11 mL, 0.770 mmol), CD$_3$CN or d$_8$-toluene and the internal standard 1,3,5-trimethoxybenzene (10 mg) were loaded into a dried Carius NMR tube under argon atmosphere. The tube was sealed and placed in an oil bath at 90 ^{o}C. The reaction was

then monitored by NMR spectroscopy. Borate ester product **6a**, **6e-h** were isolated by removing volatiles under vacuum for several hours. Isolated yield is given in parenthesis.
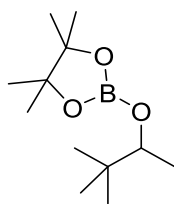
6a

6a (68%): Pale yellow liquid.

^{1}H NMR (400 MHz, CDCl$_3$): δ = 3.87 (q, ^3J = 6.4 Hz, 1H, C*H*), 1.25 (s, 12H, C*H*$_3$), 1.11 (d, ^3J = 6.4 Hz, 3H, C*H*$_3$), 0.87 (s, 9H, C*H*$_3$).

^{13}C NMR (100 MHz, CDCl$_3$): δ = 17.4 (*C*H$_3$), 24.6 (*C*H$_3$), 24.7 (*C*H$_3$), 25.6 (*C*H$_3$), 34.9 (*C*(CH$_3$)$_3$), 78.3 (*C*H), 82.5 (*C*(CH$_3$)$_2$).

^{11}B NMR (128 MHz, CDCl$_3$): δ = 21.9.

HRMS (ESI): *m/z* calcd for C$_{12}$H$_{26}$BO$_3$: 229.1975 [(*M*+*H*)]$^+$; found: 229.1968.
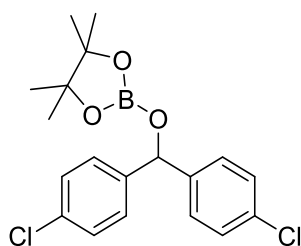
6e

6e (82%): White solid; M.p.: 135 $^{\circ}$C.

^{1}H NMR (400 MHz, CDCl$_3$): δ = 7.28 (s, 8H, Ar*H*), 6.10 (s, 1H, C*H*), 1.20 (s, 12H, C*H*$_3$).

^{13}C NMR (100 MHz, CDCl$_3$): δ = 24.7 (*C*H$_3$), 76.8 (*C*H), 83.4 (*C*(CH$_3$)$_2$), 128.0 (*C*H), 128.7 (*C*H), 133.5 (Ar*C*-R), 141.3 (*C*-Cl).

^{11}B NMR (128 MHz, CDCl$_3$): δ = 22.4.

HRMS (ESI): *m/z* calcd for C$_{19}$H$_{22}$BO$_3$Cl$_2$: 379.1039 [(*M*+*H*)]$^+$; found: 379.1048.

6f
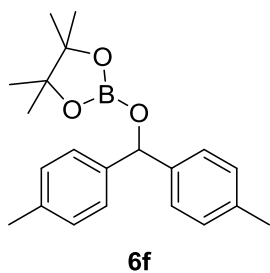
6f (85%): White solid; M.p.: 140 °C.

^{1}H NMR (400 MHz, CDCl$_3$): δ = 7.25 (d, ^3J = 8.0 Hz, 4H, Ar*H*), 7.09 (d, ^3J = 8.0 Hz, 4H, Ar*H*)

6.12 (s, 1H, C*H*), 2.30 (s, 3H, C*H*$_3$), 1.20 (s, 12H, C*H*$_3$).

^{13}C NMR (100 MHz, CDCl$_3$): δ = 21.2, (*C*H$_3$), 24.7 (*C*H$_3$), 77.7 (*C*H), 83.0 (*C*(CH$_3$)$_2$), 126.5 (*C*H),

129.0 (*C*H), 136.9 (Ar*C*-R), 140.6 (*C*-Me).

^{11}B NMR (128 MHz, CDCl$_3$): δ = 22.3.

HRMS (ESI): *m/z* calcd for C$_{21}$H$_{28}$BO$_3$: 339.2132 [(*M*+*H*)]$^+$; found: 339.2125.

6g
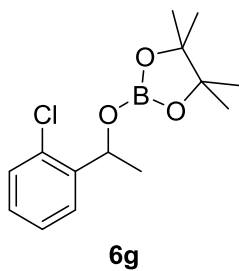
6g (72%): Pale yellow oil.

^{1}H NMR (400 MHz, CDCl$_3$): δ = 7.63 (dd, ^3J = 8.0 Hz, 1H, Ar*H*), 7.31 – 7.25 (m, 2H, Ar*H*), 7.19

– 7.17 (m, 1H, Ar*H*), 5.58 (q, ^3J = 6.4 Hz, 1H, C*H*), 1.48 (d, ^3J = 6.4 Hz, 3H, C*H*$_3$), 1.25 (s, 6H,

C*H*$_3$) 1.22 (s, 6H, C*H*$_3$).

^{13}C NMR (100 MHz, CDCl$_3$): δ = 24.0, (*C*H$_3$), 24.7 (*C*H$_3$), 69.7 (*C*H), 83.0 (*C*(CH$_3$)$_2$), 126.8 (*C*H),

127.2 (*C*H), 128.3 (*C*H), 129.2 (*C*H), 131.2 (Ar*C*-R), 142.4 (*C*-Cl).

^{11}B NMR (128 MHz, CDCl$_3$): δ = 22.0.

HRMS (ESI): *m/z* calcd for C$_{14}$H$_{21}$BO$_3$Cl: 283.1272 [(*M*+*H*)]$^+$; found: 283.1282

6h
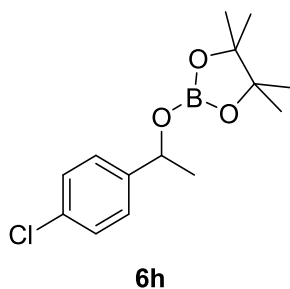
6h (79%): Colourless oil.

^{1}H NMR (400 MHz, CDCl$_3$): δ = 7.29 (s, 4H, ArH), 5.20 (q, ^3J = 6.4 Hz, 1H, CH), 1.46 (d, ^3J = 6.4 Hz, 3H, CH_3), 1.24 (s, 6H, CH_3), 1.21 (s, 6H, CH_3).

^{13}C NMR (100 MHz, CDCl$_3$): δ = 24.7, (CH$_3$), 25.5 (CH$_3$), 72.1 (CH), 83.0 (C(CH$_3$)$_2$), 126.9 (CH), 128.5 (CH), 132.9 (ArC-R), 143.3 (C-Me).

^{11}B NMR (128 MHz, CDCl$_3$): δ = 22.0.

HRMS (ESI): *m/z* calcd for C$_{14}$H$_{21}$BO$_3$Cl: 283.1272 [(*M+H*)]$^+$; found: 283.1278.

3.4.2 Kinetic studies:

General method for Eyring Plot: Compound **7** (23 mg, 0.060 mmol), HBpin (120 μL, 0.827 mmol) were dissolved in CD$_3$CN (0.40 mL) and an internal standard 1,3,5-trimethoxybenzene (10 mg, 0.059 mmol) were loaded into a dried Carius NMR tube and sealed. The reaction was monitored every 3 minutes over a range of temperature range from 40 ^{o}C to 70 ^{o}C. Based on the integration of the aryl proton signals at 7.17 ppm of **7**, the concentration of **7** was plotted against time which follows a pseudo-first order kinetic. The Eyring Plot was also obtained based on the rate at each temperature and plotted against the inverse of time.

General method for kinetic isotope effect (KIE) Studies: DBpin and Ph$_2$CO^{18} were synthesized according to literature reports using D$_2$ and H$_2$O^{18} respectively.[16] O^{18} labeled compound **7-O^{18}** was synthesized following the procedures for the synthesis of **7**. Compound **7** or **7-O^{18}** (0.060 mmol), H(D)Bpin (0.827 mmol) and an internal standard 1,3,5-trimethoxybenzene (10mg, 0.059 mmol) were dissolved in CD$_3$CN (0.40 mL) and loaded into a Carius NMR tube. The reaction was monitored every 3 minutes at 50 ^{0}C. Based on the integration of the aryl proton signals at 7.17

ppm of **7**, the concentration of **7** was plotted against time which follows a pseudo-first order reaction and kinetic isotope effect values (KIE) were determined by the rate constant k for each reaction.

3.5   References

1.   *Handbook of Metathesis*; Grubbs, R. H.; Wenzel, A. G., Eds.; WILEY-VCH Verlag GmBH & Co. KGaA: Weinheim, Germany, 2015.

2.   For selected examples, see: a) Schrock, R. R. *Acc. Chem. Res*. **2014**, *47*, 2457–2466; b) Lin, Y. A.; Boutureira, O.; Lercher, L.; Bhushan, B.; Paton, R. S.; Davis, B. G. *J. Am. Chem. Soc*. **2013**, *135*, 12156–12159; c) *Metathesis in Natural Product Synthesis: Strategies, Substrates and Catalysis*; Cossy, J.; Arseniyadis, S.; Meyer, C., Eds.; WILEY-VCH Verlag GmBH & Co. KGaA: Weinheim, Germany, 2010; d) Sutthasupa, S.; Shiotsuki, M.; Sanda, F. *Polym. J.* **2010**, *42*, 905–915; e) Binder, J.   B.; Raines, R. T. *Curr. Opin. Chem. Biol*. **2008**, *12*, 767–773; f) Liu, X.; Basu, A. *J. Organomet. Chem*. **2006**, *691*, 5148–5154.

3.   For selected reviews, see: a) Fustero, S.; Simón-Fuentes, A.; Barrio, P.; Haufe, G. *Chem. Rev*. **2015**, *115*, 871–930; b)Vougioukalakis, G. C.; Grubbs, R. H. *Chem. Rev*. **2010**, *110*, 1746–1787; c) Samojłowicz, C.; Bieniek, M.; Grela, K. *Chem. Rev*. **2009**, *109*, 3708–3742; d) Schrock, R. R.; Hoveyda, A. H. *Angew. Chem. Int. Ed*. **2003**, *42*, 4592–4633; e) Schrock, R. R. *Chem. Rev*. **2002**, *102*, 145–180; f) Trnka, T. M.; Grubss, R. H. *Acc. Chem. Res*. **2001**, *34*, 18–29; g) Fürstner, A. *Angew. Chem. Int. Ed*. **2000**, *39*, 3012–3043.

4.   For selected reviews, see: a) Fürstner, A. *Angew. Chem. Int. Ed*. **2013**, *52*, 2794–2819; b) Jyothish, K.; Zhang, W. *Angew. Chem. Int. Ed*. **2011**, *50*, 8478–8480; c) Wu, X.; Tamm, M. *Beilstein J. Org. Chem*. **2011**, *7*, 82–93; d) Fürstner, A. *Chem. Commun*. **2011**, *47*, 6505–6511; e) Tamm, M.; Wu, X. *Chem. Today* **2010**, *28*, 60–63.

5.   a) Waterman, R. *Organometallics* **2013**, *32*, 7249–7263; b) Lin, Z. *Coord. Chem. Rev*. **2007**, *251*, 2280–2291.

6.   a) Inagaki, S.; Fukui, K. *J. Am. Chem. Soc*. **1975**, *97*, 7480–7484; b) Woodward, R. B.; Hoffmann, R. *Angew. Chem. Int. Ed*. **1969**, *11*, 781–853; c) Hoffmann, R.; Woodward, R. B. *J. Am. Chem. Soc*. **1965**, *87*, 2046–2048; d) Woodward, R. B.; Hoffmann, R. *J. Am. Chem. Soc*. **1965**, *87*, 395–397.

7.   For selected examples, see: a) Ochi, N.; Nakao, Y.; Sata, H.; Sakaki, S. *J. Phys. Chem. A* **2010**, *114*, 659–665; b) Suresh, C. H.; Koga, N. *Organometallics* **2004**, *23*, 76–80; c) Upton, T. H.; Rappe, A. K. *J. Am. Chem. Soc*. **1985**, *107*, 1206–1218.

8.   Wang, Y.; Chen, W.; Lu, Z.; Li, Z. H.; Wang, H. *Angew. Chem. Int. Ed*. **2013**, *52*, 7496–7499.

9.   Nikonov, G. I.; Vyboishchikov, S. F.; Shirobokov, O. G. *J. Am. Chem. Soc*. **2012**, *134*, 5488–5491.

10.   Cui, J.; Li, Y.; Ganguly, R.; Inthirarajah, A.; Hirao, H.; Kinjo, R. *J. Am. Chem. Soc*. **2014**, *136*, 16764–16767.

11.   For recent examples of catalytic reduction reactions by main-group compounds, see: a) Yang, Z.; Zhong, M.; Ma, X.; De, S.; Anusha, C.; Parameswaran, P.; Roesky, H. W. *Angew. Chem. Int. Ed.* **2015**, *54*, 10225–10229; b) Lampland, N. L.; Pindwal, A.; Neal, S. R.; Schlauderaff, S.; Ellern, A.; Sadow, A. D. *Chem. Sci*, **2015**, *6*, 6901–6907; c) Lampland, N. L.; Hovey, M.; Mukherjee, D.; Sadow, A. D. *ACS Catal.* **2015**, *5*, 4219–4226; d) Mukherjee, D.; Ellern, A.; Sadow, A. D. *Chem. Sci.* **2014**, *5*, 959–964; e) Hadlington, T. J.; Hermann, M.; Frenking, G.; Jones, C. *J. Am. Chem. Soc*. **2014**, *136*, 3028–3031; f) Arrowsmith, M. Hadlington, T. J.; Hill, M. S.; Kociok-Köhn, G. *Chem. Commun*. **2012**, *48*, 4567–4569; g) Blake, A. J.; Cunningham, A.; Ford, A.; Teat, S. J.; Woodward, S. *Chem. Eur. J*. **2000**, *6*, 3586–3594; h) Ford, A.; Woodward, S. *Angew. Chem. Int. Ed*. **1999**, *38*, 335–336.

12.   a) Cho, B. T. *Chem. Soc. Rev*. **2009**, *38*, 443–452; b) *Catalytic Functionalization*; Togni, A.; Grützmacher, H., Eds.; Wiley-VCH Verlag GmbH: Weinheim, Germany, 2001.

13.   Gaussian09 (Revision D.01), Frisch, M. J. et al. Gaussian, Inc.; Wallingford CT, **2009**.

14.   Reed, A. E.; Curtis, L. A.; Weinhold, F. *Chem. Rev*. **1998**, *88*, 899–926.

15.   For examples of ^{18}O-KIE, see a) Angeles-Boza, A. M.; Ertem, M. Z.; Sarma, R.; Ibañez, C. H.; Maji, S.; Llobet, A.; Cramer, C. J.; Roth, J. P. *Chem. Sci*. **2014**, *5*, 1141–1152; b) Angeles-Boza, A. M.; Roth, J. P. *Inorg. Chem*. **2012**, *51*, 4722–4729.

16.   a) Braunschweig, H.; Guethlein, F.; Mailander, L.; Marder, T. B. *Chem. Eur. J.* **2013**, *19*, 14831–14835; b) Zheng, H.; Lejkowski, M.; Hall, D. G. *Chem. Sci.* **2011**, *2*, 1305–1310.

4.1   Introduction

The adverse effects of global warming and climate change have led to various strategies to limit the emission of greenhouse gases, in particular, carbon dioxide (CO_2).[1] A promising methodology in reduction emission of carbon dioxide is the valorisation of CO_2,[2] which involves utilizing CO_2 as a non-toxic, abundant and cheap C1 source for production of valuable chemicals.[3] A notable example is the large-scale methanol production from CO_2, a key concept in the methanol economy.[4] An important aspect in transforming CO_2 requires the activation of the thermodynamically stable C-O bond. Several transition metal catalysts were shown to reduce CO_2 which afforded useful chemicals including formic acid derivatives, methane, methanol, CO or formaldehyde.[5]

Metal-free catalysis presents another viable method for CO_2 valorisation to the prevailing use of transition metal catalysts.[6] A ground breaking work by Grimme, Stephan, and Erker demonstrated the potential use of FLPs for CO_2 capture.[7] Subsequently, various main group systems have been developed for the activation of CO_2.[8] All in all, the coordination mode of CO_2 can be classified into three main types: a Lewis base (LB) coordinated-CO_2 adduct (**I**), coordination of one Lewis base (LB) and one Lewis acid (LA) to CO_2 (**II**) and lastly, CO_2 with one Lewis base (LB) and two Lewis acid (LA) moieties (**III**) (Figure 4.1a).[9] These coordination modes are known to be key intermediates for the facile activation of CO_2 which is evident from the hydrosilylation of CO_2 catalysed by NHC. Ying and co-workers suggest that the initial step for the catalytic cycle involves the formation NHC-CO_2 adduct based on experimental and theoretical studies.[10] Recently, Li and co-workers proposed a new activation mode which involves an S_N2-type mechanism in involving activation of Si-H bond by NHC-CO_2 adduct, allowing hydride transfer to CO_2 in a concerted manner.[11] However, DFT study by Wang and co-workers proposed that the first step of the catalytic reaction should involve activation of Si-H by NHC.[12]

Another activation mode involves the direct insertion of E-H bond of main group hydrides to the C=O bond in CO_2 to produce formate derivatives. This has been reported for group 13 and 14 elements which include B, Al, Ga, Ge, and Sn (Figure 4.1b).[13] The insertion process occurs due to the presence of the polarized $E(\delta+)$–$H(\delta-)$ bond, which hence, exhibits hydride donor ability and electrophilicity at the E centre. In the case of group 15 elements, Cavell and co-workers reported the insertion of CO_2 into the P(V)-N bond of $Me(F_3C)_3P$-NMe_2 to yield a hexacoordinated phosphorus species (Figure 4.2a, **IV**).[14] Similarly, Stephan and co-workers showed that the strained amido-phosphoranes reacted readily with CO_2 to afford P(V) heterocycles (Figure 4.2a, **Va-b**).[15] More recently, Fontaine and co-workers described activation of CO_2 using phosphazenes and analogously, a CO_2 insertion into P(V)-N was also proposed as the transition state (Figure 4.2a, **VI**).[16] In those examples, the electrophilic P(V) centre could coordinate to the O of CO_2 while the nucleophilic N centre could coordinate to C of CO_2, which is similar to coordination mode **II** as shown in Figure 4.1a.

a) *Basic mode of activation* b) *[E]-H insertion*
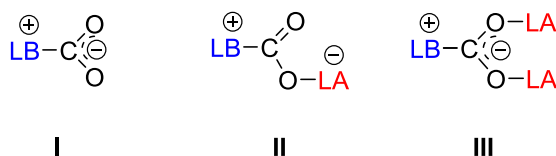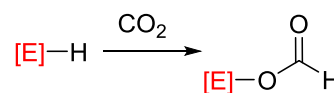
Figure 4.1 a) Three main types of coordination mode of CO_2 by main group compounds; b) direct [E]-H insertion into CO_2.

a) *P^V-N bond CO$_2$ insertion*

| IV | Va | Vb | VI |
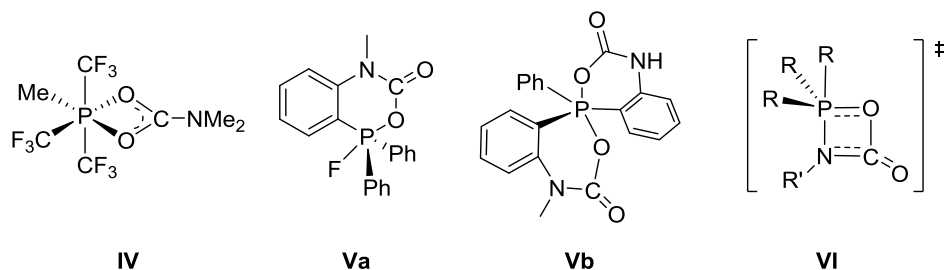
b) *P^{III}-N bond CO$_2$ insertion*
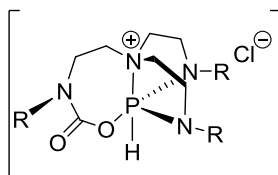
Figure 4.2   a) Products / transition state for P^V-N insertion into CO$_2$; b) Proposed intermediate for the azaphosphatrane-catalysed cyclic carbonate formation using CO$_2$ and epoxides.

Sequestration of CO$_2$ using R$_3$P(III) is relatively uncommon.[17] In 2013, Martinez and Dufaud demonstrated the catalytic activity of azaphosphatranes for the synthesis cyclic carbonate using CO$_2$ and epoxides. Notably, they proposed a mechanistic pathway involving a CO$_2$ insertion into the P-N bond, forming a tricyclic phosphorylcarbamate intermediate (Figure 4.2b).[18] The insertion of a P-H bond into CO$_2$, or in other words, hydrophosphination of CO$_2$, to yield phosphorus formate, R$_2$P-OCOH (similar to Figure 4.1b) was not reported as R$_3$P(III) are generally categorized as a nucleophile, hence, coordination with CO$_2$ should generate Lewis base-CO$_2$ adduct (Figure 4.1a).[3d, 8h, 8q,]

As aforementioned, the umpolung nature of the P-H bond in compound **1** was well established as evident from the reaction of **1** with aldehydes and ketones. Therefore, we hypothesized that compound **1** could undergo similar reaction with CO$_2$, hence, achieving hydrophosphination. Further addition of a suitable hydride source could also regenerate compound **1** and afford a formate derivative, originating from CO$_2$ as the C1 source. In this chapter, we discuss the catalytic hydrosilylation of CO$_2$ as well as its application in the catalytic N-formylation of amines.

4.2 Results and Discussions

4.2.1 Stoichiometric Reaction between 1, CO_2 and Ph_2SiH_2

When a CD_3CN solution of compound **1** was exposed to CO_2 (1 atm) (Scheme 4.1a), a dark brown solution was formed, showing a singlet peak at 111.5 ppm in the ^{31}P NMR spectrum. After work-up, compound **8** was isolated in 93% yield. The ^1H NMR spectrum of **8** showed a distinctive peak at 8.10 ppm (Appendix A, Figure A4-1a) and the $^{13}C\{^1H\}$ spectrum showed a singlet at 164.2 ppm, which implies the presence of a formate moiety (Appendix A, Figure A4-1b). We also performed the reaction using ^{13}C-labelled carbon dioxide ($^{13}CO_2$) which gave the corresponding product **8**-^{13}C. In the ^1H NMR spectrum, a doublet appeared at 8.13 ppm due to the coupling ($^1J_{C-H} = 210.8$ Hz) with the ^{13}C atom (Appendix A, Figure A4-2a) and an intense peak at 164.4 ppm corresponding to the ^{13}C atom in the formate moiety was observed in the $^{13}C\{^1H\}$ NMR spectrum (Appendix A, Figure A4-2b). The solid-state IR spectrum of **8** displays a peak at 1720 cm^{-1} which could correspond to the C=O stretching frequency (Appendix A, Figure A4-3). The solid-state molecular structure of **8** was confirmed by X-ray diffraction analysis (Figure 4.3). The P1-O1 distance (1.808(1) Å) is much longer than a typical P-O single bond (1.63 Å), hence, implying a certain degree of zwitterionic character **8'**. This is evident from the ^{31}P NMR for compound **8** (111.5 ppm) which slightly more downfield as compared to that of compound **7** (93.0 ppm).

Similar to the case for the hydroboration of aldehydes and ketones, we hypothesized that the presence of hydride source could regenerate **1** which hence, could be employed as a catalyst for the reduction of CO_2. To examine our hypothesis, we studied the reaction of compound **8** with diphenylsilane (Ph_2SiH_2) (Scheme 4.1b) given that the formation of the strong Si-O bond could favour the reaction thermodynamically. The addition of half equivalent of Ph_2SiH_2 to compound **8** afforded $Ph_2Si(OCHO)_2$ as the major product with some formation of siloxane, $(Ph_2SiO)_3$ in a ratio of 2.3: 1 (Figure 4.4a). $Ph_2Si(OCHO)_2$ was further converted to $(Ph_2SiO)_3$ after 18 h at ambient temperature which was confirmed by both ^1H and ^{29}Si NMR spectroscopy (Figure 4.4b-c).[19] The formation of $Ph_2Si(OCHO)_2$ suggested that the formate moiety was transferred from **8** to

silane and regenerate **1**. However, only the peak for compound **8** was observed during the reaction, presumably due to the rapid reaction between **1** and CO_2.
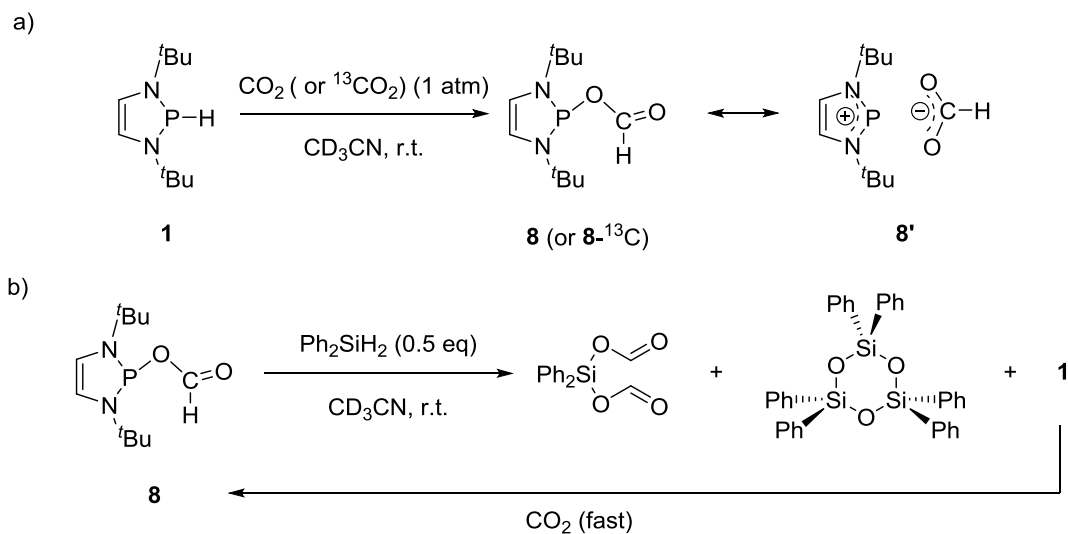
Scheme 4.1 Stoichiometric reactions performed at r.t. between a) **1** and CO_2 (or $^{13}CO_2$); b) compound **8** and Ph_2SiH_2 (0.5 eq).
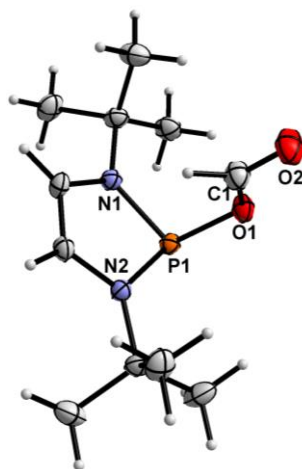
Figure 4.3 ORTEP drawing of **8** with thermal ellipsoids set at 30% probability level. Selected bond lengths [Å] and angles [°] for **8**: P1-N1 1.6829(11) P1-N2 1.6828(11) P1-O1 1.801(1), O1-C1 1.3189(2), C1-O2 1.1954(2), N1-P1-N2 89.77(5) P1-O1-C1 123.11(9) O2-C1-O1 124.07(1).
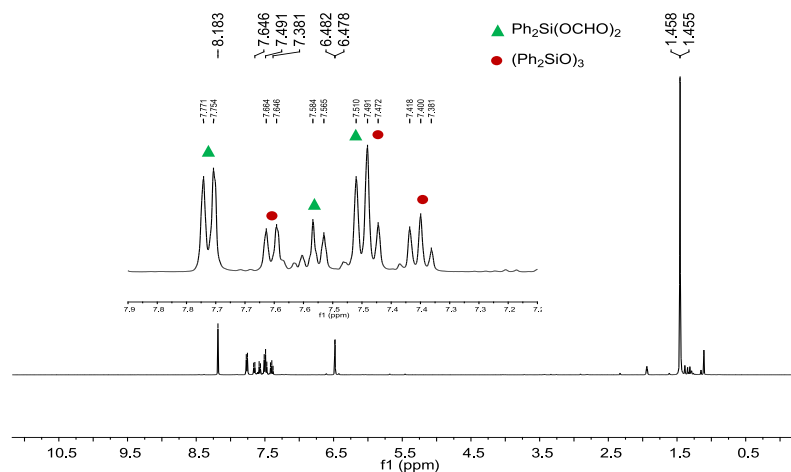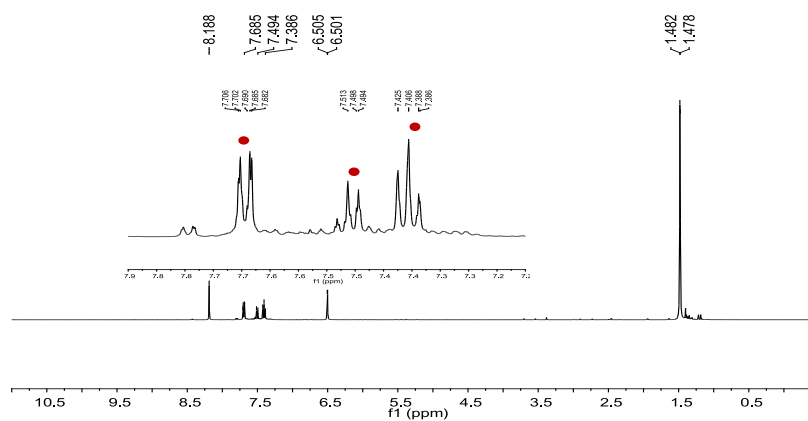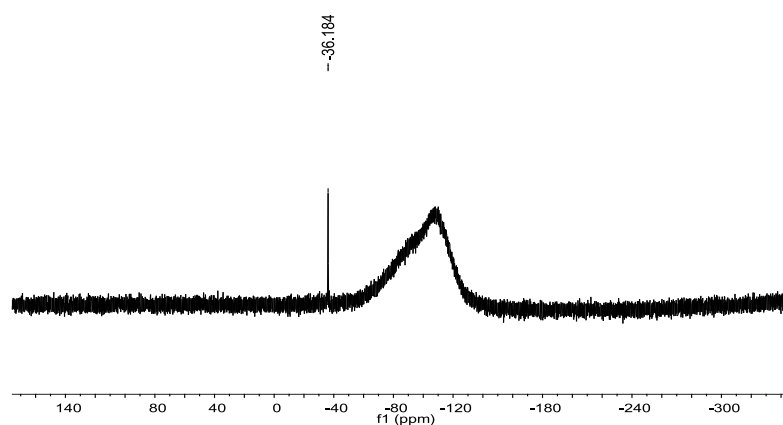
Figure 4.4 The ^{1}H NMR spectra in CD$_3$CN for the a) stoichiometric reaction between **8** and 0.5 eq Ph$_2$SiH$_2$; b) conversion of Ph$_2$Si(OCHO)$_2$ to (Ph$_2$SiO)$_3$ upon standing for 18 h;c) ^{29}Si NMR taken after 18 h shows a clean formation of (Ph$_2$SiO)$_3$. (Enlarge versions of the phenyl region were shown in the inset).

4.2.2   Catalytic Hydrosilylation of CO$_2$ using 1

With the above stoichiometric result in mind, we attempted the hydrosilylation of CO$_2$ using a catalytic amount of **1**. CO$_2$ (45 mg) were introduced into a dried Carius NMR tube filled with a CD$_3$CN solution of Ph$_2$SiH$_2$ and 5 mol% of **1**. The ^{1}H NMR spectroscopy showed the almost complete conversion of Ph$_2$SiH$_2$ to Ph$_2$Si(OCHO)$_2$ (> 95%) with only small amount (< 5%) of siloxane, (Ph$_2$SiO)$_3$ after 1 h (Scheme 4.2, Figure 4.5a-b). The ^{29}Si NMR spectrum was measured after the reaction (Figure 4.5c) and corresponded well with the reported data[20] as well as that obtained from the independent synthesis of Ph$_2$Si(OCHO)$_2$ from Ag(OCHO) and Ph$_2$SiCl$_2$. When we employed ^{13}CO$_2$ for the same reaction, a clean formation of Ph$_2$Si(O^{13}CHO)$_2$ was confirmed based on the characteristic doublet peak at δ = 8.29 ppm corresponding to the coupling with ^{13}C ($^1J_{\text{C-H}}$ = 232.5 Hz) in the ^{1}H NMR spectrum and an intense peak (δ = 160.7 ppm) was observed in the ^{13}C NMR spectrum corresponding to the -^{13}CHO formate moiety (Figure 4.6a-b).
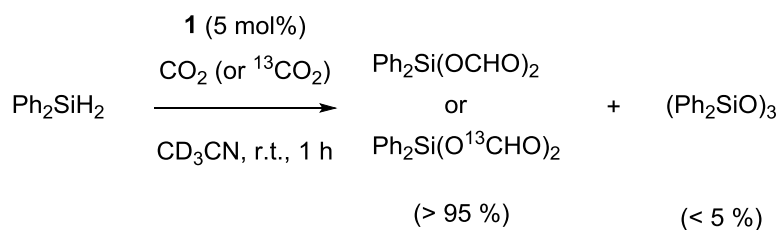
Scheme 4.2   Hydrosilylation of CO$_2$ employing 5 mol% of **1**.

a)
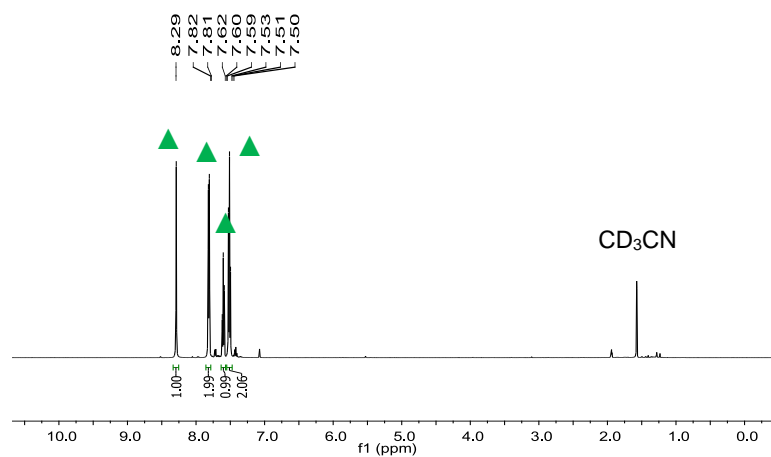
b)
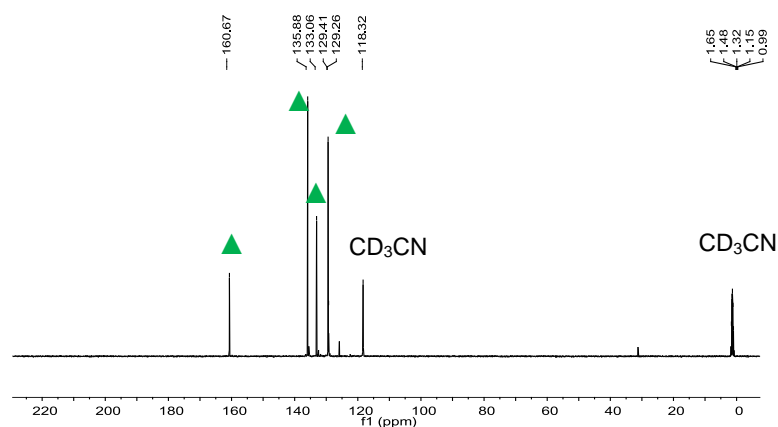
c)
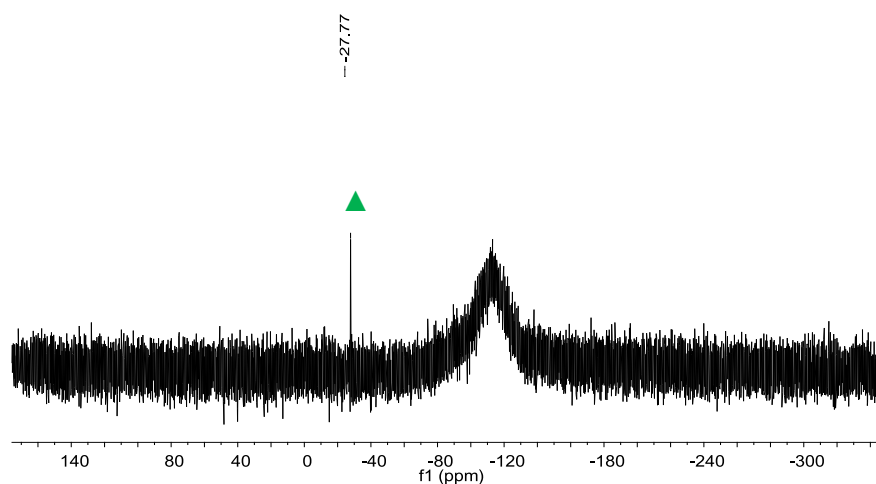
Figure 4.5   a) The ^{1}H NMR spectrum in CD_3CN, for the catalytic hydrosilylation of CO_2 using 5 mol% of **1**. [▲: $Ph_2Si(OCHO)_2$]; b) The ^{13}C NMR spectrum in CD_3CN, for catalytic hydrosilylation of CO_2 using 5 mol% of **1** [▲: $Ph_2Si(OCHO)_2$]; c) The ^{29}Si NMR spectrum for catalytic hydrosilylation of CO_2 using **1**. [▲: $Ph_2Si(OCHO)_2$]

a)

b)
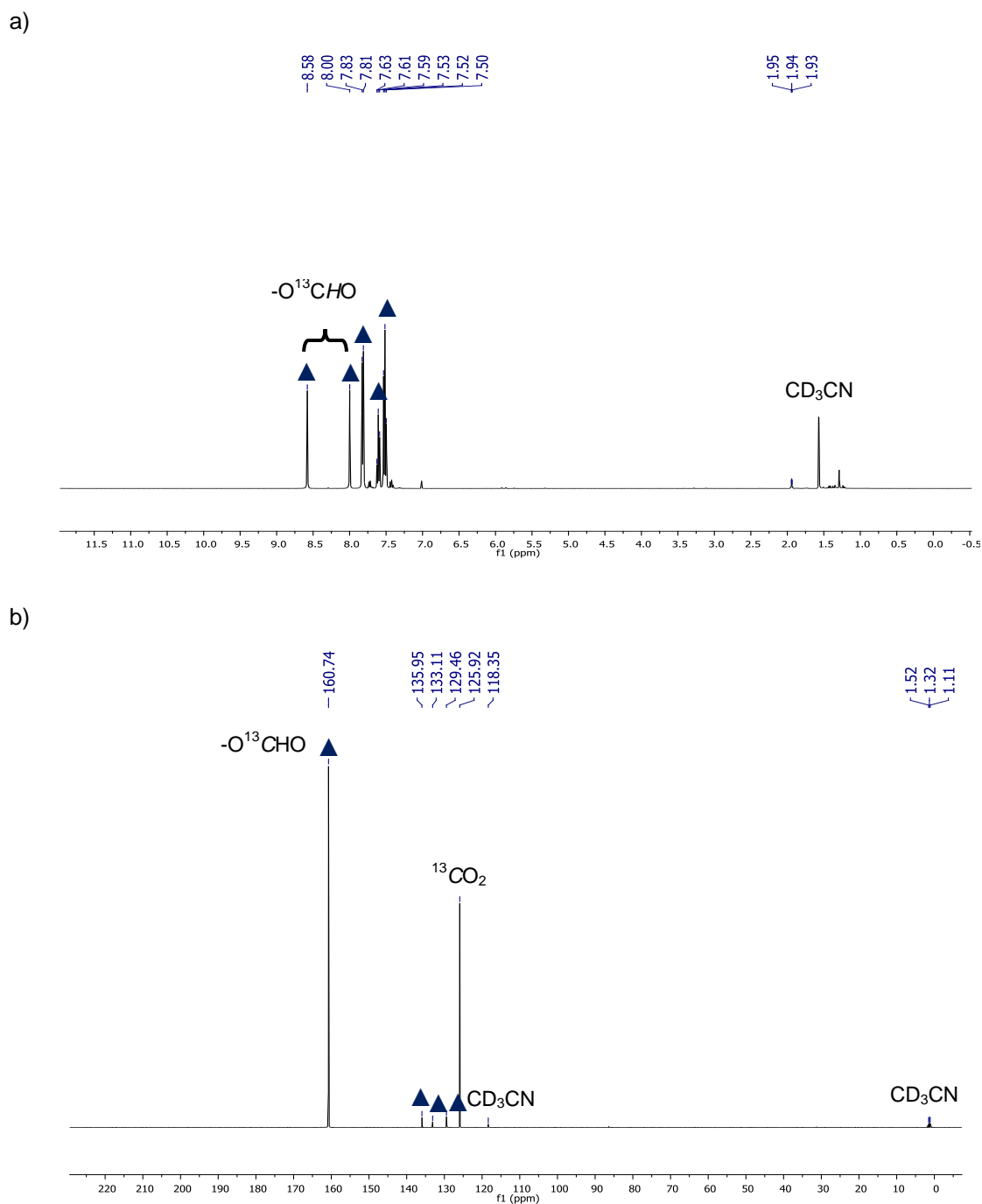
Figure 4.6 (a) The ^{1}H NMR spectrum for the catalytic hydrosilylation of $^{13}CO_2$ after 1 h. A peak for the formyl proton with a C-H coupling constant of 232.5 Hz was observed at 8.29 ppm; (b) The $^{13}C\{^1H\}$ NMR spectrum for catalytic hydrosilylation of $^{13}CO_2$.

4.2.3 N-formylation of amines using CO_2 catalyzed by **1**

In recent years, several organocatalysts have shown to catalyse the N-formylation or N-methylation of amines using CO_2 as the C1 source (Figure 4.7).[21] In these reactions, formate derivatives are considered to be an important intermediate in the reaction mechanism.[17-22] Hence,

79

we examined a one-pot N-formylation of amines using **1** as the catalyst. To examine the reaction, N-methylaniline was used as a model substrate. Without any catalysts, no desired product was obtained (Table 4.1, entry 1). When 1 mol% of **1** was employed, N-methyl-N-phenylformamide was obtained in 26% yield (Table 4.1, entry 2). 5 mol% of **1** afford the corresponding N-methyl-N-phenylformamide in excellent yield (95%) after 4 h (Table 4.1, entry 3). The use of one equivalent of Ph_2SiH_2 or in neat condition resulted in slightly lower yields after 4 h (Table 4.1, entries 4 – 5). Screening of several hydride sources revealed that Ph_2SiH_2 is the most suitable for the reaction (Table 4.1, entries 6 – 8).
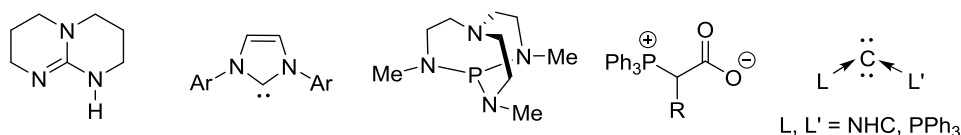
Figure 4.7   Organocatalysts employed in the N-formylation or N-methylation of CO_2.

Table 4.1   Optimisation of the reaction condition for the N-formylation of N-methylaniline[a].
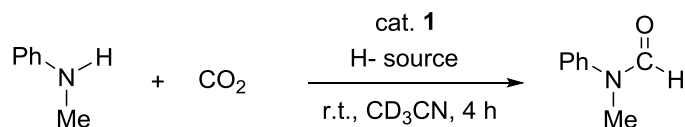
Entry	Cat loading of 1	H- Source	Equivalent	Yield (%)[b]
1	None	Ph_2SiH_2	3	0
2	1 mol%	Ph_2SiH_2	3	26
3	**5 mol%**	**Ph_2SiH_2**	**3**	**95**
4	5 mol%	Ph_2SiH_2	1	69
5	5 mol%	Ph_2SiH_2	neat	50
6	5 mol%	$PhSiH_3$	3	66
7	5 mol%	Et_3SiH	3	0
8	5 mol%	HBpin	3	54

(a)   Reaction conditions: N-methylaniline (0.45 mmol), CO_2 (45 mg), CD_3CN (0.4 ml). Catalyst loading relative to N-methylaniline.

(b)   Yields are determined by ^{1}H NMR using 1,3,5-trimethoxybenzene as an internal standard.

Having the optimised condition in hand, we conducted substrate screening with a variety of secondary amines (Figure 4.8). Less sterically hindered aliphatic amines gave corresponding N-

formylamines product in excellent yields (**9a**: 95%, **9c**, 94%, **9e**: 94%). On the contrary, bulkier and highly basic amines such as diisopropylamine and 2,2,4,4,-tetramethylpiperidine afforded N-methylated amines (**10b**: 61%, **10d**: 53%). The N-methylated product might be generated by further reduction of the corresponding N-formylamines.[23] Secondary amines containing aryl substituents (**9f–k**) were also tolerated and afforded the corresponding products in good to excellent yields (64–94%). In addition, we also tested primary amines and those were well tolerated to give the corresponding formamides (**9l-u**) in reasonable yields (72–99%). When $^{13}CO_2$ was employed for the N-formylation of N-methylaniline, ^{13}C-labelled N-methyl-N-phenylformamide was formed which was isolated in 64% yield (Figure 4.9).
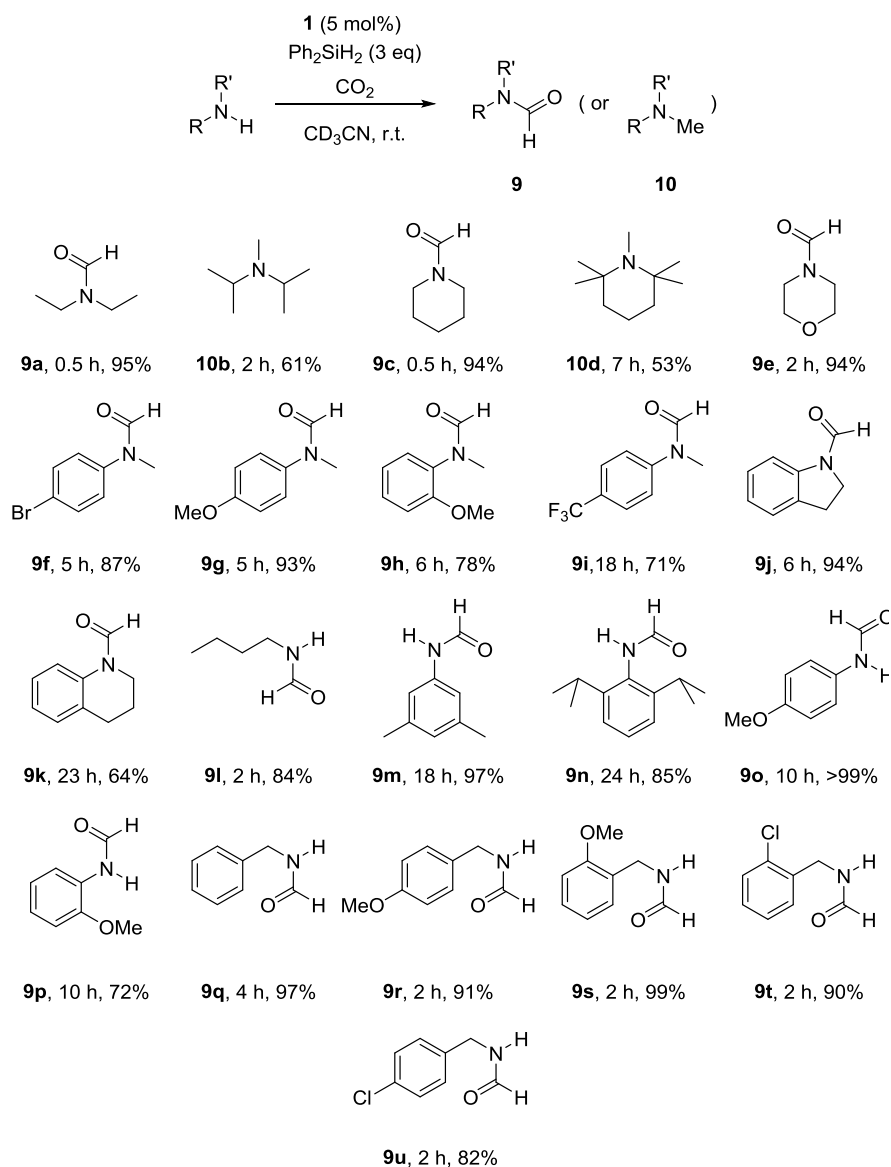
Figure 4.8 NMR yields and reaction times for the N-formylation of amines using Ph_2SiH_2 (3 eq), CO_2 (45 mg) and 5 mol% **1** at r.t.

To elucidate the reaction mechanism, several controlled reactions were performed. Without Ph_2SiH_2, a mixture of N-methylaniline and **1** under CO_2 only afforded compound **8** at room temperature, and no further reaction between **8** and N-methylaniline was observed. The addition of compound **1** to Ph_2SiH_2 did not result in any apparent reactions. We also observed that $Ph_2Si(OCHO)_2$ is relatively unstable in the presence of **1** but much stable in the presence of compound **8**. On the other hand, the addition of N-methylaniline to $Ph_2Si(OCHO)_2$ gave N-methyl-N-phenylformamide in approximately 50% NMR yield, even after 2 h at room temperature in the absence of compound **1** and **8**. Hence, the reaction mechanism can be summarized as follows: firstly, an insertion of P-H bond of **1** into CO_2 to generate **8**; this is followed by formate transfer from **8** to Ph_2SiH_2 to regenerate **1** concomitant with formation of $Ph_2Si(OCHO)_2$; lastly, the reaction of amines with $Ph_2Si(OCHO)_2$ results in the formation of N-formamides and silane products such as silanol and $(Ph_2SiO)_3$ (Scheme 4.3).

a)
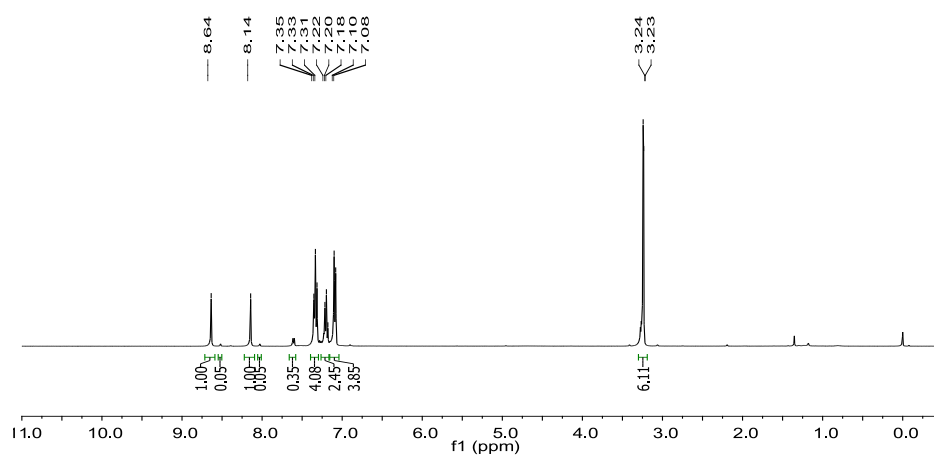
b)
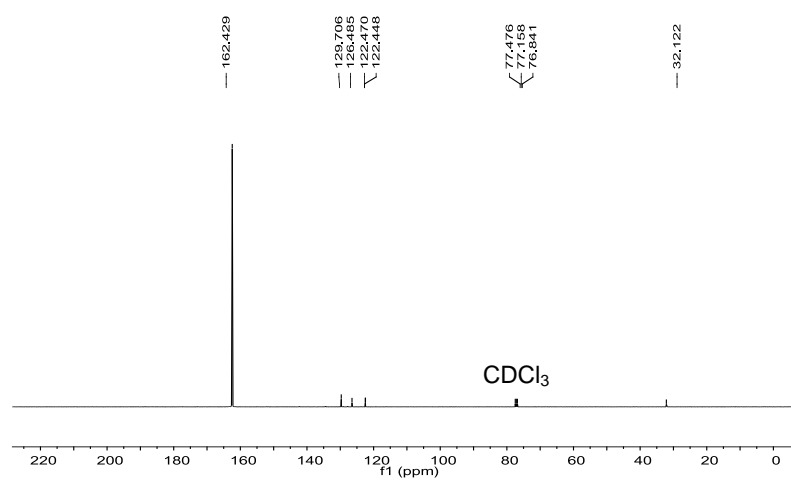
Figure 4.9   a) ^1H NMR spectra of (Ph)(Me)N-^{13}CHO; b) ^{13}C NMR spectra of (Ph)(Me)N-^{13}CHO in $CDCl_3$.
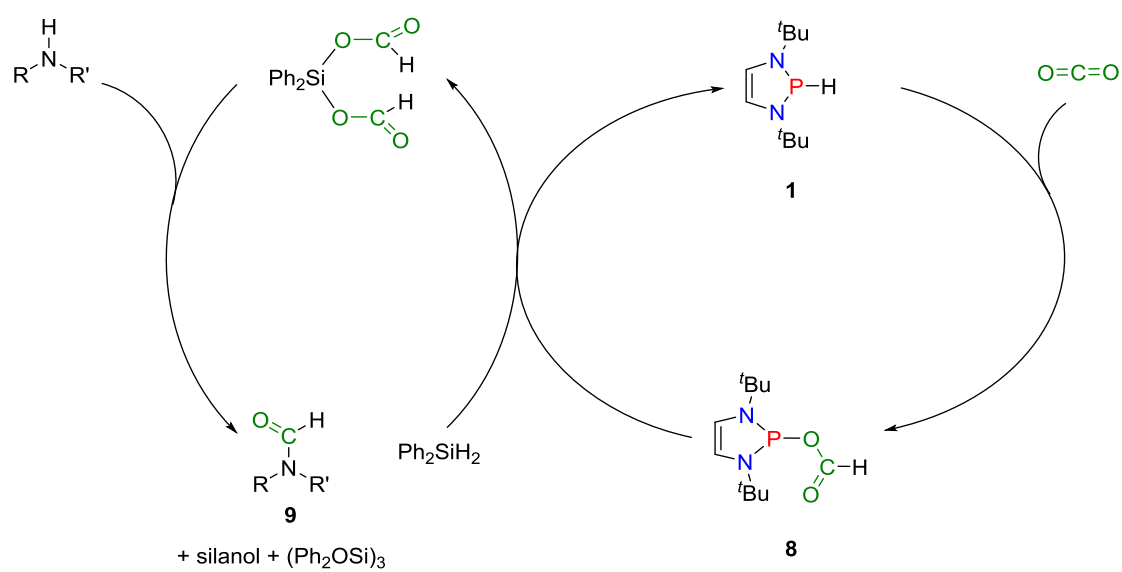
Scheme 4.3 Plausible mechanism for the catalytic N-formylation of amines using CO_2 by 5 mol% of **1**.

4.3   Conclusion

In conclusion, we showed that **1** could undergo hydrophosphination with CO_2 to afford compound **8** which has been successfully characterized by X-ray diffraction analysis, IR and NMR spectroscopy. Subsequent formate transfer from compound **8** to Ph_2SiH_2 give $Ph_2Si(OCHO)_2$ as the hydrosilylated product. These stoichiometric reactions can be extended to a catalytic scale: 5 mol% of **1** could catalyse the hydrosilylation of CO_2 at room temperature to afford $Ph_2Si(OCHO)_2$ as the major product. The formation of $Ph_2Si(OCHO)_2$ was further confirmed by independent synthesis of $Ph_2Si(OCHO)_2$ as well as reaction with $^{13}CO_2$.

In addition, the introduction of N-methylaniline to $Ph_2Si(OCHO)_2$ resulted in the formation of N-formamide. Thus, a one pot synthesis of N-formamide can be performed using 5 mol% of **1** in the presence of Ph_2SiH_2 and amines under CO_2 atmosphere. Controlled experiments suggest that the generation of $Ph_2Si(OCHO)_2$ is the key intermediate for the formation of N-formamides.

4.4   Experimental Section

4.4.1   Synthesis, physical and spectroscopic data for all new compounds

General considerations: All reactions were performed under an atmosphere of argon by using standard Schlenk or dry box techniques; solvents were dried over Na metal, K metal or CaH_2. Traces of moisture in CO_2 were removed by passing through concentrated H_2SO_4 before use. All amines substrates are commercially available and dried using CaH_2. ^1H, $^{13}C\{^1H\}$, and ^{19}F NMR spectra were obtained with a Bruker AV 500, Bruker AV 400 or AVIII 400 MHz BBFO2 spectrometers at 298 K unless otherwise stated. Coupling constants *J* are given in Hz. Electrospray ionization (ESI) mass spectra were obtained at the Mass Spectrometry Laboratory at the Division of Chemistry and Biological Chemistry, Nanyang Technological University. Compound **1** was prepared according to the literature procedures (refer to Chapter 1 reference 52). The spectroscopic data for products **10b** were similar to those as reported[24] while **10d** was compared with the commercially available sample.

Stoichiometric reaction between NHPH and CO_2 or $^{13}CO_2$: Compound **1** (25 mg, 0.125 mmol) in CD_3CN was subjected to two cycles of freeze-pump-thaw and filled with CO_2 at 1 atm. The reaction was shaken and NMR spectroscopy confirmed the full conversion to compound **8**. Compound **8** was isolated by recrystallization from benzene at room temperature.

8 (93%): Brown solid; M.p. 47.5 $^{\circ}C$.

^1H NMR (400 MHz, CD_3CN): $\delta = 8.10$ (s, 1H, C*H*O), 6.41 (d, $^3J_{P-H} = 1.6$ Hz, 2H, *H*C=C*H*), 1.45 (d, $^4J_{P-H} = 1.6$ Hz, 18H, C*H*$_3$).

$^{13}C\{^1H\}$ NMR (125 MHz, CD_3CN): $\delta = 31.1$ (d, $^4J_{P-C} = 10.4$ Hz, *C*H$_3$), 55.2 (d, $^2J_{P-C} = 11.3$ Hz, *C*(CH$_3$)$_3$), 116.3 (d, $^2J_{P-C} = 8.6$ Hz, *C*H), 164.2 (*C*HO).

^{31}P NMR (160 MHz, CD_3CN): $\delta = 111.5$.

HRMS (ESI): *m/z* calcd for $C_{11}H_{22}N_2O_2P$: 245.1419 [(*M*+*H*)]$^+$; found: 245.1423.

8-^{13}C (90%):

^{1}H NMR (400 MHz, CD$_3$CN): δ = 8.13 (d, $J_{C\text{-}H}$ = 210.8 Hz, 1H, C*H*O), 6.42 (d, $^3J_{P\text{-}H}$ = 2.0 Hz, 2H, *H*C=C*H*), 1.47 (d, $^4J_{P\text{-}H}$ = 1.6 Hz, 18H, C*H*$_3$).

^{13}C{^{1}H} NMR (100 MHz, CD$_3$CN): δ = 31.1 (d, $^3J_{P\text{-}C}$ = 11.0 Hz, *C*H$_3$), 55.4 (d, $^2J_{P\text{-}C}$ = 13.0 Hz, *C*(CH$_3$)$_3$), 116.7 (d, $^2J_{P\text{-}C}$ = 10.0 Hz, *C*H), 164.4 (^{13}*C*HO).

^{31}P NMR (200 MHz, CD$_3$CN): δ = 114.9 (br).

HRMS (ESI): *m/z* calcd for ^{12}C$_{10}$^{13}CH$_{22}$N$_2$O$_2$P: 246.1452 [(*M*+*H*)]$^+$; found: 246.1454.

Stoichiometric reaction between 8 and Ph$_2$SiH$_2$: Compound **8** (30 mg, 0.123 mmol) and Ph$_2$SiH$_2$ (11 μL, 0.0593 mmol) were loaded into a dried Carius NMR tube at room temperature under argon atmosphere. The sample was then monitored by NMR spectroscopy.

Independent Synthesis of Ph$_2$Si(OCHO)$_2$: For comparative studies, an independent synthesis of Ph$_2$Si(OCHO)$_2$ was attempted. Ph$_2$SiCl$_2$ (0.34 mL, 1.62 mmol) and HCOOAg[25] (0.5 g, 3.27 mmol) were mixed in CH$_2$Cl$_2$ and stirred overnight at room temperature. The reaction mixture was filtered and the solvent was removed from the filtrate in vacuo to yield Ph$_2$Si(OCHO)$_2$ in 63 % yield. The spectroscopic data are similar to those as reported.[18]

^{1}H NMR (400 MHz, CD$_3$CN): δ = 8.30 (s, 1H, C*H*O), 7.83 (d, ^3J = 8.0 Hz, 4H, Ar*H*), 7.61 (t, ^3J = 8.0 Hz, 2H, Ar*H*), 7.52 (t, ^3J = 8.0 Hz, 4H, Ar*H*).

^{13}C NMR (100 MHz, CD$_3$CN): δ = 129.1 (^{Ar}*C*-Si), 129.4 (*C*H), 133.0 (*C*H), 135.8 (*C*H), 160.4 (*C*HO).

^{29}Si NMR (79.5 MHz, CD$_3$CN): δ = -27.5.

4.4.2   Crystal Structure Determination of Compound 8

X-ray data collection and structural refinement. Intensity data for compounds **8** were collected using a Bruker APEX II diffractometer at 153(2) K. The structure was solved by direct phase determination (SHELXS-97) and refined for all data by full-matrix least squares methods on F^2.[26] All non-hydrogen atoms were subjected to anisotropic refinement. The hydrogen atoms

were generated geometrically and allowed to ride on their respective parent atoms; they were assigned appropriate isotropic thermal parameters and included in the structure-factor calculations. CCDC-1405652 contains the supplementary crystallographic data for this paper. The data can be obtained free of charge from the Cambridge Crystallography Data Centre via www.ccdc.cam.ac.uk/data_request/cif

Table 4.2 Summary of Data Collection and Structure Refinement for compound **8**.

	8
Formula	$C_{11}H_{21}N_2O_2P$
Fw	244.27
Cryst Syst	monoclinic
space group	$P\,1\,2_1/c\,1$
Size (mm^3)	0.14 x 0.28 x 0.42
T, K	153(2)
a, Å	11.2962(5)
b, Å	9.5410(4)
c, Å	12.6825(6)
α, deg	90
β, deg	97.406(2)
γ, deg	90
V, A^3	1355.48(10)
Z	4
d_{calcd} g·cm^{-3}	1.197
μ, mm^{-1}	0.193
Refl collected	15240
T_{min}/ T_{max}	0.9230 / 0.9730
N$_{measd}$	4346
[R_{int}]	[0.0537]
R [I>2sigma(I)]	0.0407
R_w[I>2sigma(I)]	0.0984
GOF	1.025
Largest diff peak/hole[e·Å^{-3}]	0.317/-0.342

4.4.3 Catalytic Studies

Catalytic hydrosilylation of CO_2 ($^{13}CO_2$) using 1: **1** (4.5 mg, 0.0225 mmol), Ph_2SiH_2 (84 μL, 0.450 mmol) and CD_3CN (0.5 mL) were loaded into a dried Carius NMR tube at room temperature under argon atmosphere. The sample was subjected to two cycles of freeze-pump-thaw and filled

with CO_2 ($^{13}CO_2$) at –196 °C. The mass of the Carius NMR tube before and after the introduction of CO_2 was measured. Approximately 45 mg of CO_2 / $^{13}CO_2$ was introduced into the reaction mixture and the reaction mixture was shaken. NMR spectroscopy confirmed the formation of $Ph_2Si(OCHO)_2$ as the major product after 1 h.

Procedure for the reductive functionalization of $^{13}CO_2$ using Ph_2SiH_2 and N-methylaniline: Compound **1** (4.5 mg, 0.0225 mmol), Ph_2SiH_2 (0.25 mL, 1.35 mmol), N-methylaniline (49 μL, 0.452 mmol) and CD_3CN (0.40 mL) were loaded in a dried Carius NMR Tube under argon atmosphere. The reaction mixture in the Carius NMR Tube was subjected to two cycles of freeze-pump-thaw and was then filled with $^{13}CO_2$ at –196 °C. The mass of the Carius NMR tube before and after the introduction of $^{13}CO_2$ was measured. Approximately 45 mg of $^{13}CO_2$ was introduced into the reaction mixture and the reaction mixture was shaken. The reaction was monitored by NMR spectroscopy which confirmed the formation of $PhNMe(^{13}CHO)$ with a NMR yield of 90 % after 5 h. $PhNMe(^{13}CHO)$ was isolated by preparative TLC using ethyl acetate/hexane as solvent.

PhNMe^{13}CHO (Colourless oil, 64 %) as a mixture of rotamers (95 : 5).

Major rotamer: ^1H NMR ($CDCl_3$, 400 MHz): 8.39 (d, $^1J_{C-H}$ = 200.1 Hz, 1H, C*H*O), 7.33 (t, ^3J = 8.0 Hz, 2H, Ar*H*), 7.23 – 7.18 (m, 1H, Ar*H*), 7.09 (d, ^3J = 8.0 Hz, 2H, Ar*H*), 3.24 (d, $^3J_{C-H}$ = 4.0 Hz, 3H, C*H*$_3$).

$^{13}C\{^1H\}$ NMR ($CDCl_3$, 100 MHz): 32.1 (*C*H$_3$), 122.5 (*C*H), 126.5 (*C*H), 129.7 (*C*H), 142.3 (^{Ar}*C*-N), 162.4 (^{13}*C*HO).

HRMS (ESI): *m/z* calcd for $C_7 \, ^{13}CH_{10}NO$: 137.0796 [(*M+H*)]$^+$; found: 137.0791.

General catalytic procedure for the functionalization of CO_2 using Ph_2SiH_2 and Amines: Compound **1** (4.5 mg, 0.0225 mmol), Ph_2SiH_2 (0.25 mL, 1.35 mmol), amines (0.45 mmol) and CD_3CN (0.40 mL) were loaded in a dried Carius NMR Tube under argon atmosphere. The reaction mixture in the Carius Tube was subjected to two cycles of freeze-pump-thaw and was then filled with CO_2 at –196 °C. The mass of the Carius NMR tube before and after the introduction of CO_2 was measured. Approximately 45 mg of CO_2 was introduced into the reaction

mixture, and the reaction mixture was shaken. The reaction was monitored by NMR spectroscopy. The products can be isolated by preparative TLC using hexane/ethyl acetate mixed solvent. Isolated yields are given in parenthesis.

9a
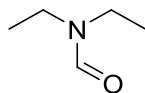
9a[27](40 %).

^{1}H NMR (400 MHz, CDCl$_3$): δ = 8.05 (s, 1H, CHO), 3.37 (q, ^3J = 8.0 Hz, 2H, CH_2), 3.28 (q, ^3J = 8.0 Hz, 2H, CH_2), 1.19 (t, ^3J = 8.0 Hz, 3H, CH_3), 1.13 (t, ^3J = 8.0 Hz, 3H, CH_3).

^{13}C NMR (100 MHz, CDCl$_3$): δ = 12.9 (*C*H$_3$), 15.0 (*C*H$_3$), 36.7 (*C*H$_2$), 42.0 (*C*H$_2$), 162.3 (*C*HO).

HRMS (ESI): *m/z* calcd for C$_5$H$_{12}$NO: 102.0919 [(*M+H*)]$^+$; found: 102.0923.
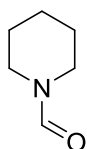
9c

9c[28] (42 %).

^{1}H NMR (300 MHz, CDCl$_3$): δ = 7.99 (s, 1H, CHO), 3.46 (t, ^3J = 6.0 Hz, 2H, CH_2), 3.29 (t, ^3J = 6.0 Hz, 2H, CH_2), 1.69 – 1.63 (m, 2H, CH_2), 1.60 – 1.50 (m, 4H, CH_2).

^{13}C NMR (75 MHz, CDCl$_3$): δ = 24.8 (*C*H$_2$), 25.2 (*C*H$_2$), 26.7 (*C*H$_2$), 40.8 (*C*H$_2$), 47.1 (*C*H$_2$), 161.1 (*C*HO).

HRMS (ESI): *m/z* calcd for C$_6$H$_{12}$NO: 114.0919 [(*M+H*)]$^+$; found: 114.0914.
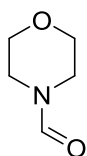
9e

9e[26] (46 %).

^{1}H NMR (300 MHz, CDCl$_3$): δ = 8.04 (s, 1H, CHO), 3.70 – 3.63 (m, 4H, CH_2), 3.58 – 3.56 (m, 2H, CH_2), 3.40 – 3.37 (m, 2H, CH_2).

^{13}C NMR (75 MHz, CDCl$_3$): δ = 40.8 (CH$_2$), 45.9 (CH$_2$), 66.5 (CH$_2$), 67.3 (CH$_2$), 161.0 (CHO).

HRMS (ESI): *m/z* calcd for C$_5$H$_{10}$NO: 116.0712 [(*M+H*)]$^+$; found: 116.0710.
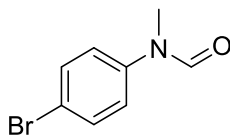
9f

6f[29] (61 %); 93: 7 mixture of rotamers.

Major rotamer: ^{1}H NMR (400 MHz, CDCl$_3$): δ = 8.43 (s, 1H, C*H*O), 7.51 – 7.46 (m, 2H, Ar*H*), 7.04 – 7.02 (m, 2H, Ar*H*) 3.27 (s, 3H, C*H*$_3$).

^{13}C NMR (100 MHz, CDCl$_3$): δ = 32.0 (*C*H$_3$), 119.7 (*C*Br), 123.8 (*C*H), 132.8 (*C*H), 141.3 (*C*N), 162.0 (*C*HO).

HRMS (ESI): *m/z* calcd for C$_8$H$_9$BrNO: 213.9868 [(*M+H*)]$^+$; found: 213.9866.
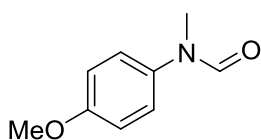
9g

9g[30] (56 %); 94: 6 mixture of rotamers.

Major rotamer: ^{1}H NMR (500 MHz, CDCl$_3$): δ = 8.33 (s, 1H, C*H*O), 7.10 (t, ^3J = 9.0 Hz, 2H, Ar*H*), 6.93 (t, ^3J = 9.0 Hz, 2H, Ar*H*), 3.82 (s, 3H, OC*H*$_3$), 3.27 (s, 3H, C*H*$_3$).

^{13}C NMR (125 MHz, CDCl$_3$): δ = 32.8 (*C*H$_3$), 55.6 (O*C*H$_3$), 114.9 (*C*H), 124.8 (*C*H), 135.3 (^{Ar}*C*-N), 158.4 (^{Ar}*C*-OMe), 162.6 (*C*HO).

HRMS (ESI): *m/z* calcd for C$_9$H$_{12}$NO$_2$: 166.0868 [(*M+H*)]$^+$; found: 166.0863.
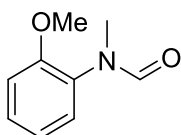
9h

9h[31] (48 %); 94: 6 mixture of rotamers.

Major rotamer: ^{1}H NMR (400 MHz, CDCl$_3$): δ = 8.16 (s, 1H, CHO), 7.34 – 7.28 (m, 1H, ArH), 7.12 – 7.10 (m, 1H, ArH), 7.00 – 6.96 (m, 2H, ArH), 3.84 (s, 3H, OCH_3), 3.20 (s, 3H, CH_3).

^{13}C NMR (100 MHz, CDCl$_3$): δ = 32.8 (CH$_3$), 55.7 (OCH$_3$), 112.1 (CH), 121.0 (CH), 127.9 (CH), 129.1 (CH), 134.5 (^{Ar}C-N), 155.1 (^{Ar}C-OMe), 163.6 (CHO).

HRMS (ESI): m/z calcd for C$_9$H$_{12}$NO$_2$: 166.0868 [(M+H)]$^+$; found: 166.0871.
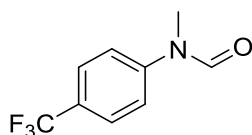
9i

9i (Colourless oil, 48 %); 92: 8 mixture of rotamers.

Major rotamer: ^{1}H NMR (400 MHz, CDCl$_3$): δ = 8.60 (s, 1H, CHO), 7.70 – 7.65 (m, 2H, ArH), 7.31 – 7.29 (m, 2H, ArH), 3.36 (s, 3H, CH_3).

^{13}C NMR (100 MHz, CDCl$_3$): δ = 31.7 (CH$_3$), 121.5 (CH), 127.0 (q, ^{C-F}J = 4.0 Hz, CH), 127.6 (q, $^1J_{C-F}$ = 247.7 Hz, CF$_3$), 128.2 (q, $^2J_{C-F}$ = 33.0 Hz, ^{Ar}C-CF$_3$), 145.2 (^{Ar}C-N), 162.0 (CHO).

^{19}F NMR (376 MHz, CDCl$_3$): δ = -62.4 (s).

HRMS (ESI): m/z calcd for C$_9$H$_9$F$_3$NO: 204.0636 [(M+H)]$^+$; found: 204.0637.
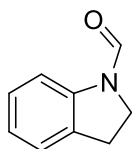
9j

9j[20e] (61 %); 82: 18 mixture of rotamers.

^{1}H NMR (400 MHz, CDCl$_3$): δ = 8.92 (s, 0.82H, CHO), 8.51 (s, 0.18H, CHO), 8.06 (d, ^3J = 8.0 Hz, 0.18H, ArH), 7.27 – 7.16 (m, 2.87H, ArH), 7.14 – 7.03 (m, 1.06H, ArH), 4.10 – 4.03 (m, 2H, CH_3), 3.20 – 3.12 (m, 2H, CH_3).

^{13}C NMR (100 MHz, CDCl$_3$): δ = 27.2 (CH$_2$), 27.8 (CH$_2$), 44.7 (CH$_2$), 47.0 (CH$_2$), 109.4 (CH), 116.7 (CH), 124.3 (CH), 124.6 (CH), 124.9 (CH), 126.1 (CH), 127.6 (CH), 132.0 (^{Ar}C-C), 132.1 (^{Ar}C-C), 141.1 (^{Ar}C-N), 157.6 (CHO), 159.4 (CHO).

HRMS (ESI): m/z calcd for C$_9$H$_{10}$NO: 148.0762 [(M+H)]$^+$; found: 148.0758.

9k
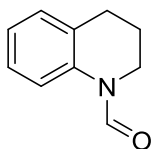
9k[32](44 %); 93: 7 mixture of rotamers.

Major rotamer: ^{1}H NMR (400 MHz, CDCl$_3$): δ = 8.78 (s, 1H, CHO), 7.21 – 7.08 (m, 4H, ArH), 3.80 (t, ^3J = 8.0 Hz, 2H, CH_2), 2.81 (t, ^3J = 8.0 Hz, 2H, CH_2), 1.96 (m, 2H, CH_2).

^{13}C NMR (100 MHz, CDCl$_3$): δ = 22.3 (CH_2), 27.3 (CH_2), 40.4 (CH_2), 117.1 (CH), 124.6 (CH), 127.2 (CH), 129.0 (^{Ar}C-C), 129.7 (CH), 137.3 (^{Ar}C-N), 161.2 (CHO).

HRMS (ESI): m/z calcd for C$_{10}$H$_{12}$NO: 162.0919 [$(M+H)$]$^+$; found: 162.0921.

9l
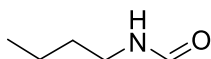
9l[33](43 %); 79: 21 mixture of rotamers.

^{1}H NMR (500 MHz, CDCl$_3$): δ = 8.13 (s, 0.79H, CHO), 8.01 (d, ^3J = 10.0 Hz, 0.21H, CHO), 6.06 (br, 0.21H, NH), 5.86 (br, 0.79H, NH), 3.27 (q, ^3J = 7.0 Hz, 1.68H, CH_2), 3.19 (q, ^3J = 7.0 Hz, 0.42H, CH_2), 1.49 (quint, ^3J = 7.0 Hz, 2H, CH_2), 1.34 (sext, ^3J = 7.0 Hz, 2H, CH_2), 0.91 (t, ^3J = 7.0 Hz, 3H, CH_3).

^{13}C NMR (125 MHz, CDCl$_3$): δ = 13.6 (CH_3), 13.7 (CH_3), 19.6 (CH_2), 20.1 (CH_2), 31.6 (CH_2), 33.3 (CH_2), 38.0 (CH_2), 41.7 (CH_2), 161.4 (CHO), 165.0 (CHO).

HRMS (ESI): m/z calcd for C$_5$H$_{12}$NO: 102.0919 [$(M+H)$]$^+$; found: 102.0919.
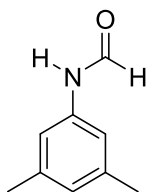
9m

9m (Colourless solid, 42 %); M.p. 76.1 °C; 60: 40 mixture of rotamers.

^{1}H NMR (400 MHz, CDCl$_3$): δ = 8.68 (d, ^3J = 11.2 Hz, 0.60H, C*H*O), 8.41 (br, 0.40H, N*H*), 8.34 (s, 0.40H, C*H*O), 7.41 (br, 1H, N*H*), 7.17 (s, 0.80H, Ar*H*), 6.82 (s, 0.60H, Ar*H*), 6.78 (s, 0.40H, Ar*H*), 6.71 (s, 1.20H, Ar*H*), 2.31 (s, 3.60H, C*H*$_3$), 2.29 (s, 2.40H, C*H*$_3$).

^{13}C NMR (100 MHz, CDCl$_3$): δ = 21.4 (*C*H$_3$), 21.4 (*C*H$_3$), 116.6 (*C*H), 117.8 (*C*H), 126.7 (*C*H), 127.1 (*C*H), 136.7 (^{Ar}C-N), 136.8 (^{Ar}C-N), 139.0 (^{Ar}C-C), 139.7 (^{Ar}C-C), 159.1 (*C*HO), 162.9 (*C*HO).

HRMS (ESI): *m/z* calcd for C$_9$H$_{12}$NO: 150.0919 [(*M*+*H*)]$^+$; found: 150.0910.
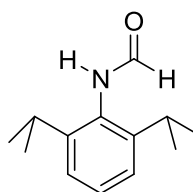
9n

9c[34] (43 %); 63: 37 mixture of rotamers.

^{1}H NMR (400 MHz, CDCl$_3$): δ = 8.46 (s, 0.37H, C*H*O), 8.03 (d, ^3J = 11.6 Hz, 0.63H, C*H*O), 7.35 – 7.30 (m, 1H, Ar*H*), 7.21 – 7.18 (m, 2H, Ar*H*), 6.85 (s, 0.38H, N*H*), 3.23 (sept, ^3J = 6.8 Hz, 1.26H, C*H*), 3.11 (sept, ^3J = 6.8 Hz, 0.74H, C*H*), 1.22 (d, ^3J = 6.8 Hz, 12H, C*H*$_3$).

^{13}C NMR (100 MHz, CDCl$_3$): δ = 23.8 (*C*H$_3$), 28.6 (*C*H), 28.9 (*C*H), 123.7 (*C*H), 124.0 (*C*H), 128.9 (*C*H), 129.1 (*C*H), 129.6 (^{Ar}C-N), 130.1 (^{Ar}C-N), 146.3 (^{Ar}C-C), 146.9 (^{Ar}C-C), 160.7 (*C*HO) 165.4 (*C*HO).

HRMS (ESI): *m/z* calcd for C$_{13}$H$_{20}$NO: 206.1545 [(*M*+*H*)]$^+$; found: 206.1552.
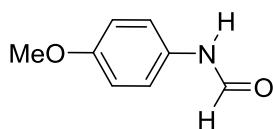
9o

9o[20e] (55 %); 50: 50 mixture of rotamers.

^{1}H NMR (400 MHz, CDCl$_3$): δ = 8.51 (d, ^3J = 11.6 Hz, 0.50H, C*H*O), 8.31 (m, 1.00H, C*H*O and N*H* overlap), 7.55 (br, 0.50H, N*H*), 7.45 (d, ^3J = 8.8 Hz, 1.00H, Ar*H*), 7.04 (d, ^3J = 8.8 Hz, 1.00H, Ar*H*), 6.90 – 6.85 (m, 2.00H, Ar*H*), 3.80 (s, 3.00H, OC*H*$_3$).

<superscript>13</superscript>C NMR (100 MHz, CDCl$_3$): δ = 55.6 (CH$_3$), 55.7 (CH$_3$), 114.3 (CH), 115.0 (CH), 121.7 (CH), 121.9 (CH), 129.7 (^{Ar}C-N), 130.1 (^{Ar}C-N), 156.8 (^{Ar}C-O), 157.7 (^{Ar}C-O), 159.1 (CHO), 161.3 (CHO).

HRMS (ESI): *m/z* calcd for C$_8$H$_{10}$NO$_2$: 152.0712 [(*M*+H)]$^+$; found: 152.0717.

9p
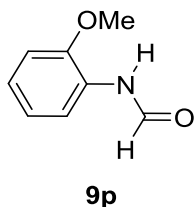
9p[35](64 %); 70: 30 mixture of rotamers.

^{1}H NMR (400 MHz, CDCl$_3$): δ = 8.73 (d, ^3J = 11.6 Hz, 0.30H, CHO), 8.45 (s, 0.70H, CHO), 8.36 (d, ^3J = 8.0 Hz, 0.70H, ArH), 7.88 (br, 0.70H, NH), 7.74 (br, 0.30H, NH), 7.19 (d, ^3J = 8.0 Hz, 0.30H, ArH), 7.15 – 7.05 (m, 1H, ArH), 6.98 – 6.88 (m, 2H, ArH), 3.88 (s, 2.10H, OCH$_3$), 3.86 (s, 0.90H, OCH$_3$).

^{13}C NMR (100 MHz, CDCl$_3$): δ = 55.8 (CH$_3$), 110.2 (CH), 111.4 (CH), 116.8 (CH), 120.6 (CH), 121.2 (CH), 124.4 (CH), 125.3 (CH), 126.3 (^{Ar}C-N), 126.8 (^{Ar}C-N), 147.9 (^{Ar}C-O), 148.8 (^{Ar}C-O), 158.9 (CHO), 161.6 (CHO).

HRMS (ESI): *m/z* calcd for C$_8$H$_{10}$NO$_2$: 152.0712 [(*M*+H)]$^+$; found: 152.0709.

9q
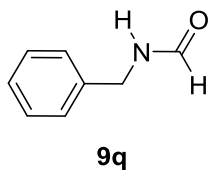
9q[26] (49 %); 85: 15 mixture of rotamers.

^{1}H NMR (500 MHz, CDCl$_3$): δ = 8.19 (s, 0.85H, CHO), 8.10 (d, ^3J = 12.0 Hz, 0.15H, CHO), 7.36 – 7.22 (m, 5H, ArH), 6.32 (br, 0.85H, NH), 6.17 (br, 0.15H, NH), 4.43 (d, ^3J = 6.0 Hz, 1.70H, CH$_2$), 4.36 (d, ^3J = 6.5 Hz, 0.30H, CH$_2$).

^{13}C NMR (125 MHz, CDCl$_3$): δ = 42.2 (CH$_2$), 45.7 (CH$_2$), 127.0 (CH), 127.7 (CH), 127.8 (CH), 128.0 (CH), 128.8 (CH), 129.0 (CH), 137.7 (^{Ar}C-C), 161.3 (CHO), 164.8 (CHO).

HRMS (ESI): *m/z* calcd for C$_8$H$_{10}$NO: 136.0762 [(*M*+H)]$^+$; found: 136.0763.

9r
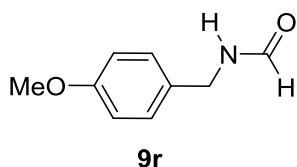
9r[36](66 %); 85: 15 mixture of rotamers.

^{1}H NMR (500 MHz, CDCl$_3$): δ = 8.19 (s, 0.85H, C*H*O), 8.12 (d, [3]*J* = 12.0 Hz, 0.15H, C*H*O), 7.20 (d, [3]*J* = 8.0 Hz, 1.70H, Ar*H*), 7.15 (d, [3]*J* = 8.0 Hz, 0.30H, Ar*H*), 6.89 – 6.84 (m, 2H, Ar*H*), 6.16 (br, 0.85H, N*H*), 6.05 (br, 0.15H, N*H*), 4.38 (d, [3]*J* = 6.0 Hz, 1.70H, C*H*$_2$), 4.31 (d, [3]*J* = 6.5 Hz, 0.30H, C*H*$_2$), 3.80 (s, 0.45H, OC*H*$_3$), 3.78 (s, 2.55H, OC*H*$_3$).

^{13}C NMR (125 MHz, CDCl$_3$): δ = 41.7 (*C*H$_2$), 45.2 (*C*H$_2$), 55.4 (*C*H$_3$), 55.4 (*C*H$_3$), 114.2 (*C*H), 114.3 (*C*H), 128.4 (*C*H), 129.2 (*C*H), 129.6 ([Ar]*C*-C), 129.8 ([Ar]*C*-C), 159.2 ([Ar]*C*-O), 161.1 (*C*HO), 164.6 (*C*HO).

HRMS (ESI): *m/z* calcd for C$_9$H$_{12}$NO$_2$: 166.0868 [(*M*+*H*)]$^+$; found: 166.0870.

9s
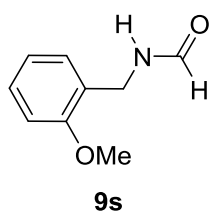
9s[37](57 %); 80: 20 mixture of rotamers.

^{1}H NMR (400 MHz, CDCl$_3$): δ = 8.16 (s, 0.80H, C*H*O), 8.12 (d, 0.20H, overlapping, C*H*O), 7.32 – 7.24 (m, 1.80H, Ar*H*), 7.16 (d, [3]*J* = 7.2 Hz, 0.20H, Ar*H*), 6.94 – 6.86 (m, 2H, Ar*H*), 6.33 (br, 0.80H, N*H*), 6.15 (br, 0.20H, N*H*), 4.46 (d, [3]*J* = 6.0 Hz, 1.60H, C*H*$_2$), 4.33 (d, [3]*J* = 6.4 Hz, 0.40H, C*H*$_2$), 3.84 (s, 3H, OC*H*$_3$).

^{13}C NMR (100 MHz, CDCl$_3$): δ = 38.0 (*C*H$_2$), 42.1 (*C*H$_2$), 55.3 (*C*H$_3$), 55.3 (*C*H$_3$), 110.4 (*C*H), 110.5 (*C*H), 120.7 (*C*H), 120.7 (*C*H), 125.7 ([Ar]*C*-C), 126.0 ([Ar]*C*-C), 128.7 (*C*H), 129.1 (*C*H), 129.5 (*C*H), 129.7 (*C*H), 157.3 ([Ar]*C*-O), 157.6 ([Ar]*C*-O), 161.0 (*C*HO), 164.9 (*C*HO).

HRMS (ESI): *m/z* calcd for C$_9$H$_{12}$NO$_2$: 166.0868 [(*M*+*H*)]$^+$; found: 166.0871.

9t
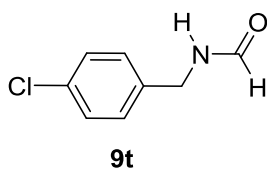
9t[34] (69 %); 88: 12 mixture of rotamers.

^{1}H NMR (400 MHz, CDCl$_3$): δ = 8.24 (s, 0.88H, C*H*O), 8.15 (d, ^3J = 12.0 Hz, 0.12H, C*H*O), 7.35 – 7.27 (m, 2H, Ar*H*), 7.22 – 7.18 (m, 2H, Ar*H*), 6.12 (br, 1H, N*H*), 4.43 (d, ^3J = 6.0 Hz, 1.76H, C*H*$_2$), 4.38 (d, ^3J = 6.8 Hz, 0.24H, C*H*$_2$).

^{13}C NMR (100 MHz, CDCl$_3$): δ = 41.6 (C*H*$_2$), 45.1 (C*H*$_2$) 128.4 (*C*H), 129.0 (*C*H), 129.2 (*C*H), 129.4 (*C*H) 133.7 (^{Ar}*C*-Cl), 134.0 (^{Ar}*C*-Cl), 136.1 (^{Ar}*C*-C) 136.3 (^{Ar}*C*-C), 161.1 (*C*HO), 164.6 (*C*HO).

HRMS (ESI): *m/z* calcd for C$_8$H$_9$NOCl: 170.0373 [(*M*+*H*)]$^+$; found: 170.0381.

9u
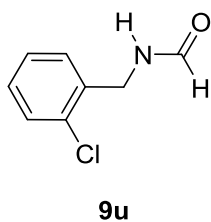
9u (Colourless solid, 59 %); M.p. 75.4 ^{o}C; 85: 15 mixture of rotamers.

^{1}H NMR (400 MHz, CDCl$_3$): δ = 8.21 (s, 0.85H, C*H*O), 8.16 (d, ^3J = 12.0 Hz, 0.15H, C*H*O), 7.37 – 7.35 (m, 1.84H, Ar*H*), 7.28 – 7.21 (m, 2.26H, Ar*H*), 6.41 (br, 0.85H, N*H*), 6.24 (br, 0.15H, NH), 4.54 (d, ^3J = 6.0 Hz, 1.7H, C*H*$_2$), 4.47 (d, ^3J = 6.4 Hz, 0.30H, C*H*$_2$).

^{13}C NMR (100 MHz, CDCl$_3$): δ = 40.1 (C*H*$_2$), 43.8 (C*H*$_2$), 127.2 (*C*H), 127.4 (*C*H), 129.0 (*C*H), 129.2 (*C*H), 129.5 (*C*H), 129.6 (*C*H), 129.9 (*C*H), 130.2 (*C*H), 133.3 (^{Ar}*C*-Cl), 133.6 (^{Ar}*C*-Cl), 135.1 (^{Ar}*C*-C), 135.3 (^{Ar}*C*-C), 161.3 (*C*HO), 164.9 (*C*HO).

HRMS (ESI): *m/z* calcd for C$_8$H$_9$NOCl: 170.0373 [(*M*+*H*)]$^+$; found: 170.0383.

4.5   References

1.   a) D'Alessandro, D. M.; Smit, B.; Long, J. R. *Angew. Chem. Int. Ed*. **2010**, *49*, 6058–6082; b) Jacobson, M. Z. *Energy Environment. Sci*. **2009**, *2*, 148–173; c) Olah, G.; Goeppert, A.; Prakash, G. K. S. *J. Org. Chem*. **2009**, *74*, 487–498; d) *Carbon Dioxide Capture and Storage*; Metz, B.; Davidson, O.; de Coninck, H.; Loos, M.; Meyer, L., Eds.; Intergovernmental Panel on Climate Change (IPCC), Cambridge University Press, New York, 2005.

2.   Aresta, M.; Dibenedetto, A.; Angelini, A. *Chem. Rev*. **2014**, *114*, 1709–1742.

3.   a) Liu, Q.; Wu, L.; Jackstell, R.; Beller, M. *Nat. Commun*. **2015**, *6*, 5933; b) Tlili, A.; Blondiaux, E.; Frogneux, X.; Cantat, T. *Green. Chem*. **2015**, *17*, 157–168; c) Yeung, C. S.; Dong, V. M. *Top. Catal*. **2014**, *57*, 1342–1350; d) Maeda, C.; Miyazaki, Y.; Ema, T. *Catal. Sci. Technol*. **2014**, *4*, 1482–1497; e) Appel, A. M.; Bercaw, J. E.; Bocarsly, A. B.; Dobbek, H.; DuBois, D. L.; Dupuist, M.; Ferry, J. G.; Fujita, E.; Hille, R.; Kenis, P. J. A.; Kerfeld, C. A.; Morris, R. H.; Peden, C. H. F.; Portis, A. R.; Ragsdale, S. W.; Rauchfuss, T. B.; Reek, J. N. H.; Seefeldt, L. C.; Thauer, R. K.; Waldrop, G. L. *Chem. Rev*. **2013**, *113*, 6621–6658; f) Riduan, S. N.; Zhang, Y. *Dalton Trans*. **2010**, 39, 3347–3357; g) Sakakura, T.; Choi, J. –C.; Yasuda, H. *Chem. Rev*. **2007**, *107*, 2365–2387.

4.   Olah, G. A. *Angew. Chem. Int. Ed*. **2005**, *44*, 2636–2639.

5.   For selected recent examples, see: a) Jin, G.; Werncke, G.; Escudié, Y.; Sabo-Etienne, S.; Bontemps, S. *J. Am. Chem. Soc*. **2015**, *137*, 9563–9566; b) Rezayee, N. M.; Huff, C. A.; Sanford, M. S. *J. Am. Chem. Soc*. **2015**, *137*, 1028–1031; c) Suh, H. –W.; Guard, L. M.; Hazari, N. *Chem. Sci*. **2014**, *5*, 3859–3872; d) Moret, S.; Dyson, P. J.; Laurenczy, G. *Nat. Commun*. **2014**, *5*, 4017; e) Bontemps, S.; Vendier, L.; Sabo-Etienne, S. *J. Am. Chem. Soc*. **2014**, *136*, 4419–4425; f) Berkefeld, A.; Pier, W. E.; Parvez, M.; Castro, L.; Maron, L.; Eisenstein, O. *Chem. Sci*. **2013**, *4*, 2152–2162; g) Bontemps, S.; Sabo-Etienne, S. *Angew. Chem. Int. Ed*. **2013**, *52*, 10253–10255; h) Dorovetsky, R.; Stephan, D. W. *Angew. Chem. Int. Ed*. **2013**, *52*, 2516–2519; See also: i) Lescott, C.; Nielsen, D. U.;

Makarov, I. S.; Lindhardt, A. T.; Daasbjerg, K.; Skrydstrup, T. *J. Am. Chem. Soc.* **2014**, *136*, 6142–6147.

6. Fontaine, F. –G.; Courtemanche, M. –A.; Légaré, M. –A. *Chem. Eur. J.* **2014**, *20*, 2990–2996.

7. Mömming, C. M.; Otten, E.; Kehr, G.; Fröhlich, R.; Grimme, S.; Stephan, D. W. *Angew. Chem. Int. Ed.* **2009**, *48*, 6643–6646.

8. For selected recent examples, see: a) Courtemanche, M. –A.; Pulis, A. P.; Rochette, E.; Légaré, M. –A.; Stephan, D. W.; Fontaine, F. –G. *Chem. Commun.* **2015**, *51*, 9797–9800; b) Ménard, G.; Gilbert, T. M.; Hatnean, J. A.; Kraft, A.; Krossing, I.; Stephan, D. W. *Organometallics* **2013**, *32*, 4416–4422; c) Ménard, G.; Stephan, D. W. *Angew. Chem. Int. Ed.* **2011**, *50*, 8396–8399; d) Zhao, X.; Stephan, D. W. *Chem. Commun.* **2011**, *47*, 1833 –1835; e) Dickie, D. A.; Coker, E. N.; Kemp, R. A. *Inorg. Chem.* **2011**, *50*, 11288–11290; f) Ménard, G.; Stephan, D. W. *J. Am. Chem. Soc.* **2010**, *132*, 1796–1797; Selected examples of catalytic transformation of CO_2: g) Wang, T.; Stephan, D. W. *Chem. Eur. J.* **2014**, *20*, 3036–3039; h) Wang, T.; Stephan, D. W. *Chem. Commun.* **2014**, *50*, 7007–7010; i) Das Neves Gomes, C.; Blondiaux, E.; Thuéry, P.; Cantat, T. *Chem. Eur. J.* **2014**, *20*, 7098–7106; j) Courtemanche, M. –A.; Légaré, M. –A.; Maron, L.; Fontaine, F. –G. *J. Am. Chem. Soc.* **2013**, *135*, 9326–9329; k) Wang, Y. –B.; Wang, Y. –M.; Zhang, W. –Z.; Lu, X. –B. *J. Am. Chem. Soc.* **2013**, *135*, 11996–12003; l) Wehmschulte, R. J.; Saleh, M.; Powell, D. R. *Organometallics* **2013**, *32*, 6812–6819; m) Courtemanche, M. –A.; Larouche, J.; Légaré, M. –A.; Bi, W.; Maron, L.; Fontaine, F. –G. *Organometallics* **2013**, *32*, 6804–6811; n) Schäfer, A.; Saak, W.; Haase, D.; Müller, T. *Angew. Chem. Int. Ed.* **2012**, *51*, 2981–2984; o) Khandelwal, M.; Wehmschulte, R. J. *Angew. Chem. Int. Ed.* **2012**, *51,* 7323–7326; p) Riduan, S. N.; Zhang, Y.; Ying, J. Y. *Angew. Chem. Int. Ed.* **2009**, *48*, 3322–3325; q) Kayaki, Y.; Yamamoto, M.; Ikariya, T. *Angew. Chem. Int. Ed.* **2009**, *48*, 4194–4197.

9. a) Murphy, L. J.; Robertson, K. N.; Kemp, R. A.; Tuononen, H. M.; Clyburne, J. A. C. *Chem. Commun.* **2015**, *51*, 3942–3956; b) Purushothaman, I.; De, S.; Parameswaran, P. *RSC Adv.* **2014**, *4*, 60421–60428.

10. Riduan, S. N.; Ying, J. Y.; Zhang, Y. *ChemCatChem* **2013**, *5*, 1490–1496.

11. Zhou, Q.; Li, Y. *J. Am. Chem. Soc.* **2015**, *137*, 10182–10189.

12. Huang, F.; Lu, G.; Zhao, L.;Li, H.; Wang, Z. –X. *J. Am. Chem. Soc.* **2010**, *132,* 12388–12396.

13. For B, see: a) Knopf, I.; Cummins, C. C. *Organometallics* **2015**, *34*, 1601–1603; b) Lu, Z.; Hausmann, H.; Becker, S.; Wegner, H. A. *J. Am. Chem. Soc.* **2015**, *137*, 5332–5335; c) Fujiwara, K.; Yasuda, S.; Mizuta, T. *Organometallics* **2014**, *33*, 6692–6695; d) Peuser, I.; Neu, R. C.; Zhao, X.; Ulrich, M.; Schirmer, B.; Tannert, J. A.; Kehr, G.; Fröhlich, R.; Grimme, S.; Erker, G.; Stephan, D. W. *Chem. Eur. J.* **2011**, *17*, 9640–9650; e) Berkefeld, A. Piers, W. E.; Parvez, M. *J. Am. Chem. Soc.* **2010**, *132*, 10660–10661; f) Ashley, A. E.; Thompson, A. L.; O'Hare, D. *Angew. Chem. Int. Ed.* **2009**, *48*, 9839–9843; g) Wartik, T.; Pearson, R. K. *J. Inorg. Nucl. Chem.* **1958**, *7*, 404–411; h) Wartik, T.; Pearson, R. K. *J. Am. Chem. Soc.* **1955**, *77*, 1075; For Al, see: i) Ménard, G.; Stephan, D. W. *Dalton Trans.* **2013**, *42*, 5447–5453; j) Kuo, P. –C.; Chen, I. –C.; Chang, Jr. –C.; Lee, M. –T.; Hu, C. –H.; Hung, C. –H.; Lee, H. M.; Huang, J. –H. *Eur. J. Inorg. Chem.* **2004**, 4898–4906; For Ga, see: k) Abdalla, J. A. B.; Riddlestone, I. M.; Tirfoin, R.; Aldridge, S. *Angew. Chem. Int. Ed.* **2015**, *54*, 5098–5102; For Ge, see: Chapter 1, ref. 46; For Si, see: l) Arya, P.; Boyer, J.; Corriu, R. J. P.; Lanneau, G. F.; Perrot, M. *J. Organomet. Chem.* **1968**, *346*, C11-C14; For Sn, see: m) Jana, A.; Roesky, H. W. Schulzke, C.; Döring, A. *Angew. Chem. Int. Ed.* **2009**, *48*, 1106–1109; n) Albertin, G.; Antoniutti, S.; Castro, J.; García- Fontán, S.; Zanardo, G. *Organometallics* **2007**, *26*, 2918–2930.

14. a) Cavell, R. G.; The, K. I.; Van de Griend, L. *Inorg. Chem.* **1981**, *20*, 3813–3818; b) The, K. I.; Van de Griend, L.; Whitla, W. A.; Cavell, R. G. *J. Am. Chem. Soc.* **1977**, *99*, 7379–7380.

15. Hounjet, L. J.; Caputo, C. B.; Stephan, D. W. *Angew. Chem. Int. Ed*. **2012**, *51*, 4714–4717.

16. Courtemanche, M. –A.; Légaré, M. –A.; Rochette, E.; Fontaine, F. –G. *Chem. Commun*. **2015**, *51*, 6858–6861.

17. a) Kindra, D. R.; Casely, I. J.; Fieser, M. E.; Ziller, J. W.; Furche, F.; Evans, W. J. *J. Am. Chem. Soc*. **2013**, *135*, 7777–7787; b) Yin, S. –F.; Maruyama, J.; Yamashita, T.; Shimada, S. *Angew. Chem. Int. Ed*. **2008**, *47*, 6590–6593; c) Light, R. W.; Hutchins, L. D.; Paine, R. T.; Campana, C. F. *Inorg. Chem*. **1980**, *19*, 3597–3604; d) Oertel, G.; Malz, H.; Holtschmidt, H. *Eur. J. Inorg. Chem*. **1964**, *97*, 891–902.

18. Chatelet, B.; Joucla, L.; Dutasta, J.–P.; Martinez, A.; Szeto, K. C.; Dufaud, V. *J. Am. Chem. Soc*. **2013**, *135*, 5348–5351.

19. Endo, H.; Takeda, N.; Umo, M. *Organometallics* **2014**, *33*, 4184–4151.

20. Jansen, A.; Görls, H.; Pitter, S. *Organometallics* **2000**, *19*, 135–138.

21. a) Chen, W. –C.; Shen, J. –S.; Jurca, T.; Peng, C. –J.; Lin, Y. –H.; Wang, Y. –P.; Shih, W. –C.; Yap, G. P. A.; Ong, T. –G. *Angew. Chem. Int. Ed*. **2015**, *54*, 15207–15212; b) Zhou, H.; Wang, G. –X.; Zhang, W. –Z.; Lu, X. –B. *ACS Catal.* **2015**, *5*, 6773–6779; c) Das Neves Gomes, C.; Jacquet, O.; Villiers, C.; Thuéry, P.; Ephritikhine, M.; Cantat, T. *Angew. Chem. Int. Ed*. **2012**, *51*, 187–190; d) O. Jacquet, Das Neves Gomes, C.; Ephritikhine, M.; Cantat, T. *J. Am. Chem. Soc*. **2012**, *134*, 2934–2937; e) Blondiaux, E.; Pouessel, J.; Cantat, T. *Angew. Chem. Int. Ed*. **2014**, *53*, 12186–12190; f) Das, S.; Bobbink, F. D.; Laurenczy, G.; Dyson, P. J. *Angew. Chem. Int. Ed*. **2014**, *53*, 12876–12879.

22. a) Zhou, Q.; Li, Y. *J. Am. Chem. Soc*. **2015**, *137*, 10182–10189; b) Wang, B.; Cao, Z. *RSC Adv*. **2013**, *3*, 14007–14015; c) González-Sebastían, L.; Flores-Alamo, M.; García, J. J. *Organometallics* **2013**, *32*, 7186–7194; d) Itagaki, S.; Yamaguchi, K.; Mizuno, N. *J. Mol. Catal. A* **2013**, *366*, 347–352; e) Shintani, R.; Nozaki, K. *Organometallics* **2013**, *32*, 2459–2462.

23.   a) González-Sebastían, L.; Flores-Alamo, M.; García, J. J. *Organometallics* **2015**, *34*, 763–769; b) Sorribes, I.; Junge, K.; Beller, M. *Chem. Eur. J.* **2014**, *20*, 7878–7883; c) Jacquet, O.;Frogneux, X.; Das Neves Gomes, C.; Cantant, T. *Chem. Sci.* **2013**, *4*, 2127–2131; d) Sattler, W.; Parkin, G. *J. Am. Chem. Soc.* **2012**, *134*, 17462–17466.

24.   Wadsworth, D. H.; Detty, M. R.; Murray, B. J.; Weidner, C. H.; Haley, N. F. *J. Org. Chem.* **1984**, *49*, 2676–2681.

25.   Oshima, M.; Sakamoto, T.; Maruyama, Y.; Ozawa, F.; Shimizu, I.; Yamamoto, A. *Bull. Chem. Soc. Jpn.* **2000**, *73*, 453–464.

26.   Sheldrick, G. M. SHELXL-97; Universität Göttingen, Germany, 1997.

27.   Li, G.; Kung, K. K.; Wong, M. *Chem. Commun.* **2012**, *48*, 4112–4114.

28.   Nguyen, T. B.; Sorres, J.; Tran, M. Q.; Ermolenko, L.; Al-Mourabit, A. *Org. Lett.* **2012**, *14*, 3202–3204.

29.   Taneda, H.; Inamoto, K.; Kondo, Y. *Chem. Commun.* **2014**, *50*, 6523–6525.

30.   Hoffmann, R. V.; Salvador, J. M. *J. Org. Chem.* **1992**, *57*, 4487–4490.

31.   Klapars, A.; Huang, X.; Buchwald, S. L. *J. Am. Chem. Soc.* **2002**, *124*, 7421–7428.

32.   Tao, L.; Zhang, Q.; Li, S.; Liu, X.; Liu, Y.; Cao, Y. *Adv. Synth. Catal.* **2015**, *357*, 753–760.

33.   Kamer, P. C. J.; Nolte, R. J. M.; Drenth, W. *J. Am. Chem. Soc.* **1988**, *110*, 6818–6825.

34.   Sattler, W.; Ener, M. E.; Blakemore, J. D.; Rachford, A. A.; LaBeaume, P. J.; Thackeray, J. W.; Cameron, J. F.; Winkler, J. R.; Gray, H. B. *J. Am. Chem. Soc.* **2013**, *135*, 10614–10617.

35.   Komati, R.; Jursic, B. S. *Tetrahedron Lett.* **2014**, *55*, 1523–1527.

36.   Ortega, N.; Richter, C.; Glorius, F. *Org. Lett.* **2013**, *15*, 1776–1779.

37.   Pigge, F. C.; Coniglio, J. J.; Fang, S. *Organometallics* **2002**, *21*, 4505–4512.

5.1 Introduction

Heterocyclic compounds containing phosphorus and nitrogen atoms are useful in areas such as polymerisation, nucleotide synthesis and energetic materials.[1] They could also act as strong bases or catalysts in organic reactions.[2] The first inorganic P,N-heterocyclic compound can be traced back to the work by Liebig and Wöhler in which the reaction of PCl_5 and NH_3 generated various P,N-heterocycles with an empirical formula of $PNCl_2$.[3] Recently, Cummins et al. reported the isolation of a rare aromatic P,N-heterocyclic compound.[4] This aromatic anion, namely diphosphatriazolate anion $(P_2N_3^-)$ was formed from the reaction of an anthracene-based source of P_2 with [Na-kryptofix-221]N_3 (Scheme 5.1). Remarkably, the stabilisation of the $P_2N_3^-$ anion can be attributed solely to the aromaticity of the heterocyclic moiety as no steric stabilisation from bulky substituents is present.
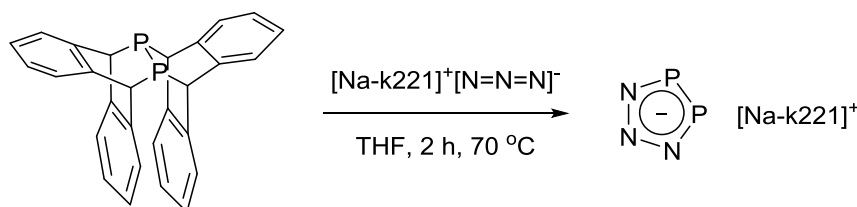
Scheme 5.1   Synthesis of inorganic aromatic P,N-heterocycle, [Na-k221]$^+$[P$_2$N$_3$]$^-$.

Besides binary P,N-heterocycles, a common class of phosphorus-nitrogen heterocycles is the ternary heterocyclic system **A**-**D** featuring additional carbon atoms linked with phosphazane type P-N-P moieties (Figure 5.1). Particularly, five-membered N-heterocyclic phosphanes (NHPX) (**B**) and its cationic species (**C**) have been extensively explored by Gudat et al. Derivatives **B** can be obtained from the corresponding α-diimines in a single step. In addition, substituent X on the phosphorus centre can be readily modified by a simple nucleophilic substitution method starting from P-chloro-derivatives (X = Cl). For instance, Gudat et al. reported the reaction of P-chlorodiazaphospholene with $LiPPh_2$ or $LiPC_4Et_4$ which afforded P-phosphino-derivatives

(Scheme 5.2a).[5] Those P-phosphino-derivatives possess a highly reactive P-P bond which could catalyse the P-C bond cross coupling reaction (Scheme 5.2b)[6] or participate in the phosphination of nitrile (Scheme 5.2c).[7]

Figure 5.1 Common P,N-heterocycles featuring C_2 or C_3-fragments.

Scheme 5.2 a) Synthesis of P-phosphino-derivatives using salt elimination method; b) NHP-PPh$_2$-catalysed C-P bond formation; c) Phosphination of MeCN using NHP-PC$_4$Et$_4$ and W(CO)$_4$(cod).

Another notable example is the synthesis of P-amino-derivatives from the reaction of NHPCl and NaNH$_2$ in liquid ammonia (Scheme 5.3a).[8] Interestingly, the reaction of NaNH$_2$ and N-mesityl-substituted derivative yielded an amino-diazaphospholine whereas an imino-

bis(diazaphospholene) was observed from a similar reaction with a diazaphospholene featuring aliphatic substituents (R = ^{t}Bu) on the N atoms. Gudat et al. also reported the synthesis P-azido-diazaphospholene from the reaction of P-chloro-derivative and sodium azide (Scheme 5.3b).[9] Under heating condition, N$_2$ was liberated and dimerization of the possible P-N nitrene intermediate afforded a novel cyclodiphosphazene compound (Scheme 5.3b).
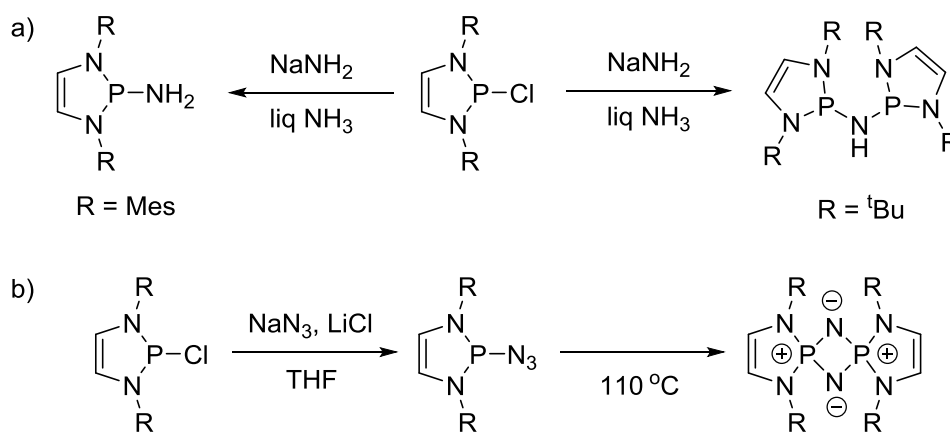
Scheme 5.3   a) Formation of P-amino-derivatives from the reaction of NHPCl and NaNH$_2$; b) Synthesis and thermolysis of P-azido-derivative.

Those examples demonstrate that the derivatives of N-heterocyclic Phosphanes (NHP) are easily synthesized and could undergo further reaction to form novel NHP-containing molecules with unique properties.

Imidazolin-2-iminato, an imidazole-based ligand featuring exocyclic -NR moiety at 2-position of the N-heterocycle (Figure 5.2), are highly nucleophilic species as shown by its resonance forms.[10]
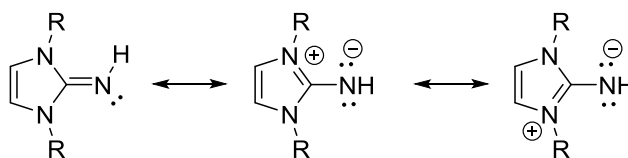
Figure 5.2   Resonance structures related to imidazolin-2-iminato.

Imidazolin-2-iminato derivatives have been employed as (2σ, 4π)-electron donor in the various transition metal complexes, that could be utilised for polymerisation and metathesis

reactions.[11] In recent times, imidazolin-2-iminato has also been used as a supporting ligand to stabilised reactive main group species. Notable examples include acyclic silylene, phosphorus mononitride, phosphinonitrene, aluminium dihydride, cationic $[B=S]^+$ species and Al=Te double bond species (Figure 5.3).[12].
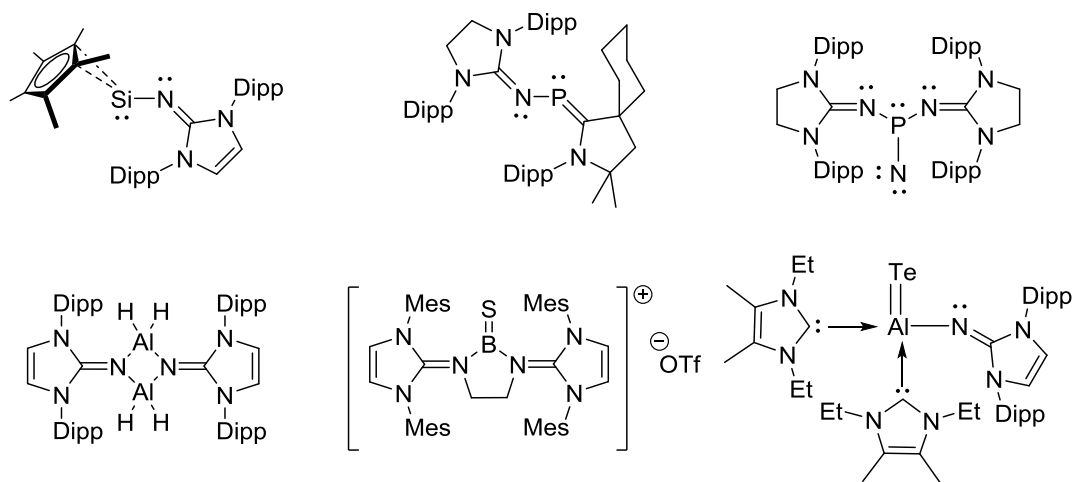
Figure 5.3   Various reactive main group species featuring imidazolin-2-iminato as supporting ligand.

Given the unique electronic and structural properties of NHP and imidazolin-2-iminato, we decided to explore the possibility of incorporating imidazolin-2-iminato onto NHP moiety and to investigate its reactivity.

5.2　Results and Discussions

5.2.1　*Synthesis and characterisation of phosphinoimino-4-imidazoline 12*

Imidazolin-2-iminato **11** was synthesized by following the method reported by Tamm et al. (Scheme 5.4a).[11e] Deprotonation of **11** using [n]BuLi afforded the corresponding lithium species *in situ* and was subsequently reacted with 2-chloro-diazaphospholidine **1'** to give the desired phosphinoimino-4-imidazoline species **12** in 58% yield (Scheme 5.4b).
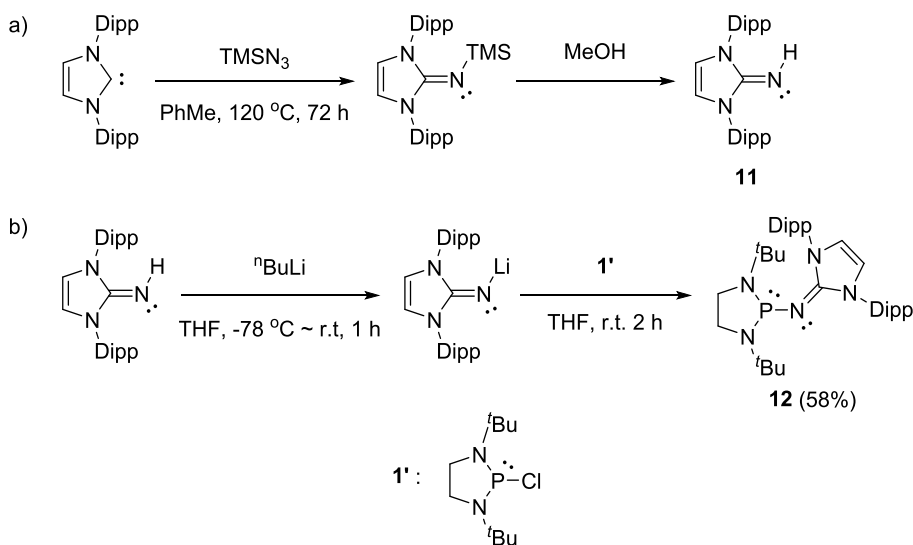
Scheme 5.4　a) Synthesis of imidazolin-2-iminato **11**; b) Synthesis route of phosphinoimino-4-imidazoline species **12**.

The ^{31}P NMR spectrum of compound **12** shows a peak at 90.0 ppm in C_6D_6 which is slightly downfield as compared to that of P-amino-derivatives (NHP-NH$_2$) shown in Scheme 5.3a. A single crystal of **12** was grown from a benzene solution at room temperature and subjected to X-ray diffraction analysis (Figure 5.4a). The phosphorus centre displays a distorted trigonal pyramidal geometry. The P1-N3 bond length is 1.693(2) Å, which is slightly longer than those observed in NHP-NH$_2$ derivative (1.6743 Å) and bisdiazaphospholenyl-imine (1.683 Å) as shown in Scheme 5.3a. The N3-C1 bond length (1.284(3) Å) is within the range of a typical $C(sp^2)=N$ and is comparable with that in **11** (1.2888 Å).[13]

To investigate the electronic structure, DFT calculations were performed for **12** at B3LYP/6-31G(d) level of theory. The HOMO of **12** mainly consists of the lone pairs of electron

on the P atom and the adjacent N atom connected to the imidazole moiety (Figure 5.4b). Hence, compound **12** contains two nucleophilic sites available for coordination. On the other hand, the LUMO for **12** localised on the aryl substituents on the imidazole ring (Figure 5.4c). Natural bond orbital (NBO) analysis was also carried out at the same level of theory. The hybridization of the lone pair of electrons on the P1 and N3 atoms are $sp^{0.68}$ and $sp^{3.19}$ respectively. The Wiberg bond index (WBI) for P1-N3 and C1-N3 are 0.8108 and 1.6132 respectively, suggesting no significant exocyclic n(N)-σ*(P-N) hyperconjugative interactions between P1 and N3

a)

b)

c)
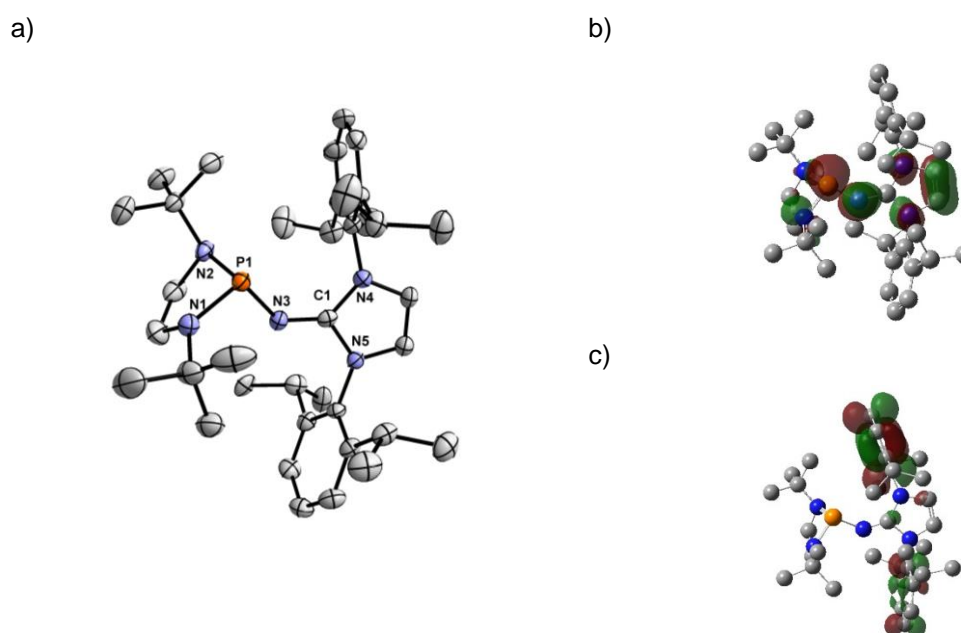
Figure 5.4   a) ORTEP drawing of **12** with thermal ellipsoids set at 30% probability level. Selected bond lengths [Å] and angles [°] for **12**: P1-N1 1.711(3), P1-N2 1.722(2), P1-N3 1.693(2), N3-C1 1.284(3), C1-N4 1.387(3), C1-N5 1.395(3), P1-N3-C1 127.4(2), N2-P1-N1 91.39(12), N4-C1-N5 103.8(2); b) Calculated HOMO for **12**; c) Calculated LUMO for **12**. Hydrogen atoms are omitted for clarity.

5.2.2   Reactivity of N-heterocyclic phosphino-imidazolidin-2-iminato

Next, several reactions were performed to explore the potential application of compound **12**. Firstly, we attempted to isolate a radical cationic species of **12**. When $[Ph_3C]^+[B(C_6F_5)_4]^-$ (1 eq) was added to **12** in benzene at room temperature, a dark solution was obtained. The room temperature EPR spectrum (Figure 5.5a-b) of the resulting solution displays a signal which is split into multiple lines but no large and distinct hyperfine coupling for the P atom was detected in the

EPR spectrum, suggesting that the phosphorus moiety is not involved in the product.[14] Attempts to obtain the crystal structure for the final product were unsuccessful, hence, we simulated an EPR spectrum (Figure 5.5d) to match the experimental EPR data. The multiple splitting pattern can be attributed to the hyperfine coupling with the two adjacent nitrogen atoms ($a_{N1,2}$ = 7.03 MHz), four nitrogen atoms (a_{N1-4} = 3.81 MHz) and four hydrogen atoms (a_{H1-4} = 0.84 MHz) on the imidazole ring. Thus, the EPR spectrum suggests that a dinitrogen radical cation-stabilised by two NHC(Dipp) moieties could be a possible structure (Figure 5.5c). Such urea azine can be seen formally as a bis(N-heterocyclic carbene)-stabilised dinitrogen radical cation. Interestingly, a similar compound has been reported recently by Himmel and co-workers.[15]

a)

b)

c)

d)
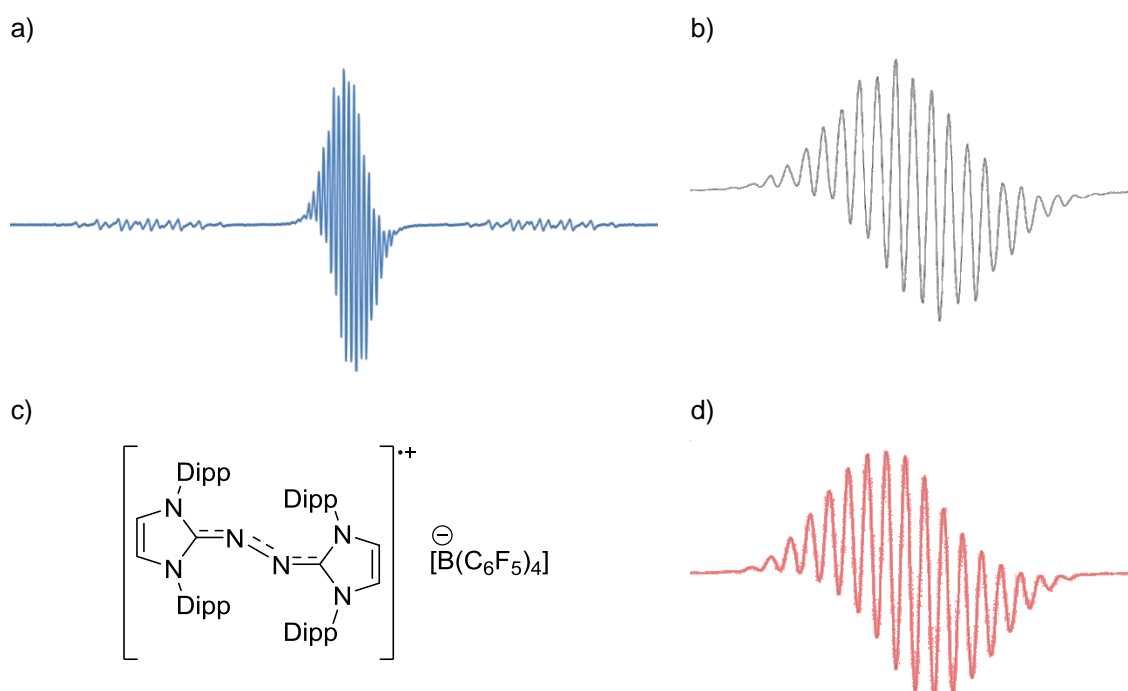
Figure 5.5   a) EPR spectrum for oxidation of **12** using [Ph$_3$C]$^+$[B(C$_6$F$_5$)$_4$]$^-$ at 298 K in fluorobenzene, SW = 99.9 G, g = 2.0034; b) Enlarge EPR spectrum of the centre band; c) Proposed structure for the radical species based on simulated EPR; d) Simulated EPR spectrum, $a_{N1,2}$ = 2.506 G; a_{N1-4} = 1.357 G; a_{H1-4} = 0.300 G, LW = 0.475.

As aforementioned, **12** consists two nucleophilic sites which can be classified as soft P nucleophile and hard N nucleophile. Hence, compound **12** could exhibit coordination selectivity with different Lewis acids. Indeed, addition of BH$_3$, a typical soft Lewis acid, to a toluene solution

of **12** (Scheme 5.5) resulted in a upfield shift in the ^{31}P NMR from 90.0 ppm to 80.0 ppm. The formation of **12[BH$_3$]** adduct was unanimously confirmed by X-ray diffraction analysis (Figure 5.6a). The phosphorus centre adopts a distorted tetrahedral geometry and the P1-N3 bond length (1.6241(16) Å) is slightly shorter than that in **3** (1.693(2) Å) while the P1-N3-C1 angle increases from 127.4(2)^o in **3** to 131.05(14)^o. In addition, the N3-C1 bond length increases slightly to 1.299(2) Å from 1.284(3) Å in **3s**. A DFT study on **3[BH$_3$]** conducted at a similar level of theory [B3LYP/6-31G(d)] reveals that the HOMO lies mainly on the lone pairs of electron on the exocyclic N3 atom with some contribution from the endocyclic N1 atom (Figure 5.6b). On the other hand, the LUMO remains largely on the phenyl substituents on the imidazole ring (Figure 5.6c). A further NBO analysis [B3LYP/6-311G(d,p)] suggests a slight increase in the Wiberg bond order for P1-N3 to 0.8755 from 0.8108 in **3**, whilst that of N3-C1 decreases from 1.6132 to 1.4745.

Reactions with hard acids (MeOTf, HCl) resulted in the cleavage of the exocyclic P-N bond to form the NHP-X species (X = OTf, Cl) concomitant with the formation of **11** or its derivatives (Scheme 5.5) as confirmed by both ^{1}H NMR and ^{31}P NMR spectroscopy. Given the electrophilic nature of the P atom in the NHP fragment, it is reasonable to suggest that after the initial coordination of H$^+$ or Me$^+$ to the harder nitrogen atom on the imidazolin-2-iminato moiety, the heterolytic cleavage of the exocyclic P-N bond occurs to form the products (Scheme 5.6). Compound **12** is also found to be thermally stable when subjected to heating in toluene overnight, however, it hydrolyses rapidly to give the NHP(O)H and **11** (Scheme 5.5).
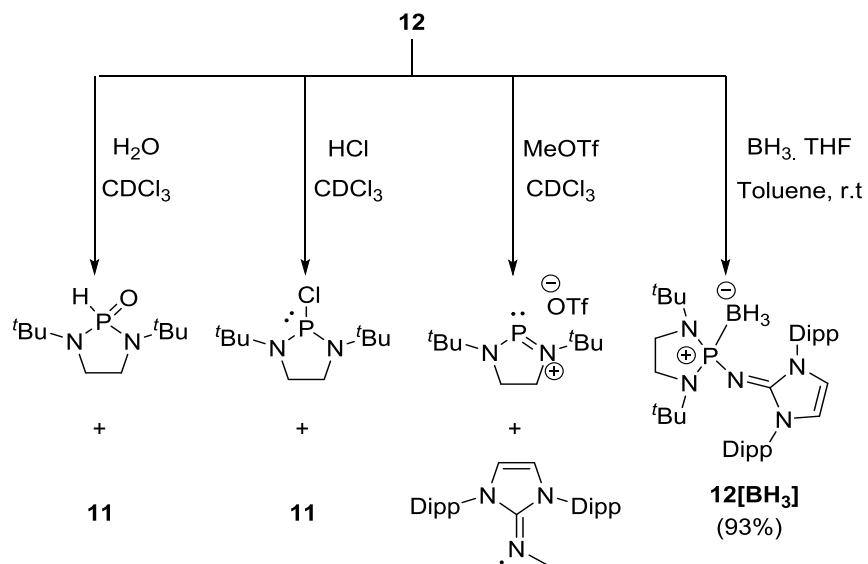
Scheme 5.5   Reactions of **12** with BH_3.THF, MeOTf, HCl and H_2O.
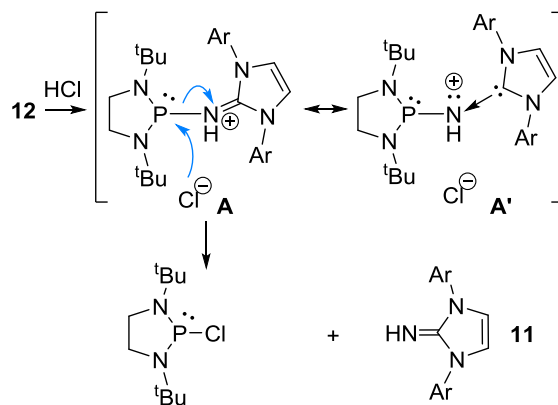
Scheme 5.6   Proposed mechanism for the reaction of **12** with HCl.

a)
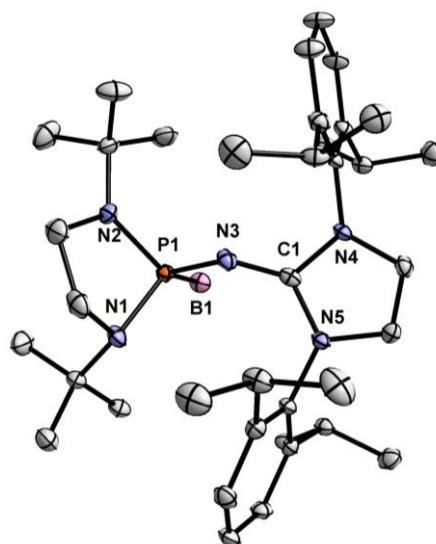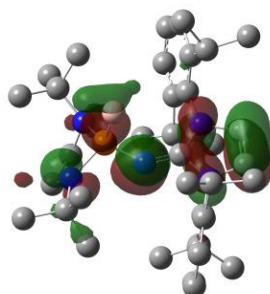
b)   c)
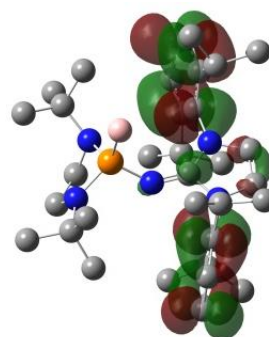
Figure 5.6   ORTEP drawing of **12[BH₃]** with thermal ellipsoids set at 30% probability level. Selected bond lengths [Å] and angles [°]: P1-N1 1.6823(16), P1-N2 1.7085(16), P1-N3 1.6241(16), P1-B1 1.915(2), N3-C1 1.299(2), C1-N4 1.381(2), C1-N5 1.377(2), P1-N3-C1 130.64(13), N1-P1-N2 94.34(8), N4-C1-N5 104.74(15). b) HOMO of **12[BH₃]**; c) LUMO of **12[BH₃]**. Hydrogen atoms are omitted for clarity.

5.2.3   *Synthesis of cationic P^III Heterocycle featuring Bis(NHC-olefin) ligand*

Replacing the exocyclic nitrogen in imidazoline-2-iminato **11** with a carbon atom, formally known as enediamines, gives an NHC-olefin containing an ylidic carbon centre (Figure 5.7a). Rivard et al. reported the utilisation of such NHC-olefin for the stabilisation of Sn and Ge hydrides of low oxidation states (Figure 5.7b).[16] Robinson et al. also employed NHC-olefin for the stabilisation of a borenium cation (Figure 5.7c).[17] Furthermore, their application in catalytic polymerisation reaction and CO_2 reduction has also been reported.[18]
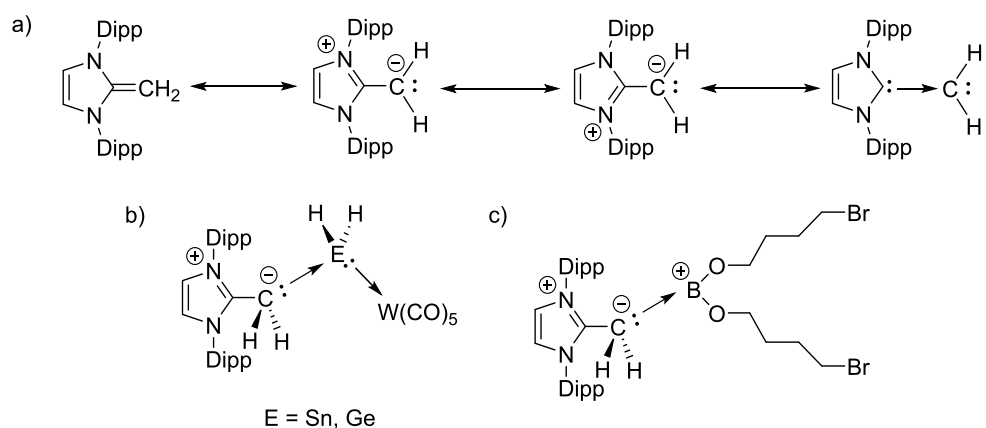
Figure 5.7 a) Resonance structures of ylidic NHC-olefin; b) NHC-olefin-stabilised Sn(II) or Ge(II) hydrides; c) NHC-olefin-stabilised borenium cation.

In addition, functionalisation of NHC-olefin featuring aryl substituent has been achieved by both von Wangelin and Mayr (Scheme 5.7).[19] Similar to the case for NHC-olefin, these deoxy-Breslow intermediates are nucleophilic at the α- and γ-position of the exocyclic double bond as shown by its resonance structures (Figure 5.8).
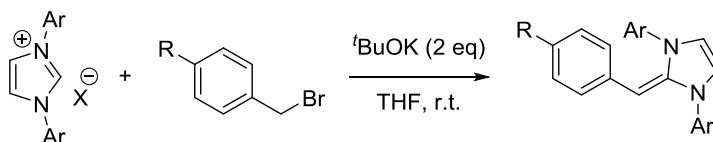
Scheme 5.7 General synthetic route for the deoxy-Breslow intermediates.
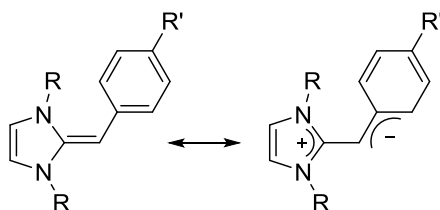
Figure 5.8 Resonance structures of deoxy-Breslow intermediate.

Those pioneering works prompted us to design and develop new P(III) heterocyclic ligands featuring two ylidic (NHC-olefin) moieties. Initially, the synthesis of bis(NHC-olefin) ligands **13a-b** was performed using α,α'-dibromo-o-xylene with NHC (**L$_a$** or **L$_b$**) employing similar procedures as shown in Scheme 5.6, however, the reaction did not proceed cleanly. The

desired ligands **13** were obtained after stirring in THF for 2 days at room temperature when excess NHCs were used (Scheme 5.8). Products **13a-b** were characterised by both ^{1}H NMR and ^{13}C NMR spectroscopy. It is important to note that compounds **13** are reactive towards chlorinated solvents and Brønsted acids like HCl.
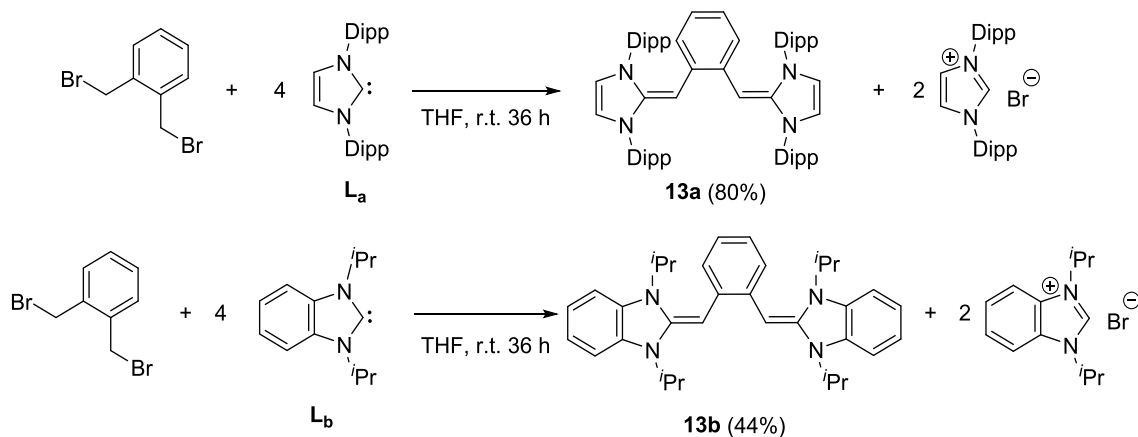
Scheme 5.8   Synthesis of ylidic bis(NHC-olefin)-based ligand **13**.

Addition of PCl_3 (1 eq) in the presence of excess NEt_3 (6 eq) afford the corresponding bis(NHC-olefin) chlorophosphindole in reasonable yields (Scheme 5.8, **14a**: 91 %; **14b**: 45 %). The ^{31}P NMR spectrum of **14b** in $CDCl_3$ ($\delta = 170.1$ ppm) is slightly upfield compared with that of **14a** ($\delta = 184.2$ ppm) which might be due to the stronger donor ability of L_b as compared to L_a.

A single crystal for **14a** was subjected to X-ray diffraction analysis (Figure 5.9a). The structure for **14a** shows a two-coordinated cationic phosphorus centre with Cl⁻ as the counterion. The stabilisation of its cationic form could be due to the strong donating ability of the ylidic carbons which increases the electron density around the phosphorus centre. The C2-C3 (1.427(3) Å) and the C4-C5 1.428(3) Å bond distances are slightly shorter than the average $C(sp^2)$-C(Ar) single bond (1.470 Å).[13] On the other hand, the C1-C2 and the C5-C6 bonds (1.443(3) Å and 1.449(3) Å respectively) are slightly longer than the average $C(sp^2)$-$C(sp^2)$ double bond (1.317 Å).[13] The C-N bond lengths for the two imidazole moieties in **14a** are comparable to one another, hence suggesting some degree of delocalisation for the N-C-N moieties. To account for these structure parameters, several possible canonical forms **I**-**VI** for the cationic form of **14** were

drawn (Scheme 5.9) and in particular, resonance structure **IV** provides a matching description to those solid state structural parameters.

13a (R = Dipp)
13b (R = ^{i}Pr)

14a (91%) ^{31}P NMR: 184.2
14b (45%) ^{31}P NMR: 170.1

1. NEt$_3$ (6 eq)
2. PCl$_3$ (1 eq)

toluene, 40 °C, 36 h
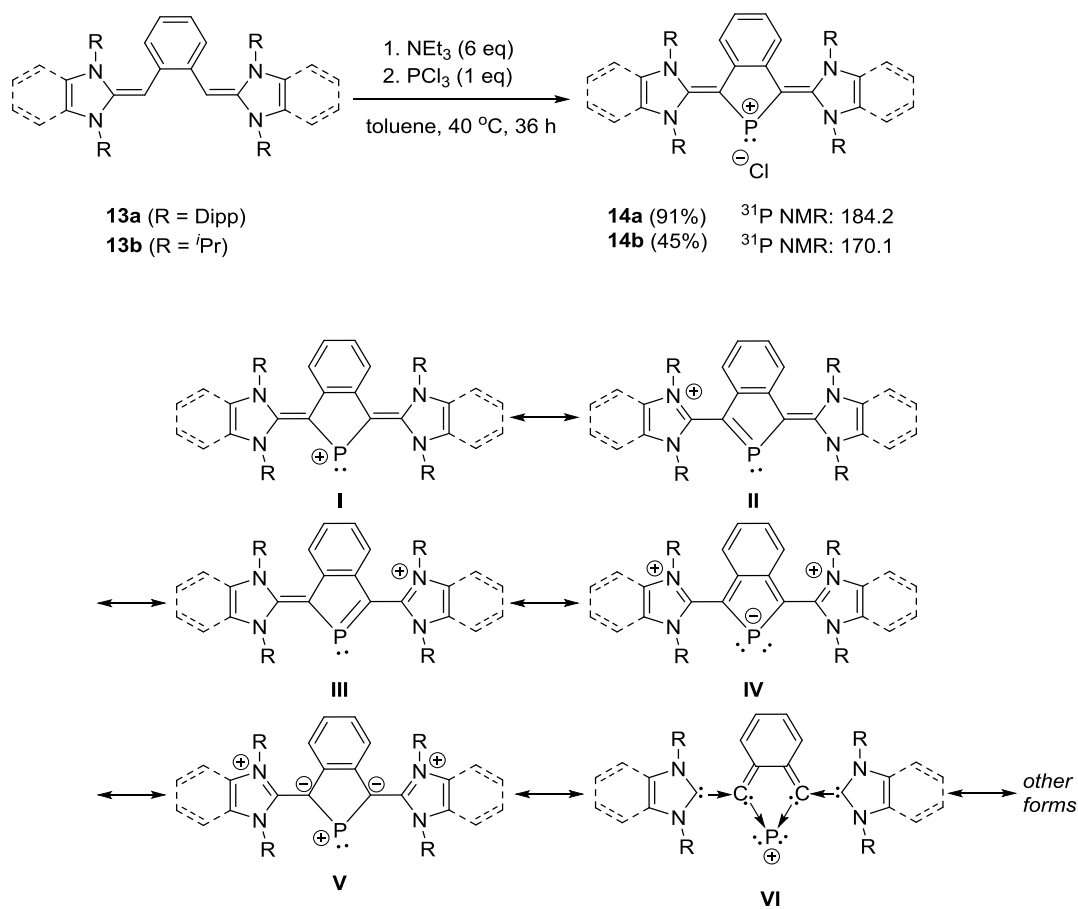
Scheme 5.9   Synthetic route for chlorophosphinodole **14** and the selected resonance forms of the cation in **14**.

a)
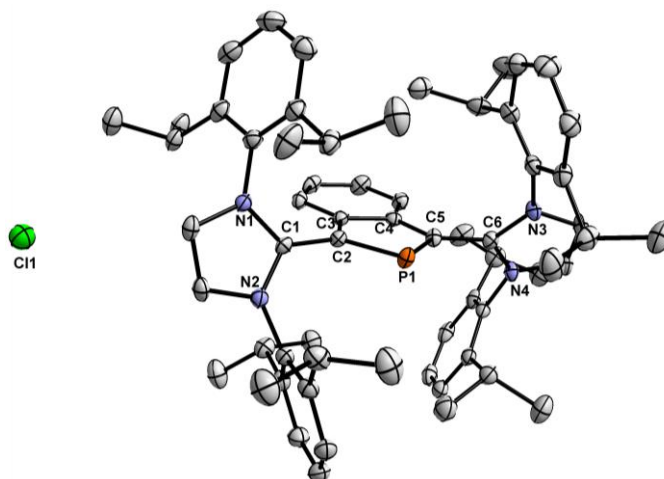
b)
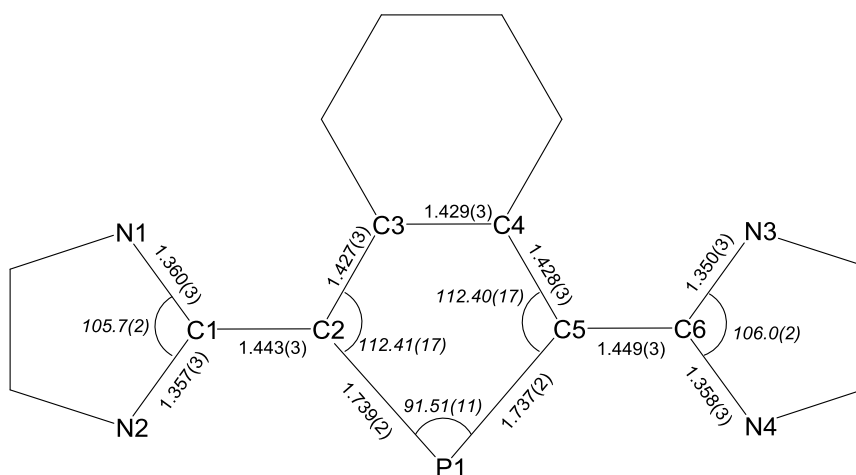
Figure 5.9 a) ORTEP drawing of **14a** with thermal ellipsoids set at 30% probability level; b) Summary of selected bond lengths (Å) and bond angles (°) of **14a** encapsulating the phosphindole moiety. Hydrogen atoms are omitted for clarity.

To gain further insights into the electronic structure of **14**, theoretical studies were performed at B3LYP/6-311G(d,p) level of theory for a model compound of **14a**, (**14a[H]**[+]).[20] Natural bond orbital (NBO) analysis[21] was also carried out at M052X/6-311G(d,p) level of theory. The Wiberg bond index (WBI) values (Figure 5.10) suggest a partial double bond character around the 5-membered ring phosphole moiety, hence, implying the aromatic nature of the cationic 6π-phosphole moiety. Indeed, the HOMO of **14a[H]**[+] shows the π-system of the benzophosphole moiety with some contribution from the two imidazole groups (Figure 5.11b).

Moreover, the HOMO-1 of **14a[H]**[+] locates mainly on the [ylide]C-P-[ylide]C fragment, hence, implying a certain extent of nucleophilicity on the phosphorus centre (Figure 5.11a). The LUMO of **14a[H]**[+] consists of mainly the p-orbital on the P atom as well as the π-systems on the ylidic (NHC-olefin) (Figure 5.11c).
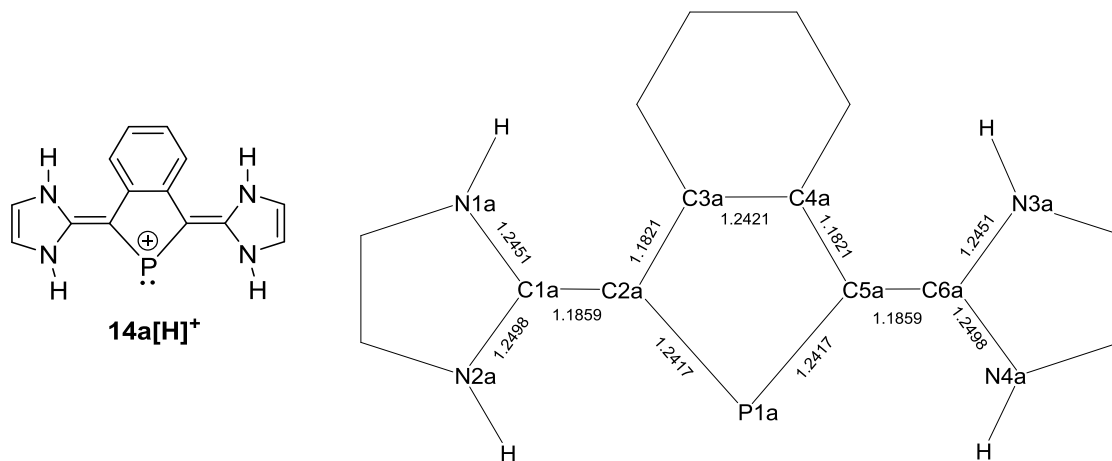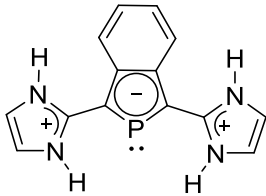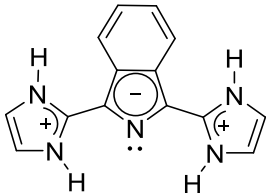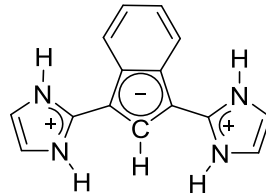
Figure 5.10   Selected WBI values for compound **14a[H]**[+].
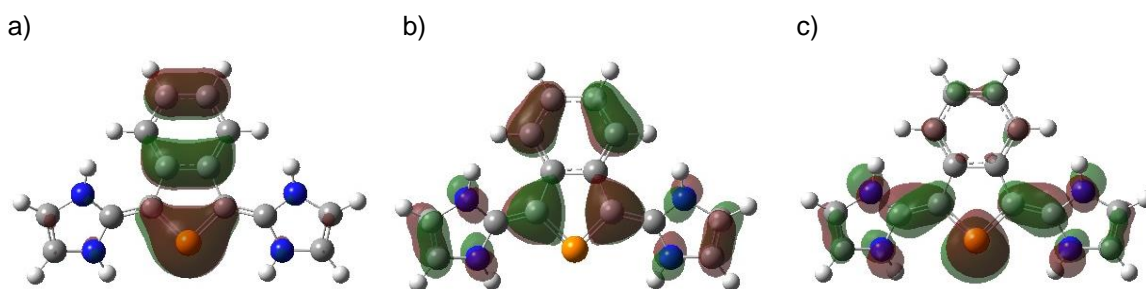
Figure 5.11   Calculated a) HOMO-1, b) HOMO and c) LUMO for compound **14a[H]**[+] at B3LYP/6-311G(d,p) level of theory.

A further analysis of the aromaticity of **14a[H]**[+] was conducted using nucleus-independent chemical-shift values NICS(0) and NICS(1).[22] For comparative purpose, the NICS(0) and NICS(1) values for analogous cationic structures featuring isoindole (**IsoN**[+]), isoindene (**IsoC**[+]) were also calculated at the same level of theory (B3LYP/6-311G(d,p)) (Figure 5.12). The NICS values for **14a[H]**[+] are found to be significantly negative, indicating aromaticity, which is in contrast to the case for the neutral non-aromatic phosphole featuring pyramidal phosphorus centre.[23] In addition, NICS values for **14a[H]**[+] are comparable to those of isoindene derivative and the isoindole derivative.

	14a[H]⁺	IsoN⁺	IsoC⁺
NICS(0)	-8.89	-8.62	-8.08
NICS(1)	-8.98	-9.55	-8.44

Figure 5.12 Calculated NICS(0) and NICS(1) values for **14a[H]⁺**, isoindole (**IsoN⁺**) and isoindene (**IsoC⁺**) derivatives at B3LYP/6-311G(d,p) level of theory.

To investigate the coordination ability of compound **14**, CuCl (1 eq) was added to dichloromethane solution of **14a**. However, no reaction was observed according to ³¹P NMR spectroscopy. This could be due to the steric hindrance exerted by the two bulky –Dipp substituents on the two imidazole moieties. In contrast, addition of CuCl (1 eq) to a dichloromethane solution of **14b** resulted in a shift in ³¹P NMR to 144.2 ppm from 170.1 ppm (**14b**). After work-up, compound **15** was obtained in 81% yield (Scheme 5.10). A single crystal of **15** can be obtained from an acetonitrile solution and its solid-state structure was unanimously confirmed by single crystal X-ray diffraction analysis (Figure 5.13a). The P1-Cu1 bond length is 2.1784(13) Å, which is shorter than the P-Cu bond length (2.35 Å) in (Ph₃P)₃CuCl but comparable to that found in tris(2,4,6-trimethoxyphenyl)phosphine copper(I) chloride complex (2.177 Å).[24] The sum of angles around the P1 atom is 360° indicating a trigonal planar geometry with the sp²-hybridisation.
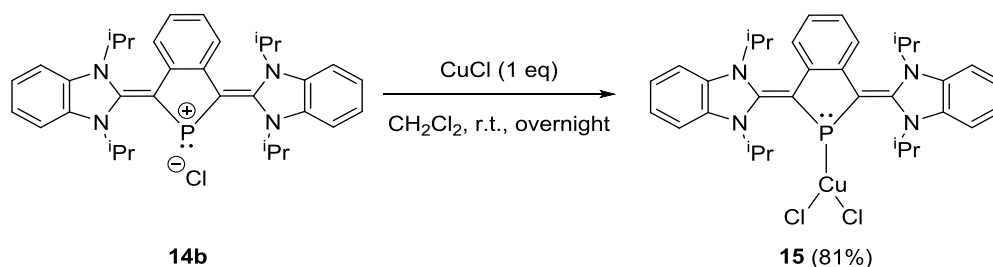
Scheme 5.10 Synthetic route for compound **15** from compound **14b**.

a)
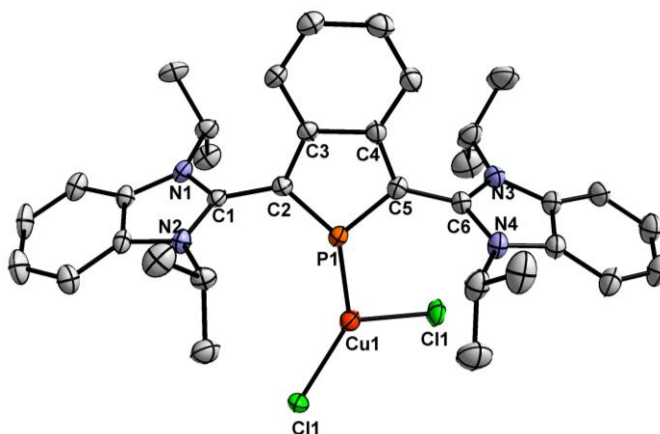
b)
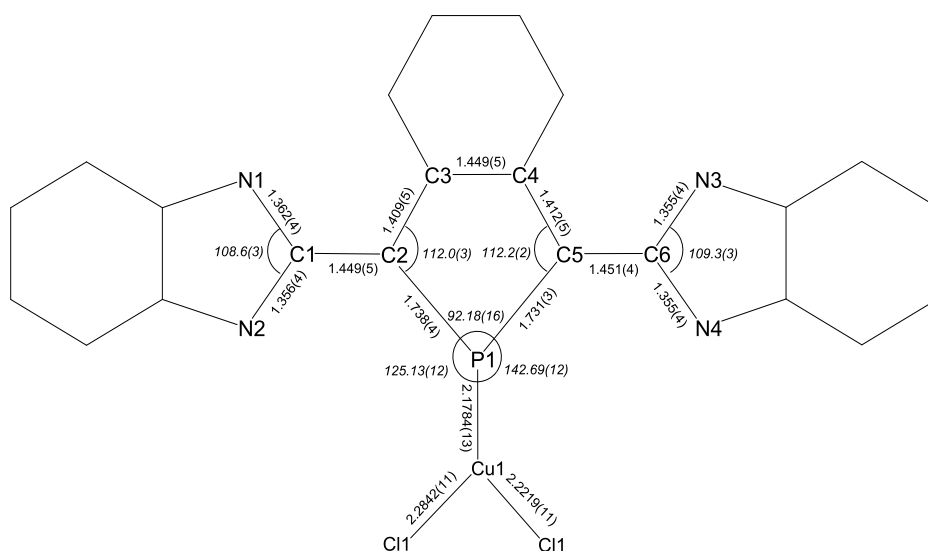
Figure 5.13   a) ORTEP drawing of **15** with thermal ellipsoids set at 30% probability level; b) Summary of selected bond lengths (Å) and bond angles (°) of **15**. Hydrogen atoms are omitted for clarity.

To gain further insights into the electronic feature of **15**, DFT calculations were performed at B3PW/6-31G(d,p) level of theory, with the LANL2DZ pseudo-potential applied for Cu atom. The optimised geometry around the phosphorus centre shows a distorted pyramidal shape (sum of angles around the P atom = 334.1°) which deviates from the trigonal planar of **15** (sum of angles around the P atom = 359.9°). Nonetheless, the HOMO of **15** is contributed by both the π-orbitals around 5-membered phosphole moiety and a d-orbital on the Cu centre (Figure

5.14a). On the other hand, the LUMO of **15** lies mainly on the p-orbital of the phosphorus atom with some contribution from π-orbitals from the two adjacent ylidic carbons (Figure 5.14b). Interestingly, the LUMO for **15** is similar to that in **14[H]** (Figure 5.11b), hence, implying that the electrophilicity on the phosphorus centre somewhat unperturbed despite being coordinated to the Cu centre. We also performed natural bond order (NBO) analysis for compound **15** (Figure 5.14c). The Wiberg bond index (WBI) values show partial double bond character for the 5-membered phosphole moiety, therefore, implying that the aromaticity is retained. In addition, the characteristic donor-acceptor interaction was found between the lone pair (LP) orbital on the P atom and the partially vacant d-orbital on the Cu, with a stabilisation energy of 107.97 kcalmol^{-1}.

a)

b)

c)
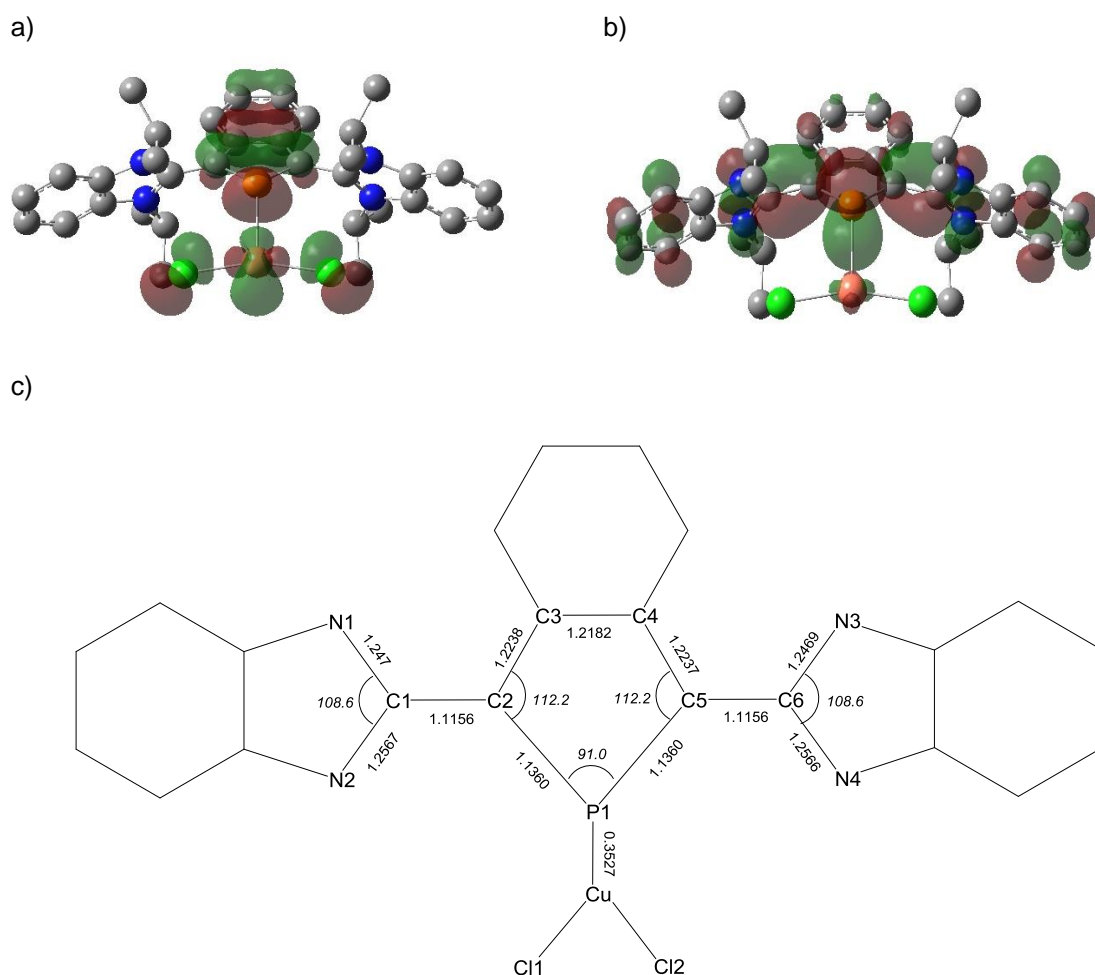
Figure 5.14   a) HOMO, b) LUMO and, c) selected WBI values and bond angles (^{o}) for compound **15** calculated at B9PW/6-31G(d,p) with LANL2DZ pseudo-potential level of theory. Hydrogen atoms are omitted for clarity.

5.3   Conclusion

We have successfully synthesized an N-heterocyclic phosphine **12** featuring imidazolin-2-iminato moiety. Attempt to perform one-electron oxidation using $[Ph_3C]^+[B(C_6F_5)_4]^-$ resulted in a radical species. The EPR and simulated EPR spectra predicted that the radical cation species could be a radical cation of bis(carbene)-stabilised N_2. Reacting of **12** with soft Lewis acid BH_3 resulted in the coordination of BH_3 to the softer P atom while hard acids (MeOTf, HCl) induced the cleavage of the exocyclic P-N bond upon coordination to the harder N atom.

We also synthesized a new P^{III} heterocycle, **14** using bis(NHC-olefin) ligands **13**. Both X-ray diffraction analysis and DFT calculations suggest aromatic nature on the 5-membered phosphole ring. Despite the cationic property of **14b**, the lone pair on the phosphorus centre could act as nucleophile as seen from the reaction of CuCl with **14b** which afforded a new phosphenium cation-Cu complex **15**.

5.4 Experimental Section

5.4.1 Synthesis, physical and spectroscopic data for all new compounds

General considerations: All reactions were performed under an atmosphere of argon by using standard Schlenk or dry box techniques; solvents were dried over Na metal, K metal or CaH_2. ^1H, $^{13}C\{^1H\}$, and ^{19}F NMR spectra were obtained with a Bruker AV 500, Bruker AV 400 or AVIII 400 MHz BBFO2 spectrometers at 298 K unless otherwise stated. Continuous wave X-Band EPR spectrum was obtained with a Bruker ELEXSYS E500 EPR spectrometer. Coupling constants *J* are given in Hz. Electrospray ionisation (ESI) mass spectra were obtained at the Mass Spectrometry Laboratory at the Division of Chemistry and Biological Chemistry, Nanyang Technological University. Compounds **1'**[25], **11**[11e], $[Ph_3C]^+[B(C_6F_5)_4]^-$ [26], **La**[27] and **Lb**[28] were prepared according to the literature procedures.

Synthesis of Compound 12: ^nBuLi (1.6 M in hexane, 3.2 mL, 5.12 mmol) was added at −78 °C to a THF solution (30 mL) of **11** (2.02 g, 5.00 mmol). The reaction mixture was warmed to room temperature and stirred for 2 h. **1'** was then dissolved in THF, added dropwise to the reaction mixture at room temperature and stirred for overnight. THF was then removed under vacuo and toluene was added to the residue. After filtration of LiCl, the solvent was removed in vacuo to yield an oily residue. Washing with pentane (10 mL) and filtration gives an off white compound **12**. (58% yield). Mp: 208 °C.

^1H NMR (400 MHz, C_6D_6): δ = 7.24 (t, ^3J = 7.6 Hz, 2H, Ar*H*), 7.14 (d, ^3J = 7.6 Hz, 4H, Ar*H*), 5.88 (s, 2H, NC*H*), 3.28 (sept, ^3J = 6.8 Hz, 4H, C*H*(CH₃)₂), 3.19 (m, 2H, NC*H₂*), 2.91 (m, 2H, NC*H₂*), 1.47 (d, ^3J = 6.8 Hz, 12H, CH(C*H₃*)₂), 1.20 (d, ^3J = 6.8 Hz, 12H, CH(C*H₃*)₂), 0.96 (d, $^4J_{P-H}$ = 0.8 Hz, 18H, C(C*H₃*)₃).

^{13}C NMR (100 MHz, C_6D_6): δ = 148.0 (Ar*C*-N), 143.3 (d, $^2J_{P-C}$ = 15.0 Hz, *C*=N), 135.7 (Ar*C*-C), 129.4 (Ar*C*-H), 123.8 (Ar*C*-H), 115.3 (NC*H*), 52.7 (d, $^2J_{P-C}$ = 10.0 Hz, q-*C*(CH₃)₃), 44.5 (d, $^2J_{P-C}$ = 8.0 Hz, *C*H₂), 29.7 (d, $^3J_{P-C}$ = 12.0 Hz, *C*H₃), 29.1 (*C*H), 24.9 (*C*H₃), 22.9 (*C*H₃).

^{31}P NMR (160 MHz, C_6D_6): δ = 90.0.

HRMS (ESI): *m/z* calcd for $C_{37}H_{59}N_5P$: 604.4508 $[(M+H)]^+$; found: 604.4508.

Attempted one-electron oxidation using [Ph₃C]⁺[B(C₆F₅)₄]⁻: **12** (0.25 g, 0.41 mmol) and [Ph₃C]⁺ [B(C₆F₅)₄]⁻ (0.38 g, 0. 41 mmol) were dissolved in degassed and dry benzene at room temperature. Upon addition of benzene, a dark brown solution was formed and the reaction mixture was stirred for 1 hour. The solvent was removed in vacuo and degassed hexane was added. After filtration, the resulting residue was then dried in vacuo to give a dark compound.

Synthesis of Compound 12[BH₃]: **12** (0.25 g, 0.41 mmol) and BH₃·THF (1.0 M in THF, 0.50 ml, 0.50 mmol) were dissolved in 20 mL of toluene and stirred for 1 h. The solvent was then removed in vacuo and recrystallized from benzene to give a colourless crystal of **1[BH₃]** (53% yield). Mp. 139 °C(decomposed).

^{1}H NMR (400 MHz, C₆D₆): δ = 7.23 (t, ^{3}J = 7.8 Hz, 2H, *p-CH*), 7.14 (d, ^{3}J = 7.8 Hz, 4H, *m-CH*), 6.06 (s, 2H, NC*H*), 3.31 (sept, ^{3}J = 6.8 Hz, 4H, C*H*(CH₃)₂), 3.00 (m, 2H, NC*H*₂), 2.89 (m, 2H, NC*H*₂), 1.47 (d, ^{3}J = 6.8 Hz, 12H, CH(C*H*₃)₂), 1.11 (d, ^{3}J = 6.8 Hz, 12H, CH(C*H*₃)₂), 1.02 (s, 18H, C(C*H*₃)₃).

^{13}C NMR (100 MHz, C₆D₆): δ = 147.7 (Ar*C*-N), 143.5 (d, $^{2}J_{P-C}$ = 10.0 Hz, *C*=N), 135.0 (Ar*C*-C), 129.7 (Ar*C*-H), 124.4 (Ar*C*-H), 116.6 (N*C*H), 54.3 (d, $^{2}J_{P-C}$ = 4.0 Hz, *q-C*(CH₃)₃), 45.2 (*C*H₂), 30.1 (d, $^{3}J_{P-C}$ = 3.0 Hz, *C*H₃), 28.8 (*C*H), 25.7 (*C*H₃), 22.9 (*C*H₃).

^{31}P NMR (160 MHz, C₆D₆): 80.0 (br).

^{11}B NMR (128 MHz, C₆D₆): -31.0 (br).

HRMS (ESI): *m/z* calcd for C₃₇H₆₂N₅PB: 618.4836 [(*M*+*H*)]⁺; found: 618.4807.

General Procedures for the Reactions of 12 with MeOTf, MeOH and HCl: **12** (25 mg, 0.041 mmol) and 1 equivalent of the corresponding reactant were added to 0.5 ml of CDCl₃ in a Carius NMR tube at room temperature.

Synthesis of 13: **L_a** or **L_b** (10 mmol) and α,α'-dibromo-o-xylene (0.65 g , 2.5 mmol) were dissolved in THF (50 mL) and stirred for 36 h at room temperature. The THF solvent was removed under vacuo and toluene (80 mL) was added to the resulting residue. After filtering

corresponding imidazolium salt, the filtrate was then removed under vacuo to afford compound **13**. Further purification for **13** can be carried out by washing the residue with hexane (20 mL).

13a (80 %): Yellow solid; M.p. 250 $^{\circ}$C (decomposed).

^{1}H NMR (300 MHz, C$_6$D$_6$): δ = 7.32 (t, ^{3}J = 8.0 Hz, 2H, Ar*H*), 7.19 (d, ^{3}J = 8.0 Hz, 4H, Ar*H*), 7.00 (t, ^{3}J = 8.0 Hz, 2H, Ar*H*), 6.85 (d, ^{3}J = 8.0 Hz, 4H, Ar*H*), 6.35 (dd, ^{3}J = 8.0 Hz, J = 3.6 Hz, 2H, Ar*H*), 5.95 (d, ^{3}J = 4.0 Hz, 2H, =C*H*), 5.90 (dd, ^{3}J = 8.0 Hz, J = 3.6 Hz, 2H, Ar*H*), 5.82 (d, ^{3}J = 4.0 Hz, 2H, =C*H*), 3.97 (s, 2H, $^{\text{ylide}}$C*H*), 3.39 (sept, ^{3}J = 8.0 Hz, 4H, C*H*Me$_2$), 3.29 (sept, ^{3}J = 8.0 Hz, 4H, C*H*Me$_2$), 1.24 (d, ^{3}J = 8.0 Hz, 12H, CH(C*H$_3$*)$_2$), 1.12 – 1.07 (m, 36H, CH(C*H$_3$*)$_2$).

^{13}C NMR (75 MHz, C$_6$D$_6$): δ = 148.8 (Ar*C*-N), 145.9 (N*C*N), 145.6 (Ar*C*-N), 137.3 (Ar*C*-C), 135.6 (Ar*C*-C), 131.4 (Ar*C*-C), 129.3 (Ar*C*-H), 128.4 (Ar*C*-H), 125.9 (Ar*C*-H), 124.9 (Ar*C*-H), 123.9 (Ar*C*-H), 118.4 (Ar*C*-H), 117.7 (*C*H), 115.6 (*C*H), 69.2 ($^{\text{ylide}}$*C*H), 28.8 (*C*H), 28.3 (*C*H), 25.7 (*C*H$_3$), 24.4 (*C*H$_3$), 23.8 (*C*H$_3$), 22.4 (*C*H$_3$).

HRMS (ESI): *m/z* calcd for C$_{62}$H$_{79}$N$_4$: 879.6305 [(*M*+*H*)]$^+$; found: 879.6376.

13b (44 %): Pale orange solid; M.p. 147 $^{\circ}$C.

^{1}H NMR (400 MHz, C$_6$D$_6$): δ = 7.64 (dd, ^{3}J = 5.7 Hz, J = 3.5 Hz, 2H, Ar*H*), 7.09 (dd, ^{3}J = 5.7 Hz, J = 3.5 Hz, 2H, Ar*H*), 6.91 – 6.79 (m, 8H, Ar*H*), 4.91 (s, 2H, $^{\text{ylide}}$C*H*), 4.54 (sept, ^{3}J = 8.0 Hz, 2H, C*H*Me$_2$), 4.25 (sept, ^{3}J = 8.0 Hz, 2H, C*H*Me$_2$), 1.23 (d, ^{3}J = 8.0 Hz, 12H, CH(C*H$_3$*)$_2$), 1.16 (d, ^{3}J = 8.0 Hz, 12H, CH(C*H$_3$*)$_2$).

^{13}C NMR (100 MHz, C$_6$D$_6$): δ = 148.4 (N*C*N), 138.4 (Ar*C*-C), 135.9 (Ar*C*-C), 135.5 (Ar*C*-C), 126.8 (Ar*C*-H), 122.4 (Ar*C*-H), 120.4 (Ar*C*-H), 119.1 (Ar*C*-H), 110.1 (Ar*C*-H), 107.4 (Ar*C*-H), 71.5 ($^{\text{ylide}}$*C*H), 50.4 (*C*H), 47.1 (*C*H), 19.6 (*C*H$_3$), 19.2 (*C*H$_3$).

HRMS (ESI): *m/z* calcd for C$_{34}$H$_{43}$N$_4$: 507.3488 [(*M*+*H*)]$^+$; found: 507.3504.

Synthesis of 14: NEt$_3$ (3.3 mL, 24 mmol) was added to a solution of **13** (4 mmol) in 30 mL toluene. After which, PCl$_3$ (0.4 mL, 4.6 mmol) was added to the mixture at room temperature. The reaction was then stirred at 40 $^{\circ}$C for 36 h. Toluene was then removed under vacuo and the solid residue was dissolved in dichloromethane. The dichloromethane solution was then washed twice

with water (20 mL). The organic extract was then dried using $MgSO_4$ and removed under vacuum to yield corresponding phosphole **14**.

14a (91 %): Yellow solid; M.p. 288 ^{o}C.

^{1}H NMR (500 MHz, CDCl$_3$): δ = 7.54 (s, 4H, =C*H*), 7.28 (t, ^3J = 8.0 Hz, 4H, Ar*H*), 6.99 (d, ^3J = 8.0 Hz, 8H, Ar*H*), 6.73 (m, 2H, Ar*H*), 6.58 (m, 2H, Ar*H*), 2.59 (sept, ^3J = 6.5 Hz, 8H, C*H*Me$_2$), 1.10 (d, ^3J = 6.5 Hz, 24H, CH(C*H*$_3$)$_2$), 0.64 (d, ^3J = 6.5 Hz, 24H, CH(C*H*$_3$)$_2$).

^{13}C NMR (125 MHz, CDCl$_3$): δ = 152.4 (d, $^2J_{P\text{-}C}$ = 25.0 Hz, NC*N*), 145.2 (Ar*C*-N), 137.9 (Ar*C*-C), 131.6 (Ar*C*-C), 130.9 (Ar*C*-H), 124.7 (Ar*C*-H), 124.4 (=*C*-H), 119.3 (Ar*C*-H), 117.1 (Ar*C*-H), 115.3 (d, $^1J_{P\text{-}C}$ = 38.0 Hz, ^{ylide}*C*-P), 29.2 (*C*H), 26.0 (*C*H), 22.5 (*C*H$_3$).

^{31}P NMR (200 MHz, CDCl$_3$): δ = 184.2.

HRMS (ESI): *m/z* calcd for C$_{62}$H$_{76}$N$_4$P: 907.5808 [*M*]$^+$; found: 907.5789

14b (45 %): Pale orange solid; M.p. 252 ^{o}C.

^{1}H NMR (400 MHz, CDCl$_3$): δ = 8.00 (dd, ^3J = 6.3 Hz, J = 3.2 Hz 4H, Ar*H*), 7.66 (dd, ^3J = 6.3 Hz, J = 3.2 Hz 4H, Ar*H*), 7.20 – 7.13 (m, 4H, Ar*H*), 4.95 (sept, ^3J = 7.0 Hz, 8H, C*H*Me$_2$), 1.79 (d, ^3J = 7.0 Hz, 12H, CH(C*H*$_3$)$_2$), 1.68 (d, ^3J = 7.0 Hz, 12H, CH(C*H*$_3$)$_2$).

^{13}C NMR (100 MHz, CDCl$_3$): δ = 152.8 (d, $^2J_{P\text{-}C}$ = 24.1 Hz, NC*N*), 139.0 (Ar*C*-N), 130.56 (Ar*C*-C), 126.0 (Ar*C*-H), 121.0 (Ar*C*-H), 117.6 (Ar*C*-H), 116.5(d, $^1J_{P\text{-}C}$ = 37.2 Hz, ^{ylide}*C*), 114.8 (^{Ar}*C*-H), 52.2 (*C*H), 21.3 (*C*H$_3$).

^{31}P NMR (160 MHz, CDCl$_3$): δ = 170.1.

HRMS (ESI): *m/z* calcd for C$_{34}$H$_{40}$N$_4$P: 535.2991 [*M*]$^+$; found: 535.3015

Synthesis of 15: CuCl (35 mg, 0.35 mmol) and **14b** (0.200 g, 0.35 mmol) were dissolved in dichloromethane and the reaction was stirred overnight. Solvent was then removed to yield yellow solid of compound **15** (81 %). M.p. 255 ^{o}C (decomposed).

^{1}H NMR (400 MHz, CDCl$_3$): δ = 7.92 (br, 4H, Ar*H*), 7.62 (br, 4H, Ar*H*), 7.07 (m, 4H, Ar*H*), 4.86 (sept, ^3J = 7.0 Hz, 8H, C*H*Me$_2$), 1.69 (m, ^3J = 7.0 Hz, 12H, CH(C*H*$_3$)$_2$).

^{13}C NMR (100 MHz, CDCl$_3$): δ = 151.7 (d, $^2J_{\text{P-C}}$ = 22.0 Hz, NCN), 138.2 (ArC-N), 130.7 (ArC-C), 125.8 (ArC-H), 121.0 (ArC-H), 117.8 (ArC-H), 115.0 (ArC-H), 110.5 (br, $^{\text{ylide}}C$-P), 52.4 (CH), 21.6 (CH$_3$).

^{31}P NMR (160 MHz, CDCl$_3$): δ = 144.2.

HRMS (ESI): m/z calcd for C$_{34}$H$_{40}$N$_4$P: 535.2991 [M]$^+$; found: 535.2991.

5.4.2   Crystal Structure Determination of Compounds *12*, *12[BH$_3$]*, *14a*, *15*.

X-ray data collection and structural refinement. Intensity data for compounds **12, 12[BH$_3$], 14a** and **15b** were collected using a Bruker APEX II diffractometer. The crystals of **12, 12[BH$_3$], 14a** were measured at 103(2) K while that of **15** was measure at 153(2) K. The structure was solved by direct phase determination (SHELXS-97) and refined for all data by full-matrix least squares methods on F^2.[29] All non-hydrogen atoms were subjected to anisotropic refinement. The hydrogen atoms were generated geometrically and allowed to ride on their respective parent atoms; they were assigned with appropriate isotropic thermal parameters and included in the structure-factor calculations.

Table 5.1 Summary of Data Collection and Structure Refinement for **12**, **12[BH₃]**, **14a** and **15**.

	12	**12[BH₃]**	**14a**	**15(CH₃CN)₂**
Formula	$C_{37}H_{58}N_5P$	$C_{43}H_{67}BN_5P$	$C_{68}H_{94}ClN_4O_3P$	$C_{38}H_{46}Cl_2CuN_6P$
Fw	603.85	695.79	1081.89	752.22
Cryst Syst	orthorhombic	triclinic	Monoclinic	triclinic
space group	P b c a	P -1	P 21/n	P -1
Size (mm³)	0.160 x 0.200 x 0.280	0.160 x 0.220 x 0.260	0.400 x 0.200 x 0.060	0.100 x 0.110 x 0.200
T, K	103(2)	103(2)	103(2)	153(2)
a, Å	19.3330	9.9932(5)	11.7627(11)	10.494(4)
b, Å	19.333(2)	12.8508(6)	22.295(2)	10.900(4)
c, Å	19.625(2)	32.4198(16)	24.911(2)	19.793(7)
α, deg	90	91.6290(18)	90	78.535(5)
β, deg	90	95.1147(17)	99.493(3)	89.373(5)
γ, deg	90	91.5658(17)	90	63.043(5)
V, A³	7335.1(11)	4143.3(3)	6443.3(11)	1969.6(13)
Z	8	4	4	2
d_{calcd} g·cm⁻³	1.094	1.115	1.115	1.268
μ, mm⁻¹	0.106	0.101	0.131	0.765
Refl collected	110868	100259	111090	11835
T_{min}/T_{max}	0.9710 / 0.9833	0.9740/ 0.9840	0.7462/0.5929	0.9270/0.8620
N_{measd}	6737	18865	20627	8176
$[R_{int}]$	0.1591	0.0905	0.1563	0.1003
R [I>2sigma(I)]	0.0633	0.0547	0.0731	0.0594
R_w[I>2sigma(I)]	0.1404	0.1180	0.1582	0.1338
GOF	1.135	1.021	1.019	1.025
Largest diff peak/hole[e·Å⁻³]	0.725/-0.748	0.337/-0.409	0.772/-0.456	0.622/-0.806

5.5 References

1.   a) Mark, J. E.; Allock, H. R.; West, R. *Inorganic Polymers*, 2nd ed.; Oxford University Press, New York, 2005; b) Göbel, M.; Karaghiosoff, K.; Klapötke, T. M. *Angew. Chem. Int. Ed.* **2006**, *45*, 6037–6040; c) Venkatesan, N.; Kim, S. J.; Kim, B. H. *Curr. Med. Chem*. **2003**, *10*, 1973–1991; d) Wilk, A.; Grajkowski, A.; Phillips, L. R.; Beaucage, S. L. *J. Am. Chem. Soc*. **2000**, *122*, 2149–2156; e) Jones, A. S.; McGuigan, C.; Walker, R. T. *J. Chem. Soc. Perkin Trans. 1* **1985**, 199–202.

2.   Verkade, J. G.; Urgaonkar, S. *Proazaphosphatrane, e-EROS Encyclopedia of Reagents for Organic Synthesis*, 2012.

3.   Holleman, A. F.; Wiberg, E.; Wiberg, N. *Lehrbuch der Anorganischen Chemie*. 102nd ed.; De Gruyter, Berlin, 2007, pp 814.

4.   Velian, A.; Cummins, C. C. *Science* **2015**, *348*, 1001–1004.

5.   a) Burck, S.; Götz, K.; Kaupp, M.; Nieger, M.; Weber, J.; auf der Günne, J. S.; Gudat, D. *J. Am. Chem. Soc*. **2009**, *131*, 10763–10774; b) Burck, S.; Gudat, D.; Nieger, M. *Angew. Chem. Int. Ed.* **2004**, *43*, 4801–4804.

6.   Burck, S.; Förster, D.; Gudat, D. *Chem. Commun*. **2006**, 2810–2812.

7.   a) Burck, S.; Gudat, D.; Nieger, M. *Organometallics* **2009**, *28*, 1447–1452; b) Burck, S.; Gudat, D.; Nieger, M.; Vinduš, D. *Eur. J. Inorg. Chem*. **2008**, 704–707; c) Burck, S.; Gudat, D.; Nieger, M. *Angew. Chem. Int. Ed*. **2007**, *46*, 2919–2922.

8.   Burck, S.; Gudat, D.; Lissner, F.; Nättinen, K.; Nieger, M.; Schleid, T. *Z. Anorg. Allg. Chem*. **2005**, *631*, 2738–2745.

9.   Burck, S.; Gudat, D.; Nieger, M.; Schalley, C. A.; Weilandt, T. *Dalton Trans*. **2008**, 3478–3485.

10. Kuhn, N.; Göhner, M.; Grathwohl, M.; Wiethoff, J.; Frenking, G.; Chen, Y. *Z. Anorg. Allg. Chem*. **2003**, *629*, 793–802.

11. a) Panda, T. K.; Trambitas, A. G.; Bannenberg, T.; Hrib, C. G.; Randoll, S.; Jones, P. G.; Tamm, M. *Inorg. Chem*. **2009**, *48*, 5462–5472; b) Beer, S.; Brandhorst, K.; Hrib, C. G.;

Wu, X.; Haberlag, B.; Grunenberg, J.; Jones, P. G.; Tamm, M. *Organometallics* **2009**, *28*, 1534–1545; c) Beer, S.; Brandhorst, K.; Grunenberg, J.; Hrib, C. G.; Jones, P. G.; Tamm, M. *Org. Lett.* **2008**, *10*, 981–984; d) Beer, S.; Hrib, C. G.; Jones, P. G.; Brandhorst, K.; Grunenberg, J.; Tamm, M. *Angew. Chem. Int. Ed.* **2007**, *46*, 8890–8894; e) Tamm, M.; Petrovic, D.; Randoll, S.; Beer, S.; Bannenberg, T.; Jones, P. G.; Grunenberg, *J. Org. Biomol. Chem.* **2007**, *5*, 523–530; f) Tamm, M.; Randoll, S.; Herdtweck, E.; Kleigrewe, N.; Kehr, G.; Erker, G.; Rieger, B. *Dalton Trans.* **2006**, 459–467; g) Tamm, M.; Randoll, S.; Bannenberg, T.; Herdtweck, E. *Chem. Commun.* **2004**, 876–877.

12. a) Franz, D.; Szilvási, T.; Irran, E.; Inoue, S. *Nat. Commun.* **2015**, *6*, 10037; b) Franz, D.; Irran, E.; Inoue, S. *Angew. Chem. Int. Ed.* **2014**, *53*, 14264–14268; c) Franz, D.; Irran, E.; Inoue, S. *Dalton Trans.* **2014**, *43*, 4451–4461; d) Dielmann, F.; Back, O.; Henry-Ellinger, M.; Jerabek, P.; Frenking, G.; Bertrand, G. *Science* **2012**, *337*, 1526–1528; e) Inoue, S.; Leszczyńska, K. *Angew. Chem. Int. Ed.* **2012**, *51*, 8589–8593; f) Kinjo, R.; Donnadieu, B.; Bertrand, G. *Angew. Chem. Int. Ed.* **2010**, *49*, 5930–5933. See also: g) Ochiai, T.; Franz, D.; Wu, X. –N.; Inoue, S. *Dalton Trans.* **2015**, *44*, 10952–10956; h) Ochiai, T.; Franz, D.; Irran, E.; Inoue, S. *Chem. Eur. J.* **2015**, *21*, 6704–6707; i) Lui, M. W.; Merten, C.; Ferguson, M. J.; McDonald, R.; Xu, Y.; Rivard, E. *Inorg. Chem.* **2015**, *54*, 2040–2049.

13. Allen, F. H.; Kennard, O.; Watson, D. G.; Brammer, L.; Orpen, A. G.; Taylor, R. *J. Chem. Soc. Perkin Trans. II* **1987**, S1–S19.

14. a) Griffin, N. A.; Hendsbee, A. D.; Roemmele, T. L.; Lundsen, M. D.; Pye, C. C.; Masuda, J. D. *Inorg. Chem.* **2012**, *51*, 11837–11850; b) Edge, R.; Less, R. J.; McInnes, E. J. L.; Muther, K.; Naseri, V.; Rawson, J. M.; Wright, D. S. *Chem. Commun.* **2009**, 1691–1693.

15. Herrmann, H.; Reinmuth, M.; Wiesner, S.; Hübner, O.; Kaifer, E.;Wadepohl, H.; Himmel, H.-J. *Eur. J. Inorg. Chem.* **2015**, 2345–2361.

16. Al-Rafia, S. M. I.; Malcolm, A. C.; Liew, S. K.; Ferguson, M. J.; McDonald, R.; Rivard, E. *Chem. Commun.* **2011**, *47*, 6987–6989.

17. Wang, Y.; Abraham, M. Y.; Gilliard, R. J.; Sexton, D. R.; Wei, P.; Robinson, G. H. *Organometallics* **2013**, *32*, 6639–6642.

18. a) Naumann, S.; Thomas, A. W.; Dove, A. P. *Angew. Chem. Int. Ed*. **2015**, *54*, 9550–9554; b) Wang, Y.-B.; Wang, Y.-M.; Zhang, W.-Z.; Lu, X.-B. *J. Am. Chem. Soc*. **2013**, *135*, 11996–12003.

19. a) Maji, B.; Horn, M.; Mayr, H. *Angew. Chem. Int. Ed*. **2012**, *51*, 6231–6235; b) Knappe, C. E. I.; Arduengo, III, A. J.; Jiao, H.; Neudörfl, J. –M.; von Wangelin, A. J. *Synthesis* **2011**, *23*, 3784–3795.

20. Gaussian09 (Revision D.01), Frisch, M. J. et al. Gaussian, Inc.; Wallingford CT, **2009**.

21. a) Weinhold, F. *J. Comput. Chem*. **2012**, *33*, 2363–2379; b) Reed, A. E.; Curtis, L. A.; Weinhold, F. *Chem. Rev*. **1998**, *88*, 899–926.

22. a) Chen, Z.; Wannere, C. S.; Corminboeuf, C.; Puchta, R.; Schleyer, P. v. R. *Chem. Rev.* **2005**, *105*, 3842–3888; b) Schleyer, P. v. R.; Maerker, C.; Dransfeld, A.; Jiao, H.; van Eikema Hommes, N. J. R. *J. Am. Chem. Soc*. **1996**, *118*, 6317–6318.

23. a) Quin, L. D.; Quin, G. S. *Phosphorus-Carbon Heterocyclic Chemistry: The Rise of a New Domain*; Mathey, F., Ed.; Elsevier Science Ltd, Oxford, 2001, pp 307–362; b) Mathey, F. *Chem. Rev*. **1988**, *88*, 429–453.

24. a) Bowmaker, G. A.; Cotton, J. D.; Healy, P. C.; Kildea, J. D.; Silong, S. B.; Skelton, B. W.; White, A. H. *Inorg. Chem*. **1989**, *28*, 1462–1466; b) Barron, P. F.; Dyason, J. C.; Healy, P. C.; Engelhardt, L. M.; Pakawatchai, C.; Patrick, V. A.; White, A. H. *J. Chem. Soc. Dalton Trans.* **1987**, 1099–1106.

25. King, R. B.; Sundaram, P. M. *J. Org. Chem*. **1984**, *49*, 1784–1789.

26. Scott, V. J.; Çelenligil-Çetin, R.; Ozerov, O. V. *J. Am. Chem. Soc*. **2005**, *127*, 2852–2853.

27. Arduengo, III, A. J.; Krafczyk, R.; Schmutzler, R. *Tetrahedron* **1999**, *55*, 14523–14534.

28. Crudden, C. M.; Horton, J. H.; Ebralidze, I. I.; Zenkina, O. V.; McLean, A. B.; Drevniok, B.; She, Z.; Kraatz, H. –B.; Mosey, N. J.; Seki, T.; Keske, E. C.; Leake, J. D.; Rousina-Webb, A.; Wu, G. *Nat. Chem*. **2014**, *6*, 409–414.

29. G. M. Sheldrick, SHELXL-97; Universität Göttingen, Göttingen, Germany, 1997.

Conclusion

As mentioned in Chapter 1, the aim of the project is to investigate the catalytic activity of 1,3,2-diazaphospholene **1**. To our delight, **1** could perform efficiently in several catalytic reduction reactions.

In Chapter 2, **1** (5 mol%) was shown to catalyse the transfer hydrogenation of various azo-compounds using ammonia-borane under mild conditions. Theoretical and kinetic studies suggested a concerted hydrogenolysis transition state involving the cleavage of N-H and B-H bonds in the catalytic cycle.

In Chapter 3, we explored the catalytic hydroboration of aldehydes and ketones using **1** as the catalyst. The hydroboration of aldehydes occurs at room temperature in the presence of **1** (0.5 mol%) and HBpin. Subsequently, hydroboration of ketones were also examined and a harsher condition is required (10 mol% of **1** and at a temperature of $90^{o}C$). Stoichiometric reactions suggest that the initial step involves the insertion of P-H across the C=O bond, forming an alkoxyphosphine intermediate. Subsequently, the cleavage of P-O bond in the presence of HBpin affords the corresponding boric ester and regenerates catalyst **1**. The mechanism for the catalytic cycle was investigated using kinetic studies and theoretical calculations. Both results suggest that the second step of the hydroboration reaction occurs via a σ-bond metathesis mechanism.

Chapter 4 describes the catalytic reduction of a greenhouse gas, CO_2 using Ph_2SiH_2 in the presence of 5 mol% of **1** to generate $Ph_2Si(OCHO)_2$ as the major product. $Ph_2Si(OCHO)_2$ could react with amines to form formamides. The reaction could be conducted in a one-pot manner and hence, demonstrates the utilization of CO_2 as a C_1 source.

Lastly, Chapter 5 depicts the synthesis and characterization of a NHP-derivative **12** and a novel heterocyclic phosphorus(III) compound **14**. Despite containing two adjacent nucleophilic sites, **12** shows coordination selectivity with different acids. For compound **14**, the crystal structure and theoretical studies imply aromatic nature on the 5-membered phosphole ring moiety.

Remarkably, compound **14** could react with CuCl to afford a phosphenium cation-Cu complex **15** which could act as a potential catalyst.

## List of Publications related to this Thesis

1.   **Chong, C. C**.; Hirao, H.; Kinjo, R. A Concerted Transfer Hydrogenolysis: 1,3,2-Diazaphospholene-Catalyzed Hydrogenation of N=N Bond with Ammonia-Borane. *Angewandte Chemie International Edition*, **2014**, *53*, 3342–3346.

2.   **Chong, C. C**.; Hirao, H.; Kinjo, R. Metal-Free σ-Bond Metathesis in 1,3,2-Diazaphospholene-Catalyzed Hydroboration of Carbonyl Compounds. *Angewandte Chemie International Edition*, **2015**, *54*, 190–194.

3.   **Chong, C. C**.; Kinjo, R. Catalytic Hydroboration of Carbonyl Derivatives, Imines, and Carbon Dioxide. *ACS Catalysis*, **2015**, *5*, 3238–3259.

4.   **Chong, C. C**.; Kinjo, R. Hydrophosphination of CO_2 and Subsequent Formate Transfer in 1,3,2-Diazaphospholene-Catalyzed N-Formylation of Amines. *Angewandte Chemie International Edition*, **2015**, *54*, 12116–12120.

Chapter 2

a)
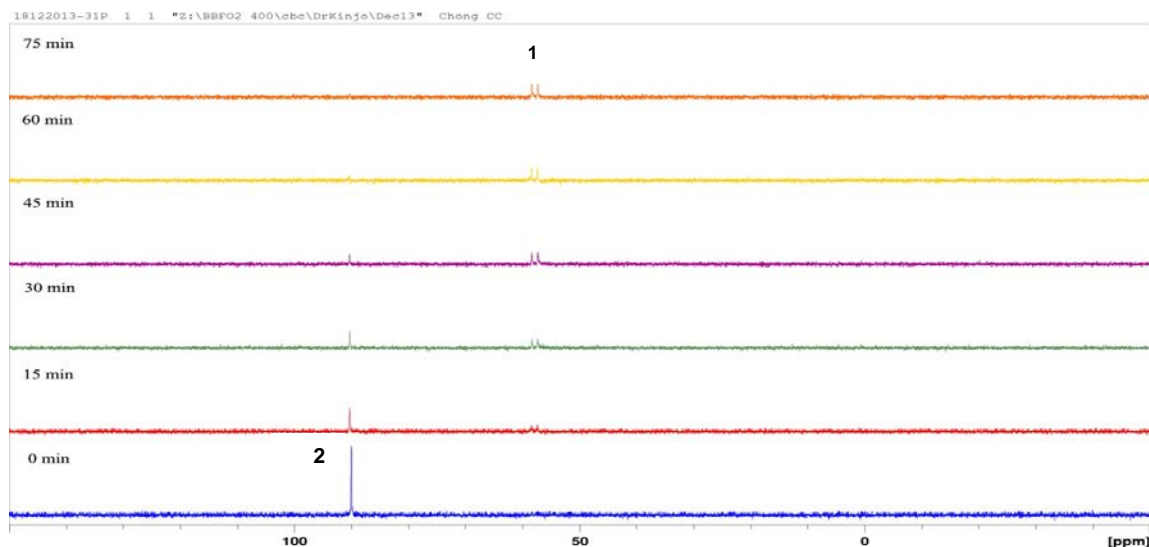
b)
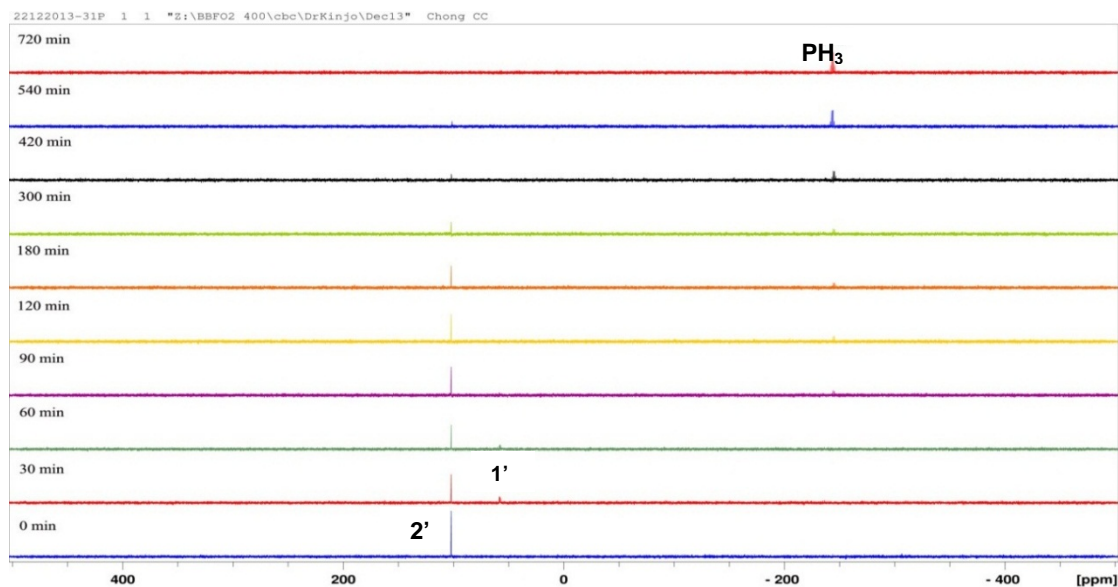
Figure A2-1   a) ^{31}P NMR plot for the reaction of **2** and H_3NBH_3 at 50 ^{o}C in CD_3CN at 15 minutes intervals. Signals observed: **2** at δ = 90.0 ppm and **1b** at δ = 57.8 ppm (d, ^{P-H}J = 165.2 Hz); b) ^{31}P NMR plot for the reaction of **2'** and H_3NBH_3 at 50 ^{o}C in CD_3CN. Signals observed: **2a** at δ 101.9 ppm, **1a** at δ = 57.3 ppm (d, ^{P-H}J = 153.1 Hz), and PH_3 at δ = –243.8 ppm (q, ^{P-H}J = 191.2 Hz).
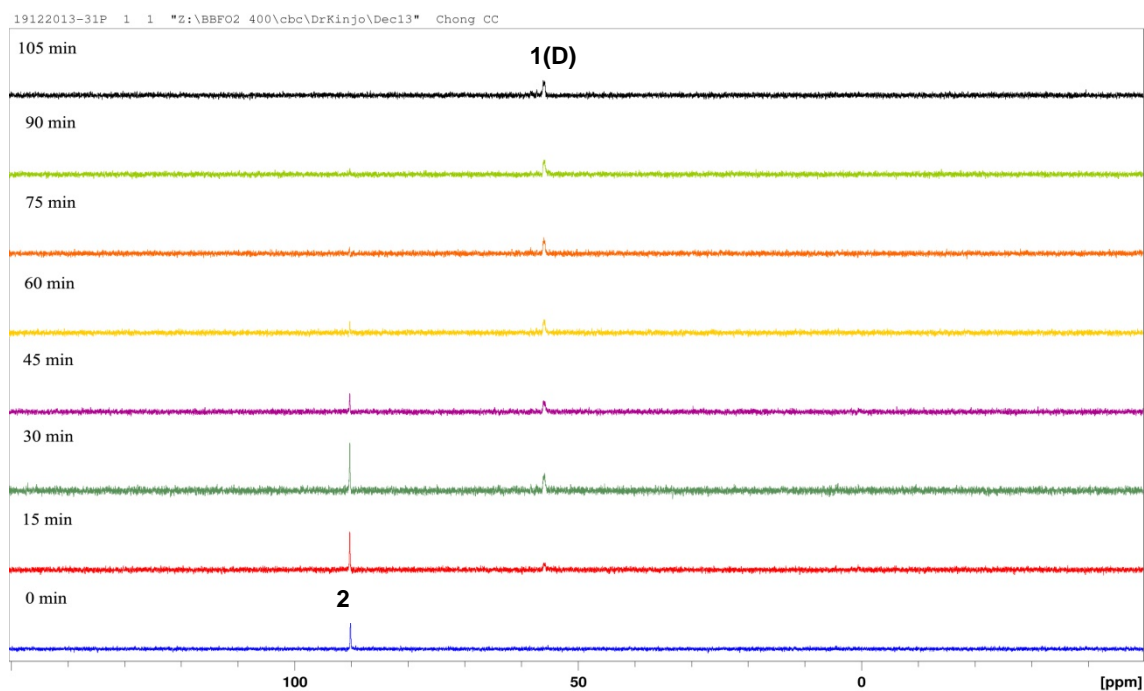
Figure A2-2 ^{31}P NMR plot for the reaction of **2** and H$_3$NBD$_3$ at 50 $^{\circ}$C in CD$_3$CN with 15 minutes interval. Signals observed: **2** at δ = 90.0 ppm and **1(D)** at δ = 57.8 ppm (br).

a)
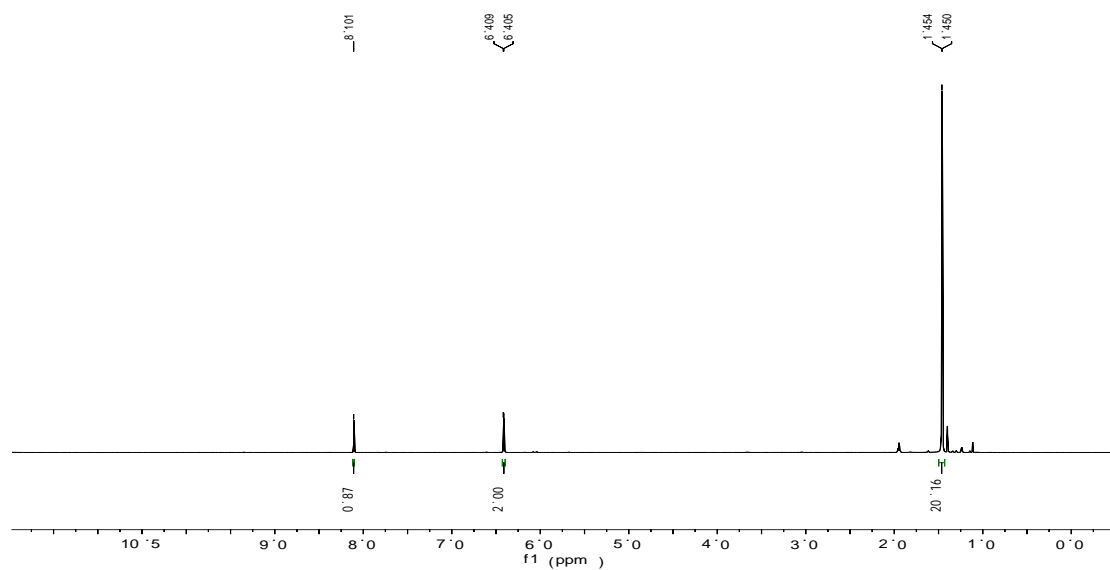

b)
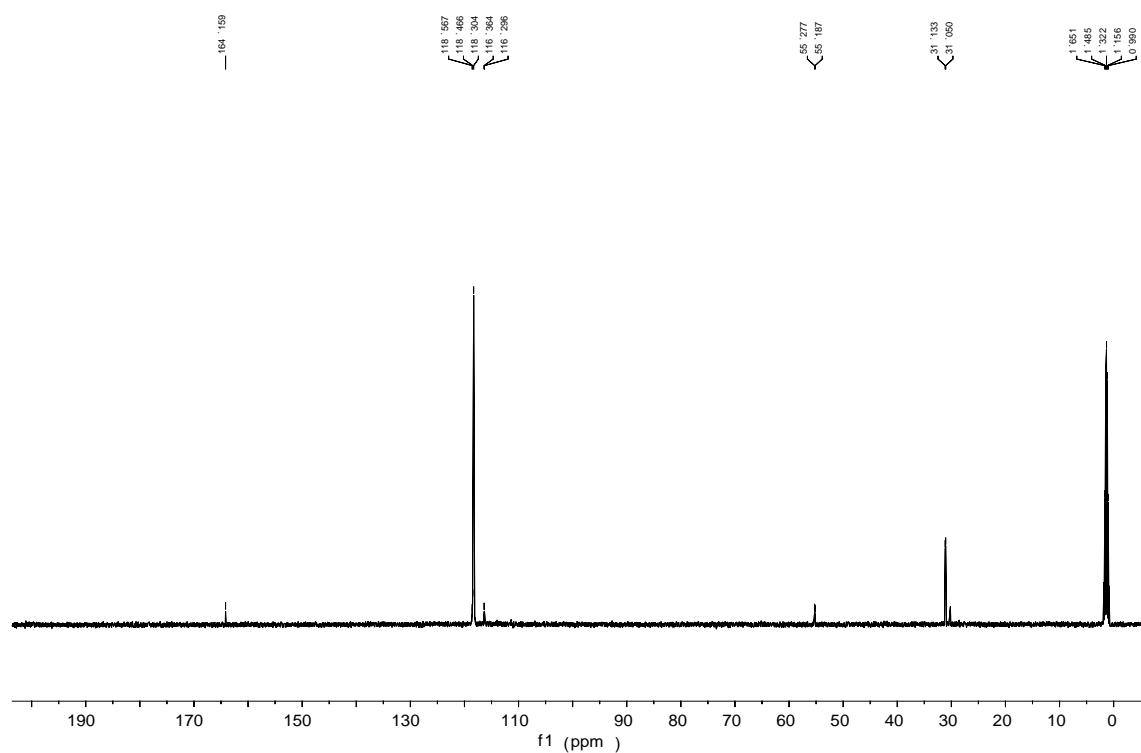
Figure A4-1 a) ¹H NMR spectrum of compound **8** in CD₃CN; b) ¹³C NMR spectrum of compound **8** in CD₃CN. .

a)
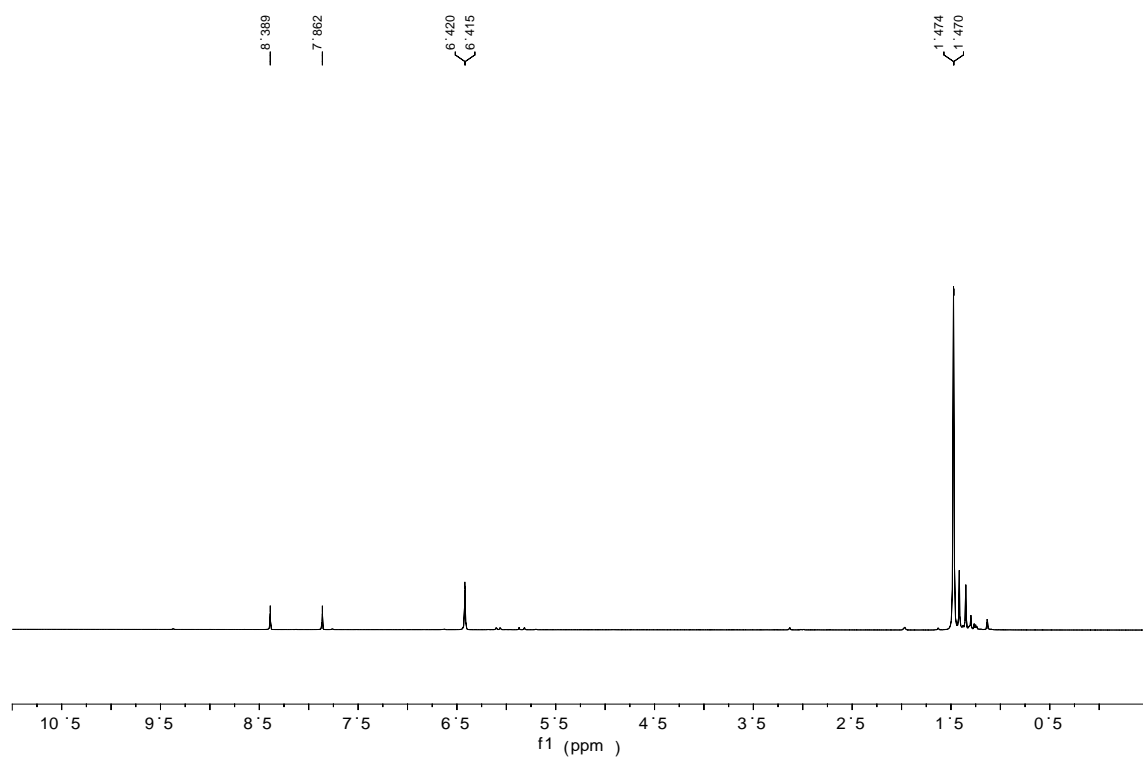
b)
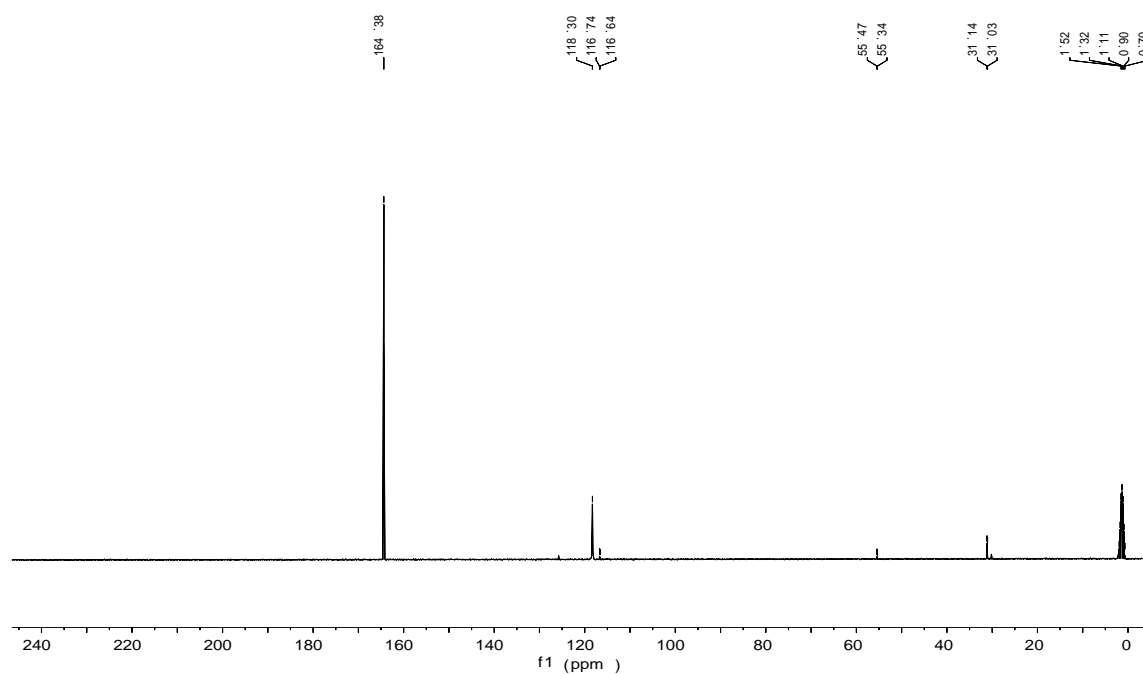
Figure A4-2   a) ^{1}H NMR spectrum of compound **8-**^{13}C in CD$_3$CN; b) ^{13}C NMR spectrum of compound **8-**^{13}C in CD$_3$CN.

137
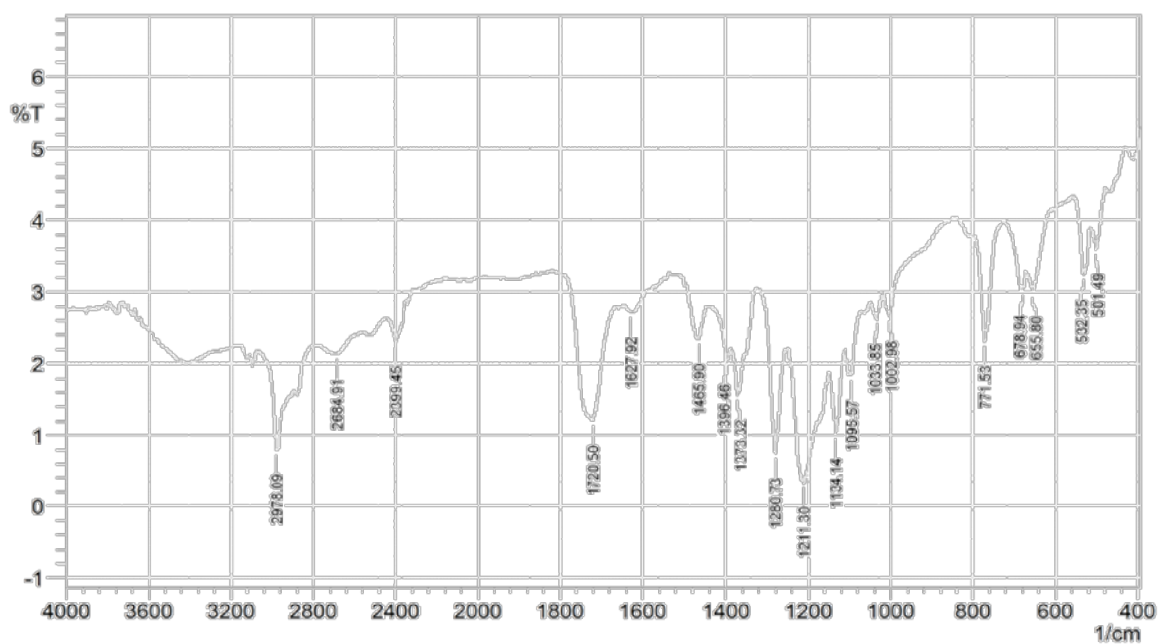
Figure A4-3   The solid-state IR spectrum of **8**: A peak at 1720 cm^{-1} corresponds to the $\nu_{C=O}$ in compound **8**.

Appendix B **Kinetic Data**

Chapter 2
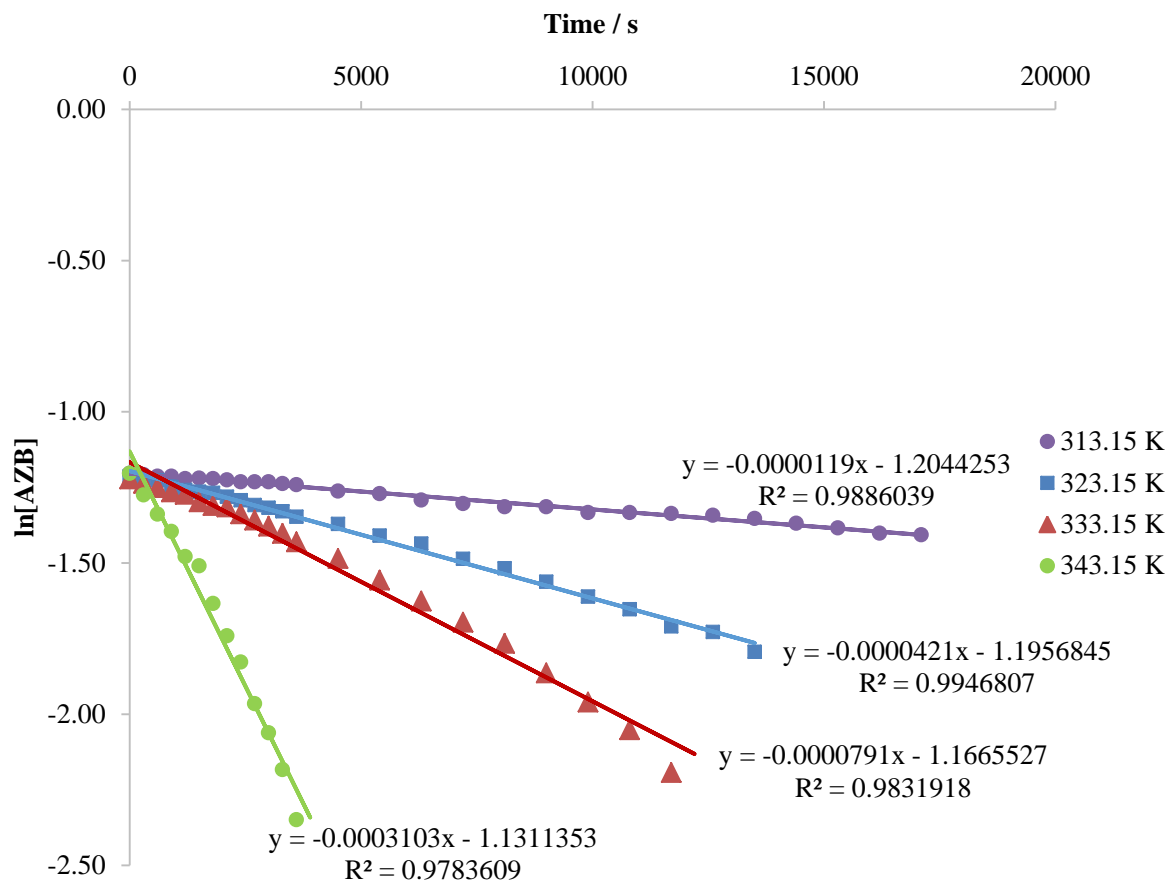
Figure B2-1 First-order plot of In(azobenzene) against time, *t* at various temperatures. Rate constant, *k*, can be obtained from the gradient of the graph.

Table B2-1 Various parameters for the determination of Eyring Plot for catalytic transfer hydrogenation of azobenzene.

T / K	1 / (*T* / K^{-1})	*k* / s^{-1}	(*k* / s^{-1}) / (*T* / K)	In(*k* / *T*)
313.15	0.003193	1.185E-05	3.785E-08	-17.09
323.15	0.003095	4.215E-05	1.356E-07	-15.82
333.15	0.003002	7.907E-05	2.447E-07	-15.22
343.15	0.002914	3.103E-04	9.315E-07	-13.89

$$\ln\frac{k}{T} = -\frac{\Delta H^{\ddagger}}{R}\left(\frac{1}{T}\right) + \ln\frac{k_B}{T} + \frac{\Delta S^{\ddagger}}{R} \qquad \text{(B1)}$$
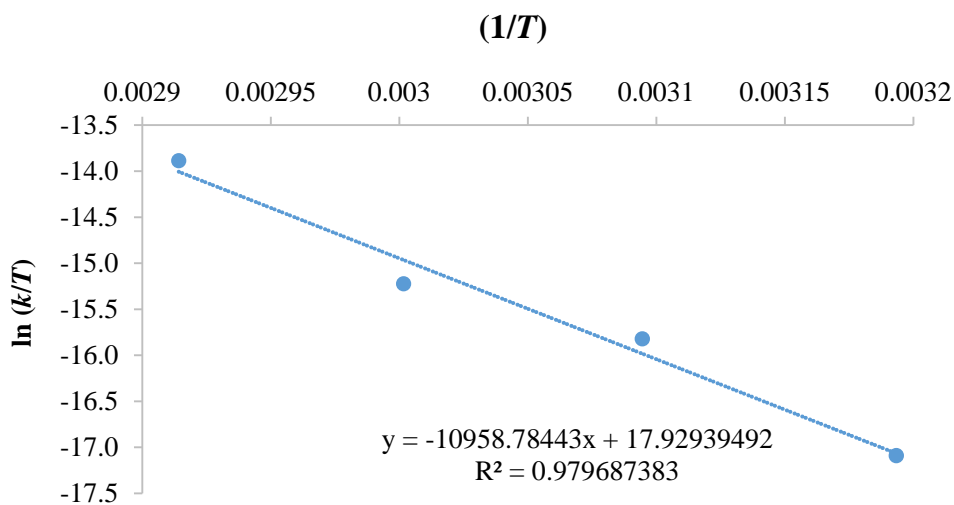
Figure B2-2   Eyring plot of the reaction of azobenzene with **AB** catalysed by **1**. Based on eq B1, the thermodynamic parameters are: $\Delta H^{\ddagger} = 21.8 \pm 2.2$ kcal/mol, $\Delta G^{\ddagger}_{(298)} = 25.2 \pm 4.2$ kcal/mol, $\Delta S^{\ddagger} = -11.6 \pm 6.8$ e.u.
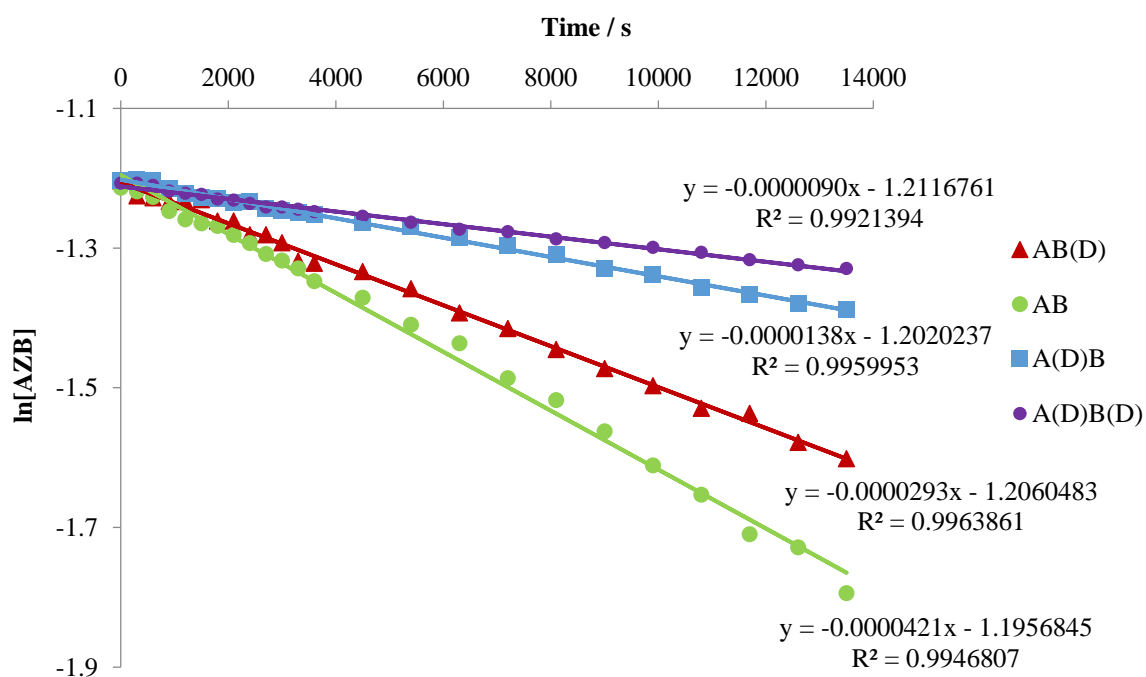
Figure B2-3   Kinetic plots for the reaction of azobenzene with deuterated ammonia-borane catalysed by 5 mol % **1**; H_3NBD_3: **AB(D)**, D_3NBH_3: **A(D)B**, D_3NBD_3: **A(D)B(D)**.

Table B2-2   Calculated   (M05-2X(SCRF)/6-311G(d,p)//M05-2X/6-311G(d,p)   level)   and experimental DKIE values for the reaction of azobenzene with deuterated **AB** at 298.15K, 1 atm.

Deuterated ammonia-boranes	Calculated KIE	Experimental KIE
BD_3NH_3	1.35	1.44
BH_3ND_3	2.31	3.05
BD_3ND_3	3.11	4.67

a)

7

b)

y = -0.0001289x - 2.1524328
R² = 0.9977152

● 313.15 K
■ 323.15 K
▲ 333.15 K
● 343.15 K

y = -0.00024011x - 2.18175088
R² = 0.99817881

y = -0.0004212x - 2.1630055
R² = 0.9980395

y = -0.0008784x - 2.0884638
R² = 0.9919319
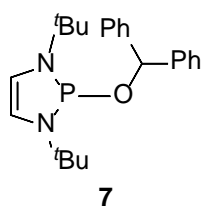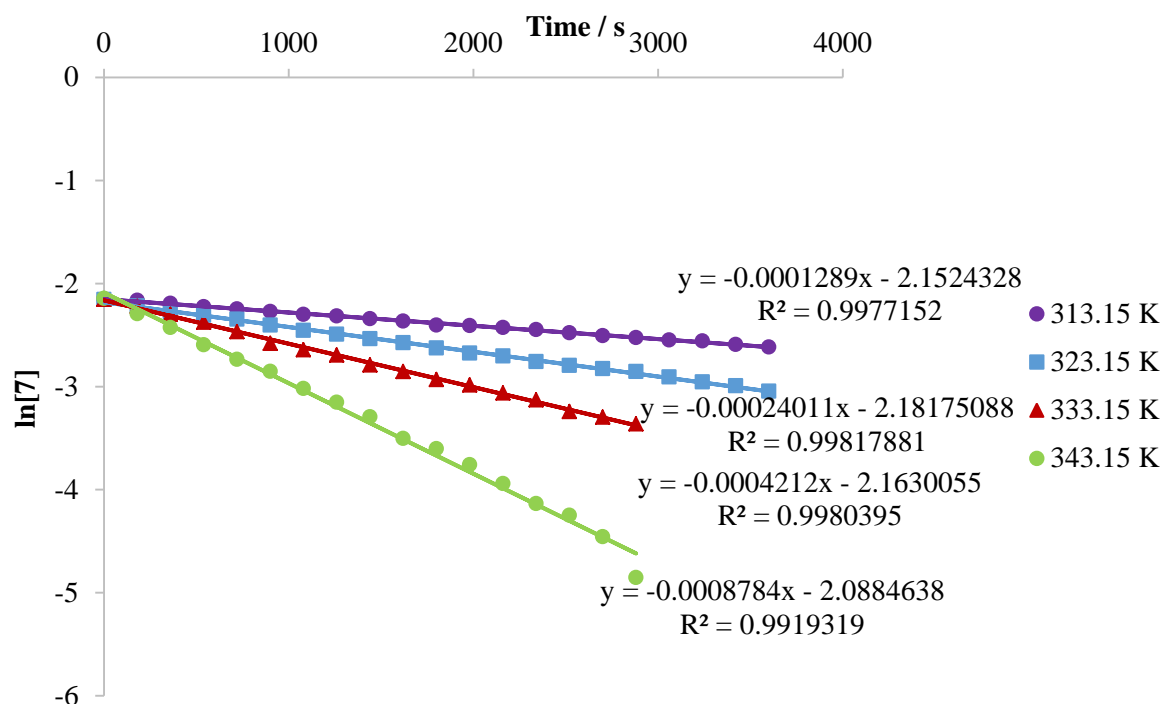
Figure B3-1   a) Structure of compound **7**. b) Pseduo-first order plot for the reaction of **7** and HBpin.

Table B3-1   Various parameters for the determination of Eyring Plot for reaction of **7** with HBpin.

T / K	$1 / (T / K^{-1})$	k / s^{-1}	$(k / s^{-1}) / (T / K)$	$\ln(k / T)$
313.15	0.003193	0.0001289	3.989E-07	-14.73
323.15	0.003095	0.0002401	7.430E-07	-14.11
333.15	0.003002	0.0004212	1.264E-06	-13.58
343.15	0.002914	0.0008784	2.560E-06	-12.88

$$y = -6555.2x + 6.1735$$
$$R^2 = 0.9949$$
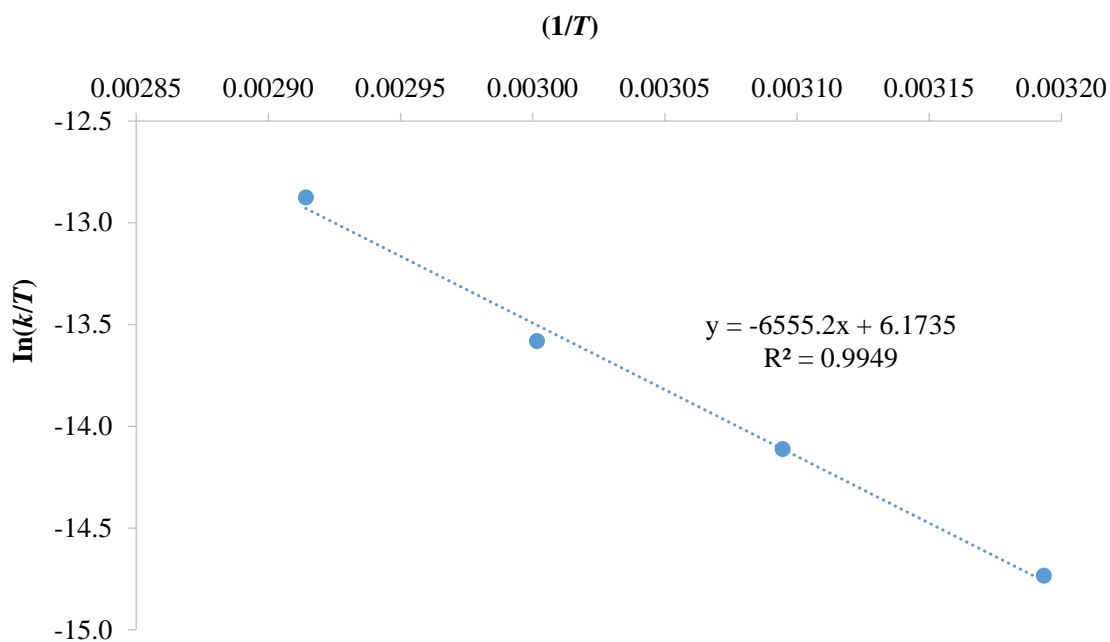
Figure B3-2   Eyring Plot of the reaction of **7** with HBpin. Based on eq B1, the thermodynamic parameters are: $\Delta H^{\ddagger} = +13.0 \pm 0.6$ kcal/mol, $\Delta G^{\ddagger}_{(298)} = +23.4 \pm 1.2$ kcal/mol, $\Delta S^{\ddagger} = -34.9 \pm 2.0$ e.u.

$$y = -0.00024011x - 2.18175088$$
$$R^2 = 0.99817881$$

$$y = -0.00022961x - 2.19561419$$
$$R^2 = 0.99720595$$

$$y = -0.00008934x - 2.16422084$$
$$R^2 = 0.98896376$$

$$y = -0.00008127x - 2.20569335$$
$$R^2 = 0.97241077$$
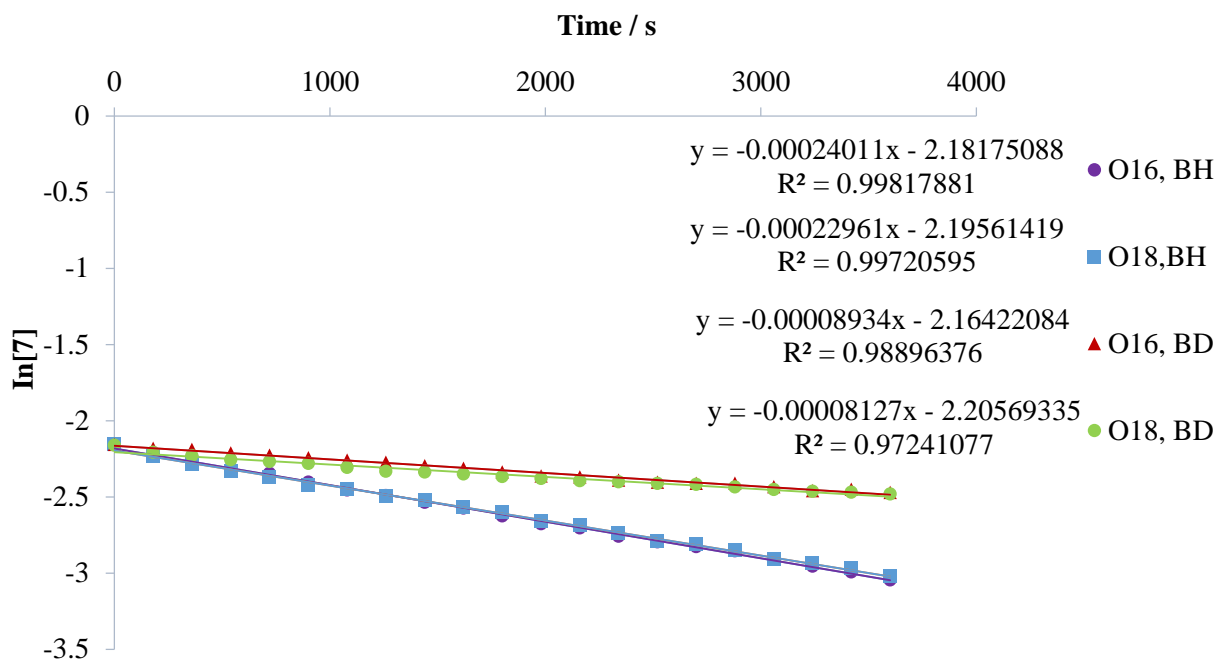
Figure B3-3   Plot of In[**7**] against time for (O^{16}, HBpin), (O^{18}, HBpin), (O^{16}, DBpin) and (O^{18}, DBpin). Simulated reaction rate constant, $k_{(O16, HBpin)} = 0.00024011$ s^{-1}, $k_{(O18, HBpin)} = 0.00022961$ s^{-1}, $k_{(O16, DBpin)} = 0.00008934$ s^{-1}, $k_{(O18, DBpin)} = 0.00008127$ s^{-1}.

Appendix C   **DFT Calculations**

Gaussian 09 was used for all density functional theory (DFT) calculations. [1] Geometry optimisation and frequency calculations were performed using the level of theory as stated in each chapter. Specific details for the DFT calculations for each chapter are stated as follow:

Chapter 1

Geometry optimisation and frequency calculations for compound **1** were performed at B3LYP/6-311G(d,p) level of theory.

XYZ coordinates for the optimized structure of **1**:

```
=== 1 ===
C    -0.671796   1.482759  -0.658013
C     0.671428   1.482802  -0.657632
H    -1.283930   2.371408  -0.714188
H     1.283522   2.371506  -0.713423
P     0.000025  -0.956325  -0.954671
H     0.000246  -0.775341  -2.376687
N    -1.283234   0.202350  -0.648977
N     1.282892   0.202492  -0.648405
C    -2.430041  -0.070879   0.270266
C    -3.486887   1.031254   0.077318
H    -4.389535   0.777405   0.638639
H    -3.140203   2.001175   0.440508
H    -3.752061   1.128083  -0.978210
C    -3.050419  -1.418841  -0.127656
H    -3.388791  -1.393868  -1.166501
H    -2.331741  -2.234667  -0.019704
H    -3.908762  -1.643240   0.511002
C    -1.981431  -0.108820   1.743679
H    -1.482570   0.824069   2.018276
H    -2.837517  -0.247534   2.411035
H    -1.284104  -0.932700   1.916225
C     2.430071  -0.070827   0.270229
C     3.051090  -1.418129  -0.129024
H     3.389634  -1.391937  -1.167781
H     3.909405  -1.642856   0.509557
H     2.332709  -2.234346  -0.022052
C     1.981804  -0.110349   1.743714
H     1.285003  -0.934801   1.915682
H     2.838116  -0.249138   2.410769
H     1.482444   0.822008   2.019217
C     3.486278   1.032053   0.078060
H     4.389208   0.778113   0.638878
H     3.751157   1.130058  -0.977439
H     3.139205   2.001454   0.442289
```

Geometry optimisation and frequency calculations were performed at the M05-2X/6-311G(d,p) level (M05-2X: Minnesota 05, Global Hybrid Functional with 56% HF exchange). The frequency calculations yielded zero-point energy (ZPE), enthalpy correction (Hcorr), and free energy correction (Gcorr) values. Single-point energy calculations were also performed at the same level with a self-consistent reaction field (SCRF) method called integral equation formalism variant (IEFPCM) to describe the solvent effect of acetonitrile.[2] NBO calculations for RC2, TS4 and Pro were performed using B3LYP/6-311+G(d,p) level of theory.[3] Frequency calculations show one imaginary frequency for all of the transition states calculated.
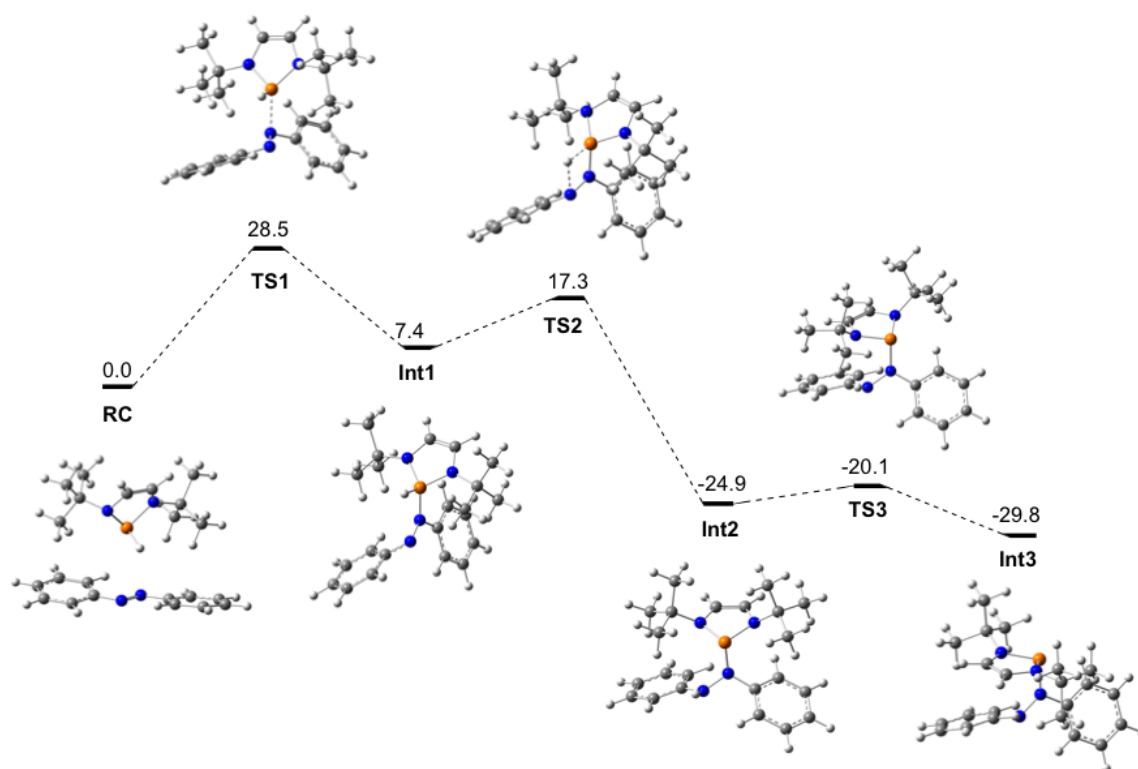
Figure C2-1   Free energy profiles (298.15 K, 1 atm) for the first step of the transfer hydrogenation reaction in solution obtained at the M05-2X(SCRF)/6-311G(d,p)//M05-2X/6-311G(d,p) level.
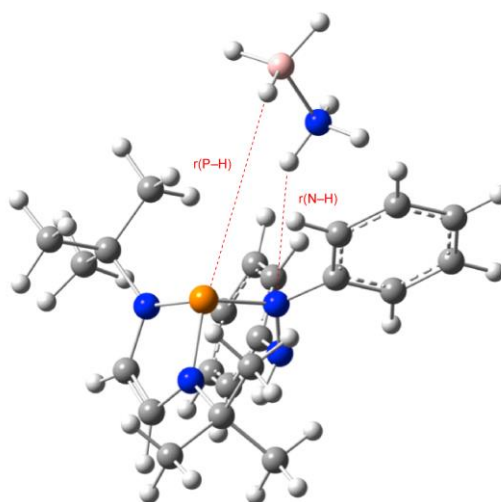
(a) Energy change with decreasing N–H distance
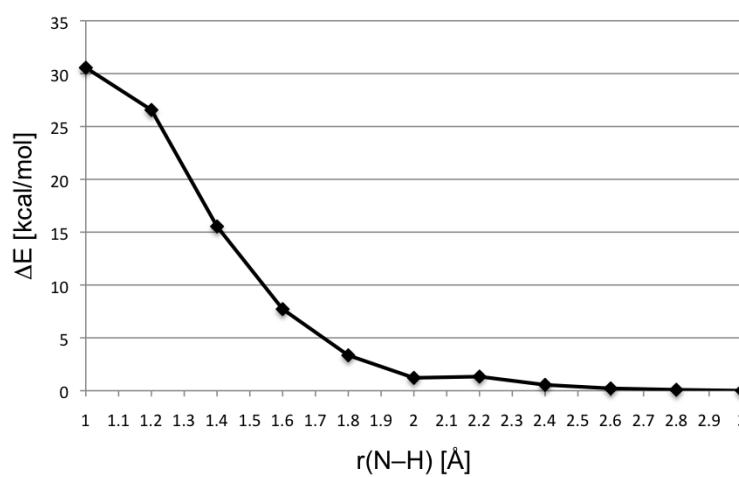
(b) Energy change with decreasing P–H distance
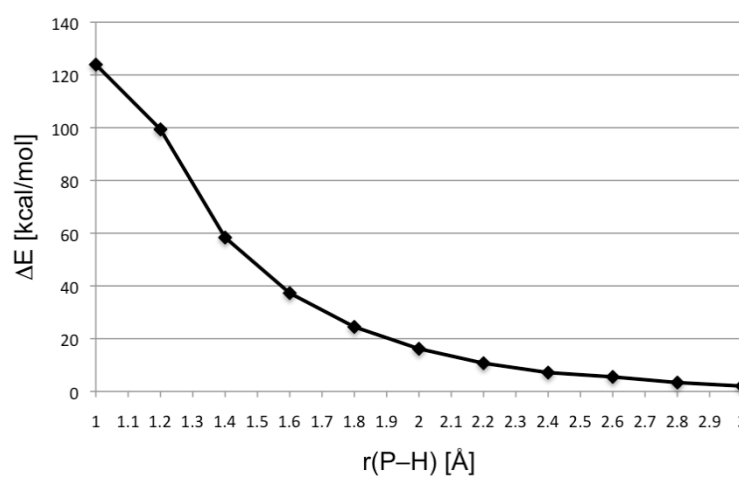
Figure C2-2   Energy scan calculations of stepwise H-transfer mechanisms (M05-2X/6-311G(d,p)).

Table C2-1   Raw energy data for various reactants (RC), transition states(TS), intermediates(Int) and Products(Pro).

a) Δ(E+ZPE)

Optimized Structure	E[au]	ZPE[au]	ΔE[kcal/mol]	Δ(E+ZPE)[kcal/mol]
First Step				
RC	-1417.453374	0.497153	0.0	0.0
TS1	-1417.408378	0.497254	28.2	28.3
Int1	-1417.439815	0.500004	8.5	10.3
TS2	-1417.425981	0.496653	17.2	16.9
Int2	-1417.501764	0.501351	-30.4	-27.7
TS3	-1417.495848	0.501958	-26.7	-23.6
Int3	-1417.512752	0.502546	-37.3	-33.9
Second Step				
RC2	-1500.737257	0.573755	0.0	0.0
TS4	-1500.691496	0.571833	28.7	27.5
Pro	-1500.734942	0.572088	1.5	0.4

b) ΔH and ΔG

Optimized Structure	E(solv)^a [au]	Hcorr^b [au]	Gcorr^c [au]	ΔH[kcal/mol]	ΔG[kcal/mol]
First Step					
RC	-1417.463869	0.526412	0.435477	0.0	0.0
TS1	-1417.423299	0.524813	0.440386	24.5	28.5
Int1	-1417.460797	0.527580	0.444173	2.7	7.4
TS2	-1417.441733	0.524171	0.440918	12.5	17.3
Int2	-1417.512403	0.529394	0.444351	-28.6	-24.9
TS3	-1417.507268	0.529013	0.446847	-25.6	-20.1
Int3	-1417.522072	0.530416	0.446154	-34.0	-29.8
Second Step					
RC2	-1500.755758	0.607303	0.508875	0.0	0.0
TS4	-1500.720203	0.603737	0.510480	20.1	23.3
Pro	-1500.746079	0.605473	0.505749	4.9	4.1

^{a} Energy in solvent. ^{b} Enthalpy correction. ^{c} Free energy correction.

The coordinates (XYZ) for various optimized structures are shown as follow:

=== **RC** ===
```
C     -1.124419   -2.778913   -1.370737
C     -0.026947   -3.141285   -0.696347
H     -1.583569   -3.339970   -2.167142
H      0.541794   -4.039385   -0.876560
P     -0.476140   -0.746093    0.017307
N     -1.690391   -1.538218   -0.941674
N      0.340767   -2.260229    0.330995
C     -3.087089   -1.570267   -0.427128
C      1.643412   -2.359215    1.002775
C     -3.576863   -0.130279   -0.293932
H     -3.533300    0.368767   -1.262418
H     -4.607111   -0.120664    0.065705
H     -2.966646    0.436176    0.410133
C     -3.962490   -2.293793   -1.450759
H     -3.805687   -1.870243   -2.443574
H     -3.747669   -3.361797   -1.479606
H     -5.011007   -2.170969   -1.178531
C     -3.164568   -2.294156    0.920167
H     -2.703012   -3.279592    0.837734
H     -2.637833   -1.726847    1.689118
H     -4.202886   -2.418039    1.233977
C      1.667763   -1.347257    2.147824
H      1.596174   -0.323102    1.778501
H      0.834706   -1.528941    2.827572
H      2.604748   -1.441994    2.697537
C      2.785772   -2.060111    0.024285
H      2.696571   -1.049638   -0.376082
H      3.750773   -2.142355    0.527522
H      2.769476   -2.762483   -0.810621
C      1.803715   -3.763123    1.589872
H      0.963034   -3.988757    2.246009
H      1.852928   -4.524226    0.811439
H      2.729378   -3.817371    2.164307
N      0.371397    2.553099   -0.514982
H      0.326359   -0.332868   -1.104301
N      1.218829    2.271511    0.342615
C     -0.910794    2.883128   -0.001901
C     -1.845960    3.285300   -0.949208
C     -1.264359    2.788326    1.345509
C     -3.137251    3.610194   -0.555596
H     -1.536437    3.334614   -1.983873
C     -2.553738    3.111749    1.730719
H     -0.525981    2.458174    2.060066
C     -3.491157    3.522327    0.783875
H     -3.864157    3.924849   -1.291117
H     -2.837249    3.036898    2.771423
H     -4.497026    3.769378    1.094354
C      2.478544    1.874127   -0.183105
C      2.712786    1.609182   -1.533799
C      3.495914    1.710869    0.752268
C      3.969854    1.186837   -1.933466
H      1.906583    1.731458   -2.240887
C      4.755099    1.293354    0.343690
H      3.274745    1.917712    1.790371
C      4.991545    1.028466   -0.999220
H      4.156142    0.972655   -2.976774
H      5.546276    1.170497    1.070037
H      5.968556    0.695340   -1.320911
```

=== **TS1** ===

C	1.555552	2.872327	-0.165044
C	2.446275	2.188875	0.560063
H	1.706393	3.834990	-0.615740
H	3.449211	2.494792	0.797199
P	0.415126	0.621112	0.337458
N	0.352371	2.172699	-0.359986
N	1.977252	0.923874	0.936396
C	-0.823720	2.681607	-1.114160
C	2.618863	0.079192	1.964520
C	-2.062499	2.519181	-0.233313
H	-1.936551	3.074172	0.697193
H	-2.940874	2.899364	-0.755691
H	-2.260724	1.472818	0.000147
C	-0.633829	4.160948	-1.435505
H	-0.475769	4.746902	-0.529634
H	0.196447	4.323443	-2.122975
H	-1.541069	4.519694	-1.920012
C	-0.969956	1.889236	-2.414635
H	-0.081044	2.022672	-3.033176
H	-1.098969	0.828032	-2.204835
H	-1.839377	2.242656	-2.970679
C	2.031220	-1.327110	1.860094
H	0.938302	-1.346604	1.952006
H	2.304314	-1.783677	0.909517
H	2.430930	-1.941628	2.666718
C	2.336466	0.680141	3.342886
H	1.263536	0.694569	3.538976
H	2.821497	0.087870	4.119690
H	2.712925	1.702654	3.397589
C	4.121921	0.008285	1.701719
H	4.304381	-0.316569	0.677207
H	4.613078	0.967167	1.868223
H	4.569436	-0.714622	2.384018
N	-1.191280	-1.570437	0.505461
H	-0.492923	0.526279	1.447348
N	-0.518414	-1.028533	-0.489377
C	-2.540998	-1.211313	0.501088
C	-3.248235	-1.315757	1.707728
C	-3.247664	-0.823163	-0.648705
C	-4.596171	-1.007624	1.771460
H	-2.702547	-1.634627	2.585741
C	-4.599028	-0.514642	-0.574752
H	-2.726883	-0.788235	-1.594710
C	-5.283516	-0.594321	0.632376
H	-5.117413	-1.087710	2.716366
H	-5.126047	-0.222832	-1.474210
H	-6.336339	-0.354763	0.683638
C	0.529009	-1.821964	-1.037682
C	0.586192	-3.190853	-0.788749
C	1.466386	-1.237460	-1.896168
C	1.587338	-3.958200	-1.375017
H	-0.156566	-3.621268	-0.135066
C	2.459642	-2.011478	-2.471050
H	1.416856	-0.175423	-2.106041
C	2.531487	-3.378554	-2.210166
H	1.623973	-5.020497	-1.173929
H	3.179768	-1.547759	-3.131597
H	3.307614	-3.979892	-2.662044

=== **Int1** ===

C	-2.399478	1.919027	0.703604

```
C    -3.077576    0.953414    0.076801
H    -2.766469    2.575251    1.470666
H    -4.103186    0.674451    0.233809
P    -0.676816    0.692256   -0.708372
N    -1.059083    2.001844    0.269238
N    -2.285510    0.250882   -0.850051
C    -0.065958    2.938485    0.858171
C    -2.782878   -0.906214   -1.643138
C     1.130231    3.031587   -0.088434
H     0.818702    3.401940   -1.066473
H     1.854590    3.732293    0.325570
H     1.646209    2.076024   -0.205325
C    -0.710140    4.319042    0.977779
H    -1.112556    4.635387    0.015515
H    -1.508314    4.337516    1.719032
H     0.048460    5.034745    1.293687
C     0.372752    2.426347    2.228590
H    -0.486250    2.328907    2.894905
H     0.853680    1.453321    2.134432
H     1.080981    3.123136    2.678348
C    -1.757198   -1.215460   -2.734073
H    -1.669651   -0.374247   -3.424864
H    -0.764233   -1.453123   -2.339403
H    -2.102553   -2.079085   -3.301812
C    -4.104891   -0.504631   -2.297269
H    -3.983428    0.419534   -2.862271
H    -4.417910   -1.295147   -2.979018
H    -4.899214   -0.367629   -1.563560
C    -2.980331   -2.119415   -0.735789
H    -2.028792   -2.464887   -0.334435
H    -3.637378   -1.875270    0.100523
H    -3.435756   -2.929923   -1.306412
N     1.271656   -0.823103   -1.298615
H    -0.061871    1.083952   -1.894298
N     0.384163   -0.474006   -0.241476
C     2.572143   -0.538252   -0.973150
C     3.534145   -0.718150   -1.995937
C     3.054551   -0.114686    0.284844
C     4.872896   -0.469088   -1.777980
H     3.178507   -1.052631   -2.961495
C     4.408974    0.133728    0.485398
H     2.371042   -0.005856    1.115187
C     5.334461   -0.033023   -0.533194
H     5.574541   -0.613462   -2.590159
H     4.740671    0.453036    1.465898
H     6.384482    0.160866   -0.367502
C     0.112946   -1.383218    0.811814
C     0.755555   -2.619452    0.810707
C    -0.789285   -1.065717    1.829911
C     0.472141   -3.536508    1.812592
H     1.454914   -2.831638    0.016502
C    -1.065684   -1.998224    2.820283
H    -1.289156   -0.105884    1.854354
C    -0.439859   -3.238224    2.818472
H     0.974608   -4.493997    1.805711
H    -1.771202   -1.747405    3.600748
H    -0.652941   -3.958734    3.595359
```

=== **TS2** ===
```
C     2.333127    1.902859   -1.082869
C     3.076769    0.986053   -0.456140
H     2.638662    2.542374   -1.890127
```

H	4.103614	0.738212	-0.655828
P	0.739843	0.751427	0.553412
N	1.028400	1.983990	-0.557316
N	2.367346	0.321295	0.557432
C	-0.032979	2.837639	-1.145797
C	2.973486	-0.731711	1.410523
C	-1.169336	2.966720	-0.132427
H	-0.803756	3.398690	0.800536
H	-1.935488	3.624915	-0.541026
H	-1.647566	2.007587	0.073486
C	0.544257	4.224883	-1.423657
H	0.998896	4.634390	-0.521651
H	1.288530	4.207443	-2.219264
H	-0.261138	4.885973	-1.742647
C	-0.542625	2.193933	-2.434903
H	0.272182	2.070618	-3.150578
H	-0.972223	1.216139	-2.218730
H	-1.310417	2.820883	-2.889856
C	1.987151	-1.084996	2.523207
H	1.804931	-0.222284	3.166963
H	1.028587	-1.445386	2.141725
H	2.421147	-1.875255	3.135041
C	4.253243	-0.173693	2.034923
H	4.040450	0.753525	2.566880
H	4.656201	-0.900415	2.740568
H	5.019229	0.021146	1.284316
C	3.283340	-1.971353	0.570836
H	2.368298	-2.419371	0.186499
H	3.922873	-1.717826	-0.276025
H	3.805329	-2.705669	1.185911
N	-1.145945	-0.628668	1.266546
H	-0.240864	0.696237	1.723040
N	-0.334604	-0.475672	0.105401
C	-2.486111	-0.399211	1.002202
C	-3.347392	-0.294190	2.111574
C	-3.057103	-0.296137	-0.278683
C	-4.699753	-0.066068	1.946279
H	-2.913949	-0.390140	3.098410
C	-4.420792	-0.067428	-0.428693
H	-2.434587	-0.411905	-1.154514
C	-5.255419	0.055474	0.672342
H	-5.332831	0.018050	2.820336
H	-4.832670	0.005529	-1.427334
H	-6.314042	0.232147	0.546396
C	-0.046778	-1.553894	-0.742385
C	-0.591307	-2.812749	-0.490854
C	0.791493	-1.363866	-1.845572
C	-0.265699	-3.875746	-1.322997
H	-1.252551	-2.930162	0.354595
C	1.107890	-2.437476	-2.663967
H	1.200188	-0.383186	-2.055868
C	0.586299	-3.700604	-2.406946
H	-0.688585	-4.850669	-1.121610
H	1.763132	-2.283287	-3.510602
H	0.830887	-4.533659	-3.050561

=== **Int2** ===
C	0.421294	1.648387	1.414057
C	-0.902947	1.514612	1.562531
H	1.118842	1.879997	2.201954
H	-1.441989	1.621667	2.488988
P	-0.400528	0.698327	-0.791250

```
N      0.878626    1.404701    0.104615
N     -1.577007    1.125335    0.384388
C      1.976731    2.232119   -0.451294
C     -2.899672    1.700640    0.041493
C      2.271459    1.796717   -1.884135
H      1.418598    1.966883   -2.540488
H      3.114282    2.376120   -2.261691
H      2.544447    0.741505   -1.909437
C      1.572291    3.708487   -0.436168
H      0.684646    3.859883   -1.053380
H      1.342325    4.033130    0.579208
H      2.380257    4.330575   -0.824391
C      3.236569    2.012300    0.389077
H      3.104024    2.359122    1.413874
H      3.498619    0.954888    0.407024
H      4.062509    2.578056   -0.044586
C     -3.508123    0.892081   -1.103118
H     -2.890045    0.949119   -1.999568
H     -3.614806   -0.154916   -0.817828
H     -4.491436    1.295980   -1.346784
C     -2.741353    3.167259   -0.366582
H     -2.150111    3.239528   -1.281360
H     -3.714308    3.628326   -0.545401
H     -2.229417    3.721845    0.421680
C     -3.818272    1.592325    1.259024
H     -3.853294    0.561603    1.612585
H     -3.494153    2.242725    2.071178
H     -4.825172    1.898126    0.974370
N      0.970654   -1.535313   -0.925150
H      1.046257   -1.303342   -1.907864
N     -0.137300   -1.010887   -0.258697
C      2.182875   -1.562048   -0.230027
C      3.375033   -1.726223   -0.940498
C      2.221986   -1.476043    1.162767
C      4.586603   -1.790462   -0.267622
H      3.347942   -1.804771   -2.020893
C      3.440530   -1.547384    1.821106
H      1.296730   -1.334553    1.699872
C      4.631364   -1.699994    1.118457
H      5.500543   -1.912772   -0.832924
H      3.458401   -1.477577    2.900701
H      5.575539   -1.751299    1.641253
C     -1.267086   -1.871285   -0.225196
C     -1.569632   -2.750235   -1.264205
C     -2.109883   -1.809062    0.884551
C     -2.708926   -3.541075   -1.198859
H     -0.901967   -2.824974   -2.110302
C     -3.254425   -2.592517    0.937910
H     -1.838653   -1.153566    1.698778
C     -3.562802   -3.458111   -0.105468
H     -2.931709   -4.222546   -2.008577
H     -3.898246   -2.540772    1.805945
H     -4.450389   -4.073690   -0.059919

=== TS3 ===
C      1.119034    1.536773    0.810960
C     -0.027648    1.490028    1.495070
H      2.097725    1.680525    1.238894
H     -0.120047    1.606550    2.563374
P     -0.616600    0.635819   -0.834295
N      0.986975    1.242390   -0.568926
N     -1.157371    1.192977    0.703995
```

```
C      1.654836   2.123488  -1.559474
C     -2.419850   1.931956   0.964064
C      1.687477   1.407619  -2.907791
H      0.685040   1.129963  -3.235862
H      2.118966   2.064421  -3.663798
H      2.303983   0.508527  -2.849650
C      0.906539   3.453619  -1.682520
H     -0.086310   3.295095  -2.107970
H      0.797012   3.903931  -0.694481
H      1.450166   4.148330  -2.325271
C      3.090680   2.381893  -1.102113
H      3.121599   3.034489  -0.230183
H      3.586257   1.441914  -0.856749
H      3.639276   2.873069  -1.906153
C     -3.400317   1.748790  -0.193549
H     -3.021192   2.206001  -1.107076
H     -3.604660   0.699180  -0.398902
H     -4.339454   2.236093   0.069912
C     -2.132830   3.429227   1.117461
H     -1.653848   3.811039   0.214870
H     -3.065553   3.972371   1.275764
H     -1.474125   3.624298   1.963228
C     -3.043277   1.385607   2.250516
H     -3.280580   0.327880   2.139721
H     -2.361964   1.496630   3.094190
H     -3.959878   1.929331   2.483782
N      1.128275  -1.515566  -0.650675
H      1.593362  -1.088164  -1.438034
N     -0.186458  -1.086818  -0.502968
C      1.933244  -1.509080   0.497858
C      3.314291  -1.372473   0.357840
C      1.386494  -1.686678   1.767449
C      4.137698  -1.410975   1.474036
H      3.740045  -1.238584  -0.629795
C      2.219767  -1.724064   2.875397
H      0.314304  -1.774152   1.868573
C      3.596989  -1.584718   2.742250
H      5.206768  -1.302178   1.349416
H      1.785202  -1.862525   3.856521
H      4.238103  -1.613840   3.611814
C     -1.167553  -2.054885  -0.798053
C     -0.902884  -3.181513  -1.580514
C     -2.453928  -1.873827  -0.285287
C     -1.919707  -4.079460  -1.867055
H      0.100069  -3.346879  -1.942203
C     -3.469908  -2.767964  -0.597611
H     -2.628023  -1.057023   0.398147
C     -3.211871  -3.874598  -1.393892
H     -1.699508  -4.948447  -2.472713
H     -4.460040  -2.610498  -0.190791
H     -3.998482  -4.577969  -1.627025

=== Int3 ===
C     -0.927556  -2.311238  -1.354568
C     -1.688157  -1.610356  -0.505494
H     -1.267081  -2.859276  -2.216665
H     -2.755445  -1.488496  -0.555598
P      0.755040  -1.123192   0.243891
N      0.435267  -2.269654  -1.009697
N     -0.939991  -0.963782   0.489125
C      1.467434  -2.947472  -1.813277
C     -1.560233  -0.542415   1.764287
```

153

```
C      2.800344   -2.899305   -1.067110
H      2.713342   -3.372407   -0.088619
H      3.549836   -3.435941   -1.648841
H      3.153429   -1.874797   -0.932950
C      1.070940   -4.411284   -2.016823
H      0.914811   -4.891677   -1.051076
H      0.157326   -4.505625   -2.603118
H      1.864460   -4.935762   -2.550181
C      1.620379   -2.241944   -3.164856
H      0.674207   -2.239524   -3.709573
H      1.945368   -1.210845   -3.016422
H      2.363830   -2.751841   -3.779341
C     -0.582034    0.349647    2.527572
H      0.320694   -0.194953    2.806693
H     -0.306680    1.213945    1.923283
H     -1.058409    0.699199    3.443542
C     -1.901746   -1.779129    2.597845
H     -0.992132   -2.330406    2.840512
H     -2.397815   -1.491729    3.526419
H     -2.565302   -2.439420    2.037733
C     -2.825748    0.267963    1.471740
H     -2.603663    1.088008    0.790101
H     -3.612780   -0.350025    1.040118
H     -3.210461    0.677930    2.406353
N      0.204328    0.681292   -1.718984
H     -0.118298   -0.147960   -2.200109
N      1.076796    0.368301   -0.673035
C     -0.822356    1.587269   -1.422978
C     -0.613525    2.634411   -0.523680
C     -2.047036    1.484490   -2.085618
C     -1.629293    3.548335   -0.282336
H      0.342269    2.722624   -0.027026
C     -3.052288    2.407926   -1.837616
H     -2.207786    0.670562   -2.781051
C     -2.854915    3.443603   -0.931371
H     -1.456900    4.355233    0.417248
H     -3.999081    2.311824   -2.351866
H     -3.640779    4.159650   -0.738284
C      2.382720    0.893866   -0.773121
C      2.832372    1.516819   -1.939195
C      3.244949    0.813825    0.328201
C      4.124332    2.022327   -2.005048
H      2.156794    1.610051   -2.775313
C      4.537182    1.308256    0.239908
H      2.895830    0.373690    1.251110
C      4.990747    1.914561   -0.925920
H      4.452461    2.505714   -2.915460
H      5.188959    1.233659    1.099966
H      5.995456    2.307771   -0.985539

=== RC2 ===
C     -0.982316   -2.242743   -1.395262
C     -1.710323   -1.511089   -0.544332
H     -1.345801   -2.769282   -2.260966
H     -2.769005   -1.332831   -0.602081
P      0.748218   -1.146869    0.209225
N      0.383643   -2.257342   -1.057112
N     -0.934290   -0.892732    0.447042
C      1.368132   -3.047068   -1.817395
C     -1.512280   -0.496647    1.753001
C      2.703395   -3.041827   -1.075617
H      2.595435   -3.461224   -0.075037
```

```
H      3.418533    -3.648009   -1.631462
H      3.114150    -2.033657   -0.994962
C      0.878486    -4.491509   -1.940963
H      0.700406    -4.909776   -0.950426
H     -0.044579    -4.558001   -2.515951
H      1.632613    -5.092807   -2.449595
C      1.561561    -2.426495   -3.205063
H      0.616733    -2.393605   -3.750695
H      1.950555    -1.410781   -3.112201
H      2.269759    -3.014175   -3.790751
C     -0.580594     0.506297    2.431836
H      0.415370     0.096594    2.607767
H     -0.506135     1.404840    1.818760
H     -0.987949     0.784323    3.403508
C     -1.686678    -1.736313    2.631550
H     -0.715202    -2.185131    2.844808
H     -2.163469    -1.474160    3.577286
H     -2.305528    -2.474148    2.118690
C     -2.861150     0.186520    1.517441
H     -2.761504     0.977465    0.772718
H     -3.624522    -0.520506    1.192726
H     -3.201968     0.626534    2.454803
N      0.298728     0.684783   -1.765241
H      0.020270    -0.135397   -2.288188
N      1.144195     0.340520   -0.705266
C     -0.765568     1.554910   -1.494243
C     -0.604489     2.633807   -0.624328
C     -1.978835     1.397772   -2.167681
C     -1.654177     3.514626   -0.405383
H      0.351351     2.781269   -0.143075
C     -3.018206     2.290329   -1.948898
H     -2.103959     0.564804   -2.846970
C     -2.869368     3.348937   -1.060036
H     -1.517698     4.344053    0.275539
H     -3.954918     2.150966   -2.471382
H     -3.682982     4.038362   -0.887123
C      2.434580     0.902891   -0.733291
C      2.737329     1.942598   -1.620446
C      3.420133     0.488302    0.176411
C      3.983973     2.553299   -1.586004
H      1.984861     2.261790   -2.325246
C      4.662089     1.108259    0.194787
H      3.211595    -0.290535    0.894344
C      4.956982     2.149053   -0.679425
H      4.191550     3.357633   -2.278948
H      5.396389     0.777360    0.916639
H      5.924565     2.628953   -0.657040
H      3.156064     2.757908    1.453285
H      1.630110     2.204191    1.612560
H      2.001942     3.720539    2.133714
H      1.667294     2.241332    4.186432
H      3.040557     1.013657    3.361433
H      3.582901     2.855794    3.990688
B      2.697017     2.158098    3.556234
N      2.342555     2.769386    2.062606

=== TS4 ===
C     -0.268971    -2.229121   -1.299643
C     -1.322343    -1.816285   -0.552203
H     -0.295139    -2.554634   -2.324603
H     -2.343353    -1.742829   -0.878138
P      0.712761    -1.611145    0.979045
```

155

```
N      0.893535    -2.242152    -0.571196
N     -0.954583    -1.512809     0.733762
C      2.158779    -2.835623    -1.101914
C     -1.916535    -1.122960     1.825733
C      3.268842    -2.636492    -0.075013
H      3.056044    -3.157388     0.859835
H      4.192064    -3.045180    -0.484198
H      3.430319    -1.579355     0.136079
C      1.910713    -4.329531    -1.316328
H      1.610458    -4.803406    -0.381644
H      1.133594    -4.500868    -2.061587
H      2.828601    -4.799660    -1.668757
C      2.540361    -2.152203    -2.412205
H      1.768526    -2.275324    -3.172297
H      2.718003    -1.090676    -2.257217
H      3.455021    -2.609066    -2.790619
C     -1.769008     0.363521     2.140089
H     -0.749822     0.589978     2.451081
H     -2.012043     0.967643     1.269263
H     -2.443871     0.613876     2.959880
C     -1.581205    -1.966425     3.057427
H     -0.588045    -1.726019     3.438125
H     -2.299191    -1.742159     3.846085
H     -1.636935    -3.030088     2.822012
C     -3.342638    -1.422702     1.377164
H     -3.650984    -0.779959     0.552411
H     -3.469111    -2.469535     1.097579
H     -4.003675    -1.213295     2.216813
N     -0.500491     1.317303    -0.692885
H     -0.841583     0.678199    -1.393544
N      0.762240     0.951509    -0.224560
C     -0.781908     2.665099    -0.962828
C     -0.032588     3.694806    -0.394873
C     -1.877727     2.978311    -1.771838
C     -0.385254     5.014890    -0.639007
H      0.809489     3.453658     0.237678
C     -2.217201     4.301426    -2.006840
H     -2.461885     2.178972    -2.212595
C     -1.473143     5.331312    -1.443058
H      0.203955     5.805360    -0.194321
H     -3.066747     4.528261    -2.636980
H     -1.737314     6.362636    -1.627577
C      1.848878     1.149948    -1.089406
C      1.703227     1.410730    -2.454990
C      3.139440     1.034664    -0.553027
C      2.826933     1.530285    -3.264698
H      0.720728     1.543389    -2.884307
C      4.249237     1.158513    -1.374164
H      3.248542     0.841998     0.507223
C      4.104939     1.400174    -2.737996
H      2.695616     1.737379    -4.318388
H      5.237003     1.068734    -0.941570
H      4.973266     1.498780    -3.373669
H      2.274111     2.452632     2.139689
H      0.962276     1.309959     0.779530
H      0.830239     2.314461     2.825082
H      2.606762     0.858152     4.115345
H      1.069410    -0.173495     3.361736
H      2.796149    -0.106231     2.368331
B      2.032489     0.548231     3.084467
N      1.506132     1.802820     2.269501
```

=== Pro ===

156

```
C    -0.026858   -1.271845   -1.150650
C    -1.175573   -1.382519   -0.469044
H     0.066235   -0.996023   -2.188156
H    -2.154638   -1.187267   -0.877701
P     0.654215   -1.686880    1.281917
N     1.136416   -1.596032   -0.390228
N    -1.038478   -1.845225    0.844052
C     2.024026   -2.663835   -0.935337
C    -2.126679   -1.661180    1.820234
C     3.323582   -2.655571   -0.134850
H     3.143057   -2.872448    0.918267
H     4.000543   -3.416269   -0.525496
H     3.801216   -1.679196   -0.223467
C     1.343518   -4.032005   -0.851642
H     1.198217   -4.327479    0.188860
H     0.369131   -3.993154   -1.341622
H     1.950569   -4.794189   -1.343302
C     2.349966   -2.328482   -2.390831
H     1.487108   -2.472713   -3.041163
H     2.697712   -1.298783   -2.474775
H     3.140126   -2.993625   -2.740385
C    -2.443859   -0.171995    2.004948
H    -1.558112    0.377094    2.327671
H    -2.799629    0.268715    1.072448
H    -3.219814   -0.041234    2.760569
C    -1.682130   -2.259786    3.153806
H    -0.856756   -1.696077    3.593037
H    -2.513232   -2.232492    3.858341
H    -1.366635   -3.294383    3.018885
C    -3.367496   -2.411796    1.334772
H    -3.744269   -2.007777    0.395051
H    -3.130251   -3.465386    1.189427
H    -4.163867   -2.323935    2.074847
N     0.673104    1.832745   -0.184407
H     0.278666    0.972570   -0.553274
N     2.058126    1.865784   -0.191476
C    -0.009130    3.000857   -0.559371
C     0.611160    4.248541   -0.555799
C    -1.362618    2.902309   -0.891925
C    -0.126425    5.381842   -0.874018
H     1.661921    4.312561   -0.315524
C    -2.084139    4.042375   -1.208148
H    -1.836806    1.928701   -0.897566
C    -1.473455    5.291712   -1.199240
H     0.364234    6.345653   -0.871615
H    -3.131134    3.953004   -1.464051
H    -2.038150    6.179057   -1.446804
C     2.734547    1.498207   -1.361205
C     2.123173    1.577016   -2.613092
C     4.069068    1.091738   -1.275215
C     2.845389    1.251179   -3.755161
H     1.099616    1.912981   -2.696093
C     4.775648    0.768561   -2.422165
H     4.545396    1.032132   -0.304563
C     4.170070    0.844089   -3.672607
H     2.361394    1.322068   -4.719813
H     5.805960    0.450851   -2.337259
H     4.723152    0.591013   -4.565586
H     0.972352    3.381427    2.858084
H     2.443175    1.480836    0.657442
H     0.495428    2.018961    1.996032
H     0.736640    0.463532    3.999596
```

H	0.647245	-0.266919	1.506148
H	1.331148	2.165898	5.039831
B	0.967268	1.634936	4.035886
N	0.812387	2.388935	2.881248

Chapter 3

DFT calculations were performed at the B3LYP-D3(SCRF)/B2//B3LYP-D/B1 level, where B1 denotes a combination of basis sets, i.e., 6-311+G(d,p) for B, N, O, and P and 6-31+G(d,p) for C and H, and B2 stands for 6-311+G(d,p).[4,5,6] The solvent effect of acetonitrile was described by the IEFPCM-SCRF method.[2] Natural Bond Orbital (NBO) method was employed for the atomic charge distributions on the exocyclic P–O bond in (HCN^{t}Bu)$_2$P-OCHPh$_2$ **7**.[3]

The plausibility of a one-step mechanism between **7** and HBpin was also examined, which involves formation of B–O and P–H bonds as well as cleavage of B–H and P–O bonds, all of which occur in a concerted manner via a four-membered ring transition state. However, the attempts were unsuccessful, indicating that a concerted process is not likely to take place.
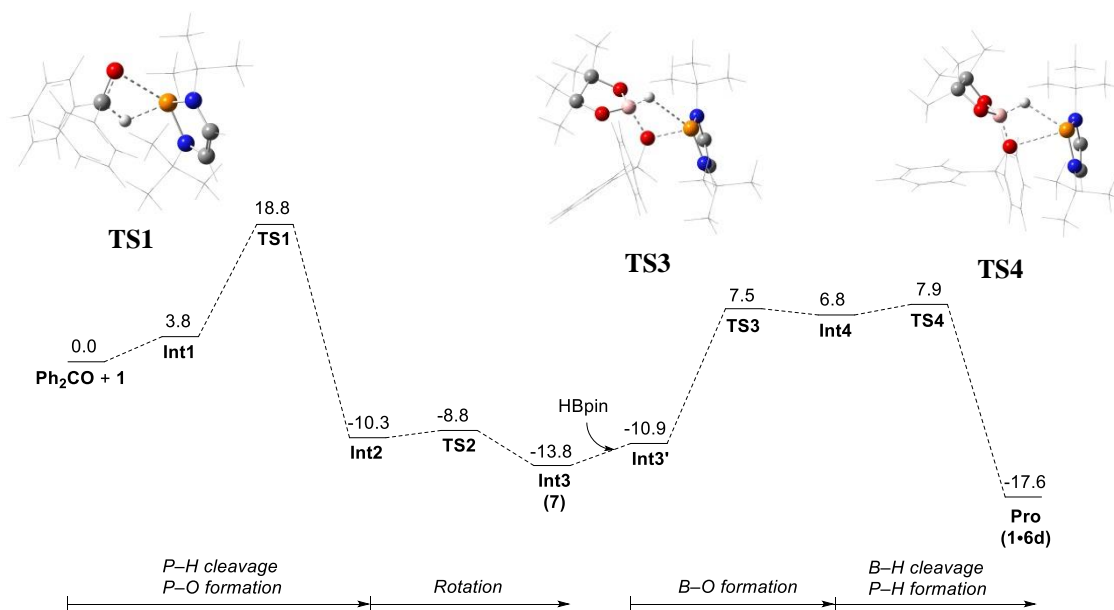
Figure C3-1   Full free energy profiles (kcal mol^{-1}) in CH$_3$CN at 298 K, as determined at the B3LYP-D3(SCRF)/B2//B3LYP-D3/B1 level**.**

158

Table C3-1. Raw energy data for various reactants, transition states, intermediates and products.

(a) B3LYP-D3/B1

Optimized Structures	E [au]	ZPE [au]	Gcorr [au]	ΔE [kcal/mol]	Δ(E+ZPE) [kcal/mol]	ΔG [kcal/mol]
			First Step			
Ph₂CO	-576.733568	0.191592	0.153861			
1	-844.704861	0.299064	0.257008			
Ph₂CO + 1	-1421.438429	0.490656	0.410869	0.0	0.0	0.0
Int1	-1421.455458	0.492164	0.431302	-10.7	-9.7	2.1
TS1	-1421.425710	0.491317	0.432677	8.0	8.4	21.7
Int2	-1421.485377	0.495305	0.437766	-29.5	-26.5	-12.6
TS2	-1421.480584	0.495018	0.435261	-26.5	-23.7	-11.1
7	-1421.490999	0.495672	0.436709	-33.0	-29.8	-16.8
			Second Step			
HBpin	-411.978170	0.190539	0.157458			
Int3 + HBpin	-1833.463548	0.685844	0.595224	-33.0	-29.8	-16.8
Int3'	-1833.482501	0.687768	0.614587	-44.9	-40.5	-16.5
TS3	-1833.458001	0.688414	0.620424	-29.5	-24.7	2.5
Int4	-1833.458013	0.688575	0.619342	-29.5	-24.7	1.8
TS4	-1833.450782	0.687745	0.619773	-25.0	-20.6	6.6
Pro	-1833.492771	0.687032	0.616111	-51.3	-47.4	-22.0

(b) B3LYP-D3(SCRF)/B2//B3LYP-D3/B1

Optimized Structures	E [au]	ZPE [au]	Gcorr [au]	ΔE [kcal/mol]	Δ(E+ZPE) [kcal/mol]	ΔG [kcal/mol]
			First Step			
Ph2CO	-576.841144	0.191592	0.153861			
1	-844.787047	0.299064	0.257008			
Ph2CO + 1	-1421.628191	0.490656	0.410869	0.0	0.0	0.0
Int1	-1421.642538	0.492164	0.431302	-9.0	-8.1	3.8
TS1	-1421.620049	0.491317	0.432677	5.1	5.5	18.8
Int2	-1421.671489	0.495305	0.437766	-27.2	-24.3	-10.3
TS2	-1421.666535	0.495018	0.435261	-24.1	-21.3	-8.8
7	-1421.675980	0.495672	0.436709	-30.0	-26.8	-13.8
			Second Step			
HBpin	-412.029397	0.190539	0.157458			
Int3 + HBpin	-1833.700885	0.685844	0.595224	-30.0	-26.8	-13.8
Int3'	-1833.715683	0.687768	0.614587	-39.3	-34.9	-10.9
TS3	-1833.692174	0.688414	0.620424	-24.5	-19.8	7.5
Int4	-1833.692174	0.688575	0.619342	-24.5	-19.7	6.8
TS4	-1833.690971	0.687745	0.619773	-23.8	-19.4	7.9
Pro	-1833.727935	0.687032	0.616111	-47.0	-43.1	-17.6

The coordinates (XYZ) for various optimized structures are shown as follow:

=== Ph₂CO ===
```
C     0.195832    2.861490   -1.310320
O    -0.275120    3.630904   -0.485989
C     1.588579    2.335270   -1.140466
C     2.412619    2.026005   -2.233744
C     2.101161    2.221723    0.161528
C     3.727193    1.604044   -2.025848
H     2.036079    2.139334   -3.244566
C     3.406009    1.779762    0.368101
H     1.460853    2.486583    0.996331
C     4.222206    1.470996   -0.726093
H     4.363652    1.381223   -2.876911
H     3.790761    1.680771    1.378676
H     5.241906    1.133584   -0.565260
C    -0.615461    2.441173   -2.497939
C    -0.484267    1.173699   -3.086300
C    -1.585948    3.329952   -2.986734
C    -1.307958    0.804923   -4.151637
H     0.241929    0.468534   -2.696539
C    -2.391751    2.968988   -4.064285
H    -1.692313    4.297349   -2.507248
C    -2.254542    1.704608   -4.648415
H    -1.211219   -0.182861   -4.592046
H    -3.129863    3.667588   -4.446706
H    -2.887526    1.420513   -5.483955
```

=== **1** ===
```
C    -0.824002   -1.732826   -1.601902
C     0.069539   -2.721473   -1.807170
H    -1.689875   -1.544959   -2.223363
H     0.021565   -3.438514   -2.616311
P     1.106056   -1.241152    0.001952
N    -0.530622   -0.863178   -0.518771
N     1.168867   -2.743399   -0.910019
C    -1.607197   -0.514889    0.453157
C     1.573987   -4.032477   -0.277520
C    -1.099327    0.635670    1.333560
H    -0.838781    1.502215    0.717814
H    -1.873713    0.933563    2.047642
H    -0.213982    0.337302    1.903614
C    -2.839798   -0.033061   -0.329518
H    -2.564580    0.764910   -1.026076
H    -3.310624   -0.844216   -0.892515
H    -3.587327    0.356902    0.368167
C    -1.982802   -1.726639    1.324553
H    -2.274051   -2.572902    0.694438
H    -1.133808   -2.034289    1.942632
H    -2.819161   -1.487396    1.990750
C     2.946264   -3.828500    0.379716
H     3.684445   -3.517601   -0.366193
H     2.901712   -3.063957    1.161560
H     3.286315   -4.761110    0.841426
C     1.704410   -5.101098   -1.375209
H     2.358085   -4.749048   -2.179259
H     2.137353   -6.011289   -0.949055
H     0.733850   -5.369433   -1.802342
C     0.541746   -4.486583    0.770352
H     0.496238   -3.776456    1.601819
H    -0.453716   -4.552512    0.320034
H     0.802168   -5.469576    1.178427
H     1.743726   -0.455292   -1.006270
```

=== **Int1** ===
```
C    -0.839546   -1.752481   -1.595468
C     0.052476   -2.743898   -1.796814
H    -1.718674   -1.578879   -2.201739
H    -0.015160   -3.482121   -2.585709
```

160

```
P      1.114221   -1.226412   -0.030540
N     -0.532424   -0.862866   -0.531695
N      1.165543   -2.748989   -0.919966
C     -1.612546   -0.516553    0.442555
C      1.584694   -4.024021   -0.271352
C     -1.093087    0.581862    1.379110
H     -0.849309    1.488520    0.821802
H     -1.862910    0.832202    2.115684
H     -0.203040    0.250730    1.922853
C     -2.816332    0.033632   -0.341776
H     -2.507608    0.849419   -1.000486
H     -3.301853   -0.739511   -0.944732
H     -3.563678    0.417547    0.359509
C     -2.031443   -1.751912    1.257993
H     -2.327917   -2.569114    0.592805
H     -1.201984   -2.100864    1.880775
H     -2.875803   -1.518376    1.915853
C      2.969508   -3.802825    0.353774
H      3.691005   -3.503924   -0.413154
H      2.936689   -3.021601    1.119689
H      3.322405   -4.724206    0.828298
C      1.694863   -5.116078   -1.347842
H      2.331077   -4.780922   -2.173025
H      2.138510   -6.016045   -0.911162
H      0.716315   -5.395565   -1.748997
C      0.575095   -4.456860    0.807250
H      0.544863   -3.726919    1.622099
H     -0.429171   -4.534670    0.379055
H      0.846256   -5.429455    1.232952
H      1.731928   -0.472108   -1.067480
C      0.211473    2.887343   -1.334700
O     -0.268191    3.648932   -0.505632
C      1.602934    2.365004   -1.155089
C      2.429064    2.027593   -2.237879
C      2.104711    2.257242    0.151442
C      3.729718    1.572847   -2.014894
H      2.061879    2.134143   -3.252484
C      3.394988    1.783096    0.373581
H      1.464130    2.539998    0.979087
C      4.209931    1.437709   -0.709825
H      4.364681    1.319688   -2.858386
H      3.765536    1.678477    1.388690
H      5.216448    1.068172   -0.537211
C     -0.598115    2.462307   -2.519092
C     -0.439787    1.206792   -3.124631
C     -1.609561    3.324633   -2.972830
C     -1.275493    0.826082   -4.175455
H      0.292432    0.506126   -2.744427
C     -2.431545    2.949316   -4.032831
H     -1.737419    4.281010   -2.476794
C     -2.265122    1.697366   -4.636967
H     -1.156564   -0.155418   -4.624266
H     -3.203627    3.626245   -4.386103
H     -2.909690    1.401453   -5.459668

=== **TS1** ===
C     -1.868581   -2.461339   -0.658990
C     -0.775987   -3.226418   -0.919410
H     -2.880903   -2.656448   -0.974094
H     -0.753466   -4.143100   -1.489657
P      0.108386   -1.147456    0.360690
N     -1.560399   -1.351800    0.113664
N      0.365357   -2.694761   -0.354076
C     -2.642450   -0.433887    0.631328
C      1.728100   -3.220403   -0.668478
C     -2.098773    0.375146    1.816508
H     -1.265571    1.008215    1.505566
H     -2.901129    1.017294    2.191936
H     -1.786637   -0.287621    2.631736
```

161

```
C    -3.075767    0.500522   -0.506107
H    -2.238519    1.145077   -0.781159
H    -3.400657   -0.070313   -1.382408
H    -3.915068    1.118930   -0.170556
C    -3.816796   -1.300981    1.117654
H    -4.340810   -1.802728    0.299181
H    -3.479299   -2.055296    1.835742
H    -4.543765   -0.653741    1.615859
C     2.772963   -2.462024    0.164165
H     2.823692   -1.401330   -0.099808
H     2.571133   -2.551151    1.236111
H     3.758507   -2.893232   -0.031952
C     2.006908   -2.997128   -2.165578
H     1.965441   -1.932113   -2.408852
H     3.004732   -3.368648   -2.417887
H     1.278830   -3.524316   -2.789392
C     1.773777   -4.713448   -0.310510
H     1.542367   -4.861737    0.748472
H     1.066855   -5.300148   -0.904317
H     2.775569   -5.106547   -0.506730
H     0.745904   -0.220179   -1.115366
C     0.660112    1.006782   -1.205341
O    -0.031991    1.442174   -0.179358
C     2.156117    1.315181   -1.212182
C     2.971261    1.031180   -2.317914
C     2.742795    1.801623   -0.038882
C     4.351597    1.228450   -2.249345
H     2.520141    0.663394   -3.235624
C     4.124398    2.000400    0.031442
H     2.084968    2.020452    0.796111
C     4.933878    1.711490   -1.071605
H     4.973268    1.011770   -3.114042
H     4.570334    2.384089    0.945371
H     6.007680    1.867733   -1.018544
C    -0.021870    1.157103   -2.565891
C    -0.583832    0.071061   -3.242572
C    -0.153841    2.438476   -3.118589
C    -1.264510    0.253067   -4.451033
H    -0.499301   -0.925983   -2.818128
C    -0.830440    2.626157   -4.323841
H     0.273367    3.285144   -2.589338
C    -1.389203    1.532287   -4.996138
H    -1.697117   -0.602524   -4.963040
H    -0.924844    3.625228   -4.740593
H    -1.917003    1.678691   -5.934166

=== Int2 ===
C    -2.184895   -2.047562    0.421186
C    -1.762712   -2.987653   -0.446169
H    -3.198202   -1.905739    0.766513
H    -2.368039   -3.748206   -0.916894
P     0.279471   -1.435845   -0.059771
N    -1.146148   -1.218879    0.881817
N    -0.376679   -2.893869   -0.700899
C    -1.418835   -0.029036    1.721954
C     0.383920   -4.051177   -1.229904
C    -0.086434    0.627397    2.110691
H     0.449652    0.997598    1.231238
H    -0.282628    1.481461    2.765697
H     0.561035   -0.075161    2.644017
C    -2.275534    0.980264    0.932767
H    -1.763679    1.260709    0.009270
H    -3.244267    0.546828    0.664693
H    -2.460899    1.877599    1.533319
C    -2.146421   -0.476794    3.001288
H    -3.111313   -0.941542    2.778134
H    -1.538041   -1.199815    3.553111
H    -2.337481    0.387086    3.645938
C     1.877353   -3.706331   -1.317136
```

162

```
H     2.060013   -2.837458   -1.956696
H     2.300343   -3.497539   -0.330976
H     2.415045   -4.557128   -1.746247
C    -0.138557   -4.393901   -2.637681
H    -0.012995   -3.542871   -3.313760
H     0.408350   -5.248685   -3.048842
H    -1.200592   -4.655634   -2.619365
C     0.203329   -5.253968   -0.285123
H     0.572522   -5.005453    0.714610
H    -0.849965   -5.534959   -0.197078
H     0.757293   -6.122179   -0.657298
H     0.584519   -1.400227   -2.836963
C     0.428994   -0.344031   -2.566847
O    -0.158125   -0.280151   -1.271163
C     1.776665    0.347517   -2.612445
C     2.803475   -0.157099   -3.416571
C     2.001025    1.512957   -1.871223
C     4.037925    0.494443   -3.487114
H     2.634945   -1.062600   -3.994899
C     3.233192    2.165039   -1.936209
H     1.203220    1.894799   -1.242992
C     4.255448    1.658482   -2.745763
H     4.827947    0.091120   -4.113997
H     3.397608    3.068008   -1.355143
H     5.214842    2.165044   -2.794566
C    -0.598871    0.205042   -3.548513
C    -0.280246    1.140049   -4.537116
C    -1.913196   -0.279688   -3.463775
C    -1.259991    1.586086   -5.431676
H     0.730766    1.526330   -4.609282
C    -2.888415    0.163626   -4.355584
H    -2.162427   -0.991320   -2.682756
C    -2.564846    1.099656   -5.345220
H    -0.999558    2.316360   -6.192548
H    -3.902899   -0.217637   -4.278419
H    -3.325009    1.446160   -6.039380

=== TS2 ===
C    -2.184895   -2.047562    0.421186
C    -1.762712   -2.987653   -0.446169
H    -3.198202   -1.905739    0.766513
H    -2.368039   -3.748206   -0.916894
P     0.279471   -1.435845   -0.059771
N    -1.146148   -1.218879    0.881817
N    -0.376679   -2.893869   -0.700899
C    -1.418835   -0.029036    1.721954
C     0.383920   -4.051177   -1.229904
C    -0.086434    0.627397    2.110691
H     0.449652    0.997598    1.231238
H    -0.282628    1.481461    2.765697
H     0.561035   -0.075161    2.644017
C    -2.275534    0.980264    0.932767
H    -1.763679    1.260709    0.009270
H    -3.244267    0.546828    0.664693
H    -2.460899    1.877599    1.533319
C    -2.146421   -0.476794    3.001288
H    -3.111313   -0.941542    2.778134
H    -1.538041   -1.199815    3.553111
H    -2.337481    0.387086    3.645938
C     1.877353   -3.706331   -1.317136
H     2.060013   -2.837458   -1.956696
H     2.300343   -3.497539   -0.330976
H     2.415045   -4.557128   -1.746247
C    -0.138557   -4.393901   -2.637681
H    -0.012995   -3.542871   -3.313760
H     0.408350   -5.248685   -3.048842
H    -1.200592   -4.655634   -2.619365
C     0.203329   -5.253968   -0.285123
H     0.572522   -5.005453    0.714610
```

```
H    -0.849965   -5.534959   -0.197078
H     0.757293   -6.122179   -0.657298
H     0.584519   -1.400227   -2.836963
C     0.428994   -0.344031   -2.566847
O    -0.158125   -0.280151   -1.271163
C     1.776665    0.347517   -2.612445
C     2.803475   -0.157099   -3.416571
C     2.001025    1.512957   -1.871223
C     4.037925    0.494443   -3.487114
H     2.634945   -1.062600   -3.994899
C     3.233192    2.165039   -1.936209
H     1.203220    1.894799   -1.242992
C     4.255448    1.658482   -2.745763
H     4.827947    0.091120   -4.113997
H     3.397608    3.068008   -1.355143
H     5.214842    2.165044   -2.794566
C    -0.598871    0.205042   -3.548513
C    -0.280246    1.140049   -4.537116
C    -1.913196   -0.279688   -3.463775
C    -1.259991    1.586086   -5.431676
H     0.730766    1.526330   -4.609282
C    -2.888415    0.163626   -4.355584
H    -2.162427   -0.991320   -2.682756
C    -2.564846    1.099656   -5.345220
H    -0.999558    2.316360   -6.192548
H    -3.902899   -0.217637   -4.278419
H    -3.325009    1.446160   -6.039380

=== 7 ===
C    -2.448344   -1.879116    0.645599
C    -2.139052   -2.612892   -0.441293
H    -3.429407   -1.750965    1.078593
H    -2.824623   -3.190837   -1.042092
P     0.080098   -1.369187    0.184855
N    -1.328260   -1.218089    1.182534
N    -0.777475   -2.525205   -0.777462
C    -1.423638   -0.414957    2.424467
C    -0.134935   -3.522246   -1.670983
C    -0.031472    0.100936    2.816400
H     0.391562    0.743127    2.038379
H    -0.115991    0.693729    3.732061
H     0.661806   -0.723856    3.005291
C    -2.355461    0.790853    2.192743
H    -1.946335    1.455688    1.427277
H    -3.351508    0.468649    1.873134
H    -2.470998    1.365392    3.117920
C    -1.966396   -1.303942    3.557774
H    -2.971554   -1.674131    3.335293
H    -1.311324   -2.167663    3.706569
H    -2.018477   -0.736912    4.492873
C     1.294725   -3.070456   -2.004058
H     1.292664   -2.089507   -2.487510
H     1.923127   -3.018701   -1.110632
H     1.747462   -3.791376   -2.691593
C    -0.930186   -3.624382   -2.984311
H    -0.995989   -2.651186   -3.472877
H    -0.429997   -4.323910   -3.661760
H    -1.944952   -3.998690   -2.821298
C    -0.099114   -4.886643   -0.958733
H     0.491154   -4.820329   -0.039184
H    -1.109994   -5.209858   -0.690693
H     0.345712   -5.651885   -1.604250
H    -1.997951    0.286613   -0.709533
C    -1.131202    0.623437   -1.289256
O     0.056646    0.059241   -0.728972
C    -1.321317    0.172012   -2.725540
C    -2.572803   -0.262190   -3.170308
C    -0.251839    0.215452   -3.628230
C    -2.761246   -0.641803   -4.502870
```

```
H    -3.398000   -0.320832   -2.466009
C    -0.433531   -0.172076   -4.955482
H     0.720633    0.547487   -3.278611
C    -1.691015   -0.599700   -5.398506
H    -3.737639   -0.982378   -4.835330
H     0.403586   -0.140064   -5.646962
H    -1.831600   -0.900794   -6.432363
C    -1.057405    2.140887   -1.181060
C    -2.171569    2.911282   -1.540479
C     0.094301    2.783606   -0.719440
C    -2.136490    4.301664   -1.436880
H    -3.068251    2.419876   -1.908742
C     0.132139    4.178318   -0.619492
H     0.950425    2.182091   -0.437731
C    -0.981003    4.941822   -0.975625
H    -3.008478    4.885835   -1.716800
H     1.033932    4.666199   -0.260262
H    -0.951433    6.024520   -0.895771

=== HBpin ===
B     3.137958    0.398214   -0.601061
H     2.640331   -0.247502    0.256355
O     3.295914   -0.053874   -1.879875
O     3.608126    1.665037   -0.404838
C     4.127104    0.914391   -2.588305
C     3.949853    2.214318   -1.713248
C     3.624468    1.032020   -4.022509
H     4.184765    1.801926   -4.563532
H     3.768502    0.078839   -4.538930
H     2.562598    1.280338   -4.058520
C     5.554956    0.359504   -2.571315
H     5.552948   -0.631275   -3.033635
H     6.239184    1.002886   -3.132064
H     5.929336    0.256965   -1.549073
C     5.204023    3.068853   -1.571406
H     5.527972    3.439308   -2.549751
H     4.988689    3.930978   -0.933957
H     6.024220    2.509173   -1.118973
C     2.763764    3.081784   -2.146299
H     2.590584    3.846891   -1.384775
H     2.961419    3.579572   -3.100161
H     1.851053    2.487657   -2.244553

=== Int3' ===
C    -2.909247   -1.817803    0.352594
C    -2.485928   -2.499201   -0.729995
H    -3.932236   -1.578574    0.603795
H    -3.106562   -2.914669   -1.509166
P    -0.299596   -1.620591    0.407935
N    -1.842176   -1.365666    1.152581
N    -1.085444   -2.573795   -0.804340
C    -2.075294   -0.719857    2.464595
C    -0.400114   -3.603296   -1.627314
C    -0.733064   -0.482333    3.171466
H    -0.078573    0.169840    2.586412
H    -0.916489    0.002670    4.134765
H    -0.206853   -1.423364    3.355177
C    -2.782422    0.633455    2.255458
H    -2.153588    1.312628    1.673212
H    -3.732751    0.505820    1.727466
H    -2.996154    1.106262    3.220017
C    -2.940560   -1.647029    3.337536
H    -3.924362   -1.819711    2.891613
H    -2.448667   -2.616550    3.461446
H    -3.094927   -1.202119    4.325924
C     1.099473   -3.279525   -1.708731
H     1.272278   -2.285184   -2.126982
H     1.577933   -3.326670   -0.726401
H     1.591242   -4.014162   -2.353877
```

C	-0.984556	-3.592954	-3.050517
H	-0.912867	-2.597899	-3.491827
H	-0.426484	-4.294898	-3.678427
H	-2.032367	-3.907100	-3.065563
C	-0.605267	-4.984393	-0.978792
H	-0.160272	-5.004298	0.021238
H	-1.672360	-5.209406	-0.881922
H	-0.140445	-5.772114	-1.582122
H	-1.960413	0.431550	-0.600762
C	-0.979918	0.624804	-1.054926
O	0.007654	-0.136948	-0.356058
C	-1.052507	0.230139	-2.515942
C	-2.290233	0.089544	-3.149275
C	0.120479	0.047285	-3.257268
C	-2.360830	-0.213781	-4.512836
H	-3.202078	0.208970	-2.570651
C	0.053045	-0.257782	-4.616504
H	1.079752	0.117672	-2.758122
C	-1.187904	-0.384572	-5.251398
H	-3.328865	-0.324051	-4.993115
H	0.969684	-0.406494	-5.180004
H	-1.238509	-0.625221	-6.309239
C	-0.663999	2.104977	-0.854732
C	-1.172426	3.074552	-1.729130
C	0.095839	2.519106	0.245362
C	-0.933869	4.431535	-1.501149
H	-1.747402	2.768493	-2.597086
C	0.332249	3.875839	0.476138
H	0.521667	1.769804	0.900260
C	-0.183922	4.838473	-0.393995
H	-1.331546	5.170079	-2.191469
H	0.933482	4.176337	1.329383
H	0.003155	5.893863	-0.218191
B	3.151442	0.389338	-0.590976
H	2.725514	-0.279583	0.281203
O	3.279293	-0.048431	-1.885244
O	3.612993	1.660781	-0.404604
C	4.117391	0.917424	-2.589146
C	3.939669	2.215336	-1.714570
C	3.633028	1.043049	-4.028997
H	4.237366	1.778971	-4.569745
H	3.739528	0.078093	-4.533689
H	2.587904	1.346625	-4.084076
C	5.541965	0.353485	-2.562023
H	5.537735	-0.636282	-3.026975
H	6.236072	0.993775	-3.114160
H	5.905552	0.245501	-1.536399
C	5.195273	3.069307	-1.576353
H	5.517691	3.438584	-2.555792
H	4.979490	3.932785	-0.940780
H	6.016436	2.510915	-1.123506
C	2.756189	3.082322	-2.149855
H	2.576049	3.847844	-1.392669
H	2.962453	3.576983	-3.103764
H	1.838733	2.499183	-2.248305

=== **TS3** ===
C	-2.467133	-1.770229	-0.280885
C	-1.737750	-2.510622	-1.137317
H	-3.520790	-1.551945	-0.351581
H	-2.089715	-2.990187	-2.037763
P	-0.004620	-1.492094	0.489989
N	-1.673360	-1.197397	0.728606
N	-0.384638	-2.559865	-0.776493
C	-2.261667	-0.683125	2.000156
C	0.547628	-3.544754	-1.407391
C	-1.194200	0.103125	2.773726
H	-0.833511	0.958823	2.197070
H	-1.629658	0.480590	3.703201

```
H    -0.337973   -0.524252    3.037903
C    -3.440164    0.255704    1.689436
H    -3.122138    1.097275    1.067583
H    -4.259222   -0.262957    1.184109
H    -3.837092    0.658082    2.626043
C    -2.744633   -1.883153    2.832588
H    -3.477495   -2.472300    2.272765
H    -1.901692   -2.534887    3.082391
H    -3.211948   -1.545520    3.763409
C     1.907879   -3.498972   -0.700209
H     2.381382   -2.521159   -0.807686
H     1.818662   -3.747043    0.362415
H     2.565006   -4.240814   -1.163937
C     0.736661   -3.196825   -2.891818
H     1.244237   -2.235815   -2.982874
H     1.349125   -3.966942   -3.372772
H    -0.220348   -3.147187   -3.419285
C    -0.063599   -4.947292   -1.242358
H    -0.229296   -5.169793   -0.183510
H    -1.019126   -5.040799   -1.766193
H     0.618268   -5.697695   -1.653972
H    -1.416895    0.872147   -0.167688
C    -0.609491    1.058667   -0.883515
O     0.448022    0.180302   -0.459182
C    -1.189200    0.693478   -2.236791
C    -2.555453    0.911231   -2.459367
C    -0.419348    0.122927   -3.251350
C    -3.143475    0.578502   -3.679946
H    -3.163987    1.341665   -1.667527
C    -1.007236   -0.220536   -4.471587
H     0.627800   -0.079616   -3.061769
C    -2.367439    0.006466   -4.693454
H    -4.203880    0.754927   -3.836758
H    -0.397561   -0.673707   -5.248576
H    -2.821104   -0.262318   -5.643100
C    -0.251846    2.530143   -0.696055
C    -0.689652    3.509630   -1.592349
C     0.444304    2.929554    0.451976
C    -0.430435    4.862614   -1.352457
H    -1.216948    3.220364   -2.494090
C     0.704817    4.276640    0.693416
H     0.828244    2.177462    1.130434
C     0.267079    5.252194   -0.208668
H    -0.768528    5.607432   -2.067249
H     1.264780    4.564024    1.578544
H     0.474816    6.302118   -0.023797
B     2.136707    0.203866   -0.694596
H     2.401048   -0.482030    0.264472
O     2.393735   -0.375906   -1.993002
O     2.703649    1.503003   -0.685165
C     3.501068    0.337677   -2.562079
C     3.320362    1.778454   -1.952314
C     3.408821    0.268780   -4.085478
H     4.210310    0.853972   -4.549281
H     3.514952   -0.770847   -4.412127
H     2.451550    0.645937   -4.449596
C     4.794677   -0.349266   -2.094313
H     4.762681   -1.400168   -2.398250
H     5.684482    0.111225   -2.535325
H     4.884624   -0.312482   -1.005274
C     4.629078    2.525563   -1.692516
H     5.192548    2.665914   -2.622150
H     4.405803    3.512837   -1.276681
H     5.255121    1.991460   -0.975461
C     2.394783    2.669829   -2.789414
H     2.130356    3.553162   -2.203909
H     2.888411    2.997483   -3.710773
H     1.469193    2.158568   -3.058208
```

=== **Int4** ===

C	-2.461133	-1.782907	-0.276935
C	-1.731174	-2.524585	-1.132580
H	-3.514639	-1.564397	-0.347866
H	-2.082102	-3.005413	-2.032597
P	-0.001471	-1.516319	0.502377
N	-1.668155	-1.214800	0.733767
N	-0.380116	-2.576039	-0.768739
C	-2.257920	-0.684421	1.999017
C	0.557762	-3.547570	-1.414422
C	-1.185733	0.095097	2.772785
H	-0.812763	0.943194	2.192809
H	-1.622039	0.483210	3.697418
H	-0.337881	-0.539757	3.046041
C	-3.425545	0.263934	1.677436
H	-3.095601	1.102510	1.058043
H	-4.245045	-0.247933	1.166025
H	-3.826219	0.670135	2.610753
C	-2.756387	-1.875177	2.835664
H	-3.494125	-2.459372	2.277077
H	-1.921431	-2.534707	3.091647
H	-3.222767	-1.527263	3.763071
C	1.920760	-3.495086	-0.713604
H	2.384129	-2.511855	-0.815497
H	1.838997	-3.752724	0.347462
H	2.582344	-4.227172	-1.186240
C	0.734972	-3.184066	-2.896347
H	1.231572	-2.216752	-2.981160
H	1.353819	-3.943345	-3.386181
H	-0.224913	-3.141523	-3.419192
C	-0.042132	-4.955701	-1.257265
H	-0.198643	-5.188949	-0.199323
H	-1.000408	-5.052007	-1.775602
H	0.642695	-5.696971	-1.680218
H	-1.399358	0.876752	-0.159005
C	-0.600348	1.063838	-0.884092
O	0.458722	0.186307	-0.465740
C	-1.196598	0.695843	-2.229635
C	-2.567906	0.903314	-2.430222
C	-0.437640	0.136424	-3.258690
C	-3.172490	0.569833	-3.642460
H	-3.167074	1.327720	-1.628063
C	-1.042189	-0.207796	-4.470664
H	0.614585	-0.056451	-3.086109
C	-2.407777	0.007723	-4.670023
H	-4.236542	0.738601	-3.782202
H	-0.440891	-0.651950	-5.259314
H	-2.874083	-0.261466	-5.613432
C	-0.247015	2.537496	-0.704375
C	-0.680604	3.510077	-1.609780
C	0.440985	2.945280	0.445711
C	-0.425507	4.865208	-1.376676
H	-1.201724	3.213812	-2.512841
C	0.696991	4.294159	0.680654
H	0.822994	2.197766	1.130452
C	0.263247	5.263183	-0.230658
H	-0.760053	5.604868	-2.098450
H	1.250558	4.588400	1.567555
H	0.467596	6.314664	-0.050880
B	2.098803	0.205723	-0.709834
H	2.396239	-0.494722	0.234349
O	2.363155	-0.362400	-2.019403
O	2.680486	1.505242	-0.691998
C	3.493192	0.334600	-2.558481
C	3.319435	1.775401	-1.946892
C	3.435167	0.273390	-4.084052
H	4.252501	0.852620	-4.527344
H	3.538034	-0.765784	-4.413432
H	2.489720	0.661672	-4.467361

```
C     4.767445   -0.371038   -2.064900
H     4.728254   -1.420508   -2.373257
H     5.672646    0.078836   -2.485123
H     4.834253   -0.338837   -0.974115
C     4.632598    2.508152   -1.667646
H     5.211140    2.644025   -2.588759
H     4.414219    3.497168   -1.253150
H     5.242295    1.966051   -0.942455
C     2.415871    2.677892   -2.797216
H     2.150615    3.562346   -2.213589
H     2.926163    3.003287   -3.710363
H     1.489608    2.175323   -3.080660

=== TS4 ===
C    -2.340335   -2.150971   -0.175333
C    -1.596400   -2.844258   -1.076173
H    -3.388522   -1.914034   -0.257249
H    -1.942544   -3.271974   -2.003141
P     0.097213   -1.990006    0.668911
N    -1.565465   -1.690248    0.870904
N    -0.265466   -2.910754   -0.708002
C    -2.127068   -1.007110    2.080456
C     0.742953   -3.665412   -1.527100
C    -1.033803   -0.127119    2.705871
H    -0.628997    0.577488    1.974895
H    -1.458607    0.428488    3.546517
H    -0.205905   -0.726952    3.097387
C    -3.324696   -0.132137    1.687415
H    -3.049176    0.585796    0.914302
H    -4.171796   -0.724016    1.329943
H    -3.661964    0.419663    2.569084
C    -2.572144   -2.101304    3.065874
H    -3.327251   -2.749547    2.610276
H    -1.720027   -2.719636    3.363233
H    -3.002940   -1.648176    3.964430
C     2.053931   -3.773579   -0.737554
H     2.474012   -2.787036   -0.527409
H     1.909092   -4.317182    0.201885
H     2.781997   -4.325315   -1.338312
C     0.974205   -2.915716   -2.845901
H     1.346318   -1.905599   -2.661730
H     1.708749   -3.459773   -3.448331
H     0.046969   -2.847389   -3.422013
C     0.190648   -5.078009   -1.778855
H    -0.041357   -5.579498   -0.834158
H    -0.710814   -5.066811   -2.397334
H     0.945157   -5.667190   -2.308025
H    -1.487246    1.555568   -0.054229
C    -0.823507    1.360837   -0.909641
O     0.146514    0.457269   -0.419864
C    -1.698400    0.715236   -1.975787
C    -3.085510    0.896836   -1.939968
C    -1.146541   -0.070851   -2.993932
C    -3.915949    0.289273   -2.885572
H    -3.522743    1.523372   -1.165979
C    -1.971859   -0.672071   -3.945817
H    -0.070224   -0.191399   -3.028827
C    -3.359622   -0.504820   -3.892207
H    -4.991237    0.438767   -2.839015
H    -1.529377   -1.271760   -4.737382
H    -3.998999   -0.977491   -4.632520
C    -0.306798    2.740496   -1.314759
C    -0.181637    3.144305   -2.647980
C    -0.010252    3.662041   -0.302189
C     0.221003    4.445202   -2.961774
H    -0.401320    2.443081   -3.444374
C     0.390399    4.961707   -0.609479
H    -0.084079    3.347936    0.735434
C     0.502616    5.360388   -1.944847
```

```
H    0.313261    4.742472   -4.002609
H    0.619589    5.660780    0.189678
H    0.812315    6.372221   -2.189606
B    1.563430    0.292675   -0.785977
H    1.764126   -0.880718   -0.329792
O    1.833955    0.342660   -2.219480
O    2.498933    1.208776   -0.168520
C    3.202477    0.709531   -2.385815
C    3.501294    1.602161   -1.102255
C    3.344962    1.446528   -3.718807
H    4.367889    1.811766   -3.862612
H    3.109221    0.761256   -4.540144
H    2.657681    2.292352   -3.774661
C    4.047422   -0.577258   -2.432492
H    3.692220   -1.201558   -3.258514
H    5.108488   -0.364548   -2.595871
H    3.946204   -1.147889   -1.506237
C    4.881251    1.355686   -0.478869
H    5.687868    1.592005   -1.183020
H    4.995023    2.001027    0.397827
H    4.992058    0.320733   -0.148545
C    3.346676    3.104852   -1.367061
H    3.378316    3.629594   -0.407999
H    4.152554    3.492104   -2.000857
H    2.392386    3.329013   -1.837912

=== Pro ===
C   -1.713429   -1.580642    0.276564
C   -1.514292   -2.286074   -0.853424
H   -2.619016   -1.053752    0.538583
H   -2.225681   -2.400133   -1.655499
P    0.750502   -2.313635    0.366504
N   -0.654436   -1.715698    1.212662
N   -0.297425   -2.999674   -0.848682
C   -0.548233   -0.780213    2.353104
C    0.259578   -3.686305   -2.038351
C    0.724435   -1.104172    3.149373
H    1.630026   -0.901323    2.567183
H    0.764519   -0.480391    4.047443
H    0.738310   -2.155024    3.452625
C   -0.488205    0.680393    1.860526
H    0.336885    0.828141    1.159191
H   -1.417481    0.953023    1.350265
H   -0.356061    1.364903    2.705799
C   -1.768964   -0.983555    3.267260
H   -2.705142   -0.765738    2.744941
H   -1.808650   -2.018194    3.620290
H   -1.709001   -0.315319    4.132838
C    1.053397   -4.910130   -1.550249
H    1.859906   -4.616399   -0.871353
H    0.395580   -5.602149   -1.016054
H    1.501524   -5.432796   -2.401798
C    1.179725   -2.740641   -2.835239
H    2.068559   -2.467616   -2.256118
H    1.523609   -3.224684   -3.755684
H    0.658556   -1.818344   -3.098471
C   -0.886630   -4.165220   -2.941720
H   -1.611077   -4.757176   -2.373506
H   -1.406327   -3.330440   -3.418930
H   -0.474351   -4.795849   -3.735227
H   -0.751207    0.727878   -1.213804
C   -0.730431    1.082002   -2.250046
O    0.543619    0.748909   -2.822111
C   -1.810916    0.342506   -3.012736
C   -3.114041    0.338940   -2.498667
C   -1.544600   -0.343440   -4.199122
C   -4.131954   -0.355497   -3.149199
H   -3.325729    0.876429   -1.578223
C   -2.566049   -1.038733   -4.856213
```

170

```
H    -0.536140   -0.341446   -4.595069
C    -3.859495   -1.052996   -4.332506
H    -5.135769   -0.357557   -2.734417
H    -2.345262   -1.573681   -5.775586
H    -4.649899   -1.598839   -4.839066
C    -0.937836    2.587232   -2.267218
C    -1.040022    3.271319   -3.485427
C    -1.001627    3.307426   -1.071418
C    -1.197013    4.656963   -3.505333
H    -0.997170    2.712480   -4.415560
C    -1.169802    4.695238   -1.087687
H    -0.898618    2.781774   -0.127902
C    -1.264684    5.373162   -2.304735
H    -1.273327    5.178731   -4.454915
H    -1.218745    5.244653   -0.151852
H    -1.391785    6.451708   -2.320388
B     1.676954    1.022107   -2.132465
H     1.100162   -1.078448   -0.339896
O     2.921186    0.839254   -2.680535
O     1.708594    1.510912   -0.846073
C     3.887659    1.028704   -1.612286
C     3.079859    1.905123   -0.577244
C     5.124956    1.705573   -2.190290
H     5.842049    1.940335   -1.396394
H     5.611052    1.031524   -2.901204
H     4.868571    2.626460   -2.716560
C     4.244634   -0.361348   -1.075562
H     4.621074   -0.970302   -1.902063
H     5.019387   -0.306138   -0.305082
H     3.368445   -0.861388   -0.655793
C     3.390953    1.617718    0.886874
H     4.440756    1.836431    1.108076
H     2.768503    2.251946    1.524624
H     3.188911    0.576493    1.143114
C     3.166593    3.408952   -0.857934
H     2.429483    3.925906   -0.237802
H     4.159477    3.804106   -0.624022
H     2.936959    3.629069   -1.904117
```

Chapter 5

Geometry optimisation and frequency calculations for compound **12**, **12[BH₃]** were conducted at B3LYP/6-31G(d) level of theory, while NBO analyses for **12** and **12[BH₃]** were conducted at B3LYP/6-311G(d,p) level of theory. Geometry optimisation, frequency calculations and nucleus-independent chemical-shift values for **14a[H]**, **IsoN**, **IsoC** were performed at B3LYP/6-311G(d,p) level of theory. NBO analysis for **14a[H]** was conducted at M05-2X/6-311G(d,p) level of theory. Geometry optimisation, frequency calculations and NBO analysis for **15** were conducted at B3PW/6-31G(d,p) level of theory with LANL2DZ pseudo-potential applied for Cu atom.

The coordinates (XYZ) for various optimized structures are shown as follow:

=== **12** ===

C	1.478830	-2.821045	0.312626
C	0.202595	-3.113222	0.006291
N	-0.505996	-1.914334	-0.172024
H	2.307495	-3.471729	0.538808
H	-0.286750	-4.065617	-0.115499
C	-1.939817	-1.957796	-0.415461
C	-2.434887	-2.021643	-1.749467
C	-2.831595	-2.104979	0.683812
C	-3.820278	-2.142557	-1.938162
C	-4.202969	-2.240305	0.414976
C	-4.705679	-2.245908	-0.876359
H	-4.203794	-2.173747	-2.954285
H	-4.886439	-2.346000	1.253336
H	-5.773205	-2.344279	-1.054277
C	2.894223	-0.774083	0.552925
C	3.795993	-0.630043	-0.538636
C	3.281530	-0.348960	1.853358
C	5.008782	0.041009	-0.317109
C	4.508778	0.315835	1.998883
C	5.362242	0.534822	0.928997
H	5.692141	0.165996	-1.152869
H	4.796881	0.658575	2.989343
H	6.303787	1.058895	1.069885
N	1.617207	-1.432738	0.347559
C	-1.622741	-2.030983	-3.052971
H	-2.372536	-2.216909	-3.832179
C	-2.480761	-2.201112	2.175142
H	-3.441154	-2.053419	2.684987
C	-0.635718	-3.207133	-3.180965
H	-1.141787	-4.159599	-2.982314
H	-0.244957	-3.245010	-4.205005
H	0.215472	-3.132430	-2.503614
C	-1.001828	-0.671204	-3.408249
H	-1.778269	0.095155	-3.493452
H	-0.293979	-0.327711	-2.655890
H	-0.478396	-0.738840	-4.370059
C	-1.544170	-1.122871	2.723717
H	-1.575835	-1.135670	3.820320
H	-0.513462	-1.303730	2.427264
H	-1.821627	-0.123370	2.374444
C	-2.011144	-3.615903	2.576461
H	-2.707995	-4.384188	2.221796
H	-1.018563	-3.840999	2.175503
H	-1.952418	-3.691191	3.669111
C	2.519323	-0.549847	3.169481
H	3.268576	-0.346228	3.945422
C	2.059157	-1.990089	3.456475
H	1.259502	-2.334094	2.801161
H	2.898501	-2.689227	3.357762
H	1.693490	-2.053785	4.488391
C	1.418065	0.507385	3.369847
H	0.701907	0.512301	2.547875
H	0.881766	0.328783	4.309823
H	1.865649	1.506700	3.421268
C	3.658211	-1.205990	-1.955469
H	4.442786	-0.698917	-2.530905
C	4.010198	-2.708393	-2.010179
H	4.956275	-2.914847	-1.497325
H	3.229557	-3.323958	-1.554143

H	4.114241	-3.028298	-3.054168
C	2.349977	-0.917546	-2.691373
H	1.516041	-1.469903	-2.263795
H	2.104396	0.147809	-2.666382
H	2.442496	-1.219372	-3.741810
C	0.369024	-0.810061	0.054109
N	0.211391	0.461049	0.064469
C	0.312769	3.319959	0.972532
C	-0.976407	2.942418	1.740565
H	0.567948	4.371825	1.146051
H	1.156829	2.708764	1.320738
H	-1.528675	3.854307	1.984544
H	-0.728133	2.451093	2.688903
P	-0.913829	1.609701	-0.552846
N	0.013354	3.078587	-0.438746
N	-1.810342	2.057047	0.890793
C	0.967139	3.574846	-1.456979
C	-3.236958	2.489849	0.728036
C	0.525613	3.095164	-2.850618
H	-0.511826	3.381245	-3.053112
H	1.164511	3.549371	-3.616463
H	0.601038	2.008349	-2.952687
C	0.926813	5.119433	-1.458764
H	-0.088935	5.475197	-1.661541
H	1.250208	5.539848	-0.500643
H	1.596333	5.517139	-2.230705
C	2.411945	3.100755	-1.185747
H	2.797749	3.512065	-0.246281
H	2.456063	2.010957	-1.111760
H	3.084107	3.428013	-1.988786
C	-3.996708	1.464991	-0.130058
H	-3.631363	1.445900	-1.160119
H	-3.897891	0.459662	0.284793
H	-5.061987	1.723747	-0.153811
C	-3.378203	3.880280	0.063716
H	-2.935926	3.876279	-0.937448
H	-4.437147	4.151075	-0.028815
H	-2.888285	4.671218	0.641594
C	-3.895745	2.510193	2.123258
H	-3.825146	1.523049	2.592717
H	-3.428961	3.238692	2.794212
H	-4.955769	2.776667	2.036589

=== **12[BH₃]** ===
B	-0.544623	1.134760	-2.570725
H	-1.338230	0.224148	-2.574687
H	-0.899776	2.098377	-3.210930
H	0.557929	0.740180	-2.867730
P	-0.408627	1.597672	-0.682128
N	0.282546	0.343725	0.155730
N	-1.836062	2.070954	0.199061
N	0.457385	3.016570	-0.234192
C	0.287878	-0.951419	0.110370
C	-1.278967	2.732769	1.398372
C	-3.049454	2.711275	-0.425439
C	-0.105670	3.629447	0.976270
C	1.820790	3.467131	-0.632158
N	-0.737708	-1.904686	0.161192
N	1.457089	-1.714974	0.146656
H	-0.909851	1.955599	2.075726
H	-2.042695	3.296868	1.932564
C	-3.616436	1.796145	-1.523615

```
C    -4.146206    2.830683    0.656449
C    -2.763181    4.107018   -1.021019
H    -0.439085    4.654887    0.767962
H     0.629838    3.683742    1.790227
C     2.890289    2.978140    0.368384
C     2.185925    2.949271   -2.029234
C     1.829134    5.011199   -0.686254
C    -0.185856   -3.187469    0.261988
C    -2.168044   -1.718032    0.242410
C     1.155408   -3.069811    0.257961
C     2.799496   -1.198917    0.163397
H    -2.949768    1.722263   -2.381299
H    -4.571817    2.206034   -1.871724
H    -3.796118    0.791081   -1.132617
H    -4.308185    1.864074    1.144295
H    -5.084970    3.137783    0.182780
H    -3.922238    3.578944    1.423662
H    -2.443041    4.817144   -0.250385
H    -3.669871    4.513852   -1.485201
H    -1.984442    4.054859   -1.787642
H     2.706842    3.355036    1.380902
H     3.884604    3.328580    0.065898
H     2.907029    1.886467    0.405666
H     2.282630    1.862644   -2.038375
H     3.150199    3.376005   -2.327656
H     1.433743    3.229331   -2.771155
H     1.051554    5.377979   -1.365197
H     2.799990    5.361062   -1.054382
H     1.671026    5.465669    0.297229
H    -0.817645   -4.055984    0.341763
C    -2.732891   -1.315428    1.474318
C    -2.965218   -2.086642   -0.864168
H     1.931649   -3.813786    0.332545
C     3.523072   -1.134147   -1.047824
C     3.369057   -0.840587    1.402058
C    -1.870486   -1.028646    2.702150
C    -4.127868   -1.261294    1.563959
C    -4.357400   -2.026685   -0.709257
C    -2.382978   -2.592377   -2.183707
C     2.926213   -1.604490   -2.372717
C     4.844679   -0.676117   -0.986566
C     4.693201   -0.384706    1.403456
C     2.608523   -0.958048    2.719416
H    -0.927708   -0.596590    2.353150
C    -2.497152   -0.011346    3.671163
C    -1.549860   -2.335349    3.460698
H    -4.592437   -0.953214    2.494685
C    -4.934963   -1.614425    0.485356
H    -4.996320   -2.306027   -1.541191
H    -1.324674   -2.316343   -2.210899
C    -2.486028   -4.130274   -2.282652
C    -3.050642   -1.955378   -3.417319
H     1.836698   -1.545673   -2.286762
C     3.304302   -3.076890   -2.645343
C     3.328871   -0.733005   -3.574722
H     5.429833   -0.613329   -1.898490
C     5.423886   -0.299835    0.222747
H     5.156709   -0.096496    2.342993
H     1.609096   -1.343559    2.499762
C     2.424778    0.410366    3.401533
C     3.286840   -1.966151    3.668000
H    -3.363918   -0.426284    4.199116
```

```
H    -2.816546    0.896989    3.152274
H    -1.762987    0.270426    4.434526
H    -2.471685   -2.806958    3.822477
H    -0.915365   -2.125957    4.330755
H    -1.025226   -3.059007    2.829406
H    -6.016959   -1.572938    0.580608
H    -1.966605   -4.638165   -1.463908
H    -2.046857   -4.479737   -3.224487
H    -3.534072   -4.452702   -2.261437
H    -4.090947   -2.281625   -3.533594
H    -2.512382   -2.258673   -4.322524
H    -3.029396   -0.864710   -3.364881
H     4.391676   -3.189543   -2.735324
H     2.850632   -3.419549   -3.582812
H     2.964356   -3.743066   -1.845882
H     4.396731   -0.820193   -3.808347
H     3.097319    0.321663   -3.405336
H     2.774674   -1.056224   -4.462577
H     6.450632    0.056279    0.244027
H     3.387847    0.864993    3.662879
H     1.849608    0.296898    4.328601
H     1.887891    1.099937    2.743823
H     3.380358   -2.953322    3.201475
H     2.699777   -2.079295    4.587067
H     4.292453   -1.636687    3.954245


=== 14a[H] ===
C    -0.715827    1.047598   -0.103037
C     0.715800    1.047618   -0.103366
C     1.403289    2.277528   -0.174845
C     0.702472    3.468034   -0.212004
C    -0.702582    3.468004   -0.211693
C    -1.403358    2.277489   -0.174234
C    -1.251445   -0.290303   -0.104463
C     1.251466   -0.290296   -0.104633
H     2.483431    2.308002   -0.261059
H     1.238808    4.407271   -0.273641
H    -1.238999    4.407203   -0.273228
H    -2.483526    2.307924   -0.260312
C     2.628788   -0.629061    0.007759
C     4.567636   -1.788748   -0.065662
C     4.826360   -0.606335    0.537954
H     5.213464   -2.615885   -0.301414
H     5.740302   -0.202872    0.936477
C    -2.628748   -0.629090    0.007776
C    -4.826369   -0.606346    0.537689
C    -4.567519   -1.788844   -0.065679
H    -5.740375   -0.202831    0.936009
H    -5.213308   -2.616019   -0.301408
N     3.219249   -1.783790   -0.390995
H     2.730771   -2.512090   -0.890421
N     3.629163    0.096144    0.568440
H     3.474340    0.972276    1.043658
N    -3.629182    0.096147    0.568285
H    -3.474378    0.972285    1.043518
N    -3.219117   -1.783905   -0.390897
H    -2.730568   -2.512262   -0.890161
P    -0.000035   -1.521910   -0.108082
```

=== IsoN ===
```
C     0.713583    1.256301    0.000002
C    -0.713583    1.256301    0.000002
C    -1.415537    2.472826   -0.000022
C    -0.704052    3.658864   -0.000063
C     0.704052    3.658864   -0.000063
C     1.415537    2.472826   -0.000022
C     1.084591   -0.134128    0.000023
C    -1.084591   -0.134128    0.000023
H    -2.499649    2.515703    0.000040
H    -1.233951    4.603650   -0.000100
H     1.233951    4.603650   -0.000100
H     2.499649    2.515703    0.000040
C    -2.368289   -0.742896    0.000010
C    -3.948377   -2.346157   -0.000045
C    -4.583543   -1.150961    0.000067
H    -4.337955   -3.348641   -0.000113
H    -5.631251   -0.908345    0.000105
C     2.368289   -0.742896    0.000010
C     4.583543   -1.150961    0.000067
C     3.948377   -2.346157   -0.000045
H     5.631251   -0.908345    0.000105
H     4.337955   -3.348641   -0.000113
N    -2.589482   -2.076331   -0.000092
H    -1.826560   -2.737238   -0.000125
N    -3.595807   -0.172573    0.000103
H    -3.759388    0.821523    0.000211
N     3.595807   -0.172573    0.000103
H     3.759388    0.821523    0.000210
N     2.589482   -2.076331   -0.000092
H     1.826560   -2.737238   -0.000125
N     0.000000   -0.939262    0.000021
```

=== IsoC ===
```
C    -0.713601    1.100215   -0.070532
C     0.713601    1.100215   -0.070532
C     1.409225    2.315550   -0.125224
C     0.700667    3.509004   -0.147063
C    -0.700667    3.509004   -0.147063
C    -1.409225    2.315550   -0.125224
C    -1.147642   -0.286474   -0.078013
C     1.147642   -0.286474   -0.078013
H     2.491002    2.351716   -0.199204
H     1.235538    4.450150   -0.188510
H    -1.235538    4.450150   -0.188510
H    -2.491002    2.351716   -0.199204
C     2.479121   -0.758955    0.000910
C     4.309725   -2.086615   -0.074946
C     4.703534   -0.881279    0.391395
H     4.868731   -2.985463   -0.265386
H     5.672222   -0.525002    0.693797
C    -2.479121   -0.758955    0.000909
C    -4.703534   -0.881279    0.391395
C    -4.309725   -2.086615   -0.074946
H    -5.672222   -0.525002    0.693797
H    -4.868731   -2.985463   -0.265386
N     2.942708   -1.997790   -0.311264
H     2.378271   -2.714537   -0.738230
N     3.572142   -0.075676    0.426642
H     3.523399    0.851509    0.819982
N    -3.572142   -0.075676    0.426642
H    -3.523399    0.851509    0.819982
```

N	-2.942708	-1.997790	-0.311264
H	-2.378271	-2.714537	-0.738230
C	0.000000	-1.097863	-0.098858
H	0.000000	-2.178404	-0.025365

=== **15** ===

Cu	-0.000849	-1.984792	-1.691895
Cl	2.219948	-2.184283	-1.978215
Cl	-2.221579	-2.185203	-1.977671
P	0.000190	-0.587184	0.430170
C	1.258676	0.607308	0.747162
C	-1.258271	0.607278	0.747457
C	2.659221	0.364135	0.501876
C	0.717429	1.871876	1.149144
C	-0.716931	1.871858	1.149238
C	-2.658865	0.364354	0.502024
N	3.429462	1.037112	-0.395463
N	3.427259	-0.572223	1.113907
C	1.406007	3.019101	1.600477
C	-1.405510	3.019072	1.600642
N	-3.428815	1.037221	-0.395598
N	-3.427132	-0.571725	1.114141
C	4.712685	0.505696	-0.371348
C	2.893681	1.977424	-1.407035
C	4.709534	-0.522237	0.584913
C	2.953232	-1.477853	2.178558
H	2.491657	3.009089	1.653559
C	0.704550	4.135627	2.016738
C	-0.704046	4.135623	2.016815
H	-2.491159	3.008985	1.653820
C	-2.892763	1.977407	-1.407149
C	-4.712139	0.506051	-0.371564
C	-4.709333	-0.521632	0.584961
C	-2.953393	-1.477143	2.179089
C	5.868167	0.816798	-1.090478
H	1.841173	2.080191	-1.135724
C	3.550300	3.352677	-1.302990
C	2.971033	1.370215	-2.806605
C	5.860463	-1.265493	0.851606
H	1.907934	-1.189312	2.315896
C	3.690079	-1.216954	3.491559
C	2.988525	-2.932333	1.715076
H	1.242703	5.010890	2.369874
H	-1.242162	5.010853	2.370070
H	-1.840232	2.079906	-1.135777
C	-2.970247	1.370172	-2.806667
C	-3.549098	3.352783	-1.302993
C	-5.867480	0.817225	-1.090903
C	-5.860450	-1.264559	0.851744
H	-1.908023	-1.188868	2.316349
C	-2.989125	-2.931803	1.716187
C	-3.690312	-1.215570	3.491939
C	7.010565	0.075106	-0.821405
H	5.881684	1.596628	-1.840830
H	3.451131	3.770352	-0.298839
H	3.052757	4.033286	-1.999761
H	4.610844	3.330886	-1.566634
H	3.999563	1.300303	-3.171196
H	2.415706	2.010715	-3.498750
H	2.534161	0.367554	-2.818768
H	5.865800	-2.068917	1.576830
C	7.007497	-0.949362	0.136364

H	4.752016	-1.469602	3.437016
H	3.243416	-1.832852	4.277503
H	3.600526	-0.168512	3.789893
H	2.517970	-3.034879	0.732805
H	2.447529	-3.550265	2.438033
H	4.008431	-3.320364	1.643691
H	-2.533680	0.367376	-2.818742
H	-2.414813	2.010525	-3.498850
H	-3.998789	1.300412	-3.171262
H	-4.609920	3.331014	-1.565521
H	-3.052171	4.033067	-2.000520
H	-3.448811	3.770790	-0.299091
H	-5.880728	1.596825	-1.841501
C	-7.010067	0.075868	-0.821746
C	-7.007334	-0.948352	0.136301
H	-5.866014	-2.067836	1.577121
H	-4.009108	-3.319710	1.645385
H	-2.447940	-3.549499	2.439231
H	-2.518883	-3.034849	0.733829
H	-3.600506	-0.167050	3.789916
H	-3.243975	-1.831339	4.278178
H	-4.752322	-1.467926	3.437261
H	7.922008	0.290133	-1.370166
H	7.916745	-1.513538	0.318005
H	-7.921408	0.290937	-1.370659
H	-7.916730	-1.512280	0.317977

References

1. Gaussian 09, Revision B.01, Frisch, M. J.; Trucks, G. W.; Schlegel, H. B.; Scuseria, G. E.; Robb, M. A.; Cheeseman, J. R.; Scalmani, G.; Barone, V.; Mennucci, B.; Petersson, G. A.; Nakatsuji, H.; Caricato, M.; Li, X.; Hratchian, H. P.; Izmaylov, A. F.; Bloino, J.; Zheng, G.; Sonnenberg, J. L.; Hada, M.; Ehara, M.; Toyota, K.; Fukuda, R.; Hasegawa, J.; Ishida, M.; Nakajima, T.; Honda, Y.; Kitao, O.; Nakai, H.; Vreven, T.; Montgomery, J. A., Jr.; Peralta, J. E.; Ogliaro, F.; Bearpark, M.; Heyd, J. J.; Brothers, E.; Kudin, K. N.; Staroverov, V. N.; Kobayashi, R.; Normand, J.; Raghavachari, K.; Rendell, A.; Burant, J. C.; Iyengar, S. S.; Tomasi, J.; Cossi, M.; Rega, N.; Millam, J. M.; Klene, M.; Knox, J. E.; Cross, J. B.; Bakken, V.; Adamo, C.; Jaramillo, J.; Gomperts, R.; Stratmann, R. E.; Yazyev, O.; Austin, A. J.; Cammi, R.; Pomelli, C.; Ochterski, J. W.; Martin, R. L.; Morokuma, K.; Zakrzewski, V. G.; Voth, G. A.; Salvador, P.; Dannenberg, J. J.; Dapprich, S.; Daniels, A. D.; Farkas, Ö.; Foresman, J. B.; Ortiz, J. V.; Cioslowski, J.; Fox, D. J. Gaussian, Inc., Wallingford CT, 2009.

2. Tomasi, J.; Mennucci, B.; Cammi, R. *Chem. Rev*. **2005**, *105*, 2999–3093.

3. Reed, A. E.; Curtis, L. A.; Weinhold, F. *Chem. Rev*. **1988**, *88*, 899–926.

4. a) Becke, A. D. *J. Chem. Phys*. **1993**, *98*, 5648–5652; b) Lee, C.; Yang, W.; Parr, R. G. *Phys. Rev. B* **1988**, *37*, 785–789; c) Vosko, H.; Wilk, L.; Nusair, M.; *Can. J. Phys*. **1980**, *58*, 1200–1211.

5. a) Hehre, W. R.; Schleyer, P. v. R.; Pople, J. A. Ab Initio Molecular Orbital Theory, John Wiley & Sons, New York, 1986. b) Krishnan, R.; Binkley, J. S.; Seeger, R.; Pople, J. A. *J. Chem. Phys.* **1980**, *72*, 650–654; c) Hariharan, P. C.; Pople, J. A. *Theor. Chim. Acta* **1973**, *28*, 213–222; d) Clark, T.; Chandrasekhar, J.; Spitznagel, G. W.; Schleyer, P. v. R. *J. Comput. Chem.* **1983**, *4*, 294–301.

6. a) Grimme, S.; Ehrlich, S.; Goerigk, L. *J. Comput. Chem*. **2011**, *32*, 1456–1465; b) Grimmer, S.; Antony, J.; Ehrlich, S.; Krieg, H. *J. Chem. Phys*. **2010**, *132*, 154104–154119; c) Johnson, E. R.; Becke, A. D. *J. Chem. Phys*. **2006**, *124*, 174104–174109; d)

Becke, A. D.; Johnson, E. R. *J. Chem. Phys*. **2005**, *123*, 154101–154109; e) Johnson, E. R.; Becke, A. D. *J. Chem. Phys.* **2005**, *123*, 024101–024107.